2010

Controls Over S-Phase And Over Nuclear Synchrony

Lee Maxine Kiang

CONTROLS OVER S-PHASE

AND OVER NUCLEAR SYNCHRONY

A Thesis Presented to the Faculty of

The Rockefeller University

in Partial Fulfillment of the Requirements for

the degree of Doctor of Philosophy

by

Lee Maxine Kiang

June 2010

CONTROLS OVER S-PHASE

AND OVER NUCLEAR SYNCHRONY

Lee Maxine Kiang, Ph.D.

The Rockefeller University 2010

Nearly forty years ago, cell fusion experiments revealed two tenets of our understanding of the cell cycle today. One, controls maintain ordered progression of the cell cycle. Two, diffusible factors in the cytoplasm promote cell cycle transitions. The studies presented here stem from those principles. In fission yeast, *Schizosaccharomyces pombe,* we have investigated the controls over S-phase within the cell cycle and over S-phase and mitosis among multiple nuclei within a common cytoplasm.

To achieve faithful replication of the genome in each cell cycle, re-initiation of S-phase is prevented in G2 and origins are restricted from re-firing within S-phase. Failure in these controls could lead to polyploidy and local gene amplification contributing to genome instability. To investigate the block to re-replication during G2 we used single cell assays (BrdU pulse labeling and live cell fluorescence microscopy) and DNA microarray analysis. Depletion of the mitotic cyclin induces periodic S-phases correlated with G1/S gene expression, cell volume doubling, and uses mostly mitotic S-phase origins to replicate the genome evenly. We conclude that cyclin dependent kinase (CDK) inhibits re-initiation of a mostly normal S-phase program during G2.

To identify features of replication origins important for amplification, we investigated origin firing and local genome amplification in the presence of excess helicase loaders using our single cell assays and microarrays. Coordination of origin firing is lost and specific origins are necessary for local amplification but act only within

a permissive chromosomal context. Origins associated with amplification are highly AT-rich, fire early during mitotic S-phase, and are located in large intergenic regions. We propose that these features predispose replication origins to re-fire within a single S-phase, or to remain active after passive replication.

Finally, we aimed to distinguish whether the decision to undergo S-phase and M-phase is nuclear autonomous or cytoplasmically driven. We demonstrate using our single-cell assays that multiple nuclei in the same cell can undergo DNA synthesis or nuclear division out of synchrony in the absence of key CDK inhibitors. We conclude that these activities are nuclear autonomous in multinucleate fission yeast cells, and propose that inhibition of CDK activity by Rum1 and Wee1 may coordinate and synchronize these cell cycle events in the common cytoplasm.

DEDICATION

To my family

for the nature

and the nurture

ACKNOWLEDGEMENTS

First and foremost, thank you Paul. Thank you for your insight and for providing me guidance, yet also allowing me the freedom to figure things out on my own. Thank you for making time when there was none. Together we have navigated the system of American graduate education and I emerge, as from a stuck elevator, having learned much about critical thinking, problem solving, calmness and performance under pressure, British English and humor.

To the current and former members of the Nurse Labs in New York and London, you have made the daily experience of my PhD wonderful. Thanks for being great scientific colleagues and true friends, especially to Jenny and to Felice, my "work spouse," for always understanding. A very special thank you to Christian, my co-author and partner in crime, for striking the perfect balance of comedic melodrama and perspective on life. It has been a joy to work with you and our collaborators Jürg Bähler and Stephen Watt.

I am grateful to the committee, Hiro Funabiki, Tom Kelly, and Dave Allis, for stimulating discussions over the years, and to Zoi Lygerou especially for travelling so far.

I would like to acknowledge my earlier scientific mentors particularly Fred Cross at Rockefeller and Henrik Dohlman at Yale University. I began my study of yeast genetics and the cell cycle in Fred's lab at the age of 16 and Fred was unfailingly patient as we did tetrad dissections, crosses, and replica plating together.

To my earliest scientific mentors, my parents, thank you for your love, support, and devotion. This simply would not have been possible without you. I am very lucky. Thank you also to my extraordinary grandmother who inspires me daily.

Lastly, I have some really wonderful friends. Thank you for always being supportive of and enthusiastic about my work, especially my dearest friend Susanna Bass who has grown up alongside me for the last 18 years. We've come a long way, Doogie.

I am grateful to the Weill Cornell/Rockefeller/Sloan-Kettering Tri-Institutional MD-PhD Program for the opportunity to pursue my scientific and medical training.

I thank the National Cancer Center for Pre-doctoral fellowship.

TABLE OF CONTENTS

LIST OF FIGURES

LIST OF TABLES

LIST OF ABBREVIATIONS

APC/C	Anaphase Promoting Complex/Cyclosome
ARS	Autonomously Replicating Sequence
BrdU	5-bromo-2-deoxyuridine
***cdc13* s/o**	*cdc13* switch-off
***cdc18 cdt1* co-oe**	*cdc18 cdt1* co-overexpression
***cdc18* oe**	*cdc18* overexpression
cdt1	*cdc10 dependent transcript*
CDK	cyclin dependent kinase
CKI	Cyclin dependent Kinase Inhibitor
DAPI	4',6-diamino-2-phenylindole
DDK	Dbf4 Dependent kinase
FACS	Fluorescence Activated Cell Sorting
fL	femtoliters
GINS	Go Ichi Ni San complex (Sld5 and Psf 1, 2 and 3)
hENT	human nucleoside transporter
HU	hydroxyurea
IF	immunofluorescence
MBF	Mlu1 cell cycle box Binding Factor
MCB	Mlu1 cell cycle box
MCM	Mini-chromosome Maintenance
MPF	Maturation/M-phase Promoting Factor
nmt	no message in thiamine (promoter)
ORC	Origin Recognition Complex
ORF	open reading frame
PIP	PCNA Interacting Protein
PreRC	Pre-Replicative Complex
SCF	Skp1-Cullin-1/Cdc53-F-box E3 ligase
SIN	Septation Initiation Network
thi	thiamine
tk	thymidine kinase

CHAPTER 1

INTRODUCTION

1.1. The Cell Cycle and maintenance of ploidy

In every cell cycle a faithful copy of the genome must be made to ensure its stable inheritance. DNA synthesis is initiated once and only once per cell cycle, and within each S-phase the genome is completely and evenly replicated (reviewed in Arias and Walter, 2007; Bell and Dutta, 2002). Initiation of S-phase is contingent upon completion of the previous mitosis (Broek et al., 1991; Moreno and Nurse, 1994) and after S-phase a G2 cell is inhibited from further initiation (Johnson and Rao, 1970; Rao and Johnson, 1970). If these inhibitory controls are lost or overcome, aberrant origin firing can lead to changes in ploidy and local amplification of regions of the genome (Dahmann et al., 1995; Gopalakrishnan et al., 2001; Hayles et al., 1994; Melixetian et al., 2004; Mihaylov et al., 2002; Nishitani et al., 2000; Schimke et al., 1986; Vaziri et al., 2003; Zhong et al., 2003)

1.2. Organization of the cell cycle

Key events in the cell cycle are DNA synthesis (S-phase), in which the genome is replicated, and mitosis (M-phase), in which the nucleus and its genomic contents are equally divided. These events are separated by Gaps, G1 and G2, during which cell growth continues. The overall sequence across a range of species and cell types is G1, S, G2, M, with exceptions mostly occurring in embryonic tissues. Orderly progression through the cell cycle with alternating S and M-phases is important for the maintenance of ploidy.

1.2.1. Historical perspective: DNA synthesis is inhibited in G2 of the cell cycle. MPF is diffusible and cytoplasmic.

By fusing HeLa cells of different cell cycle stages, Rao and Johnson (Johnson and Rao, 1970; Rao and Johnson, 1970) found that the subsequent stage in the cell cycle can be promoted, but the previous stage is not repeated. For instance, in a G1-S-phase fusion, the G1 nucleus is promoted to enter S. In an S-G2 fusion, the G2 nucleus does not re-initiate S-phase, rather the S-phase nucleus is promoted toward mitosis. Fusion of an M-phase nucleus to a G1, S-phase or G2 nucleus leads to premature chromosome condensation. Rao and Johnson observed that the ensuing mitosis was synchronous among nuclei in nearly all cases, with asynchrony observed in only 0.5% of the G1-S and G1-G2 fusions, and 11% of S-G2 fusions. Further, triple fusions showed that the promotion into the next cell cycle stage was dose dependent. For instance, in a G1-S-S fusion, the G1 cell would enter S-phase sooner than the G1 nuclei in a G1-G1-S fusion (Figure 1.1). The major implications of these results were: (1) that a diffusible factor in the common cytoplasm of fused cells can promote cell cycle transitions and (2) that controls exist to block re-initiation of S-phase once it is complete. Masui and Markert as well as Smith and Ecker then reported independently that injecting M-phase cytoplasm into G2 blocked frog oocytes could induce maturation and the term MPF, **M**aturation **P**romoting **F**actor, was coined (Masui and Markert, 1971; Smith and Ecker, 1971). When it was later established that this factor also exists in somatic cells the name **M**-phase **P**romoting **F**actor was also used. Further studies revealed that MPF consists of the active protein kinase Cdc2 bound to cyclin (Labbe et al., 1988). These players are conserved in fission yeast.

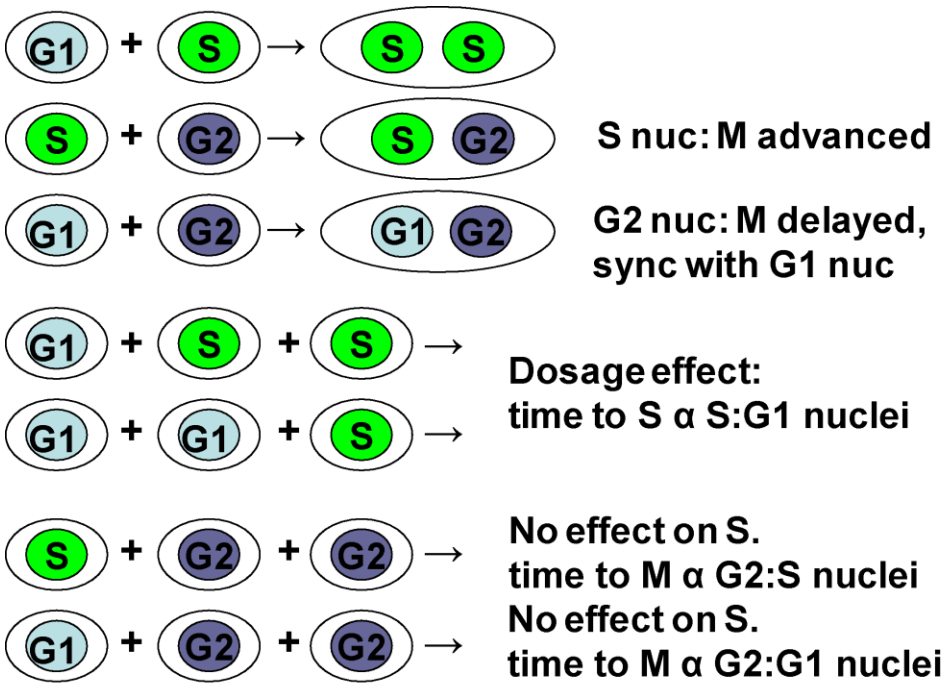

Figure 1.1 Schematic of Rao and Johnson cell fusion experiments

Cell cycle transitions could be promoted in a dose-dependent manner by exposure to cytoplasm from a subsequent cell cycle stage. Once complete, S-phase was not repeated.

1.2.2. Fission yeast mutants

Mutants in the yeasts have illuminated critical transitions in the cell cycle, and specifically mutants in the fission yeast *Schizosaccharomyces pombe* have been useful in understanding the block to re-initiation of S-phase (Hartwell et al., 1974; Nurse, 1975; Nurse et al., 1976). The isolation and analysis of mutants which tend to break these S-phase controls have defined requirements of the block, shedding light on key players and

their roles (Broek et al., 1991; Fisher and Nurse, 1996; Hayles et al., 1994; Moreno and Nurse, 1994; Nurse, 1975). Mutants of the *cdc2* protein kinase and the *cdc13* mitotic cyclin which fail to maintain their ploidy and diploidize disrupt the dependency of S-phase on completion of the previous mitosis and the block to re-initiation in G2 (Broek et al., 1991; Fisher and Nurse, 1996; Hayles et al., 1994). In mutants of *rum1*, regulator of the Cdc13-Cdc2 complex, **r**eplication is **u**ncoupled from **m**itosis (Moreno and Nurse, 1994). These and other key players are described in the following section.

1.3. Cyclins and cyclin dependent kinases

1.3.1. CDKS

Cdc2, the central essential regulator of the cell cycle in *S. pombe,* is known across species as **C**yclin **D**ependent **K**inase1 (CDK1). The CDK is a protein kinase; cyclin-bound activated CDKs drive cell cycle progression by phosphorylating substrates. CDK1 is conserved between humans and yeast to the extent that the human CDK1 can complement a *cdc2* mutant in *S. pombe* (Lee and Nurse, 1987). It is an essential CDK for all cell types in mice where it is known as CDK1 (Santamaria et al., 2007). In multicellular organisms, other CDKs exist which are required for the differentiation of specialized tissues (Malumbres et al., 2004; Rane et al., 1999). Interestingly, the requirements for specific CDKs in tumor cells can differ from the CDK requirements of the tissues from which they are derived (Tetsu and McCormick, 2003; Yu et al., 2006).

The cyclins, CDK activators, and CDK inhibitors function in combination to determine CDK activity. As such, the levels of these factors at different phases of the cell cycle are important for driving cell cycle progression. Their levels may be controlled by periodic expression or degradation, and their activity may be additionally controlled

by protein modification and intracellular localization, so factors functioning in modification and degradation of regulators are also important for CDK activity.

In the fission yeast cell cycle, Cdc2 protein levels are constant (Simanis and Nurse, 1986). Cdc2 is present in the cytoplasm throughout the cell cycle, and also localizes to the nucleus at G1/S, then accumulates on spindle pole bodies together with Cdc13 at prophase and metaphase (Decottignies et al., 2001). A mutagenesis screen for mutants which increase in ploidy isolated two alleles of *cdc2*, *cdc2-33* and *cdc2-M26* (Broek et al., 1991). When these were grown in medium lacking nitrogen to induce protease activity and then heat treated, Cdc2 protein levels decreased and DNA content was observed to double by **F**luorescence **A**ctivated **C**ell **S**orting (FACS) analysis (Broek et al., 1991). Since Cdc2 was known to act at G1 and G2 in the cell cycle (Nurse and Bissett, 1981), this led to the proposal that the cell cycle is a Cdc2 cycle with alternating S-phase and M-phase forms of Cdc2 (Broek et al., 1991). In this model, by decreasing Cdc2, cells were reset from G2 to G1 and thus could enter S-phase again. Cdc2 was established as having a critical role for establishing the order of S and M-phases in the cell cycle. Since CDKs must be activated by their cyclin binding partners, cyclins would also be expected to be important for this control.

1.3.2. Cyclins

Fourteen cyclins have been identified or predicted in fission yeast of which four are well characterized and known to bind to Cdc2: the activity of the Cdc2-Cig2 complex brings about S-phase, with Cig1 and Puc1 playing a minor roles, while the Cdc2-Cdc13 complex both inhibits re-initiation of DNA synthesis and triggers the G2-M transition (Broek et al., 1991; Fisher and Nurse, 1996; Hayles et al., 1994; Martín-Castellanos,

2000). These activities are modulated by positive and negative regulators through the cell cycle.

1.3.2.1. Cyclins: Cdc13

A second mutagenesis screen for diploidizing mutants yielded alleles of Cdc2 and Cdc13 (Hayles et al., 1994). Cdc13 is the mitotic B type cyclin in fission yeast, the only essential cyclin in *S. pombe*, and its levels are periodic in the cell cycle peaking at mitosis. The *cdc13* temperature sensitive mutants isolated re-replicated to 4C when nitrogen starved and heat treated (Fisher and Nurse, 1996; Hayles et al., 1994), and *Δcdc13* germinating spores progress through several doublings in DNA content before dying (Hayles et al., 1994). To allow further analysis of *Δcdc13*, a strain was created in which the only copy of *cdc13* is under control of the medium strength '**n**o **m**essage in **t**hiamine' (nmt) promoter so that *cdc13* can be switched on and off (*cdc13* s/o) (Fisher and Nurse, 1996). Since mutants of the binding partners Cdc2 and Cdc13 resulted in repeated DNA doublings without mitosis, the block over re-initiation of DNA synthesis was likely to be mediated by the G2/M CDK, the Cdc13-Cdc2 complex.

1.3.2.2. Cyclins: Cig2

Cig2 is a non-essential G1-S B-type cyclin thought to play the major role in the cell cycle transition to S-phase (Mondesert et al., 1996). Its levels are periodic in the cell cycle and dependent on the **M**lu1 cell cycle box **B**inding **F**actor (MBF) transcription complex which comprises Cdc10, Res1, Res2 and Rep2 (Mondesert et al., 1996). Cig2 protein and Cig2-associated kinase activity peak at G1/ S (Mondesert et al., 1996). Degradation of Cig2 depends on ubiquitination by the SCF (**S**kp1-**C**ullin-1/Cdc53-**F**-box) E3 ligase in G2 and M-phase, and by the **A**naphase **P**romoting **C**omplex/**C**yclosome

(APC/C) at anaphase/G1 (Yamano et al., 2000; Yamano et al., 2004). Localization in live cells has only been studied in overexpression, since the tagged protein is not detectable at endogenous levels; under the nmt81 promoter a pk-tagged Cig2 is nuclear at all stages of the cell cycle (Yamano et al., 2000).

1.4. The quantitative model versus cyclin specificity

Whether particular cyclins trigger specific cell cycle transitions when in complex with Cdc2 is not fully understood. Experiments showing that the Cdc13-Cdc2 complex can support cell cycle progression in the absence of the Cig1, Cig2 and Puc1 cyclins led to the proposal of a quantitative model where the level of CDK activity rather than the specific cyclins bound to Cdc2 determine cell cycle transitions (Fisher and Nurse, 1996; Stern and Nurse, 1996). In the model (schematized in Figure 1.2), it is proposed that the level of CDK activity is low at G1 allowing **P**re-**R**eplicative **C**omplex (PreRC) loading, then rises to activate S at an intermediate level. After completion of S-phase, mid-level CDK inhibits further initiation of DNA synthesis and then spikes to trigger mitosis. At the end of mitosis the CDK level drops owing to cyclin degradation by the APC/C so that the level is low as cells enter G1 again.

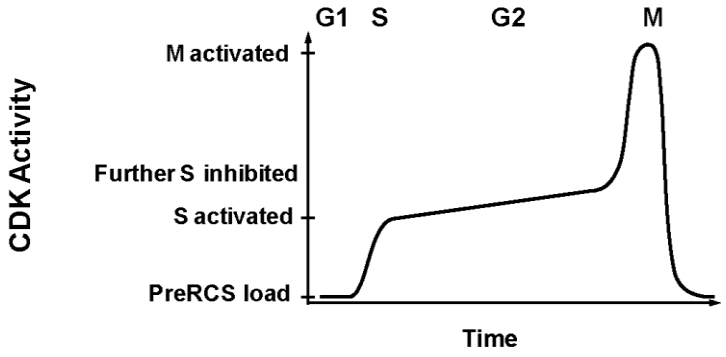

Figure 1.2 Schematic for quantitative model of cell cycle transitions. Variations exist.

By this model , a dramatic increase in CDK activity from G1 should induce mitosis rather than S-phase, as was demonstrated experimentally (Hayles et al., 1994). Evidence in favor of a cyclin specificity model finds qualitative differences among cyclins, for instance in phosphorylation of CDK substrates in budding yeast (Loog and Morgan, 2005) or differential activation of origin firing in *Xenopus* extracts (Krasinska et al., 2008). While these models are not mutually exclusive, and it is possible that both are correct to some degree, the validity of each is a matter of continuing debate.

1.5. Modulators of CDK activity

1.5.1. Rum1: CDK inhibitor

Rum1 is a stoichiometric inhibitor of the cyclin-Cdc2 complex, initially identified in a screen for genes inducing overreplication when overexpressed and named for its **r**eplication **u**ncoupled from **m**itosis (Moreno and Nurse, 1994). This may be due to 1) the inhibition of CDK activity similar to Cdc13 depletion and to 2) saturation of the SCF pathway allowing accumulation of Cdc18 which shares the pathway and can also contribute to overreplication (discussed in detail below) (Jallepalli et al., 1998; Kominami et al., 1998; Moreno et al., 1994). Rum1 is thought to influence the length of G1, the dependence of S-phase on completion of the previous mitosis, and the requirement for G1 before mitosis (Moreno and Nurse, 1994). Its levels are periodic in the cell cycle, beginning in anaphase and falling in S-phase (Correa-Bordes et al., 1997). Degradation occurs via CDK phosphorylation (Correa-Bordes et al., 1997; Moreno et al., 1994), SCF-dependent ubiquitylation, and proteolysis by the 26S proteasome at the nuclear periphery (Benito et al., 1998; Kominami et al., 1998). Rum1 strongly inhibits the Cdc13-Cdc2 complex, and weakly inhibits the Cig2-Cdc2 complex (Correa-Bordes

and Nurse, 1995). It may participate in a negative feedback loop with Cig2, as it may be phosphorylated and marked for degradation by Cig2-Cdc2 activity. Cig1-Cdc2 complex, however, is thought to play the predominant role in inhibiting Rum1, and is not inhibited by it (Figure 1.3) (Benito et al., 1998; Correa-Bordes et al., 1997).

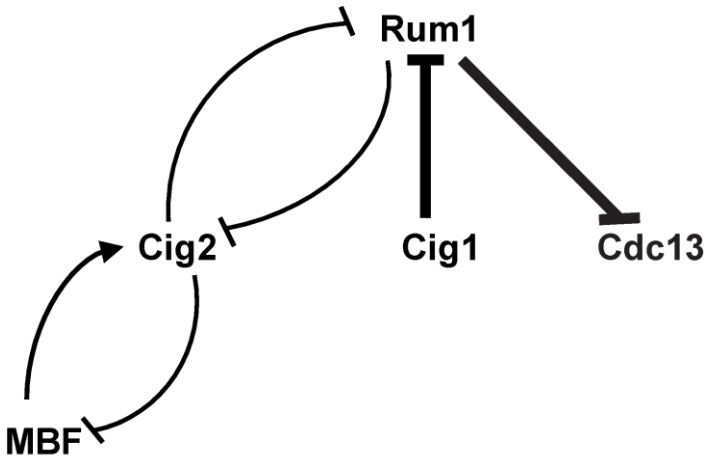

Figure 1.3 Negative feedback of Rum1 and cylins

Cyclin-Cdc2 complexes participate in these feedback loops; Cdc2 is not shown in the diagram for simplicity. Arrowhead denotes positive interaction; blunt end denotes inhibition. Line thickness represents relative strength of inhibition. (Ayté et al., 2001; Benito et al., 1998; Correa-Bordes et al., 1997; Correa-Bordes and Nurse, 1995)

1.5.2. Wee1, cdc25, and cell size at mitosis

G2/M CDK activity is inhibited by the Wee1 kinase (Russell and Nurse, 1987), which places an inhibitory phosphate on tyrosine 15 of Cdc2 (Gould and Nurse, 1989), and is activated by the opposing Cdc25 phosphatase (Russell and Nurse, 1986). Wee1 was initially identified as the *cdc9-50* mutant in which mitosis is advanced and cells divide at a smaller size than wild type (Nurse, 1975). Newly divided cells lacking Wee1 activity then undergo an extended G1 and initiate S-phase at a size smaller than the wild

type size for S-phase (Nurse and Thuriaux, 1977). This led to the idea that Wee1 influences the primary cell size control in fission yeast at the G2/M transition, and that there exists a second control over cell size at G1/S. The second control is normally cryptic because newly divided wild type cells exceed this size, but is unmasked in small cells which undergo an extended G1 to reach the minimum size for S-phase (Nasmyth et al., 1979; Nurse and Thuriaux, 1977), and is mediated by Rum1 (Moreno and Nurse, 1994). The presence of cell size requirements for cell cycle transitions coordinates cell growth with the cell cycle and contributes to cell size homeostasis (Jorgensen and Tyers, 2004). Knowing the proportions of cell cycle phases, we can therefore ascertain where a cell is in the cell cycle based on its size relative to the population, and can use cell size as a proxy for time. We have taken advantage of this principle in our studies of DNA synthesis in Chapters 2 and 3.

1.6. DNA replication

1.6.1. DNA replication origins

DNA synthesis is activated at replication origins along chromosomes; each origin will fire only once or does not fire after being passively replicated. From the activation of a population of origins, one round of replication is achieved wherein every part of the genome is copied and no portion is copied more than once.

Fission yeast origins provide a good model for origins in higher eukaryotes, as they are extended, complex, and have high AT content (Okuno et al., 1999). Replication origins in *Escherichia coli* and the budding yeast *Saccharomyces cerevisiae* have well-defined consensus sequences, and about half of budding yeast origins are used in one out of two cell cycles (Friedman et al., 1997; Poloumienko et al., 2001). In contrast,

mammalian origins and fission yeast origins lack a well-defined consensus sequence and consist of asymmetric AT-rich stretches of DNA (Dai et al., 2005; DePamphilis, 2005; Okuno et al., 1999; Segurado et al., 2003). The replication origins in mitotic S-phase in fission yeast have been mapped by several groups (Feng et al., 2006; Hayashi et al., 2007; Heichinger et al., 2006; Kiang et al., 2009); here, we refer to the set of origins and parameters as described in the most recent study of our lab (Kiang et al., 2009). Our lab has identified 904 origins used in a normal mitotic S-phase (Heichinger et al., 2006; Kiang et al., 2009). These range in efficiency, that is, the likelihood that an origin will fire in a given S-phase, from less than 10% to 76% and are located in intergenic regions. There is evidence that AT richness and length of the intergenic region occupied by the origin are correlated with the ability to act as an extrachromosomal **A**utonomously **R**eplicating **S**equence (ars) (Dai et al., 2005).

1.6.2. Control molecules and machinery

Initiation of S-phase requires the assembly of Pre-Replicative Complexes at replication origins. The Orc proteins, Cdc18 (Cdc6 in other organisms), and Cdt1 associate in a stepwise fashion and then load the **m**ini**c**hromosome **m**aintenance (MCM) complex, the likely replicative helicase (Labib et al., 2000; Liang et al., 1995; Tsuyama et al., 2005). Despite variation in the character of replication origins, the replication factors and their order of assembly are well conserved from yeasts to metazoans (reviewed in Bell and Dutta, 2002).

1.6.2.1. The Orc proteins

Orc proteins form a heterohexamer which when ATP-bound, binds DNA (Austin et al., 1999; Bell and Stillman, 1992; Chesnokov et al., 2001; Klemm et al., 1997). In *S.*

pombe, the so-called **o**rigin **r**ecognition **c**omplex (ORC) binds directly and specifically to AT rich sequences via the AT hook motifs of the Orc4 subunit of the complex (Chuang and Kelly, 1999; Kong and DePamphilis, 2001; Okuno et al., 1999) and human ORC has also been shown to bind preferentially to AT-rich polynucleotides (Vashee et al., 2003). While a basal level of ORC is origin-bound throughout the cell cycle (Lygerou and Nurse, 1999), recent evidence from our lab has shown that Orc binding varies periodically in the cell cycle, increasing at M and beginning the sequence of factor binding leading to PreRC formation for the subsequent S-phase (Wu and Nurse, 2009). The genome-wide localization of Orc1, Orc4 and Mcm6 has been mapped by ChIP-chip in the Masukata lab (Hayashi et al., 2007). These data indicate that PreRCs assemble at many more origins than are eventually active, so in each S-phase there exists a larger pool of initiation sites which have the potential to be activated.

1.6.2.2. Helicase loaders: Cdc18 and Cdt1

The next member of the PreRC to assemble is the AAA+ ATPase Cdc18, known in other organisms as Cdc6 and essential for DNA synthesis (Hartwell, 1973; Kelly et al., 1993). It is expressed periodically in the cell cycle, dependent on MBF with levels peaking at G1/S and has a short half life of only about 5 minutes (Kelly et al., 1993; Muzi-Falconi et al., 1996). Cdc18 is negatively regulated by CDK at six phosphorylation sites, 5 of which are at the N-terminus (Gopalakrishnan et al., 2001; Jallepalli et al., 1997; Lopez-Girona et al., 1998). N-terminal phosphorylation is required for Pop2 binding and thus targeting by the SCF for degradation by the 26S proteasome at the nuclear periphery (Jallepalli et al., 1997). In mammals, Cdc6 is regulated in part by nuclear export of the soluble fraction in S-phase (Saha et al., 1998), with some

chromatin-bound Cdc6 remaining nuclear (Coverley et al., 2000; Mendez and Stillman, 2000), and by ubiquitylation via the APC/C at M/G1 (Mailand and Diffley, 2005; Petersen et al., 2000).

Cdc18 is known to be important for the control of re-replication in fission yeast because its overexpression can lead to increased DNA content up to about 8-16C (Nishitani and Nurse, 1995). This is enhanced in the background of non-phosphorylatable Orp2 (Vas et al., 2001) and also when a hypophosphorylated Cdc18 is overexpressed (Jallepalli et al., 1997) or co-overexpressed with a non-phosphorylatable Cdt1 (Gopalakrishnan et al., 2001). Co-overexpression of wild type *cdc18* and *cdt1* (*cdc18 cdt1* co-oe) greatly increases this phenotype so that DNA content both increases more rapidly and attains a higher level of approximately 32C DNA content (Nishitani et al., 2000; Yanow et al., 2001).

Cdt1 was first identified in fission yeast as a **c**dc10-**d**ependent **t**ranscript (Hofmann and Beach, 1994), so like *cdc18* its expression is dependent on MBF. The interaction of Cdc18 and Cdt1 increases their respective affinities for DNA binding, and stabilizes the ORC-DNA complex (Houchens et al., 2008). In *S. pombe*, Cdt1 interacts with the C-terminus of Cdc18 to promote MCM binding (Nishitani et al., 2000), and in *Xenopus* extracts, sequential assembly of Cdc6 followed by Cdt1 is required for proper MCM loading (Tsuyama et al., 2005). In *Xenopus* it was found that Cdt1 ubiquitylation on chromatin and subsequent destruction depends on the initiation of DNA replication (Arias and Walter, 2005; Arias and Walter, 2006). *Xenopus* Cdt1 interacts with PCNA via its **P**CNA-**i**nteracting **P**rotein (PIP) box facilitating interaction with the Cul4-Ddb1^{Cdt2} E3 ubiquitin ligase. *S. pombe* Cdt1 may also be degraded by the same mechanism since

it contains a partial PIP box and its degradation during DNA damage is dependent on Cdt2 (Ralph et al., 2006), but the role for Cdt2-dependent degradation in the normal cell cycle is as yet unconfirmed. An additional level of Cdt1 regulation in *Xenopus* is the Cdt1 inhibitor geminin, and in mammals, a second Cdt1 degradation pathway constitutes yet another layer of Cdt1 regulation (Nishitani et al., 2006). Overexpression of Cdt1 alone is insufficient to induce overreplication in yeasts, but mammalian cells overexpressing Cdt1 or depleted of geminin can re-replicate (Dorn et al., 2009; Gonzalez et al., 2006; Melixetian et al., 2004).

1.6.2.3. The MCM complex: the putative replicative helicase

The MCM complex is a heterohexameric toroid of MCMs2-7 which most probably acts as the replicative helicase (Adachi et al., 1997). Assembly of the MCM complex on chromatin requires the other members of the PreRC (Tsuyama et al., 2005). Interestingly, once the complex is loaded, ORC, Cdc6 and Cdt1 are no longer required (Hua and Newport, 1998). The MCM complex is thought to be the helicase because degron studies in *S.cerevisiae* show that it functions at initiation and elongation (Labib et al., 2000). It has also been visualized at the replication fork during elongation in chorion amplification (Claycomb et al., 2002). Of the 6 subunits, Mcms 4, 6, and 7 have helicase activity and low ATPase activity *in vitro*, while Mcms 2, 3, and 5 have no helicase activity nor ATPase activity (reviewed in Bell and Dutta, 2002). The intact complex Mcms 2-7 *in vitro* has no helicase activity and high ATPase activity, suggesting that 2, 3 and 5 may serve to inhibit the helicase activity while enhancing the ATPase activity of the other subunits. Loading of the MCM complex completes PreRC formation and in

S. pombe the timing of PreRC assembly at a given origin in M through G1 is thought to establish that origin's time of firing in S-phase (Wu and Nurse, 2009).

Following PreRC assembly, the extent of Pre-IC formation at an origin is correlated with its efficiency of firing (Wu and Nurse, 2009). The Pre-Initiation Complex comprises the GINS complex (for **G**o **I**chi **N**i **S**an, referring to Sld**5** and Psf **1**, **2** and **3**), Cdc45 and others, whose ordered association depends on CDK and **D**bf4-**D**ependent **K**inase (DDK, also known as Cdc7 and Hsk1-Dpf1) (Yabuuchi et al., 2006). A single complete replication of the genome per cell cycle requires that PreRCs be formed and activated just once per cell cycle, that no origin fires more than once and that an origin does not fire after being passively replicated.

1.7. Overreplication

1.7.1. Nomenclature

Failure of these controls, resulting in continued DNA synthesis without mitosis, is known as overreplication. The nomenclature for various types of overreplication has been used with some variation in the literature. In our studies, the terms re-replication and overreplication are used synonymously to describe any increase in DNA content above a single S-phase per cell cycle or above a complete and even replication of the genome per S-phase. Endoreduplication, in which the genome is fully replicated via rounds of S-phase without intervening mitoses would be one subtype of overreplication occurring normally in development. Local amplification refers to increase in copy number of a specific segment of chromosome relative to the rest of the genome.

1.7.2. Developmentally programmed overreplication

Re-replication in nature falls in the categories of endoreduplication or amplification. Normally endoreduplicating cell types include plant endosperm, with hundreds of genomic copies (reviewed in Larkins et al., 2001), red algae (Goff and Coleman, 1990), *Drosophila* nurse cells and their surrounding follicle cells (Lilly and Spradling, 1996; Shcherbata et al., 2004), and mammalian trophoblast giant cells (Parisi et al., 2003; Ullah et al., 2008). Such cells progress through endocycles composed of gap and synthesis phases but lacking mitosis. Modulation of CDK activity has been shown to be required for the mitotic-to-endocycle switch and for maintenance of endocycling. In *Drosophila* ovarian follicle cells this occurs by upregulating Cdc25, activating mitotic cyclin degradation and establishment of fluctuating cyclin E, the G1/S cyclin (Follette et al., 1998; Shcherbata et al., 2004; Sigrist and Lehner, 1997). In human trophoblast stem cells, depletion of **f**ibroblast **g**rowth **f**actor **4** (FGF4) induces differentiation into endocycling giant cells via inhibition of CDK1 by the p57 **C**yclin dependent **K**inase **I**nhibitor (CKI) and others (Ullah et al., 2008). An interesting variant of endocycles are the endomitoses seen in megakaryocytes. After stimulation by thrombopoetin, a slightly different set of CKIs is induced and the resulting endocycles include a partial mitosis wherein chromosomes segregate within the nucleus, but the nucleus fails to divide (Baccini et al., 2001; Zhang et al., 1998). The resulting polyploid multilobulated nucleus is presumed to contain individual genome complements in each lobe. Since the transition to and maintenance of endocycles is modulated by CDK activity, regulation of CDK activity must be important for the maintenance of ploidy.

Local genome amplification is thought to be a strategy to increase gene expression by increasing the amount of template for transcription and the gene expression machinery in cells that will not undergo further divisions (Calvi et al., 1998; de Cicco and Spradling, 1984; Yao et al., 1974). In amphibians (Gall, 1968; Hourcade and Dressler, 1973), *Tetrahymena* (Donti et al., 2009; Yao et al., 1974) and flies (Gall et al., 1969; Kubrakiewicz, 2002; Kubrakiewicz and Bilinski, 1995; Tröster et al., 1990), rDNAs are excised and amplified extrachromosomally up to 10,000 fold. Amplification of chromosomal loci occurs after endoreduplication in *Drosophila* follicle cells to increase expression of chorion and eggshell proteins (Calvi et al., 1998; de Cicco and Spradling, 1984), and replication bubbles within bubbles form onion-skin structures as visualized by electron microscopy (Osheim et al., 1988). Amplification of cocoon protein genes in the salivary glands of flies also generates onion-skin structures (Lunyak et al., 2002; Monesi et al., 1995) which have been visualized by 2-D and 3-D gel electrophoresis (Liang and Gerbi, 1994; Liang et al., 1993) and form DNA 'puffs'. How amplification is controlled, what favors re-firing of selected segments of the genome while inhibiting replication of others is not well understood.

1.7.3. Induction of overreplication

Perturbations bringing about re-replication follow two themes. First, reduction in mitotic CDK activity generally results in increased ploidy, apparent by FACS analysis as discrete peaks corresponding to DNA content doublings. Second, altered abundance or regulation of helicase loaders brings about increased DNA content without discrete peaks on FACS analysis suggesting that DNA synthesis does not occur by complete doublings.

In addition to the fission yeast phenotypes previously discussed, in budding yeast, fruit flies, and mammals, disrupting G2/M CDK activity also leads to rough doublings of DNA content without mitosis (Bates et al., 1998; Dahmann et al., 1995; Itzhaki et al., 1997; Mihaylov et al., 2002; Sauer et al., 1995; Ullah et al., 2008). This increase in DNA content has generally been assumed to result from a repeated S-phase without mitosis. However, in all these organisms and in *S. pombe* it was not known whether the DNA synthesis that takes place is the consequence of induction of a normal S-phase replication program or if it represents aberrant unprogrammed DNA synthesis.

Dysregulation of the helicase loaders *cdc6* and *cdt1* can induce re-replication and polyploidy in worms, fruit flies, frogs, mice and human cell lines (Arias and Walter, 2006; Gonzalez et al., 2006; Melixetian et al., 2004; Mihaylov et al., 2002; Vaziri et al., 2003; Zhong et al., 2003). In particular, silencing the Cdt1 inhibitor geminin in *Drosophila* cell culture leads to overreplication with a broad range of DNA contents from 2C to 8C (Mihaylov et al., 2002). Budding yeast differs somewhat in its regulation of PreRC components, and in the requirements to induce bulk re-replication. In addition to regulation of Cdc6 levels, the MCM complex together with Cdt1 is exported from the nucleus, Orcs 2 and 6 are phosphorylated and Clb5 inhibits Orc6 from reforming PreRCs (Nguyen et al., 2001; Wilmes et al., 2004). Detectable overreplication by FACS analysis requires deregulation of Cdc6, non-phosphorylatable Orcs and retention of nuclear MCMs (Nguyen et al., 2001), but by more sensitive microarray analysis it was found that a low level of re-replication occurs with deregulation of just Cdc6 and the Orcs (Green et al., 2006; Tanny et al., 2006). In those organisms displaying an increase in DNA content

without discrete DNA doublings, it was suspected that the genome may be unevenly replicated.

1.7.4. Consequences of unprogrammed re-replication

Re-replication potentiates genomic instability and the resulting alterations to the genome can drive evolution but also the development of aneuploidy and cancer (Arentson et al., 2001; Karakaidos et al., 2004; Schimke et al., 1986; Seo et al., 2005). Overexpression of *cdt1* in mammalian cells leads to the formation of aberrant chromosomal structures (Seo et al., 2005) and has been found to potentiate tumorigenesis (Arentson et al., 2001). In p53 null mice, *cdt1* overexpression in T-cells can lead to lymphoma (Seo et al., 2005) while cells overexpressing *cdc6* and *cdt1* can induce tumor formation after injection in SCID mice (Liontos et al., 2007). Regulation of Cdt1 and PreRC formation seems to be critical for avoiding deleterious consequences of re-replication, which may explain why there are multiple overlapping controls in mammals.

1.8. Control of S-phase and M-phase in multinucleate cells.

Fission yeast mutants provided the opportunity to investigate the controls over S-phase in the cell cycle. We have used multinucleate fission yeast mutants to distinguish whether signals driving S-phase and M-phase are nuclear autonomous or cytoplasmic.

Multinucleate cells are found in diverse organisms including *Physarum polycephalum*, *Tetrahymena*, the filamentous fungi *Ashbya Gosypii* and *Aspergillus Nidulans* and in mammalian osteoclasts, muscle fibers and hepatocytes. They can arise from mitosis without cytokinesis or from cell fusion events, as is the case in osteoclasts and myotubes. Generally, mitoses occur synchronously (Ducommun et al., 1990) or parasynchronously, as in *Aspergillus* where a wave of mitosis spreads along the cell

(Clutterbuck, 1970). These events are assumed to be coordinated by factors shuttling between the multiple nuclei and the common cytoplasm in the same way that fused cells of different cell cycle stages became synchronized by MPF in the Rao and Johnson experiments (Johnson and Rao, 1970; Rao and Johnson, 1970). Most cases of asynchronous DNA synthesis or mitosis are seen only upon treatment with drugs or selective damage to one nucleus of a heterokaryon (Demeter et al., 2000; Krishan and Ray-Chaudhuri, 1969). Within skeletal muscle fibers, individual nuclei can be induced to locally alter gene expression in response to external signals (Rossi et al., 2000). However, differences among nuclei can also be attributed to differences in origin since a muscle fiber arises from fusion rather than acytokinetic mitosis. An exception at odds with the general rule of mitotic synchrony is *Ashbya,* which undergo asynchronous mitosis (Gladfelter et al., 2006) with nuclear divisions concentrated at growing tips and branchpoints (Helfer and Gladfelter, 2006).

Most of the *S. pombe* life cycle is spent as a mononucleate cell. During the brief interval after mitosis and before septum formation when cells are binucleate, the nuclei behave uniformly—the two sister nuclei in a wild type cell in G1 appear to enter S-phase concomitantly when assessed by autoradiography of cells pulse labeled with ^{3}H uracil (Nasmyth et al., 1979). In fission yeast, cytokinesis mutants which undergo acytokinetic mitoses become multinucleate cells. This presents the opportunity to investigate whether events are nuclear autonomous or cytoplasmically driven without the need for fusing cells of different origins and the associated caveats. In the multinucleate cells we observe, nuclei are sisters which have remained in the same constant cytoplasmic environment after division of the mother nucleus.

1.9. Overarching questions for the thesis:

How does the cell ensure: (1) that there is one S-phase per cell cycle and (2) that the genome is completely replicated in each S-phase? We approached these questions by studying fission yeast mutants in which inhibition of inappropriate DNA synthesis is lost. In *cdc13* s/o, depletion of G2/M CDK activity was known to lead to re-initiation of DNA synthesis and repeated DNA doublings without mitosis (Fisher and Nurse, 1996; Hayles et al., 1994), but whether this occurred by a normal S-phase program was not understood. Excess helicase loaders were known to induce increased DNA content without distinct DNA doublings (Gopalakrishnan et al., 2001; Jallepalli et al., 1997; Nishitani et al., 2000; Nishitani and Nurse, 1995; Yanow et al., 2001) and evidence suggested that the genome was not replicated evenly but might be locally amplified (Mickle et al., 2007). Whether local genome amplification could result from re-firing of origins was not known, nor what features might predispose origins to re-fire.

Are S-phase and M-phase driven in a nuclear autonomous fashion or coordinated within the cytoplasm of a fission yeast cell? By studying multinucleated fission yeast we aimed to distinguish nuclear-driven activity from cytoplasmic activity.

Chapter 2

CYCLIN DEPENDENT KINASE INHIBITS RE-INITIATION OF A NORMAL S-PHASE PROGRAM IN G2

2.1. Introduction

Fission yeast cells that are depleted of the mitotic Cdc13-Cdc2 G2/M CDK complex fail to undergo mitosis and then re-initiate DNA synthesis from G2, leading to approximate doublings of DNA content as assessed by fluorescence activated cell sorting (FACS) analysis (Fisher and Nurse, 1996; Hayles et al., 1994). In budding yeast, fruit flies, and mammals, disrupting G2/M CDK activity also leads to rough doublings of DNA content without mitosis (Bates et al., 1998; Dahmann et al., 1995; Itzhaki et al., 1997; Mihaylov et al., 2002; Sauer et al., 1995; Ullah et al., 2008). This increase in DNA content has generally been assumed to result from a repeated S-phase without mitosis. However, in all these organisms it is not known whether the DNA synthesis that takes place is the consequence of induction of a normal S-phase replication program or if it represents aberrant unprogrammed DNA synthesis. We have addressed this question by characterizing the DNA synthesis that occurs in fission yeast when G2/M CDK activity is depleted from G2 cells.

2.2. Does depletion of G2/M CDK lead to induction of normal S-phase program?

2.2.1. Defining a normal S-phase program

In fission yeast, a normal mitotic S-phase is characterized by (1) a burst of G1/S **M**lu1 cell cycle box **B**inding **F**actor (MBF)-dependent gene expression, (2) the initiation of DNA synthesis at a critical cell size, (3) the use of a specific set of replication origins

and (4) equal replication across the genome. To investigate whether the DNA synthesis induced when G2/M CDK is depleted from G2 cells exhibits these characteristics, we have used single cell assays for DNA synthesis and G1/S gene expression.

DNA synthesis was monitored in single cells by 5-bromo-2-deoxyuridine (BrdU) pulse labeling using a strain that expresses the human nucleoside transporter (*hENT*) and herpes simplex thymidine kinase (*tk*) (Sivakumar et al., 2004). This allows the uptake and conversion of nucleoside analog label to nucleotide label and its incorporation into cells undergoing DNA synthesis. Visualization of newly replicated DNA is monitored after fixation by immunofluorescence (Sivakumar et al., 2004). To validate this method, an asynchronous wild type culture was pulsed with BrdU for 10 minutes and signal was detected in septated and recently divided cells which are in S-phase (S-phase is at least 0.1 of a cell cycle in length, so a minimum of 20 minutes under these conditions) (Nasmyth et al., 1979) (Figure 2.1 A). Since cell cycle progression is coupled to growth, we measured the cell volume per nucleus of labeled fixed cells. The length and width of cells were measured and cell volume was estimated considering the cell as a cylinder with half-spheres at each end; cell volume was divided by two for binucleate and septated cells (Materials and methods). The percentage of BrdU-positive cells reached a maximum at about 44 femtoliters (fL) (cells shrink due to fixation and processing for immunofluorescence and so are smaller than live cells), and the peak was asymmetrical (Figure 2.1A, Table 2.1A). The smallest cell volume per nucleus at which cells were labeled was the cohort of 37 fL where already 50% of the population was labeled. The 37 fL cohort consisted of binucleate cells which had just completed mitosis. This result is consistent with the fact that there is only a very short G1 in wild type fission yeast

(Mitchison and Creanor, 1971) and S-phase is initiated soon after completion of mitosis in binucleate cells.

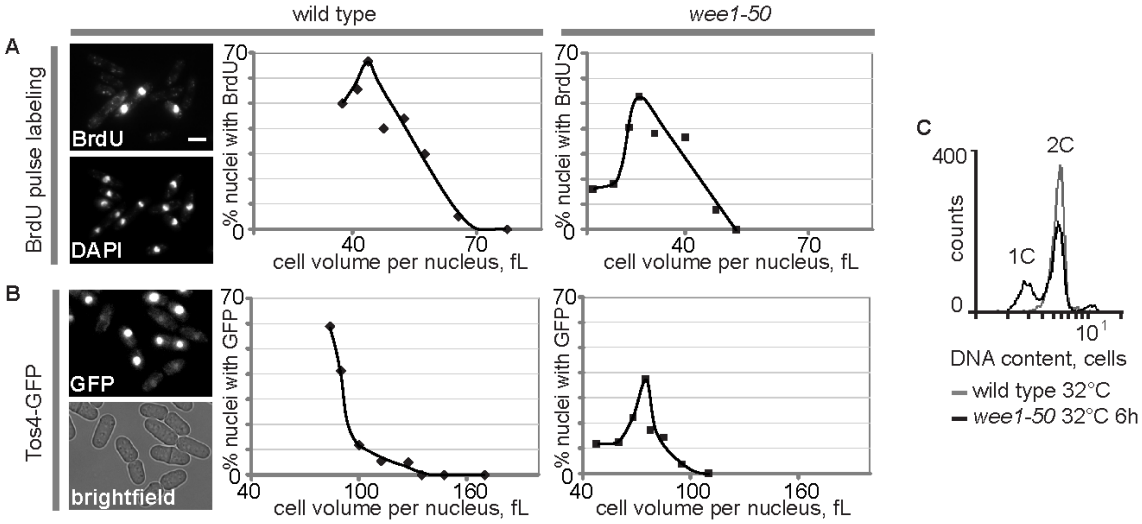

Figure 2.1 Single cell methods for studying DNA synthesis and MBF-dependent gene expression **(A)** BrdU pulse labeling of wild type and *wee1-50* cells. Left panels: A *leu1-32 his7-366 adh1-tk-his7+ adh1-hENT-leu1+* culture at 32°C was pulse labeled with BrdU. BrdU was detected by immunofluorescence and DNA visualized by DAPI (4',6-diamino-2-phenylindole) staining. The scale bar is 5 μm long. The percentage of BrdU positive nuclei was plotted as a function of fixed cell volume per nucleus. Right panel: a *wee1-50 leu1-32 his7-366 adh1-tk-his7+ adh1-hENT1-leu1+* culture at 25°C was shifted to 32°C for 6h. Cells were pulse labeled with BrdU. The percentage of BrdU positive nuclei was plotted as a function of fixed cell volume per nucleus. **(B)** MBF-dependent gene expression in wild type and *wee1-50* cells. The cell volume per nucleus with peak Tos4-GFP signal was determined. Cells not fixed. Left panels: an *ade6-M210 tos4-GFP-kanMx6* culture at 32°C. The percentage of nuclei with strong GFP signal was plotted as a function of live cell volume per nucleus. Right panel: a *wee1-50 ade6-M210 tos4-GFP-kanMx6* culture at 25°C was shifted to 32°C for 6 hours. The percentage of nuclei with strong Tos4-GFP signal was plotted as a function of live cell volume per nucleus. **(C)** FACS analysis of wild type cells at 32°C, and *wee1-50* cells shifted from 25°C to 32°C for 6 hours. *Wee1-50* cells show a 1C peak.

Table 2.1 Volume per nucleus at peak BrdU incorporation or Tos4-GFP signal for successive DNA doublings.

A.

Strain	Volume per nucleus at peak BrdU incorporation (femtoliter, fL)				
	1C→2C	**2C→4C**	**4C→8C**	**8C→16C**	**16C→32C**
wild type BrdU	44				
wee1-50 BrdU	28				
cdc13 s/o BrdU	n/a[a]	50	100	200	400

B.

Strain	Volume per nucleus at peak nuclear Tos4-GFP signal (fL)			
	1C→2C	**2C→4C**	**4C→8C**	**8C→16C**
wild type *tos4-GFP*	90			
wee1-50 tos4-GFP	75			
cdc13 s/o *tos4-GFP*	95	170	290	600

(A) Fixed cell volumes. BrdU strains contain *tk* and *hENT*.

[a] not scored. See Materials and methods for details of *cdc13* s/o pulse labeling and calculation of cell volumes.

(B) Live cell volumes

In the normal wild type mitotic cell cycle, the critical cell size threshold for entry to S-phase is cryptic, since newly divided cells are above the size threshold (Nurse, 1975; Nurse and Thuriaux, 1977) so the critical size is only revealed in small cells such as the *wee1* mutant which reduces cell size at division. In cells lacking Wee1, newly divided cells are small and G1 is lengthened as cells must grow to reach the minimum size required for S-phase. Therefore, we used temperature sensitive *wee1-50* cells which are advanced into mitosis to determine if the single cell assay could detect the reduced cell size for S-phase in these cells (Nurse and Thuriaux, 1977). *Wee1-50* cells growing exponentially at 32°C have a longer G1 than wild type cells (data not shown and Figure

2.1C) and undergo S-phase at a reduced cell volume (Figure 2.1A), and as expected the cell volume cohort with maximal labeling was smaller than wild type cells at about 28 fL (Figure 2.1A, Table 2.1A). We conclude that this assay can be used to monitor DNA synthesis and to determine the cell volume at which cells undergo DNA synthesis.

To monitor G1/S MBF-dependent gene expression, we developed a single cell assay in live cells. Factors required for DNA replication expressed at G1/S include Cdc18, Cdt1, Cig2, and Cdc22, under transcriptional control of the MBF complex which contains Cdc10, Res1, Res2 and Rep2 (reviewed in Bähler, 2005). Since these MBF-dependent gene products do not give an easily detectable signal in live cells when fluorescently labeled (S. Kearsey, personal communications), we used the non-essential gene SPAP14E8.02, related to budding yeast *TOS4,* as a marker for G1-S gene expression. This gene is periodically expressed in the cell cycle peaking at G1(Rustici et al., 2004). It has MCB1 and MCB2 (**M**lu1 **c**ell-cycle **b**ox) motifs, bound by MBF (Rustici et al., 2004). We constructed a strain in which the endogenous SPAP14E8.02 was tagged with a single GFP (S65T) at its C-terminus, and we refer to the construct here as *tos4-GFP*. To determine when Tos4-GFP signal peaks in the cell cycle, a culture was synchronized using the *cdc25-22* temperature sensitive mutation (Fantes, 1979) (Figure 2.2). Cells were blocked in G2 at the restrictive temperature of 36.5°C, and then released at 25°C allowing the population to progress synchronously through the cell cycle (Figure 2.2A).

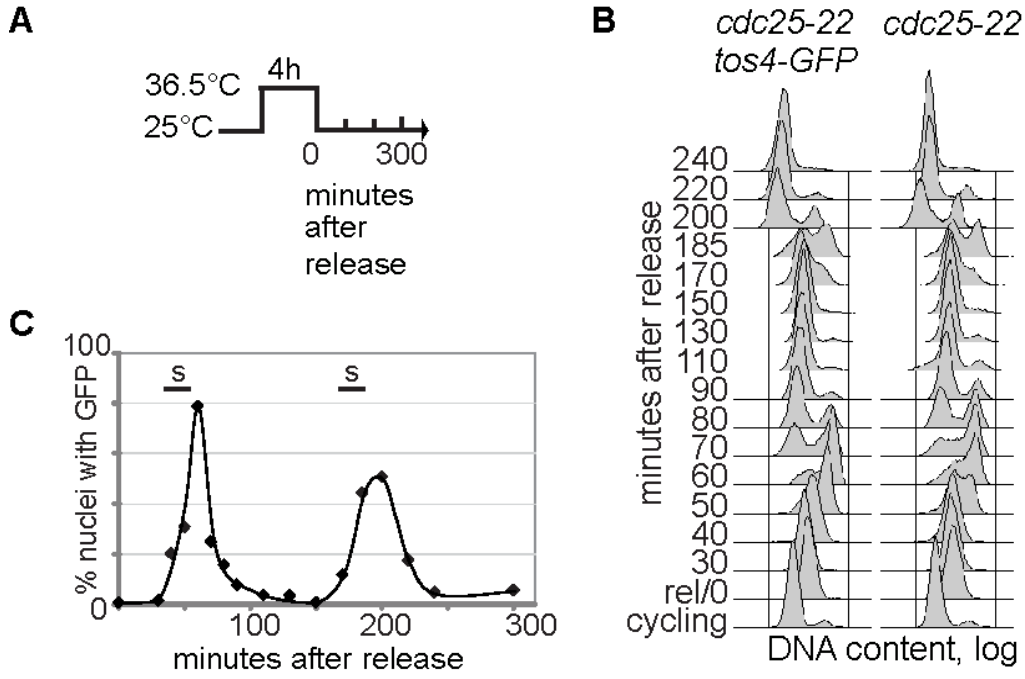

Figure 2.2 Nuclear signal of Tos4-GFP signal is periodic in the cell cycle

(A) Experiment schematic: a *cdc25-22 ade6-M210 tos4-GFP-kanMx6* culture at 25°C was shifted to 36.5°C for 4 hours, then released at 25°C. (B) FACS analysis: *cdc25-22 tos4-GFP* cycled similarly to *cdc25-22* alone. (C) The percentage of nuclei with strong Tos4-GFP signal was plotted as a function of time, peaking at the end of S-phase. Tos4-GFP localizes to the nucleus periodically during the cell cycle.

The percentage of cells with GFP signal was monitored over two cell cycles and DNA content was assessed by FACS analysis (Figure 2.2B). Fluorescent protein was seen as a high intensity signal localized to the nucleus during S-phase which decreased as cells proceeded through G2 (Figure 2.2C). This was consistent with a peak in message at G1 (Rustici et al., 2004) and the 25 minute time period needed for GFP (S65T) maturation (Heim et al., 1995) which will delay appearance of the protein to later in the cell cycle.

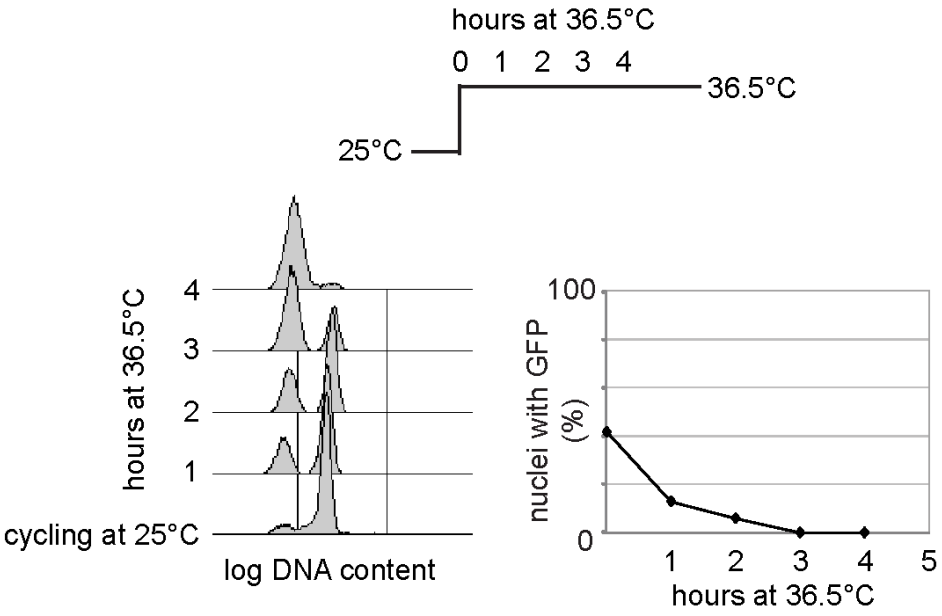

Figure 2.3 Tos4-GFP is cdc10-dependent

A cycling *cdc10-v50 Δcdc13::ura4+ pREP45 cdc13+ ade6-704 tos4-GFP-kanMx6* culture in the absence of thiamine at 25°C was shifted to 36.5°C for 4 hours. The percentage of nuclei in the culture with strong Tos4-GFP signal was assessed every hour.

To verify that *tos4-GFP* is MBF-dependent, an exponentially growing culture of *cdc10-v50 tos4-GFP* cells at 25°C was shifted to 36.5°C to inactivate the temperature sensitive mutant Cdc10 (Marks et al., 1992; Nurse et al., 1976). As cells accumulated in early G1 over 4 hours, Tos4-GFP signal disappeared, indicating that *tos4* expression depends on Cdc10, and thus the MBF complex (Figure 2.3). In contrast the Tos4-GFP signal can be readily observed in control cells with active MBF at 36.5°C (data not shown). A wild type strain with *tos4-GFP* had a normal cell size, generation time, and DNA content (data not shown). The fluorescent signal was seen in the nuclei of septated cells which are in S-phase and recently divided cells which are in S-phase and early G2 (Figure 2.1B). The smallest cell volume (per nucleus) was represented by the 90 fL

cohort which was already 60% labeled (Figure 2.1B, Table 2.IB). Labeling then gradually declined, in agreement with peak *tos4-GFP* transcription occurring immediately after mitosis. Thus Tos4-GFP levels oscillate in the normal cell cycle and appearance of the protein depends upon MBF. There was a peak in *wee1-50* cells at 75 fL; this smaller size was as expected, given that *wee1-50* cells replicate at a smaller size than wild type cells (Figure 2.1B, Table 2.IB). We conclude that the Tos4-GFP fusion can be used to monitor MBF-dependent gene expression and the cell size at which it occurs.

2.2.2. DNA synthesis and MBF-dependent gene expression in the *cdc13* switch-off strain

Cdc13 is the G2/M cyclin B which associates with the protein kinase Cdc2 to form the G2/M CDK in fission yeast cells. In the *cdc13* **s**witch-**o**ff (*cdc13* s/o) strain, the *cdc13* gene is under control of the thiamine-repressible *nmt41* promoter. Cdc2-Cdc13 CDK is depleted after thiamine addition leading to DNA synthesis in G2 cells (Fisher and Nurse, 1996; Hayles et al., 1994). Previous experiments with the *cdc13* s/o strain established that continued DNA synthesis in the absence of mitosis occurred most efficiently in cells which had been nitrogen starved, treated with thiamine, and then returned to growth medium in the presence of thiamine so that cells lack Cdc13 when they reach G2 (J. Hayles, personal communications) (Fisher and Nurse, 1996) (Materials and methods). During the subsequent 11 hours of growth, DNA content in the majority of cells increased from 2C to 32C. To determine if DNA synthesis occurred in discrete intervals that correlated with cell volume increase, samples were taken from the *cdc13* s/o *tk hENT* culture every hour and pulsed with BrdU.

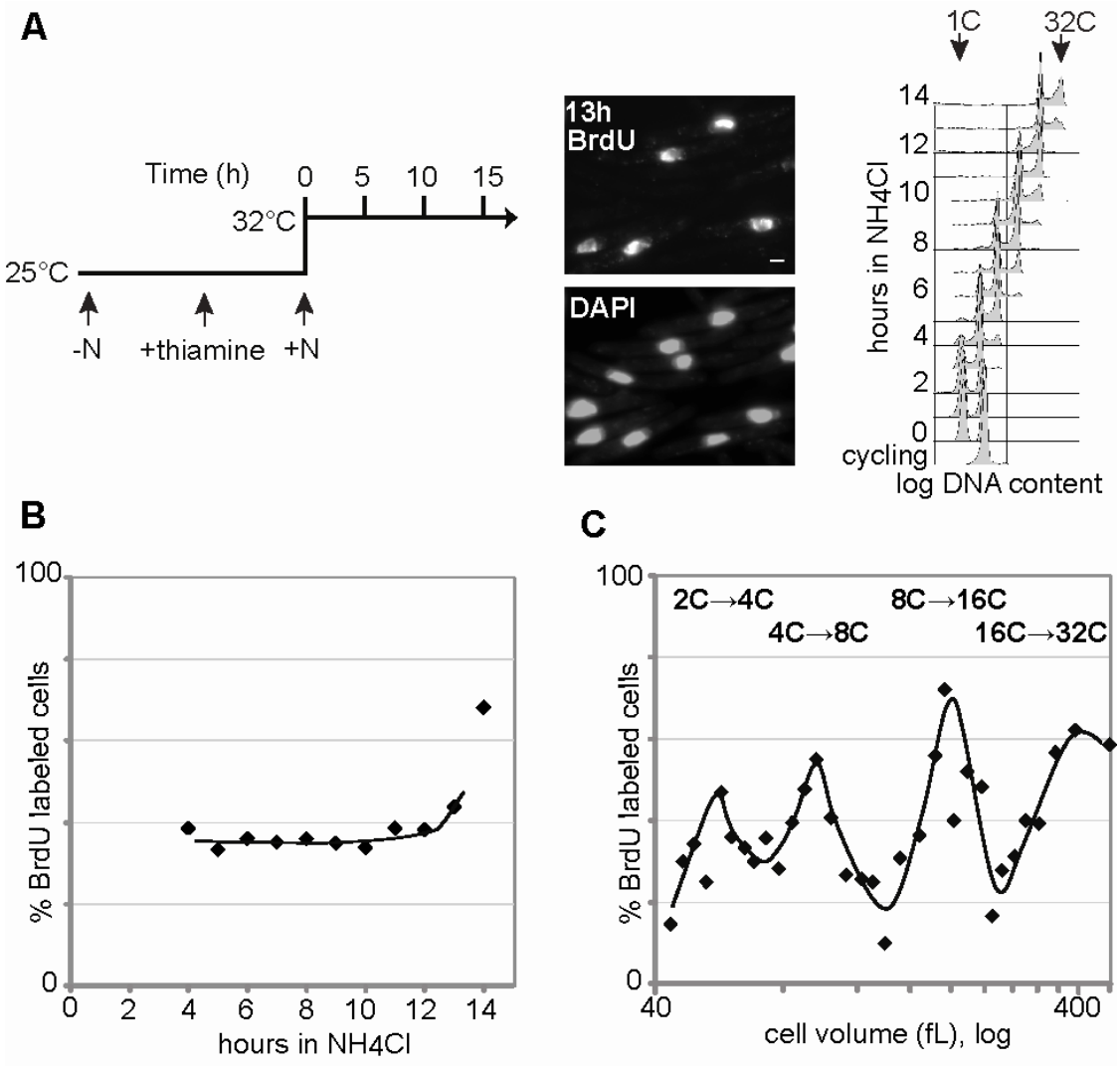

Figure 2.4 Periods of DNA synthesis correspond to cell volume doublings in *cdc13* switch-off

(A) BrdU pulse labeling of cells lacking Cdc13. An exponentially growing Δ*cdc13::ura4+ pREP45 cdc13+ ade6-704 adh1-hENT-leu1+ adh1-tk-his7+* culture was filtered and resuspended in media lacking nitrogen. After 8 hours, thiamine was added, and after an additional 12 hours, nitrogen was replenished and the culture shifted to 32°C. Cells depleted of the Cdc13 cyclin were pulse labeled with BrdU during a time course as cells underwent DNA doublings from 1C to 32C. DNA was visualized by DAPI staining and BrdU was detected by indirect immunofluorescence. Cells from 13 hours after replenishment of nitrogen are shown. The scale bar is 5μm long. **(B)** Percentage of BrdU-positive cells was plotted as a function of time **(C)** Cells of all sizes from all time points were pooled and binned according to fixed cell volume, and the percentage of cells with incorporated BrdU in each bin was plotted as a function of cell volume. Comparison of the cell size and FACS data from each time point (not shown) revealed that peaks in the percentage of BrdU-positive cells correspond to DNA doublings.

Cells from each time point were examined for BrdU incorporation into the nucleus (Figure 2.4A). The percentage of labeled cells remained essentially constant over time (Figure 2.4B) (Materials and methods). When cells from all time points were pooled and ordered according to volume similar to the assay in Figure 2.1A, three peaks of DNA synthesis and a partial fourth peak were revealed (Figure 2.4C). DNA synthesis peaked at fixed cell volumes of 50, 100 and 200 fL, with the partial fourth peak at 400 fL (Figure 2.4C, Table 2.1A). These data indicate that the *cdc13* s/o cells undergo discrete intervals of DNA synthesis in the absence of mitosis and do so periodically approximately with each cell volume doubling. Comparison of the cell size data (not shown) and FACS profile from each time point showed respectively that the peak at 50 fL corresponded to the transition from 2C to 4C, 100 fL to 4C-8C, 200 fL to 8C-16C and 400 fL to 16C-32C (Figure 2.4, Table 2.1A). These volumes are multiples of about 25 fL, close to the size of 28 fL at which cells lacking Wee1 activity undergo S-phase. We conclude that DNA synthesis is periodic and correlated to cell size doubling in the *cdc13* switch-off strain. The fact that re-initiation of DNA synthesis occurred roughly at multiples of the normal minimal size for S-phase suggests that dependence of initiation upon cell size increase is maintained.

To determine whether G1 to S-phase MBF-dependent gene expression was also periodic and accompanied the periodic DNA synthesis, we used the *cdc13* s/o strain containing the *tos4-GFP* marker. We first confirmed that Tos4-GFP was MBF-dependent in the absence of Cdc13 by inducing re-replication in a *cdc13s/o tos4-GFP* strain containing the *cdc10-v50* mutation. A re-replicating culture was shifted to 36.5°C and the Tos4-GFP signal was observed to disappear as cells blocked in G1; upon release

to 25°C Tos4-GFP reappeared demonstrating its dependence on MBF in re-replicating cells (Figure 2.5).

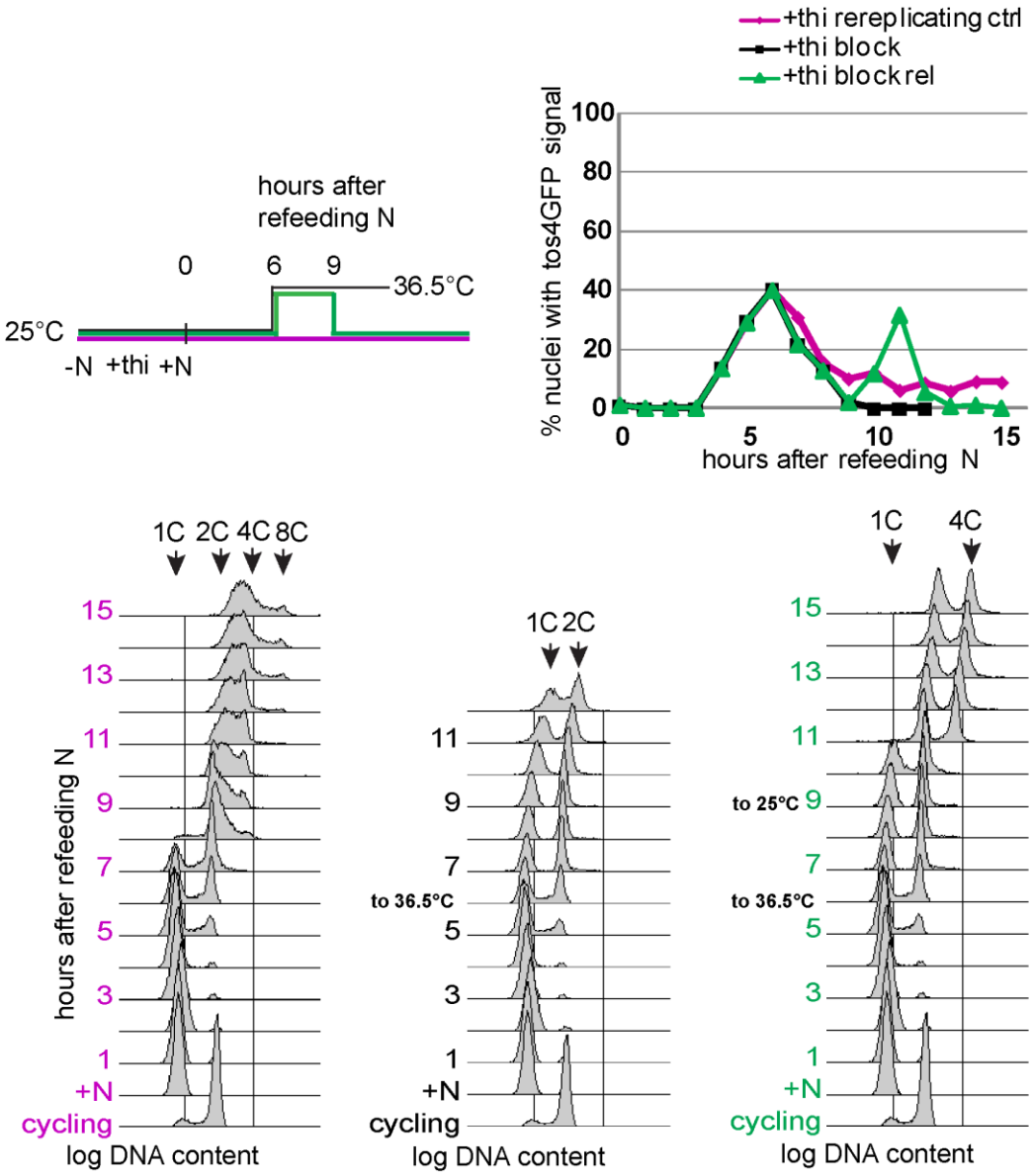

Figure 2.5 Tos4-GFP is cdc10 dependent in cdc13 s/o

Re-replication was induced by addition of thiamine (+thi) in a *cdc10-v50 Δcdc13::ura4+ pREP45 cdc13+ ade6-704 tos4-GFP-kanMx6* culture. At 6h after refeeding nitrogen, half the culture was shifted to 36.5°C for 3 hours (black line, block) while half continued to re-replicate at permissive temperature (purple line, control). At 9h, half of the blocked culture was released to 25°C (green line, block release). The percentage of nuclei with Tos4-GFP was determined at each time point.

During the experimental time course, nuclear Tos4-GFP appeared periodically during successive DNA doublings and four periods of nuclear Tos4-GFP signal coincided with the four DNA doublings (Figure 2.6, Table 2.1B). Therefore, there are periodic rounds of both DNA replication and G1/S transcription during the time course. These data also indicate that MBF-dependent gene expression does not require passage through mitosis. We conclude that in the *cdc13* s/o strain G1/S-type MBF-dependent gene expression is periodic, and that each round of DNA replication is associated with a period of gene expression. These characteristics indicate that a normal S-phase replication program is induced from G2 when the G2/M CDK is removed.

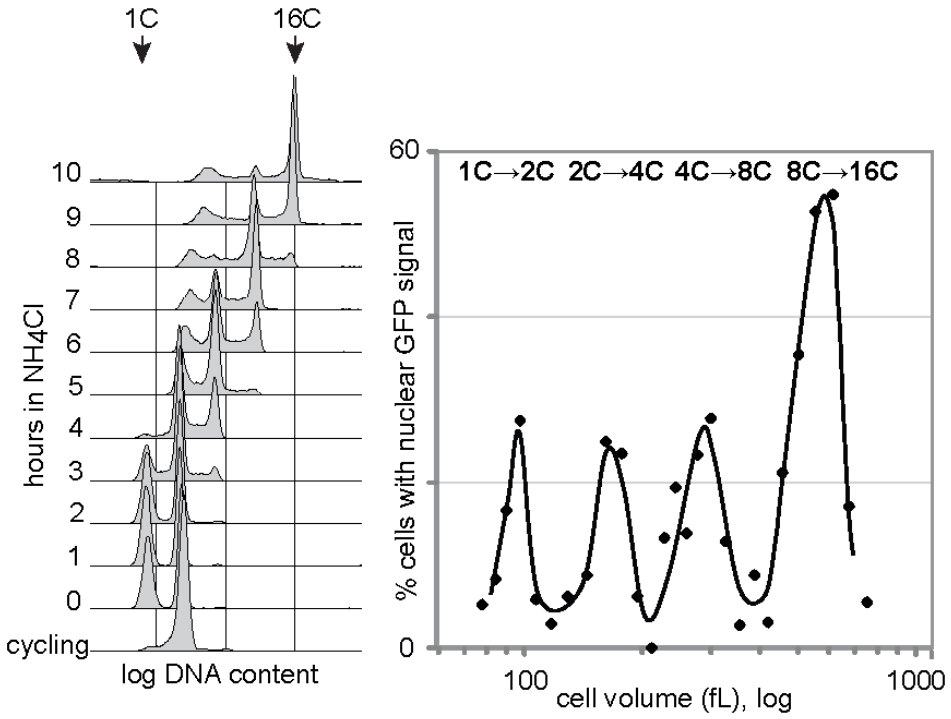

Figure 2.6 MBF-dependent gene expression is periodic in *cdc13* switch-off

Nuclear signal of Tos4-GFP in the absence of *cdc13*. Left panel: Δ*cdc13::ura4+ pREP45 cdc13+ ade6-704 tos4-GFP-kanMx6* cells depleted of Cdc13. DNA content increased to 16C. Right panel: The percentage of cells with strong nuclear GFP as a function of cell volume in femtoliters (fL).

2.3. DNA replication across the genome and replication origins

In a normal mitotic S-phase, the genome is uniformly replicated with no areas amplified relative to other regions, so there is an equal copy number of each portion of the genome. To determine whether equal rounds of replication or local amplification occurred in the *cdc13* s/o strain we assayed genomic DNA from cells which had increased their DNA content to 16C-32C. To measure the relative DNA content across the genome, we hybridized this genomic DNA against reference DNA from cell cycle-arrested cells to DNA microarrays. The signal for each microarray probe was then normalized to the median signal in the genome, yielding the relative signal ratio.. This experiment revealed that replication was essentially equal across the genome, with no region becoming significantly amplified to a higher copy number than any other (Figure 2.7). The only possible exceptions are regions very close to the telomeres where there are slight deviations from the self:self control (Figure 2.7). We conclude that although S-phase occurs in the absence of mitosis, replication is restricted to discrete and essentially full rounds of genome doubling. This establishes *cdc13* s/o as a system of endoreduplication wherein the genome is duplicated in complete rounds without mitosis as opposed to re-replication or amplification in which aberrant re-firing of origins leads to partial reduplication of the genome (reviewed in Arias and Walter, 2007; DePamphilis et al., 2006).

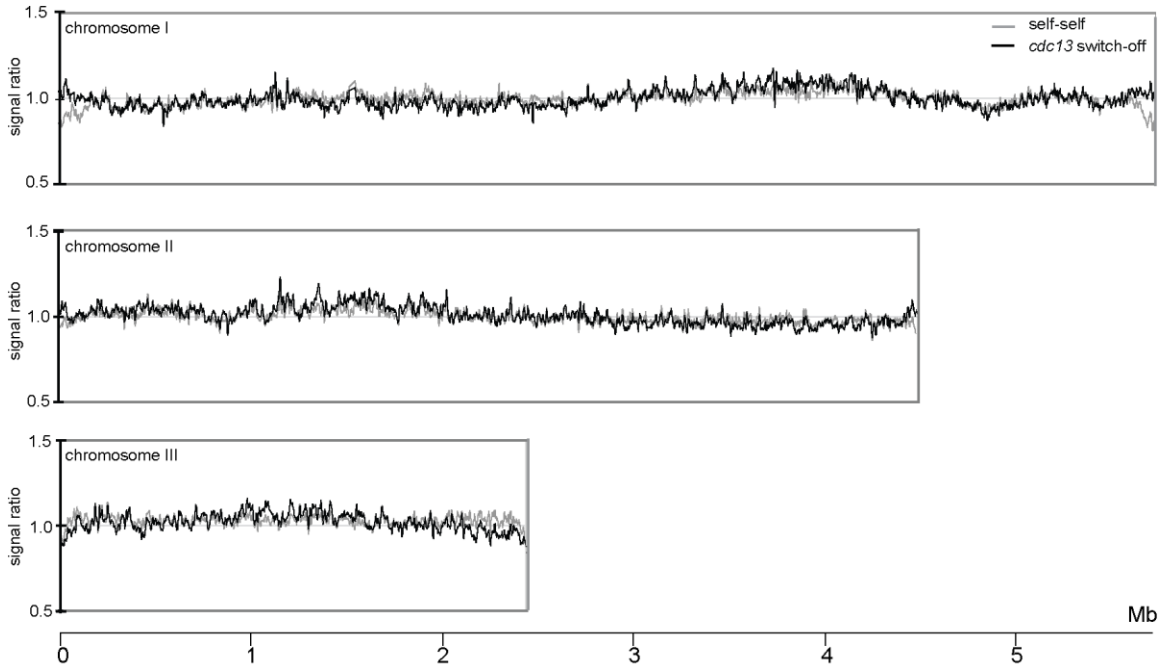

Figure 2.7 Equal replication across the genome in a *cdc13* switch-off strain

DNA from re-replicating cells which had attained 16 and 32C DNA contents in the absence of HU was hybridized against a reference to microarrays. Signal was normalized to the rest of the genome to find the relative signal ratio. Self-self is T0/T0, cdc13s/o is T8/T0.

Since the genome was found to be essentially evenly replicated as would be expected if each round of replication corresponded to a normal S-phase, we investigated whether this was the result of a normal replication program at the level of origin firing. We asked whether S-phase origins are used to reduplicate the genome, and whether origins are used with the same efficiency as in wild type cells. The replication origin profiles from the fission yeast wild type cell cycle have been identified in our previous study (Heichinger et al., 2006) using synchronous cell populations treated with **h**ydroxy**u**rea (HU) which confines DNA synthesis to the vicinity of origins (Materials and methods). We re-mapped the 904 mitotic S-phase origins (401 'strong' origins and 503 'putative weaker' origins described in Heichinger et al.), regarding origins within

clusters as distinct origins, and assigned each origin the highest signal ratio (normalized experimental/reference) value around the AT-rich island to which it maps (Appendix I) (Materials and methods).

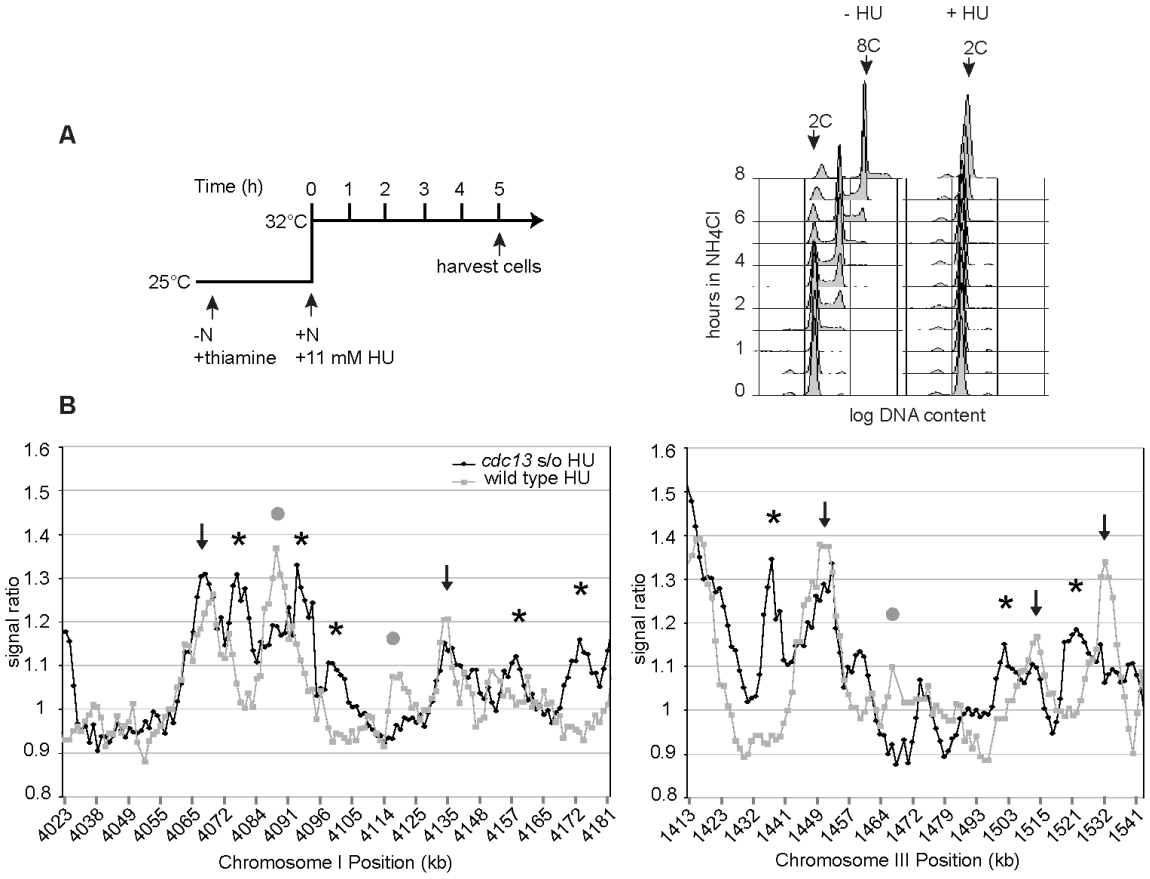

Figure 2.8 Replication origin usage in a *cdc13* cyclin switch-off

Mapping origins in endoreduplication of a *cdc13* cyclin switch-off mutant. **(A)** Left panel: Schematic of the *cdc13* cyclin switch-off time course experiment. Cells were nitrogen starved for 5 hours at 25°C in the presence of thiamine. Nitrogen was replenished and the culture shifted to 32°C, and 11 mM HU was added. Right panel: FACS analysis of the *cdc13* switch-off mutant, induced into endoreduplication with or without the addition of 11 mM HU. In the presence of HU, cells block at the onset of the first round of endoreduplication. In the absence of HU, cells undergo repeated rounds of replication without intervening mitoses. (**B**) Comparison of wild type and *cdc13* switch-off replication profiles from the average of two HU experiments. Examples of origins: arrows mark origins which are used in both a normal S-phase and in the *cdc13* s/o strain, grey circles mark normal S-phase origins not used in *cdc13* s/o, while asterisks mark new origins which are used only in the *cdc13* s/o strain. The regions were selected for illustration because they contain all three types of origins.

We identified the origins utilized in the first endoreduplication cycle of *cdc13* s/o using microarray analyses of cells treated with 11 mM HU. Samples were taken at 5 hours (Figure 2.8) when most cells of the culture not treated with HU had undergone a doubling in DNA content. Examples of the microarray profiles are given in Figure 2.8B for two regions of the genome, where peaks in the signal ratio can be observed which mark the locations of origins. These data are compared to data from wild type cells undergoing replication in a normal cell cycle to determine if the same origins are used.

A total of 799 origins were identified, a number just under the 904 identified in a normal S-phase (Table 2.2, Appendix I). Of these 799 origins, 697 are active in a normal S-phase and 102 are not used in a normal S-phase, while 207 normal S-phase origins are not fired in *cdc13* s/o (Table 2.3). Percentage AT content (Materials and methods) and intergenic length, both of which are known to be correlated with origin strength (Dai et al., 2005), did not differ on average among these groups (Tables 2.2, 2.3). The mean AT contents were similar between 72.1% and 74.0% (intergenic regions in the genome are ~70% AT on average (Dai et al., 2005; Segurado et al., 2003)), and the mean AT content for all origins activated in *cdc13* s/o was identical to that in S-phase (73.8%) (Table 2.2). The lengths of the intergenic regions in which the origins are embedded were also similar in inactive and active mitotic origins with average lengths ranging from 1349 to 1776 bp (average intergenic distance in the genome overall is 960 bp). As previously described, AT-rich sequences acting as replication origins are preferentially located in intergenic regions of divergent transcription (Segurado et al., 2003) which are longer than the average *S. pombe* intergene (Wood et al., 2002), and a similar bias was reflected in the wild type and *cdc13* s/o origins. We also found that there was no correlation of activated

or suppressed origins with loci of cell cycle regulated genes. Although many of the same origins were used, their efficiency in *cdc13* s/o was not well correlated to wild type efficiency (R^2 value of 0.3). We conclude that origins used in *cdc13* s/o are mostly similar to those of a normal S-phase, although with changes in efficiency.

Table 2.2. Origins used in mitotic S-phase and in endoreduplication of *cdc13* s/o

Replication program	No. of origins	Mean AT content (%)	Mean intergenic distance (bp)	Mean mitosis efficiency (%)
mitotic S-phase	904	73.8	1678	17.6
cdc13 s/o	799	73.8	1737	18.4[a]

For definitions of all parameters, see Materials and methods

[a] not including the additional origins which do not fire in the mitotic cell cycle

Table 2.3. Categories of origins according to usage in endoreduplication

	No. of origins in category	Mean AT-content (%)	Mean intergenic distance (bp)	Mean mitosis efficiency (%)	Mean *cdc13* s/o efficiency (%)
Mitotic origins used in *cdc13* s/o	697	74.0	1776	18.4	13.8
Non-mitotic origins used in *cdc13* s/o	102	72.1	1470	n/a[a]	18.1
Mitotic origins not used in *cdc13* s/o	207	73.2	1349	14.9	n/a[b]
Genome average		70[c]	960[d]		

Parameters are defined in Materials and methods.

[a] these origins do not fire in mitotic S-phase, so there is no mitosis origin efficiency

[b] these origins do not fire in *cdc13* s/o, so there is no *cdc13* s/o origin efficiency

[c] refers to all intergenes, genome-wide (Dai et al., 2005; Segurado et al., 2003)

[d] refers to all intergenic regions in the genome, regardless of origin activity

We examined whether the new origins activated in *cdc13* s/o were sites on the chromosome where PreRCs assemble. The new origins mapped were compared with the previously reported genome-wide localization of Orc4, a component of the PreRC, in G1 (Hayashi et al., 2007) (Appendix I). We devised a script to search the Hayashi et al. data set for Orc4 localization in the vicinity of our origins using two signal ratio thresholds (Materials and methods). With the lower threshold 96% of the 401 strong origins reported in Heichinger et al. had Orc4 localization, and 69% of the 503 weaker origins reported here were colocalized with Orc4. These values should be compared with 74% of the 102 c*dc13* s/o-activated origins which were colocalized with Orc4. Applying a higher threshold similar to Hayashi et al. (Materials and methods), 92% of the strong wild type origins colocalized with Orc4, while 50% of the activated *cdc13 s/o* origins and 50% of weaker wild type origins showed Orc4 binding. We conclude that the extent of Orc4 binding (reflecting PreRC formation) to the new origins activated in *cdc13* s/o was similar to the weaker normal S-phase origins but less than to the stronger normal S-phase origins.

2.4. The endocycling induced by G2/M CDK depletion may be driven by G1/S CDK oscillation

Since we observe periodic G1/S gene expression and S-phases in the absence of mitosis in *cdc13* s/o, we considered what might drive this endocycling. The MBF-dependent G1/S cyclin Cig2 is one candidate factor. Cig2-associated Cdc2 phosphorylates Res1 to inhibit MBF, constituting an autoregulatory negative feedback loop (Ayté et al., 2001). The role of Cig2 in endoreduplication is unclear, as previous reports are conflicting: Mondesert et al. (1996) found that Cig2 was necessary for re-

replication in germinating spores deleted for *cdc13*, while Fisher et al. (1996) found that a single DNA doubling occurred after a delay in *Δcig2 cdc13* s/o. Both studies agreed that a second G1/S cyclin Cig1 was dispensable for re-replication. To address these possible outcomes over a longer time course to detect any additional increases in DNA content and with higher temporal resolution, we created *cig1* and *cig2* deletions in the *cdc13* s/o background used for this study.

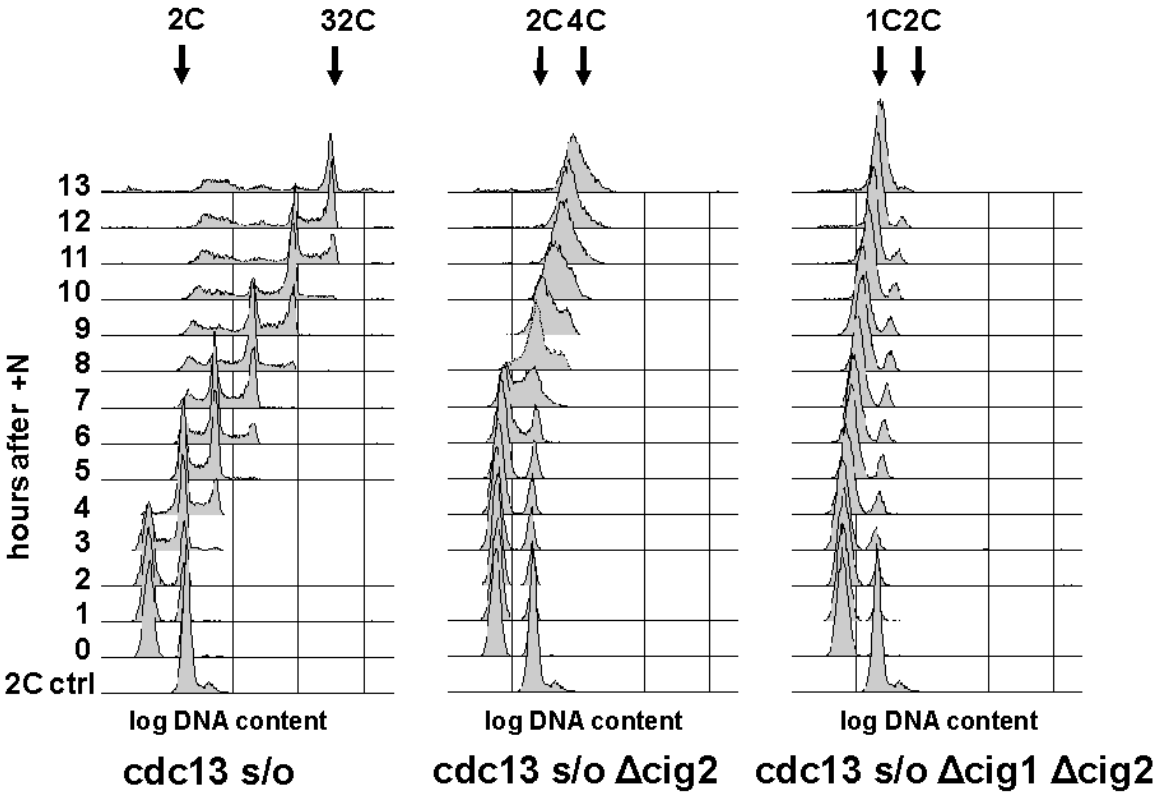

Figure 2.9 *cdc13* s/o overreplication is attenuated in the absence of *cig2* and abolished in the absence of *cig1* and *cig2*. Re-replication was induced in cycling cultures of Δ*cdc13::ura4+ pREP45 cdc13+ ade6-704,* Δ*cdc13::ura4+ pREP45 cdc13+ ade6-704* Δ*cig2::ura4+,* and Δ*cdc13::ura4+ pREP45 cdc13+ ade6-704* Δ*cig2::ura4+* Δ*cig1::ura4+*. Cultures were sampled at each hour after replenishing nitrogen and fixed in ethanol for FACS analysis.

When *cig2* alone was deleted, one round of overreplication occurred after a delay (Figure 2.9). Deletion of both *cig1* and *cig2* abolished endoreduplication in *cdc13* s/o. Our preliminary data indicate that endoreduplication is not affected by deletion of *cig1*, in agreement with both previous studies (Fisher and Nurse, 1996; Mondesert et al., 1996). Our results suggest that, consistent with Fisher et al., Cig2 is necessary for periodic cycles of endoreduplication. In the absence of *cig2*, the remaining CDK activity which may be provided by Cig1 is not sufficient to drive endoreduplication cycles beyond a single DNA doubling. This could be due to the following reasons: (1) Cig1 provides insufficient levels of CDK activity for cycling, and/or (2) Cig1 levels do not oscillate since it does not participate in the same feedback loops as Cig2. Cig2 participates in feedback loops with MBF as discussed above and with the CDK inhibitor Rum1 (Figure 2.10), whose influence will be investigated in the next section.

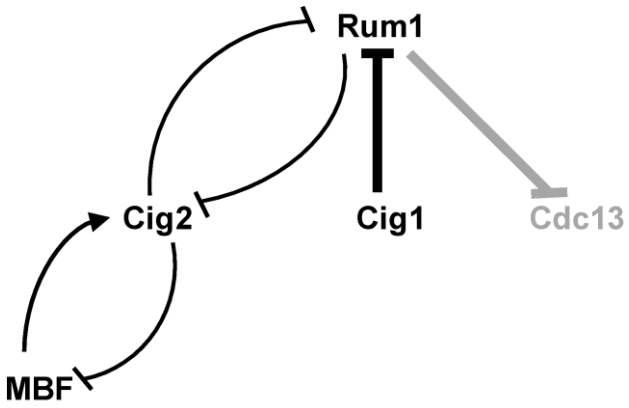

Figure 2.10 Cig2 interacts with MBF and Rum1 via feedback loops

Arrowhead denotes positive interaction; blunt end denotes inhibition. Line thickness represents relative strength of inhibition. Lines connecting with Cdc13 are shown in grey to signify Cdc13 depletion in *cdc13* s/o. (Ayté et al., 2001; Benito et al., 1998; Correa-Bordes et al., 1997; Correa-Bordes and Nurse, 1995)

2.4.1. Deletion of *rum1*, inhibitor of the Cig2-Cdc2 CDK, attenuates re-replication

To further assess the roles of Cig1 and Cig2 in endocycling, the Cig2-Cdc2 inhibitor *rum1* was deleted. When endocycling was induced, bulk DNA content increased to 4C, so the absence of *rum1* also attenuates re-replication (Figure 2.11). In the absence of inhibition by Rum1, increased Cig2-Cdc2 CDK activity may inhibit further rounds of endoreduplication beyond the 2C to 4C doubling. In support of this model, constitutive nmt1 overexpression of *cig2* or its transcription factor *cdc10* in the *cdc13* s/o background has been reported to abolish overreplication (Lopez-Girona et al., 1998) (J. Hayles, personal communication). It is possible that (1) CDK activity is too high to permit PreRC re-assembly, and/or (2) in the absence of Rum1 and its associated feedback loop, Cig2-Cdc2 CDK activity does not oscillate. Both lack of the cyclin (Cig2) and cyclin-Cdc2 inhibitor complex (Rum1) similarly attenuate re-replication though the former is expected to decrease CDK activity and the latter to increase it. We speculate that rather than simply the presence of the Cig2 cyclin, the level of CDK activity and its periodicity may be important for the ability to endocycle. Evidence from other organisms supports this concept. In *Drosophila*, evidence suggests that there must be an oscillation of the equivalent cyclin E for physiological endocycles to occur (Follette et al., 1998; Lilly and Spradling, 1996; Sauer et al., 1995). To induce endoreduplication, it seems to be necessary to first maintain CDK activity within a range low enough to allow PreRC factor binding and high enough to bring about S-phase but not mitosis, and then for the level of activity to oscillate within this range allowing PreRC assembly to occur periodically.

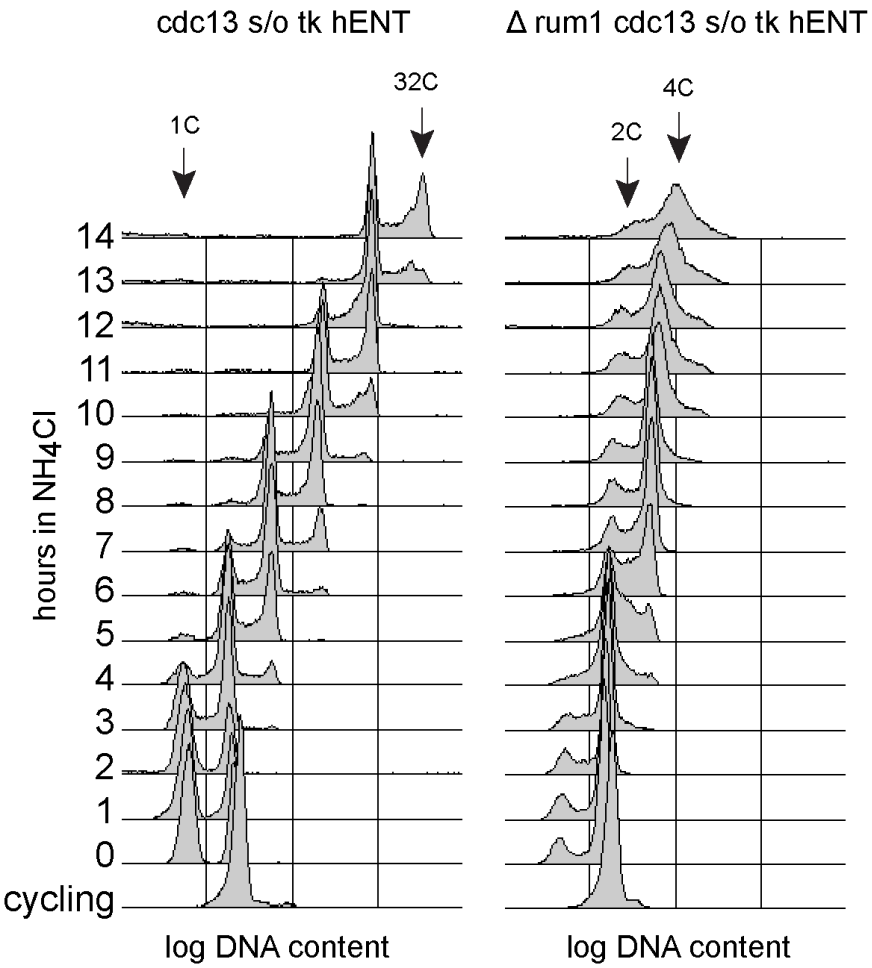

Figure 2.11 Lack of *rum1* attenuates re-replication in *cdc13* s/o

Overreplication was induced in Δ*cdc13::ura4+ pREP45-cdc13+ ade6-704* and Δ*cdc13::ura4+ pREP45-cdc13+ ade6-704* Δ*rum1:: kanMX6* cultures. Cultures were sampled at each hour after replenishing nitrogen and fixed in ethanol for FACS analysis.

2.5. Discussion

We have shown that in the absence of G2/M CDK, DNA synthesis and the accompanying G1/S transcriptional program are periodic and coordinated with cell volume increase at approximate multiples of the minimum cell size for the G1/S

transition. Most of the origins used are also utilized in a normal mitotic S-phase, although some cryptic origins are activated, mostly at sites of normal PreRC formation, and there are changes in origin efficiency compared with a normal S-phase. We have also shown that the entire genome is essentially equally replicated.

Given these results, we propose that each period of DNA synthesis largely corresponds to a complete round of DNA replication as observed in a mitotic cell cycle. In the normal cell cycle, CDK activity decreases as cells exit mitosis due to destruction of Cdc13, sending cells into G1 of a new cycle. Here, by switching off *cdc13* in G2, G2/M CDK activity is decreased to a level at which cells are unable to undergo mitosis while inhibition of S-phase is lost. Rather than undergo aberrant unprogrammed DNA synthesis, cells progress through an abbreviated cycle, returning to a G1-like state. They then re-enter a normal G1/S program and carry out S-phase. Reducing the level of CDK activity resets the cell cycle into endoreduplication, emphasizing CDK as a major cell cycle regulator important for maintenance of ploidy. What could drive periodic G1/S gene expression and S-phases in the absence of a normal cell cycle? The cyclin Cig2 is one candidate because it participates in a feedback loop with MBF (Figure 2.10) (Ayté et al., 2001). Our data and other studies suggest that Cig2 oscillation may be necessary for periodic endoreduplication in *cdc13* s/o and may drive oscillation of other MBF-dependent genes required for S-phase (Fisher and Nurse, 1996; Lopez-Girona et al., 1998; Mondesert et al., 1996; Wuarin et al., 2002). In addition, we have found that the extent of re-replication is attenuated and periodicity of endoreduplication may be abolished in the absence of *rum1*. Cig2 participates in a second negative feedback loop with Rum1, wherein the Cig2-Cdc2 complex is both inhibited by Rum1 and inhibits it via

phosphorylation, though the Cdc2-Cig1 complex is thought to play the predominant role in inhibiting Rum1(Benito et al., 1998). The oscillation of CDK activity due to Cig2 which links these two feedback loops may drive the periodic S-phases in *cdc13* s/o.

Cdc13 s/o cells replicate the genome in complete rounds, maintaining the characteristic that each part of the genome is replicated only once per S-phase. Nearly all origins used to replicate the genome in the first reduplication cycle are S-phase origins (87%), and the total number of origins is reduced but is roughly similar at 799 compared to 904 in wild type S-phase. Mitotic S-phase origins were used at slightly lower mean efficiency in endoreduplication compared with a normal S-phase (~13.8% vs ~18.4%), while the newly activated origins were used at 18.1% efficiency. These results are consistent with the view that there is a limited potential to activate a subset of potential origins or assembled PreRCs in S-phase (Dai et al., 2005; Hayashi et al., 2007; Lygeros et al., 2008; Patel et al., 2008). The program of origin usage may differ when cells are replicating from G2, perhaps because gene products normally present in S-phase are absent, or because chromatin has not been condensed by an intervening M-phase. We have found that during a normal S-phase Orc4 localizes to a significant number of the origins that are newly activated in the *cdc13* s/o strain, suggesting that PreRCs form at many of the sites which can be activated during endoreduplication. Finally, we have shown that although the efficiencies of individual origins differ, the net outcome is a complete round of replication.

Similar to fission yeast, endocycles of *Drosophila melanogaster* ovarian follicle cells show periodic BrdU incorporation. Nearly the whole genome is replicated per round of DNA synthesis, and the increase in ploidy is correlated with cell volume

increase (Calvi et al., 1998; Edgar and Orr-Weaver, 2001; Maines et al., 2004). The transition from mitosis to endocycling is brought about by inhibition of M-phase promoting CDK activity (Shcherbata et al., 2004), and periodic rounds of DNA synthesis in follicle cells rely on fluctuation of the G1/S cyclin-CDK complex (Follette et al., 1998; Lilly and Spradling, 1996; Sauer et al., 1995).

While in *Drosophila*, the decrease in mitotic CDK activity is accomplished by downregulation of String/Cdc25 and cyclins, in mammals it is mediated by upregulation of CDK inhibitors (CKIs). In the physiological transition triggering differentiation of trophoblast stem cells into endocycling trophoblast giant cells, the CKIs are p21 and p57 (Ullah et al., 2008). p57 is unique to mammals and oscillates during trophoblast endocycling. Endoreduplication can also be induced in trophoblast stem cells by addition of the drug RO3306 which inhibits CDK1 activity (Ullah et al., 2008) and in human cell lines by expression of a conditional CDK1 (Itzhaki et al., 1997). The degree of mitotic CDK inhibition seems to be critical for endocycling, since in the absence of p57, trophoblast cells progress through mitosis to become multinucleated (Ullah et al., 2008). Interestingly, this resembles the physiological endomitosis of megakaryocytes where CKIs p21 and p27, but not p57, are active and nuclei undergo cycles of G, S and partial M-phases, resulting in a multilobulated polyploid nucleus (Baccini et al., 2001; Kikuchi et al., 1997). The level of CDK activity and its oscillations appear to have a well-conserved role in determining patterns of endoreduplication across species. We conclude that more generally in eukaryotes G2/M CDK activity restricts S-phase to once per cell cycle, and its absence leads to endoreduplication with repeated S-phases in the absence of mitosis.

Chapter 3

DISTINCT FEATURES OF REPLICATION ORIGINS CAN PROMOTE LOCAL DNA AMPLIFICATION IN FISSION YEAST

3.1. Introduction

Faithful transmission of the genome requires that there is one S-phase per cell cycle so re-initiation cannot occur in G2, and that within each S-phase the genome is evenly replicated. In the previous chapter, we addressed the block to re-initiation in G2. We now turn to equal replication of the genome in S-phase.

To ensure equal replication of the genome in every eukaryotic cell cycle, replication origins fire only once each S-phase or do not fire after passive replication (reviewed in Arias and Walter, 2007). Failure in these controls can lead to local amplification (Calvi et al., 1998) which could contribute to genome instability and the development of cancer (Schimke et al., 1986; Varshavsky, 1981). To identify features of replication origins important for such amplification, we have investigated origin firing and local genome amplification in the presence of excess helicase loaders Cdc18 and Cdt1 (Gopalakrishnan et al., 2001; Mickle et al., 2007; Nishitani et al., 2000; Nishitani and Nurse, 1995; Yanow et al., 2001). We find that S-phase controls are attenuated and coordination of origin firing is lost, resulting in local amplification. Specific origins are necessary for amplification but act only within a permissive chromosomal context. Origins associated with amplification are highly AT-rich, fire efficiently and early during mitotic S-phase, and are located in large intergenic regions. We propose that these

features predispose replication origins to re-fire within a single S-phase, or to remain active after passive replication.

Cdc6 and Cdt1 are components of the Pre-Replicative Complex (PreRC) (Hartwell, 1973; Hofmann and Beach, 1994; Kelly et al., 1993; Liang et al., 1995) that bind at replication origins and recruit the MCM complex, the likely replicative helicase (Labib et al., 2000; Tanaka et al., 1999; Zou and Stillman, 2000). It was known that in fission yeast overexpression of the *CDC6* homologue *cdc18* in G2 induces re-initiation of DNA synthesis up to approximately 8-16C DNA content (Nishitani and Nurse, 1995). Co-overexpression with *cdt1* (*cdc18 cdt1* co-oe) enhances this phenotype so that DNA content both increases more rapidly and attains a higher level of approximately 32C DNA content (Gopalakrishnan et al., 2001; Nishitani et al., 2000; Yanow et al., 2001). In these cells, the S-phase controls ensuring that an origin fires no more than once per round of replication may be abrogated, since overexpression of a *cdc18* phosphorylation-site mutant brings about some local amplification, particularly at the telomeres (Mickle et al., 2007). Therefore we asked whether genome-wide coordination of origin firing is lost in *cdc18 cdt1* co-oe leading to local amplification, and if so what replication origin features might be responsible for that amplification.

3.2. Continuous DNA synthesis in *cdc18 cdt1* co-overexpression

To analyze the pattern of DNA synthesis in the presence of excess Cdc18 and Cdt1, we pulse-labeled cells with BrdU (Sivakumar et al., 2004) as cells increased their DNA content from 2C to 32C, equivalent to 4 DNA doublings (Nishitani et al., 2000; Yanow et al., 2001) (Figure 3.1). For co-overexpression of *cdc18* and *cdt1* from G2, these genes have been placed under control of the thiamine-repressible *nmt1* promoter

(Nishitani et al., 2000; Yanow et al., 2001). *Cdc18 cdt1* co-overexpressing cells containing *tk* and *hENT* were blocked in G2 at 36.5°C using the temperature sensitive *cdc25-22* mutation (Fantes, 1979) while thiamine was removed from the culture to derepress overexpression of *cdc18* and *cdt1*. By 2.5 hours (Figure 3.1A), the majority of cells were in G2 with some beginning DNA synthesis, and between 3.5 and 5.5 hours, the majority of cells increased their DNA content from 2C to 32C. Beginning at 2.5 hours, cells were BrdU pulse labeled and fixed for analysis every 30 minutes. The proportion of cells undergoing DNA synthesis gradually increased from 3 hours onwards reaching nearly 100% at 5 hours (Figure 3.1B). When cells were ordered according to cell volume (Kiang et al., 2009) no peaks in DNA synthesis were observed (Figure 3.1C). Therefore DNA synthesis appears to be continuous and there is no correlation between re-initiation of individual rounds of DNA replication and attainment of a critical cell volume, as we had found in cells depleted of the G2/M CDK (Kiang et al., 2009).

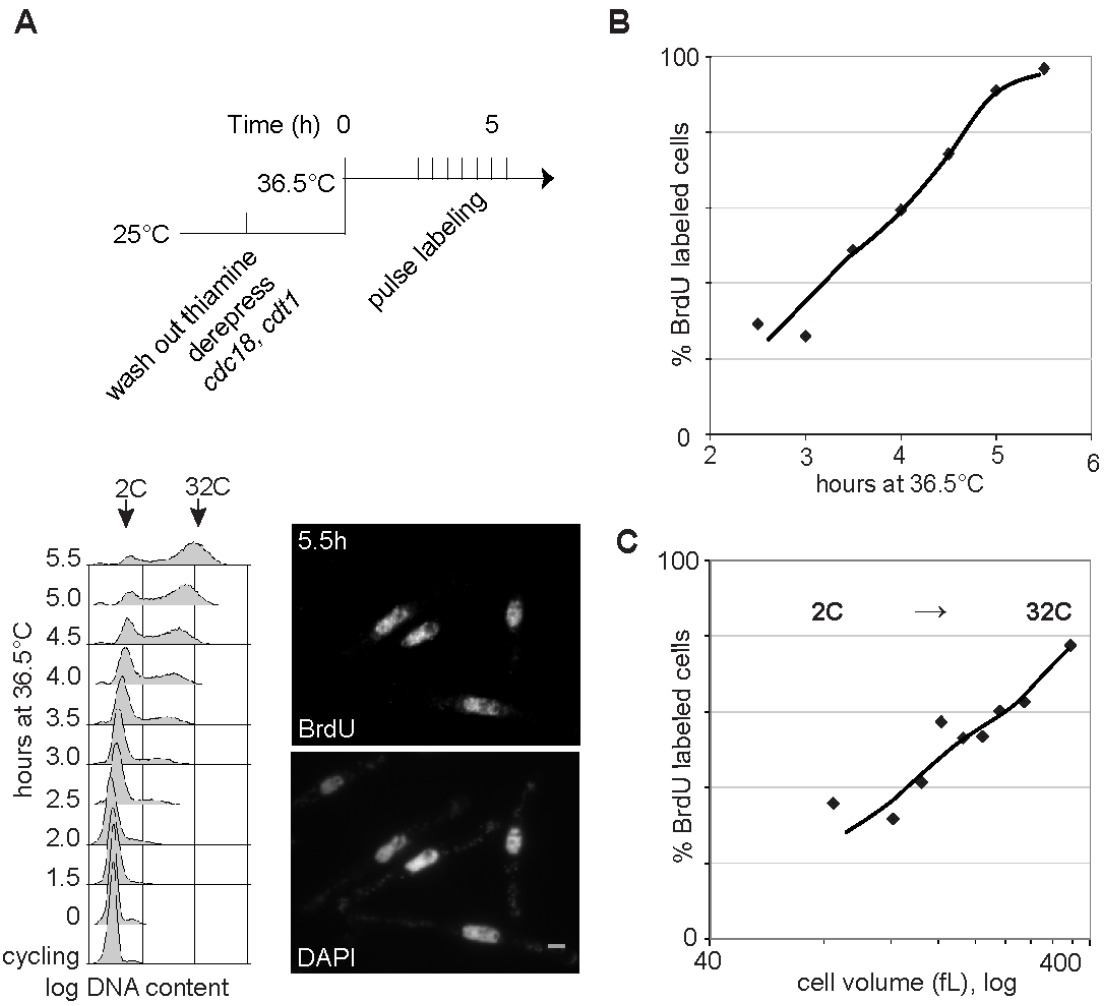

Figure 3.1 DNA synthesis is continuous in *cdc18 cdt1* co-overexpression

(A) BrdU pulse labeling of re-replicating G2 cells co-overexpressing *cdc18* and *cdt1*. Top panel: depletion of thiamine allows co-overexpression of *cdc18* and *cdt1* which are under control of the strong thiamine-repressible promoter nmt1. BrdU pulses were performed from 2.5 hours after temperature shift onwards. Bottom left: During the time course, cells increased in DNA content from 2C to about 32C. Bottom right: DNA was visualized by DAPI staining and BrdU was detected by indirect immunofluorescence. Cells from 5.5 hours after shift to 36.5°C are shown. The scale bar is 5μm long. **(B)** Percentage of BrdU-positive cells was plotted as a function of time **(C)** Cells from all time points were binned according to fixed cell volume, and the percentage of cells with incorporated BrdU in each bin was plotted as a function of fixed cell volume (Kiang et al., 2009).

3.3. DNA synthesis in *cdc18 cdt1* co-overexpression is not MBF-dependent

Next we determined if G1/S Mlu1 cell cycle box Binding Factor (MBF)-dependent transcription was associated with the DNA doublings. Normally, transcription of *cdc18* and *cdt1* in the cell cycle is mediated by MBF which ensures that Cdc18 and Cdt1 can act at the G1/S transition (Kelly et al., 1993; Rustici et al., 2004). We monitored MBF-dependent gene expression via the MBF-dependent gene product Tos4 fused to GFP (Kiang et al., 2009; Rustici et al., 2004). No Tos4-GFP signal was observed during re-replication although it was easily detected in a wild type control (data not shown). We conclude that *cdc18 cdt1* co-oe does not show characteristics of repeated, periodic S-phases requiring MBF gene expression, but rather induces an extended period of continued DNA synthesis in the absence of MBF expression, resulting in approximately 4 doublings in DNA content.

3.4. Genome-wide coordination of origin firing is reduced in the presence of excess helicase loaders

We next asked whether normal S-phase origins of replication were being used to replicate the genome and whether they fired in a coordinated fashion. First, we mapped the origins which become activated in *cdc18 cdt1* co-oe. Overreplication was induced, DNA content increased from 2C to 32C between 17 and 20h, and in a parallel culture, HU was added to inhibit fork progression (Figure 3.2A). Samples were taken at 18h from the HU culture by which point DNA content had increased beyond 8C equivalents in the cultures lacking HU. DNA content in the vicinity of fired origins was estimated using genomic **o**pen **r**eading **f**rame (ORF) and intergenic DNA microarrays (Figure

3.2B). Examples of the microarray profiles are given in Figure 3.2B for two segments of the genome with peaks in the signal ratio marking the location of origins. These data are overlaid with equivalent data from wild type cells undergoing normal replication.

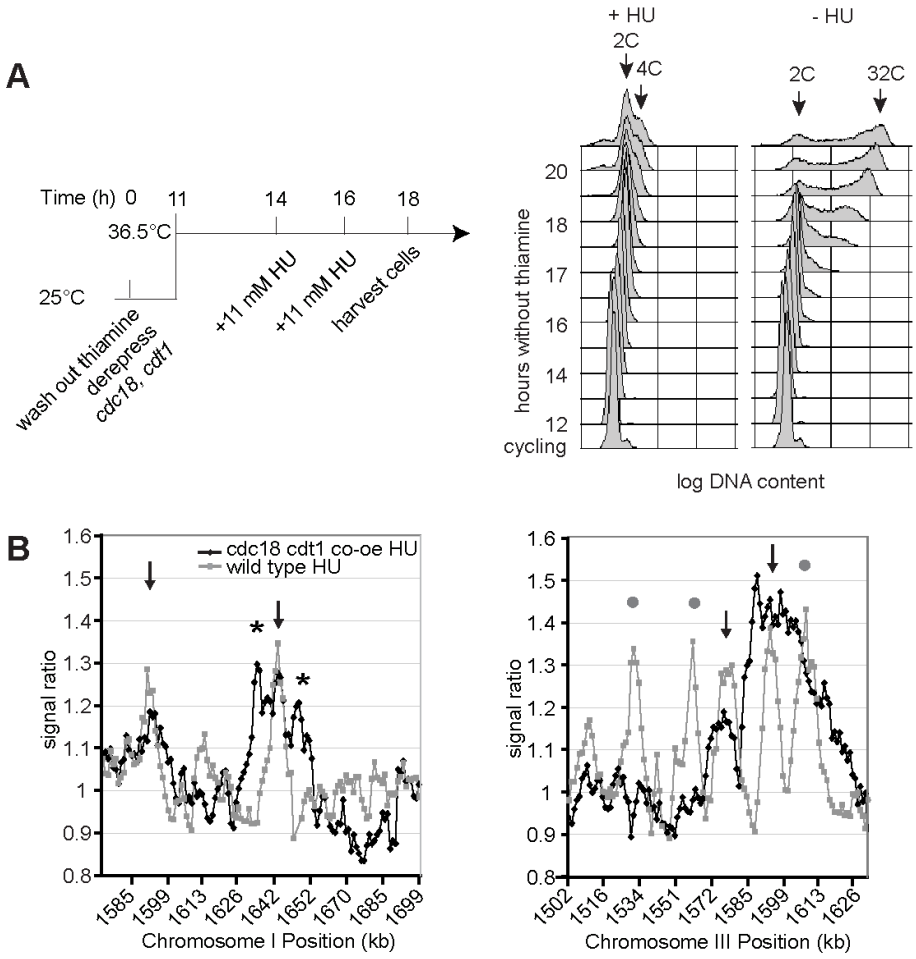

Figure 3.2 Mapping origins in re-replication of a *cdc18 cdt1* co-overexpression strain

(a) Left panel: Schematic of the *cdc18 cdt1* co-oe time course experiment. Thiamine was depleted and the culture was shifted to 36.5°C. HU was added to prior to the onset of re-replication. Samples for origin mapping were collected at 18h when the culture without HU had replicated to ~8C. (Right panel: FACS analysis) **(b)** Comparison of a wild type and the *cdc18 cdt1* co-oe replication profile, each calculated from the average of two HU experiments. (↓) origins used in both a normal S-phase and in the *cdc18 cdt1* co-oe strain, (●) normal S-phase origins not used in *cdc18 cdt1* co-oe, (*) new origins which are used only in the *cdc18 cdt1* co-oe strain. Regions from chromosomes I and III were selected to illustrate all three types of origins.

We identified 796 origins that fired in *cdc18 cdt1* co-oe (Appendix I, Tables 3.1, 3.2). In comparing origins activated in *cdc18 cdt1* co-oe versus normal mitotic S-phase, we distinguished three classes: origins that fire in both (683 of 904 S-phase origins), origins that fire in *cdc18 cdt1* co-oe but not S-phase (113), and origins that fire in S-phase but not *cdc18 cdt1* co-oe (221 of 904 normal S-phase origins) (Tables 3.1, 3.2). The different classes of origins were similar with regard to mean AT content and intergenic size, features which are correlated with the ability to act as an autonomously replicating sequence on a plasmid (Dai et al., 2005), mean efficiency of origin usage in a normal S-phase, and co-localization with sites of PreRC assembly in G1 (Hayashi et al., 2007). The only difference was that the 221 origins not activated were about half as efficient as the average origin in a normal S-phase (Table 3.2). We conclude that the majority of origins activated in *cdc18 cdt1* co-oe are also active or potential origins in a normal S-phase, although some less efficient S-phase origins are not activated.

The origins were named as follows: each origin was numbered using the format xxxx.x.x. The first four digit number represents the 401 ‘strong‘ origins mapped in (Heichinger et al., 2006). The second number describes the order of the 503 ‘weaker‘ origins which fall between strong origins. The third number denotes additional origins not activated in mitotic S-phase by their position between S-phase origins and ends with “r” for **r**e-replication. All 401 strong origins mapped in (Heichinger et al., 2006) have the suffix 0.0.

Table 3.1 Origins used in mitotic S-phase and in *cdc18 cdt1* co-overexpression

Type of DNA synthesis	Number of origins	Mean AT content (%)	Mean mitotic efficiency (%)	Mean intergenic size (bp)
Mitotic S-phase	904	73.8	18	1678
cdc18 cdt1 co-oe	796	73.8	19.7[a]	1684

[a] not including the additional origins which do not fire in the mitotic cell cycle

Table 3.2 Categories of origins according to usage in re-replication

	Total oris in group	Mean AT-content (%)	Mean mitotic efficiency (%)	Mean Intergenic size (bp)	Co-localized with PreRC[a] (%)
Mitotic oris used in *cdc18 cdt1* co-oe	683	74.1	19.7	1732	82
Non-mitotic oris used in *cdc18 cdt1* co-oe	113	72.2	n/a[b]	1397	73
Mitotic oris not used in *cdc18 cdt1* co-oe	221	73.0	10.9	1522	79
Mitotic oris centered within amplification peaks[c]	9	81.0	48.1	5269	100
Genome average		70[d]		960[d]	

[a] based on data of (Hayashi et al., 2007) using threshold 0.5, see Materials and Methods

[b] these origins do not fire in mitotic S-phase, so there is no mitosis origin efficiency

[c] subset of 683 mitotic oris used in *cdc18 cdt1* co-oe

[d] refers to all intergenes, genome-wide (Dai et al., 2005; Segurado et al., 2003)

Next, we investigated whether controls that ensure origins fire only once per round of DNA replication were still operative. We analyzed genomic DNA from cells at ~32C (equivalent to 4 rounds of replication) using ORF arrays, normalizing to the median signal ratio (Figure 3.3). If replication were equal across the genome, as in endoreduplication in the absence of the G2/M CDK (Figure 2.7) (Kiang et al., 2009), the relative signal ratio would be uniform across the genome with no large peaks above the baseline signal ratio of one. In *cdc18 cdt1* co-oe, there were 9 regions which were consistently amplified from 1.6-fold to 4-fold over baseline, indicating that although the genome had been fully replicated several times, equal replication across the genome per doubling in DNA content was not maintained (Figure 3.3). To determine whether a similar pattern would be observed if only one factor was overexpressed we performed the equivalent experiment in *cdc18* overexpression alone. We compared the regions that become amplified in *cdc18* overexpression versus *cdc18 cdt1* co-overexpression. Although the peaks are diminished in the strain overexpressing *cdc18* alone, it can be seen that they largely correspond in the two strains (Figure 3.3); some of these regions are also amplified to a low amplitude in overexpression of a non-phosphorylatable mutant form of *cdc18* (Mickle et al., 2007). The remaining 92% of the genome fell between signal ratio 0.5-1.5, indicating that the majority of the genome was equally replicated roughly 16-fold through the four doublings in DNA content. We conclude that during the extended DNA synthesis induced by *cdc18 cdt1* co-oe, the majority of origins do not re-fire within a round of replication but the 9 amplified regions must contain origins which escape this control.

Figure 3.3 Uneven replication across the genome after *cdc18 cdt1* co-overexpression

Re-replication was induced from G2 in cells overexpressing *cdc18* or both *cdc18* and *cdt1*. Genomic DNA from cells which had attained about 32C DNA content in the absence of HU was hybridized against a reference to open reading frame (ORF) microarrays. Signal was normalized to the rest of the genome. A 3-point moving average from the mean of two replicates is shown. Peak amplitudes can vary across experiments but the relative heights of peaks are maintained. The nine regions selected for further analysis were consistently >1.6 relative signal ratio over all experiments are numbered in **(A)** and labeled with the name of the origin centered under the peak in **(B)**.

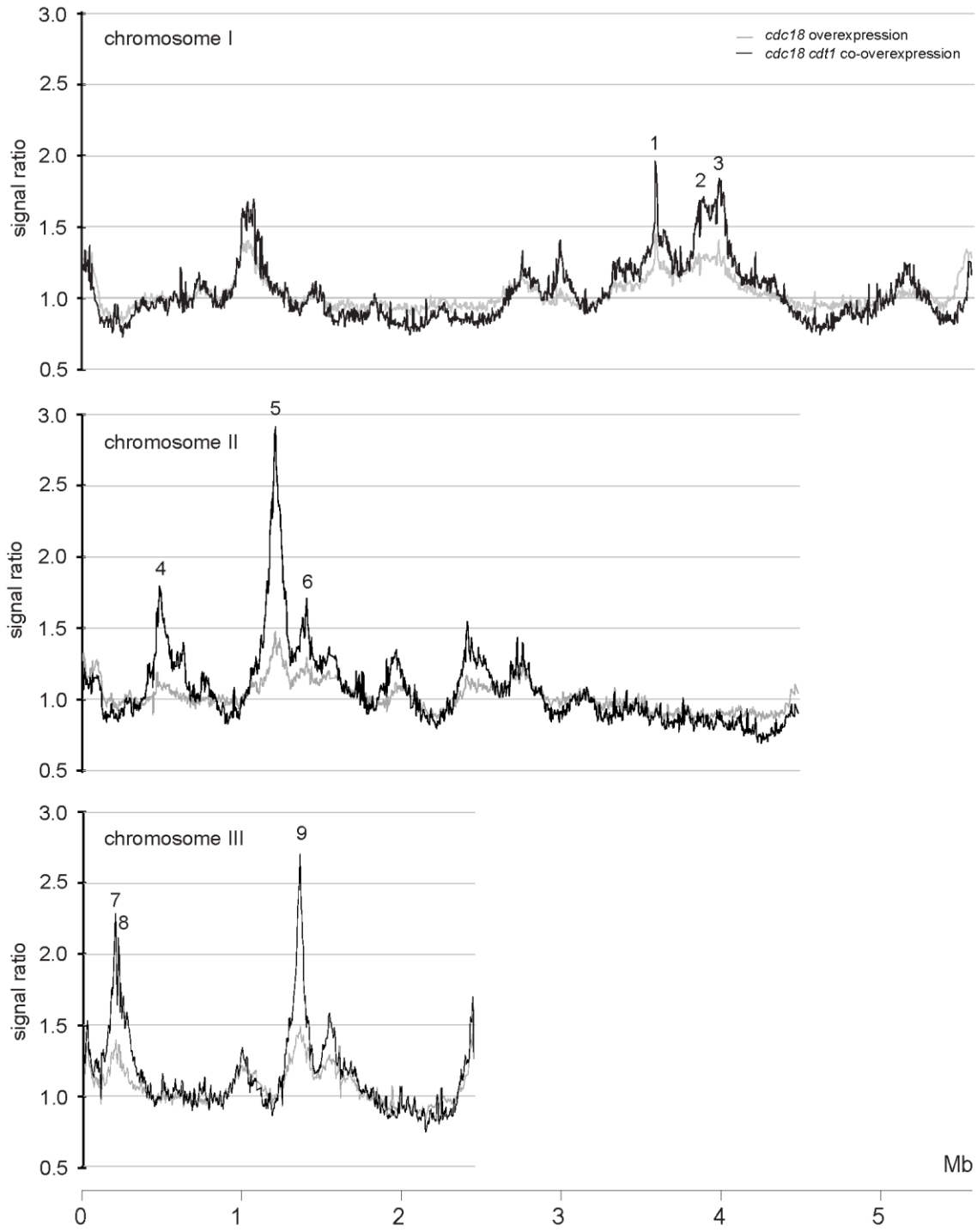
chromosome I
chromosome II
chromosome III
cdc18 overexpression
cdc18 cdt1 co-overexpression
signal ratio
Mb
1
2
3
4
5
6
7
8
9

A

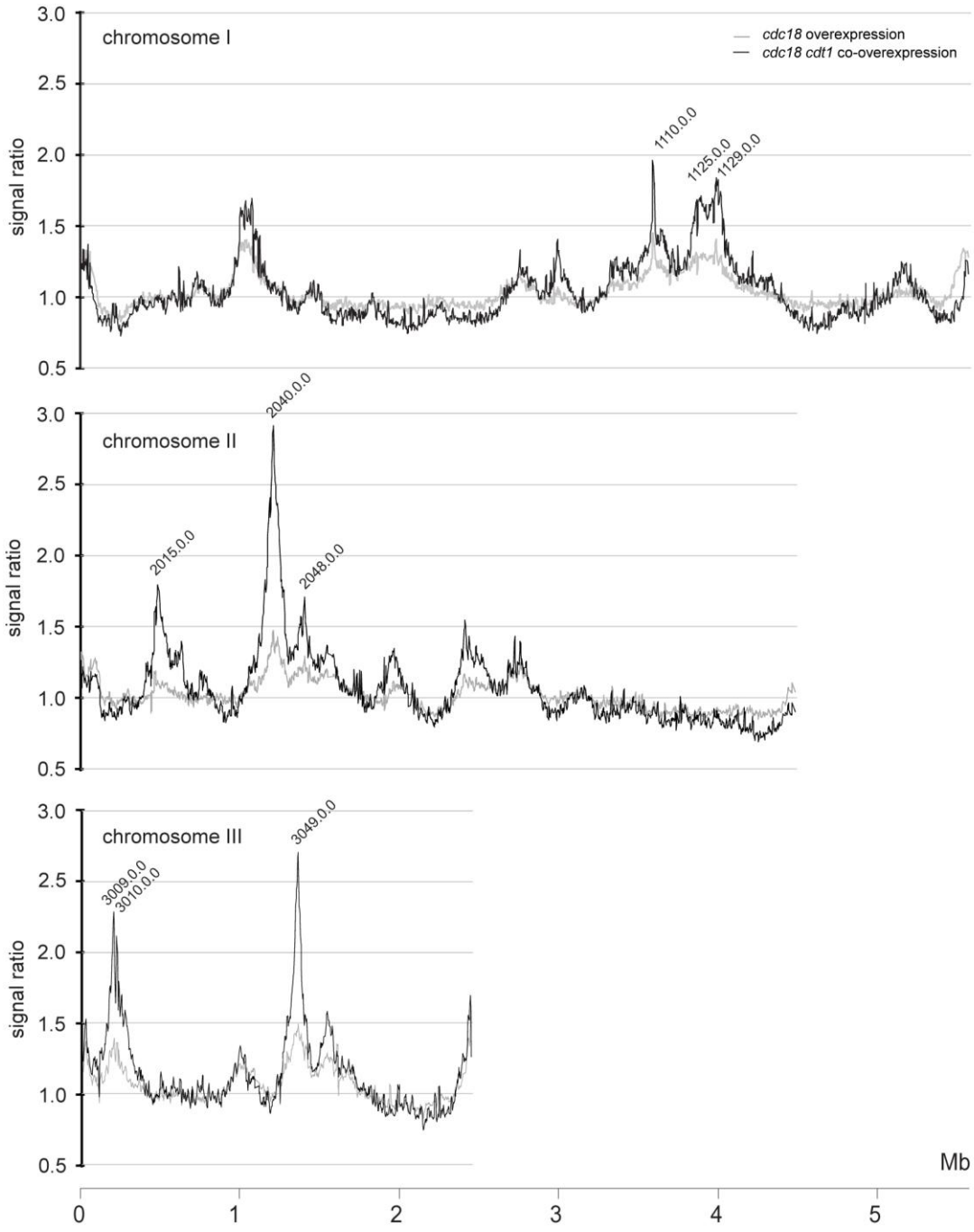
chromosome I
cdc18 overexpression
cdc18 cdt1 co-overexpression
signal ratio
1110.0.0
1125.0.0
1129.0.0
chromosome II
2040.0.0
2015.0.0
2048.0.0
chromosome III
3049.0.0
3009.0.0
3010.0.0
Mb

B

3.5. Origin 2040.0.0 is necessary but not sufficient for local genome amplification

To determine if the nine amplified regions were dependent upon specific origins we mapped the origins of replication located at the center of the two most highly amplified regions in the genome (Figure 3.4A, B). Deletion of the central origin in each amplification peak abolished amplification in these regions, (origin 2040.0.0: Figs. 3.4C, E; origin 3049.0.0: Fig. 3.4F). In contrast, deletion of neighboring origins under the peak had no effect on amplification (data not shown). These data indicate that in each region, a single specific origin is necessary to drive local amplification. To test whether such an origin is sufficient to induce amplification, a 3.65 kb sequence including the AT-rich island of origin 2040.0.0 was integrated into a nearby region of chromosome II which undergoes only limited amplification. The 3.65 kb sequence induced significantly increased amplification at this ectopic locus in a strain deleted for origin 2040.0.0 (Figure 3.4E) and in a strain containing both the endogenous origin 2040.0.0 and the ectopic origin 2040.0.0 (Figure 3.4D). Therefore, origin 2040.0.0 induces amplification outside of its normal chromosomal context. However, when this origin was inserted into a region of Chromosome II that normally shows no amplification, the ectopic origin was unable to induce amplification (Figure 3.4E). The origin does fire in this context albeit at about half the efficiency of in its native position (signal ratio ~0.2 versus ~0.44) (Figure 3.5). We conclude that single origins are likely to be necessary for amplification within each amplified region, and also that these origins can only induce local amplification in specific chromosomal contexts.

Figure 3.4 Ori2040.0.0 is necessary but not sufficient for local amplification

(A-D) ORF and intergenic tiling array analysis of genomic DNA from cells which had re-replicated to ~32C. Signal was normalized to the rest of the genome. For all analysis, cv values >30% have been removed **(A)** S-phase origins within amplification peaks. Normal *cdc18 cdt1* co-oe amplification on chromosome II, peak 5 (*cdc18 cdt1* co-oe Δorigin 3048.0.0 experiment) **(B)** Normal *cdc18 cdt1* co-oe amplification on chromosome III, peak 9 (*cdc18 cdt1* co-oe Δorigin 2040.0.0 experiment). (↓): origins centered at amplification peaks are S-phase origins active in re-replication. (↓): neighboring origins active in *cdc18 cdt1* co-overexpression. **(C and D)** Grey: Normal unperturbed amplification in *cdc18 cdt1* co-oe Δorigin 3048.0.0 strain **(C)** Δorigin 2040.0.0 in *cdc18 cdt1* co-oe. Moving averages of 3pts are shown. **(D)** A supernumary copy of origin 2040.0.0 was integrated by replacement of ars2004 (origin 2050.0.0). (*) Integration site. Moving averages of 10 points are shown. **(E)** Detecting fold amplification at native and ectopic loci by qPCR. Light grey: intact origin 2040.0.0. Dark grey: endogenous 2040.0.0 deleted and integrated at ars2004 on the left arm of chromosome II . Black: endogenous 2040.0.0 deleted and integrated at C19F5.02 on the right arm of chromosome II. White: endogenous 2040.0.0 deleted as in **(C)** (white). **(F)** Light grey: intact origin 3049.0.0. White: origin 3049.0.0 deleted. **(E-F)** Genomic DNA from cells at ~32C was analyzed by qPCR. The fold increase over a non-amplified control region was determined.

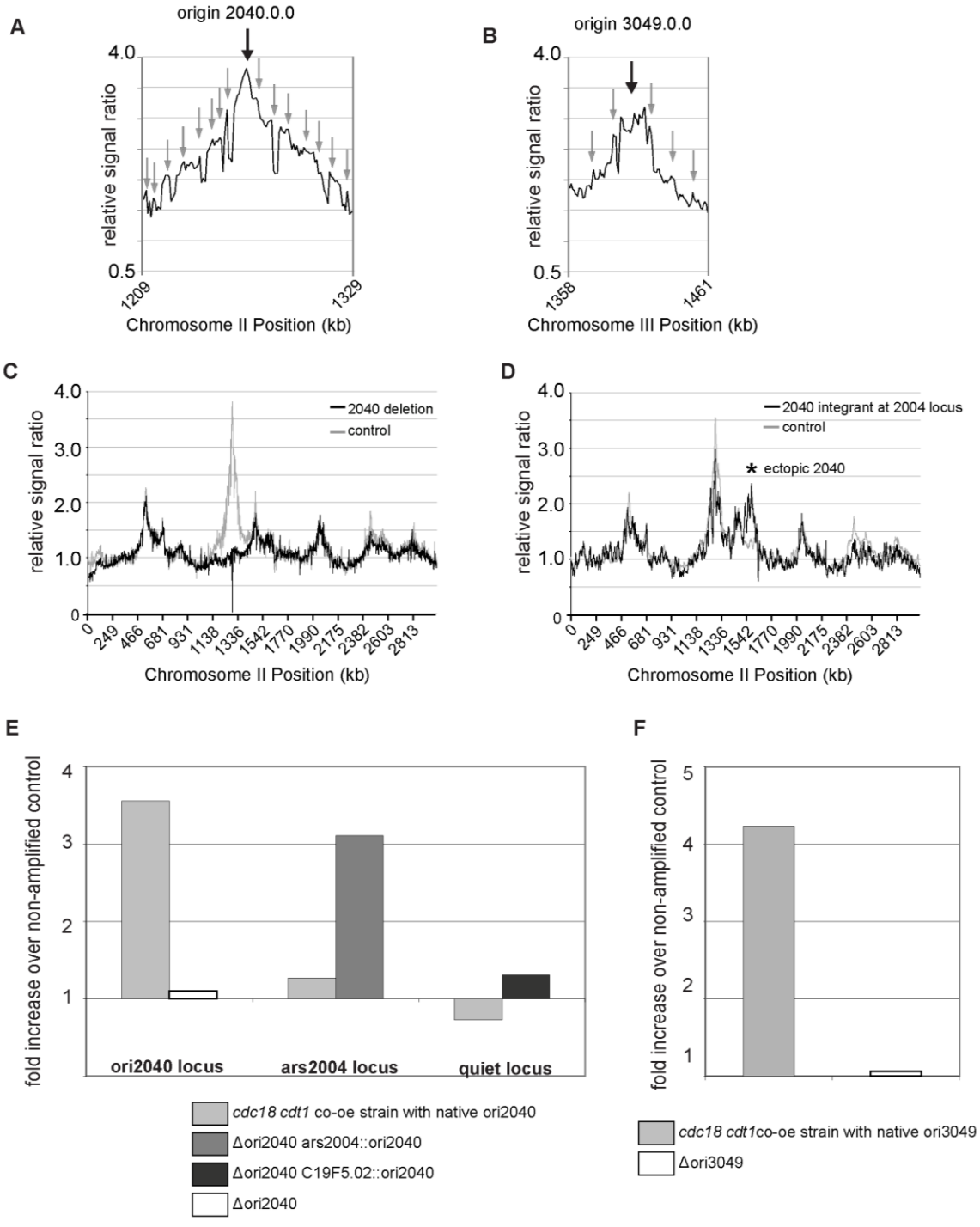
A
origin 2040.0.0
relative signal ratio
4.0
0.5
1209
1329
Chromosome II Position (kb)
B
origin 3049.0.0
relative signal ratio
4.0
0.5
1358
1461
Chromosome III Position (kb)
C
relative signal ratio
2040 deletion
control
4.0
3.0
2.0
1.0
0
0 249 466 681 931 1138 1336 1542 1770 1990 2175 2382 2603 2813
Chromosome II Position (kb)
D
relative signal ratio
2040 integrant at 2004 locus
control
* ectopic 2040
4.0
3.0
2.0
1.0
0
0 249 466 681 931 1138 1336 1542 1770 1990 2175 2382 2603 2813
Chromosome II Position (kb)
E
fold increase over non-amplified control
4
3
2
1
ori2040 locus
ars2004 locus
quiet locus
cdc18 cdt1 co-oe strain with native ori2040
Δori2040 ars2004::ori2040
Δori2040 C19F5.02::ori2040
Δori2040
F
fold increase over non-amplified control
5
4
3
2
1
cdc18 cdt1co-oe strain with native ori3049
Δori3049

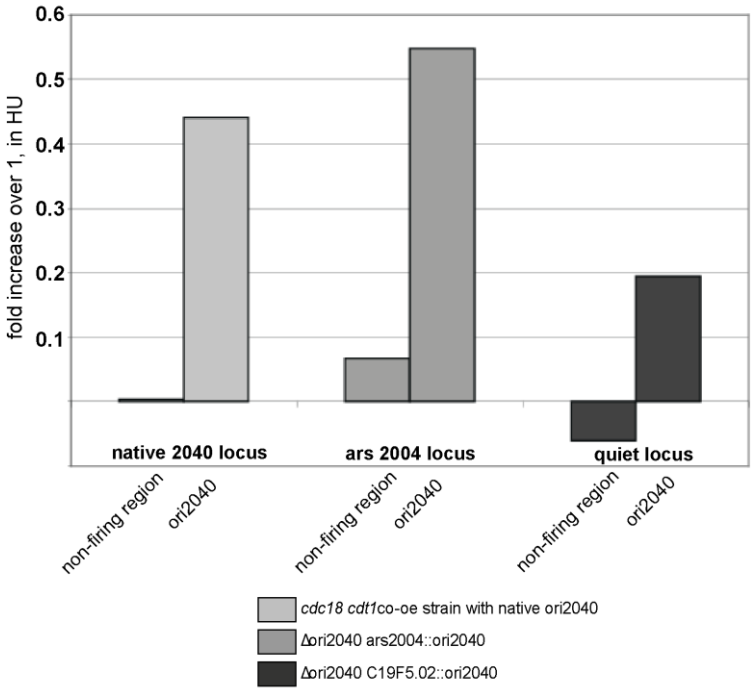

Figure 3.5 Origin 2040.0.0 fires in ectopic loci in the *cdc18 cdt1* co-oe strain

Signal ratio in the presence of 11mM HU was assessed in synchronized cultures of strains in Figure 4C to verify that origin 2040.0.0 fires in ectopic loci. Cultures were blocked in G2 at the restrictive temperature of 36.5°C, then released at 25°C allowing synchronous progression through the cell cycle in the presence of HU. Cells were collected at 120 minutes after release, genomic DNA was analyzed by qPCR and signal was normalized to a non-firing region in the genome. The fold increase over a signal ratio of 1 was determined.

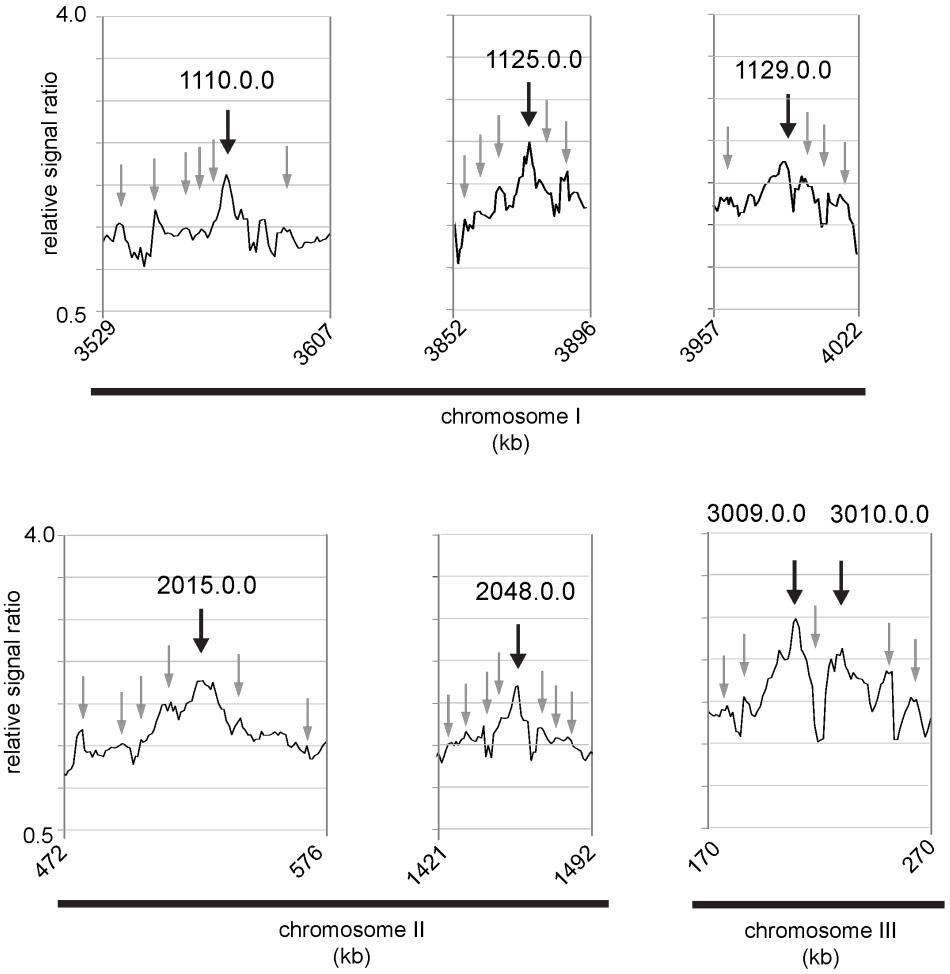

Figure 3.6 S-phase origins are centered at amplification peaks

The amplification profiles for 7 of the 9 most highly amplifying regions in the genome (peaks 1-4 and 6-8) are shown with arrows denoting the location of active origins. (↓) the central origin which is active in S-phase and overreplication. (↓) neighboring origins. Profiles shown are from the Δ3048 *cdc18 cdt1* co-oe strain for Chromosomes I and II, and from Δ2040 *cdc18 cdt1* co-oe for Chromosome III. These amplification profiles are the same as in the co-oe strain. Data from ORF and tiling arrays, moving average of 3 points, are shown.

We next identified parameters that characterize the origins driving amplification. Origins centered within the 9 amplification peaks (Figs. 3.4A, B, 3.6) were found to share three characteristics: high AT content, efficient firing in early S-phase, and chromosomal

location within long intergenic stretches (Fig. 3.7). When all S-phase origins were assessed according to efficiency versus AT content, they formed a wedge-shaped distribution with a minimum AT content of around 69% being required for origin activity (Fig. 3.7). Efficient origins are AT-rich, but AT-rich origins are not necessarily efficient. The 9 origins centrally located in the local amplification regions were highly AT-rich, with an AT content of 81.0% on average, compared to the mean for all origins at 73.8%. Their mean efficiency in S-phase is 2.7-fold greater than the average for all origins and they fire early during the first quarter of a normal S-phase, at 74 minutes on average. They are embedded in intergenic regions over 3-fold longer on average than the mean for all S-phase origins (Appendix I, Tables 3.1, 3.2) and 2.5-fold longer than origins of similar AT-content and efficiency not associated with amplification. They also all co-localize with established sites of PreRC assembly (Hayashi et al., 2007) (Table 3.2). Among these criteria, the most predictive parameter for a central origin at an amplification peak was AT content, followed by efficiency in mitotic S-phase. There was therefore no single predictor of origin amplification, rather the combination of these key parameters, together with position in the chromosome dictates amplification behavior.

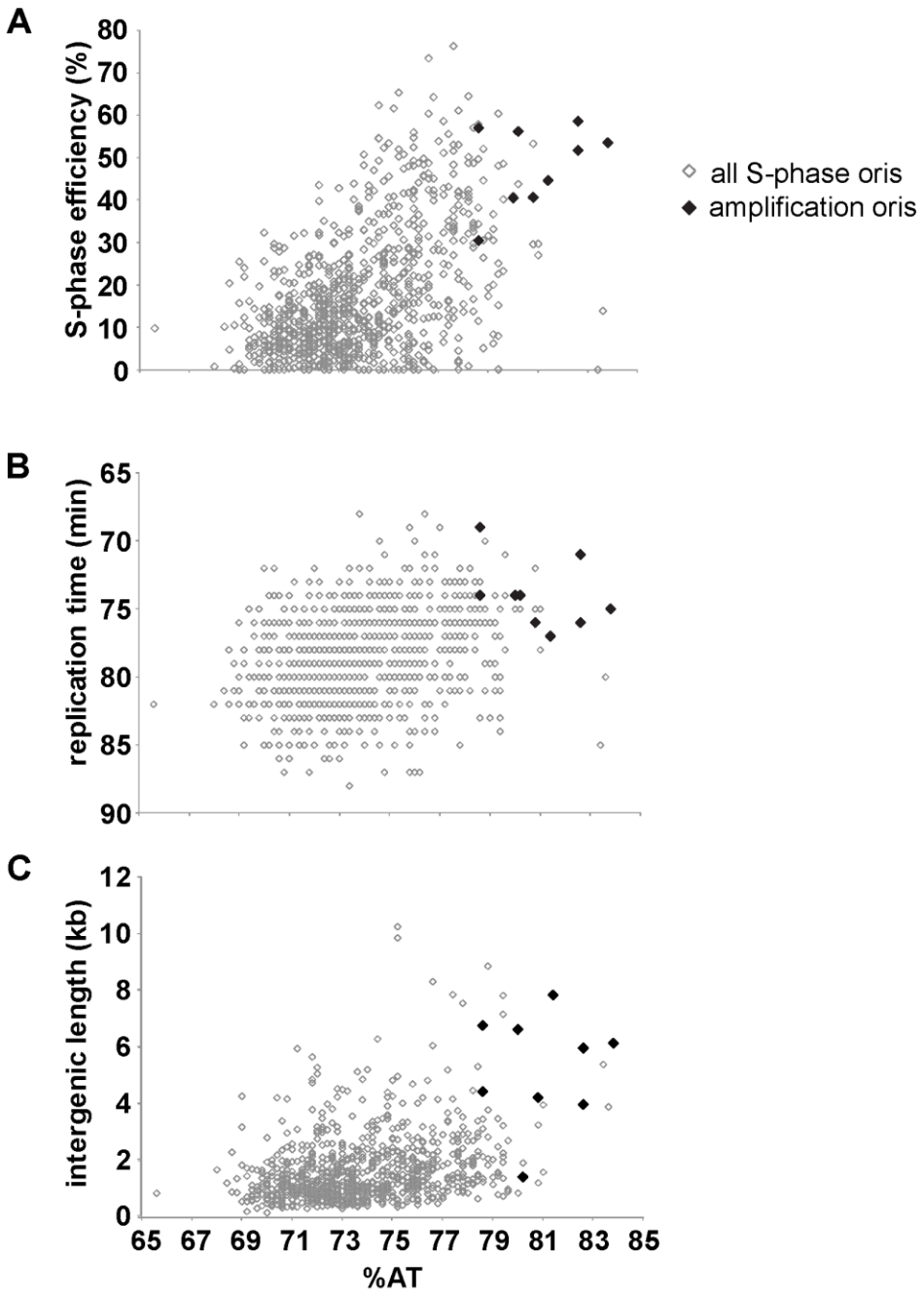

Figure 3.7 Origins associated with amplification peaks have extreme features among S-phase origins **(A)** Correlation between %AT-content and origin efficiency in a wild type mitotic S-phase. Origin efficiency for all 904 origins is plotted as a function of %AT-content. **(B)** Origin replication time in mitotic S-phase as a function of %AT-content **(C)** Length of the intergene containing each origin plotted as a function of %AT-content. The plots are coded according to origin behavior in *cdc18 cdt1* co-oe; (♦) mitotic S-phase origins centered within local peaks amplified >1.6 to 4-fold over the genome average, depending on the experiment.

3.6. Discussion

We have demonstrated here that in the presence of excess helicase loaders, normal cell cycle controls over replication are attenuated: local amplification occurs and DNA synthesis is continuous, unaccompanied by MBF-mediated G1/S gene expression, and lacks correlation between re-initiation and cell volume increase. Nine S-phase origins have been identified which bring about this local amplification, suggesting that they possess specific features allowing them to escape the once-per-S-phase firing requirement. We identified these features as high AT-richness, early and efficient firing in a normal S-phase and occupancy of extended intergenic regions. These results contrast with an earlier study (Mickle et al., 2007) which found no correspondence between re-replication peak centers and origins known to be very active in S-phase, but that study differed from the work presented here in terms of the *cdc18* allele overexpressed and the extent of amplification.

We found that the origin 2040.0.0 is necessary but not sufficient for local amplification and that the ability to induce amplification is sensitive to context within the chromosome. Our lab's initial origin mapping study showed that replication timing varies among chromosomal domains with some regions replicating earlier or later on average than others (Heichinger et al., 2006). It was also shown that origin efficiency is well correlated with timing of origin firing. Such domains of efficient, early firing origins may also influence the ability to amplify. Origin 2040.0.0 could induce amplification when integrated ectopically between its endogenous locus on the left arm of chromosome II and the centromere. Pericentromeric origins are known to be early replicating in S-phase while the right arm of chromosome II, where origin 2040.0.0 was

not sufficient to induce amplification, is later replicating. Field et al. have further analyzed fission yeast origin data by computationally modeling nucleosome occupancy in the vicinity of origins used during a normal S-phase based on the presence of 1) nucleosome-favoring periodic dinucleotides positioned every 10bp, thought to facilitate the winding of DNA around nucleosomes and 2) Poly (dA:dT) elements, thought to be nucleosome-disfavoring due to rigidity (Field et al., 2008). The model predicts *in vivo* nucleosome positions with good accuracy in the budding yeast, fly, worm, chicken and human genomes. Though the model has yet to be validated experimentally in fission yeast, it predicts high efficiency origins to be nucleosome depleted and inefficient origins to have high nucleosome occupancy. Replication factors and machinery would have ready access to the open chromatin architecture at efficient origins but would compete with nucleosomes for binding at the closed chromatin of inefficient loci (Field et al., 2008). Beyond sequence requirements for local amplification, the higher order structure of the chromosome seems to play a key role in the ability to amplify, as has been observed in *Drosophila* (de Cicco and Spradling, 1984; Zhang and Tower, 2004). Physiologically, amplifying origins might represent very efficient S-phase replication origins in a privileged chromosome context. In such a model, replication factor binding and access to replication machinery may be selectively permitted or restricted within distinct chromosomal regions, with potential influences including chromatin and subnuclear organization.

The origin features we propose as responsible for local amplification may have relevance for genome stability across a range of species as AT-richness is a conserved sequence feature for replication factor binding (Dai et al., 2005; Stanojcic et al., 2008;

Vashee et al., 2003). In support of this possibility, the chromosomal regions that overreplicate upon *cdc6* and *cdt1* overexpression in mammalian cells are also the regions replicated earliest in S-phase (Vaziri et al., 2003). Our results may also be relevant for understanding the development of cancer since NIH3T3 cells overexpressing *cdt1* accumulate structural chromosomal abnormalities (Seo et al., 2005) and gain the ability to form tumors in mice (Arentson et al., 2001), while overexpression of *cdt1* in T-cells of p53 null mice leads to the formation of lymphoblastic lymphoma (Seo et al., 2005). Origins which escape genome-wide coordination of firing may seed such alterations to the genome. Repeated re-firing of origins is known to lead to onion-skin amplification structures (Liang and Gerbi, 1994; Liang et al., 1993; Osheim et al., 1988). These might be resolved via recombination to multiple chromosomal copies of a given gene under selective pressure (Dunham et al., 2002; Koszul et al., 2004), which could eventually evolve to confer new functions (Hahn, 2009; Ohno, 1970; Ohno, 1999). Repeated firing of origins with these extreme features therefore potentiates genome instability that can drive evolution and the generation of cancer (Arentson et al., 2001; Schimke et al., 1986; Seo et al., 2005).

Chapter 4

SYNCHRONY OF S-PHASE AND MITOSIS IN A COMMON CYTOPLASM:

Distinguishing autonomous from cytoplasmically driven cell cycle events

4.1. Introduction

Fission yeast spend most of their life cycle as mononucleate cells, with a brief period between mitosis and formation of the division septum during which they are binucleate (~1/10th of the cell cycle) (Nasmyth et al., 1979). We aimed to determine whether the signals to enter S-phase or M-phase are nuclear autonomous or cytoplasmic. To investigate this question, we took advantage of fission yeast septation mutants which fail to undergo cytokinesis, yielding multiple nuclei in the same cytoplasm. In these cells we investigated whether all nuclei of a cell undergo DNA synthesis and mitosis in sync (Figure 4.1). If so, this would suggest that activities among multiple nuclei are coordinated by the cytoplasm they share, and that factors essential for DNA synthesis like CDK activity and replication factors are present in equal quantities in all the nuclei. Conversely, if we observe asynchronous S-phase or M-phase, this would imply that nuclei within a common cytoplasm can behave independently, possibly because they have different concentrations of substrates essential for DNA replication or nuclear division.

Previous work has provided two paradigms: first, the classic cell fusion experiments of Rao and Johnson showed that when nuclei of different cell cycle stages are present in the same cytoplasm, cell cycle transitions can be advanced but never go in

reverse (Johnson and Rao, 1970; Rao and Johnson, 1970). For instance, when an S-phase and G2 cell were fused, the S-phase nucleus was advanced towards mitosis, but the G2 nucleus did not repeat S-phase (Figure 1.1). In these cells, mitosis was synchronized most of the time and asynchronous mitosis was only observed in 11% of cells (Johnson and Rao, 1970; Rao and Johnson, 1970). Second, we considered the asynchronous nuclear divisions which occur in the filamentous fungus *Ashbya gosypii* (Gladfelter et al., 2006). This fungus is composed of multinucleate syncytia where nuclei are separated by semipermeable septa (Gladfelter, 2006). Nuclear division occurs asynchronously in the syncytium and preferentially at branch points (Helfer and Gladfelter, 2006). Therefore, mitotic asynchrony is unusual in cell fusion experiments while this is observed in *A. gosypii*.

To investigate whether S-phase and M-phase are nuclear autonomous or cytoplasmically driven in fission yeast we first characterized coordination of nuclear division in multinucleate cells by testing the effects of perturbing G2/M CDK activity on synchrony of division among nuclei in a common cytoplasm. Next, we investigated S-phase synchrony and perturbations resulting from altering G1/S CDK activity. We find that CDK activity has a key role in coordinating synchronous nuclear division and DNA synthesis in multinucleate cells, and when coordination is lost in the absence of CDK inhibition, division and synthesis are nuclear autonomous.

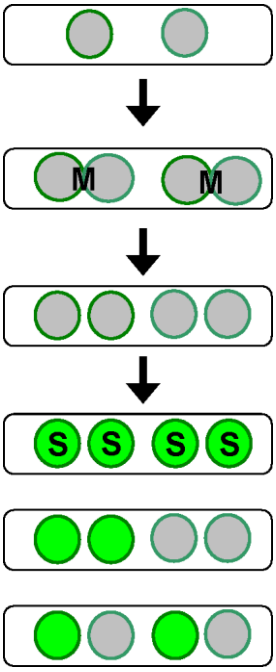

Figure 4.1 Potential patterns of S-phase and mitosis in multinucleated cells. Green represents nuclei in DNA synthesis. Note that fission yeast nuclei cross paths during division in multinucleate cells so that in the bottom cell, the green nuclei are sister nuclei.

4.2. Multinucleated cells

Mutants in the **S**eptation **I**nitiation **N**etwork (SIN) are unable to perform cell division, so after mitosis sister nuclei are retained in the same multinucleate cytoplasm. This allows us to distinguish what behaviors may be coordinated among nuclei by diffusible factors in the common cytoplasm, and what behaviors are determined by the individual nuclei. To determine the effect of perturbing G2/M CDK activity on synchrony of events in multinucleate cells, we used the conditional *wee1-50* mutant. Eliminating Wee1 activity reduces the inhibitory phosphorylation of CDK and advances

cells into the G2-M transition at a smaller size. We selected the strains *cdc15-287* (SIN) (Cdc15 coordinates re-organization of F-actin at mitosis) and *cdc15-287 wee1-50* (SIN wee) which were healthy and well suited for study. Cells of these strains are shown in Figure 4.2 after shifting to the restrictive temperature of 36.5°C.

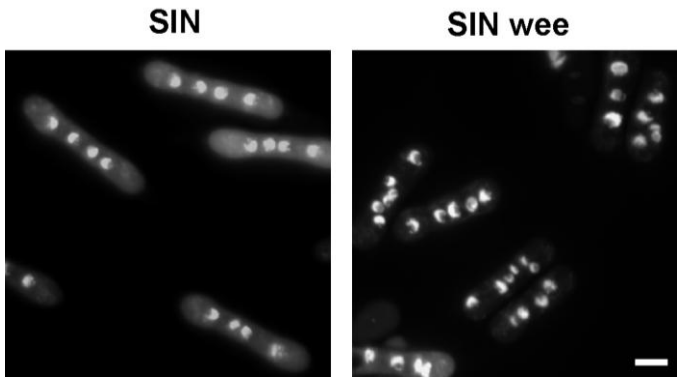

Figure 4.2 Septation Initiation Network (SIN) and *wee1-50* mutants
Cells were shifted to restrictive temperature for 5 hours, ethanol fixed and DAPI stained. The scale bar is 5μm.

4.3. SIN wee mutants

4.3.1. Cells lacking Wee1 activity are advanced in nuclear division

At any given time point after shifting to restrictive temperature, SIN wee cells appeared to have more nuclei than their SIN alone counterparts (Figure 4.2). To examine the increase in number of nuclei over time, SIN and SIN wee cells were shifted to restrictive temperature and the average nuclei per cell was determined every hour (Figure 4.3). We observed that in the SIN wee culture, the nuclei of mononucleated cells divide

within the first hour after temperature shift to become binucleated, while in the SIN mutant, nuclei of mononucleated cells divide by 3 hours. After 3 hours, the slope of the curves for average nuclei per cell versus time is the same. We conclude that SIN mutants lacking Wee1 activity are advanced by one nuclear division but thereafter maintain the same rate of nuclear divisions as SIN mutants alone.

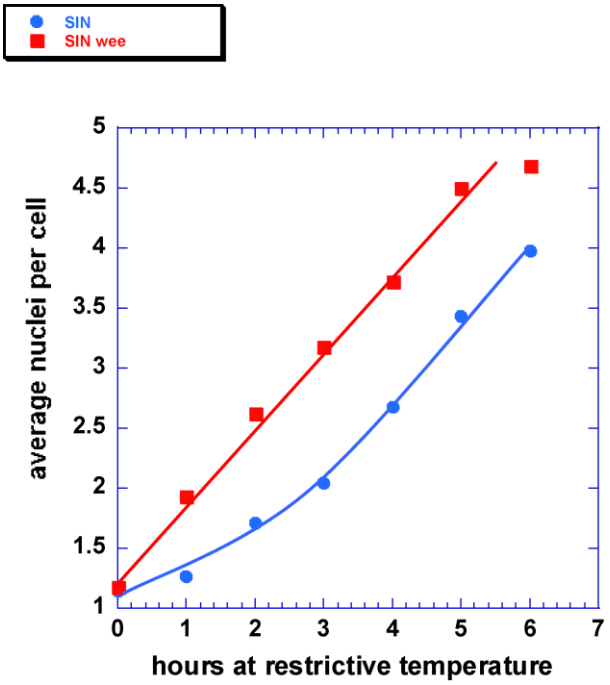

Figure 4.3 Nuclear division is advanced in the absence of Wee1 activity
Upon shift to restrictive temperature cells were collected every hour and fixed in 70% ethanol then DAPI stained to examine the nuclei. The average number of nuclei per cell was determined for each time point.

4.3.2. Wee1 activity is required for synchronous nuclear division in a common cytoplasm

While the timing of nuclear division is advanced in the SIN wee mutant, there may also be an effect on nuclear synchrony. To determine the effect of *wee1* on coordinating nuclear division, we considered the numbers of nuclei in any given cell in the cultures over time (Figure 4.4). We found that in the SIN mutant, the number of nuclei per cell doubles every few hours in an orderly fashion, as cells have one, two, then four nuclei and so forth. In contrast, in the SIN wee mutant, most cells have two nuclei at 2 hours after shift to restrictive temperature, and at 3 hours most cells are tetranucleate but there are also trinucleate cells. Thereafter we observe cells with numbers of nuclei outside of the ordered 1, 2, 4, 8 progression in the SIN mutant, and observe cells with 5, 6, 7, 9 and 10 nuclei as well.

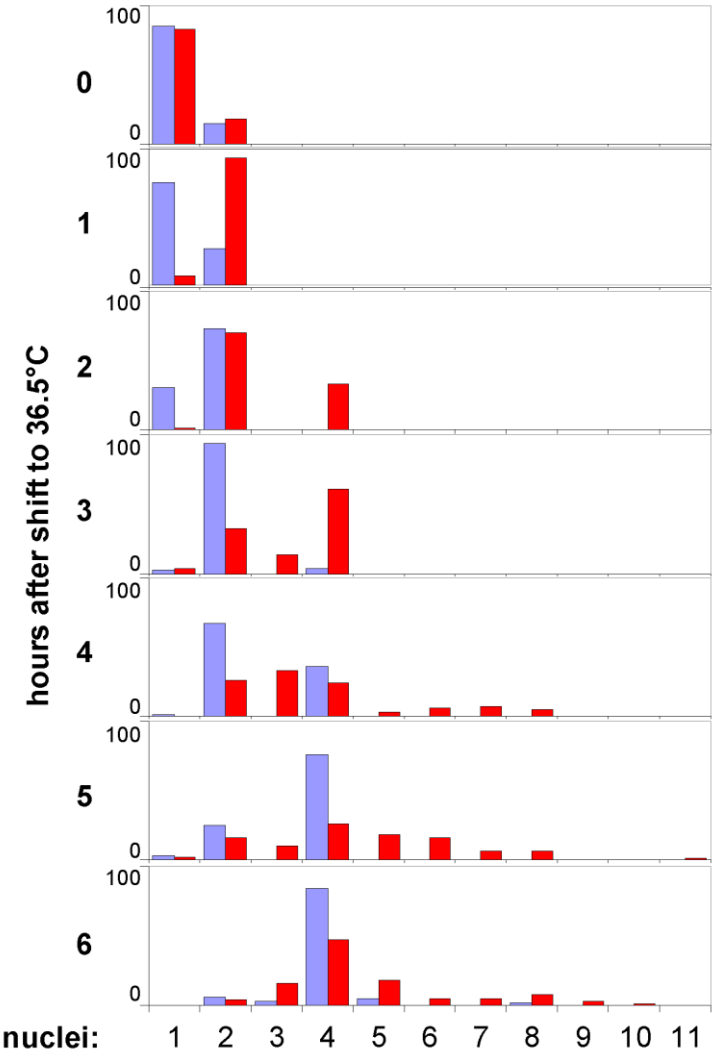

Figure 4.4 In the absence of wee1, nuclear division is advanced and asynchronous

Numbers of nuclei in SIN and SIN wee mutant cells after shift to restrictive temperature. Ethanol fixed cells were scored for nuclei by DAPI staining. Histogram for each time point shows the percentage of cells in the population with given numbers of nuclei. Blue: SIN mutant. Red: SIN wee mutant

This indicates that nuclei within SIN wee mutant cells divide more asynchronously. We therefore conclude that Wee1 activity is necessary to fully synchronize the division of multiple nuclei in the same cell since in its absence nuclei within the same cell divide less synchronously. Division of one nucleus before its sister

demonstrates that nuclei can behave autonomously despite sharing a common cytoplasm. This could be attributed to different levels of nuclear located CDK activity between those nuclei, with one nucleus reaching the threshold of mitotic activity before the other.

4.4. Though mitosis is asynchronous, DNA synthesis occurs synchronously among nuclei in a common cytoplasm

Asynchronous nuclear division in multinucleate cells may be expected to produce nuclei of different cell cycle stages in the same cytoplasm. Taking the simplest case of asynchronous division, two situations could produce a trinucleate cell from a binucleate cell. In a binucleate cell with two G2 nuclei, one nucleus could divide to produce two G1 nuclei, with the undivided nucleus remaining in G2. In a second scenario, beginning with both nuclei in G1, one of the two sisters might remain in G1while its sister progressed through S-phase and division (Figure 4.5).

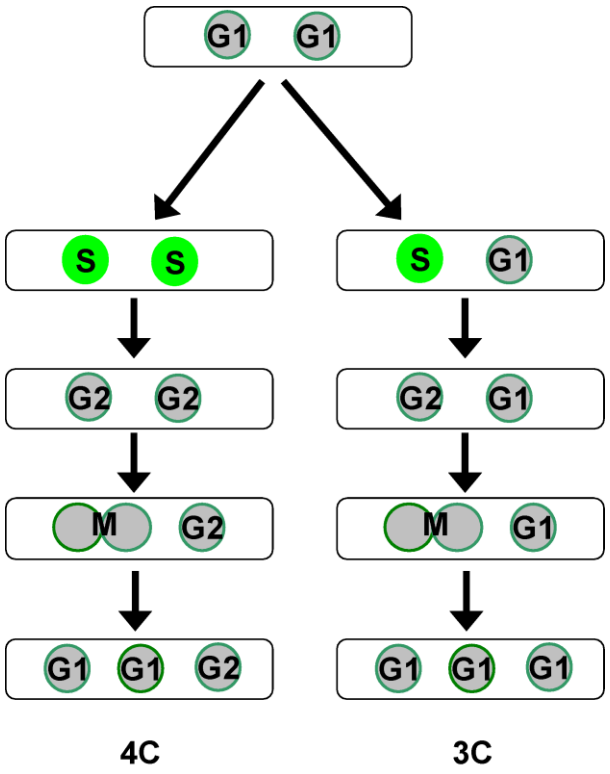

Figure 4.5 Schematic for creation of trinucleate cells from binucleates by asynchronous mitosis
Left: a trinucleate cell resulting from progression of only one G2 nucleus through mitosis would be expected to have 4C DNA content. Right: a trinucleate cell resulting from failure of one G1 nucleus to progress through S-phase and M-phase would have 3C DNA.

To differentiate between these possibilities, DNA content of cells in bulk culture was examined by flow cytometry and DNA content of single cells was estimated by DAPI staining and microscopy. In a bulk culture, DNA content of SIN wee cells increased by doublings from 2C to 4C to 8C (Figure 4.6) as assayed by FACS analysis.

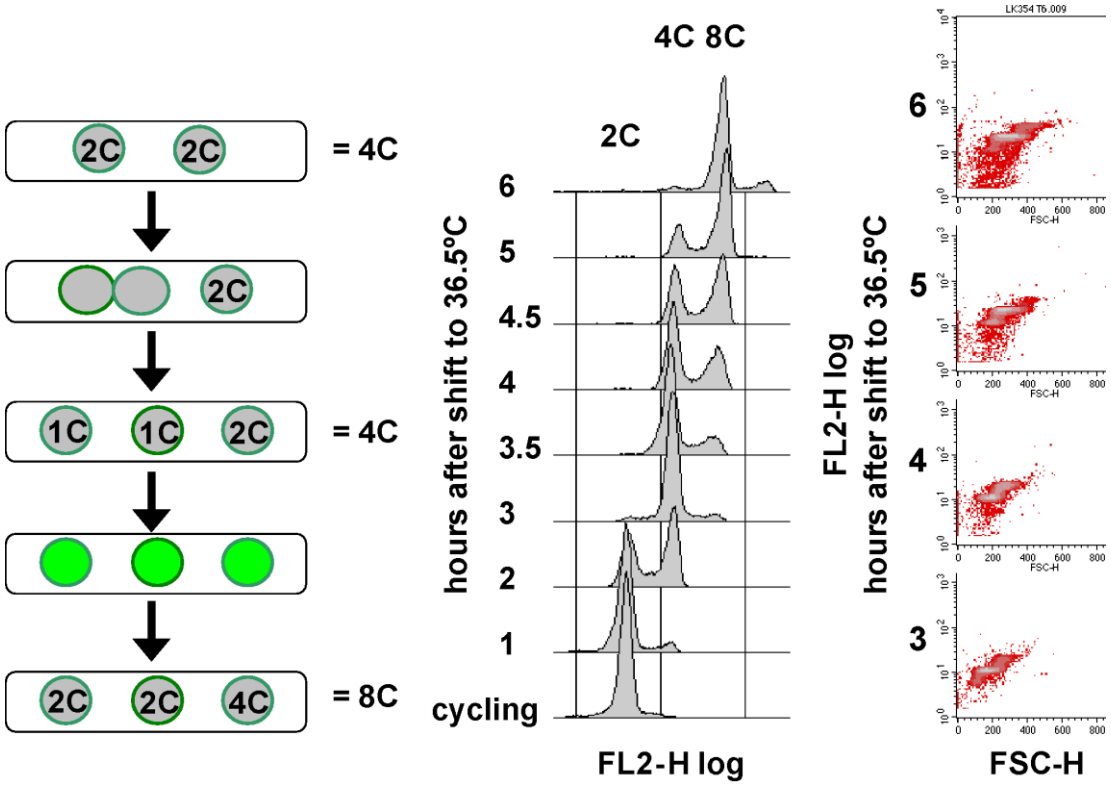

Figure 4.6 DNA content increases by doublings though cells contain nuclei which have not undergone division. After shift to restrictive temperature, SIN wee mutant *tk hENT* cells were ethanol fixed every hour and every 30 minutes between 3h and 5h. DNA was stained with propidium iodide and analyzed by flow cytometry. FL2-H represents DNA content and FSC-H represents cell length.

To estimate DNA content of single cells using DAPI staining, first we confirmed that in tetranucleate SIN wee mutants at restrictive temperature for 4 hours, the estimated DNA content was equivalent for all 4 nuclei (Figure 4.7). DNA content was estimated as:

(average pixel intensity of nucleus in medial plane – background intensity of cytoplasm) x area of nuclear cross section

Relative DNA content of nuclei within a cell was then determined by dividing each nucleus' value by the lowest value for that cell. Similar results were obtained using the

sum of a Z-stack rather than a single plane. We then examined the relative DNA content among nuclei in trinucleate cells from the same time point (Figure 4.8), and found that they had roughly a 1:1:2 ratio. Both the FACS data and estimations of DNA content in single cells are consistent with the scenario that the undivided nucleus is a G2 2C nucleus (Figure 4.5, left panel).

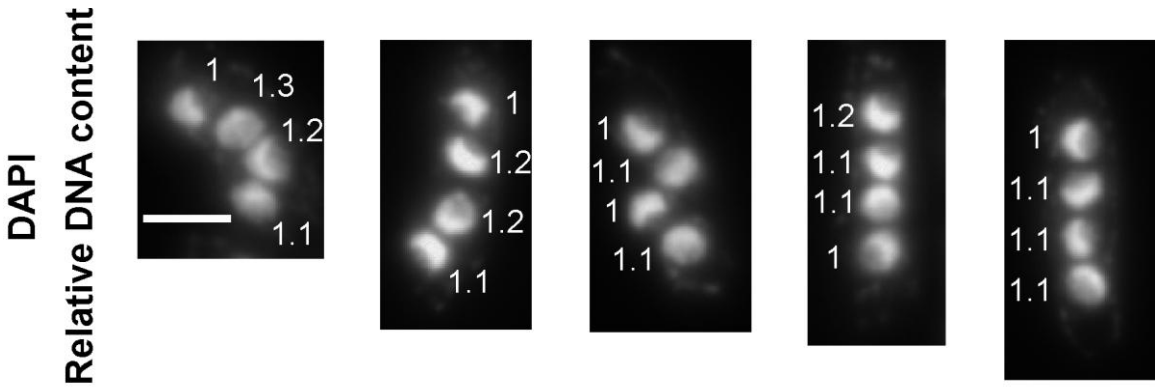

Figure 4.7 Quantification of relative DNA content among nuclei in single tetranucleate cells. After 4 hours at restrictive temperature, cells containing the SIN and wee mutations were fixed in formaldehyde and DAPI stained (see Ch. 6 for Materials and methods). DNA content was estimated from single medial plane as the product of average nuclear DAPI intensity minus background multiplied by the area of the nucleus. Estimation from the sum of a stack instead of a single plane gave similar results. The relative DNA content of nuclei within a cell is normalized to the lowest value for that cell. Each nucleus is labeled with its estimated relative DNA content. Cells shown are random and representative. Scale bar is 5μm.

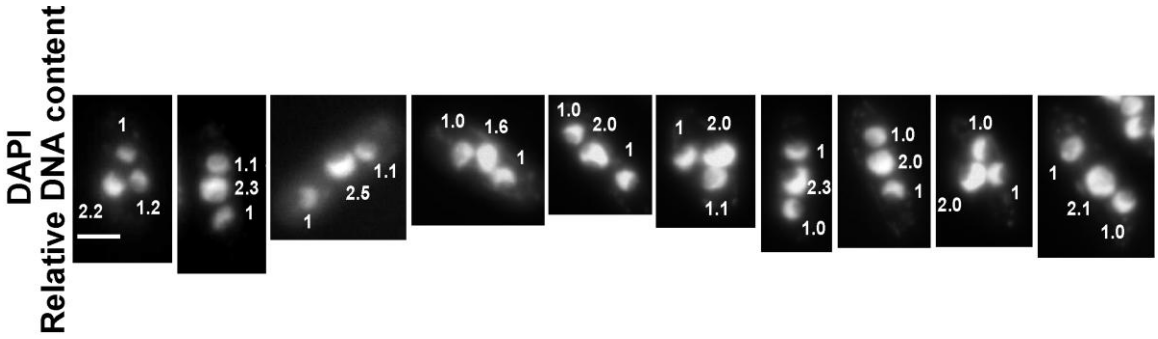

Figure 4.8 Quantification of relative DNA content among nuclei in single trinucleate cells
Cells are from the same experiment and time point as in Figure 4.7. DNA content was estimated as in Figure 4.7 and each nuclei was labeled with its relative DNA content. Cells shown are random and generally representative of the 40 cells measured. The scale bar is 5μm long.

After asynchronous nuclear division leaves one nucleus undivided with 2C DNA content, what is the consequence for DNA replication? We asked whether DNA synthesis would also be asynchronous among nuclei in such cells. Asynchronous DNA synthesis would suggest that replication is also nuclear autonomous in such cells.

SIN and SIN wee mutants containing *tk* and *hENT* were pulse labeled to assess DNA synthesis. Exponentially growing cultures at 25°C were shifted to 36.5°C. At 3.5, 4 and 4.5 hours after the shift, a sample of the culture was labeled with 300μM BrdU for 10 minutes and then fixed in formaldehyde. BrdU was visualized by indirect immunofluorescence. In the SIN mutant, BrdU incorporation among nuclei was all-or-none-- all nuclei within a cell were observed to undergo DNA synthesis in sync and no cells with only a fraction of nuclei replicating were observed. In the SIN wee mutant, all tetranucleate cells were all-or-none in terms of BrdU incorporation (Figure 4.9). We then

assessed trinucleate SIN wee cells—the simplest product of an asynchronous mitosis (Figure 4.10).

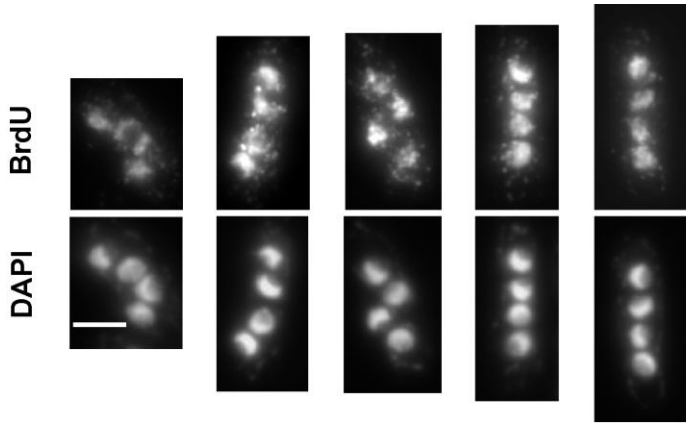

Figure 4.9 DNA synthesis in tetranucleate cells

SIN wee1-50 *tk hENT* cells shifted to restrictive temperature for 4 hours, pulse labeled for 10 minutes with BrdU, then fixed in formaldehyde (see Ch. 6 for Materials and methods). Cells from Figure 4.7 are shown. BrdU was visualized by indirect IF via Alexa 488. Scale bar is 5μm.

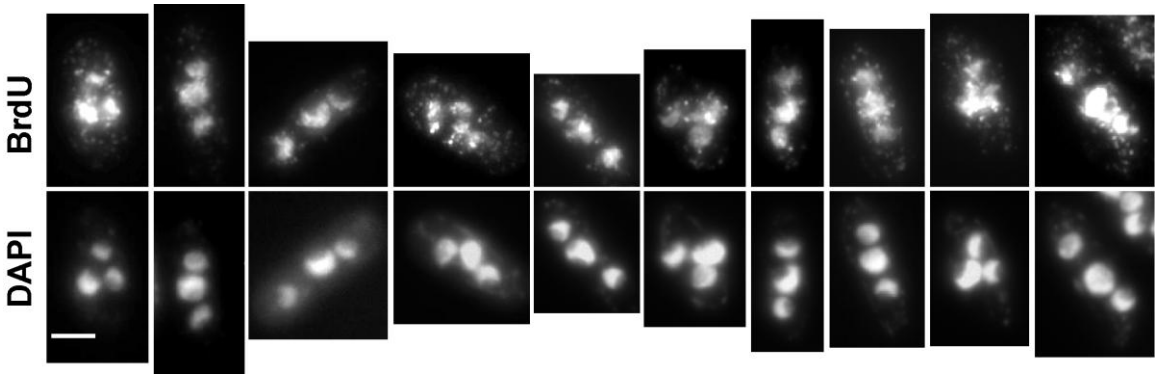

Figure 4.10 DNA synthesis in trinucleate cells

SIN wee1-50 *tk hENT* cells at restrictive temperature were pulsed with BrdU which visualized by IF. Cells from Figure 4.8 are shown. Scale bar is 5μm

Between 3.5 and 4.5 hours after shift to restrictive temperature, about 90% of the labeled trinucleates in the culture had 3 out of 3 nuclei labeled (Figure 4.10, Table 4.1).

This suggests that: 1) DNA synthesis is coordinated among multiple nuclei in the same cytoplasm despite the fact that one of the three nuclei has not divided and 2) the undivided nucleus has initiated DNA synthesis from G2 and therefore is re-replicating. The continued DNA synthesis of undivided nuclei was also reflected in the doublings of DNA content in the bulk culture over time (Figure 4.6), which resembled the FACS analysis seen in *cdc13* s/o (Figure 2.4).

Table 4.1 Scoring for trinucleate SIN wee cells between 3.5 and 4.5 hours after shift to restrictive temperature

hours at 36.5°C	% trinucleates in pop.	Of trinucleates, % labeled	Of labeled cells, % with 3 of 3 nuclei labeled	% 2 of 3	% 1 of 3
3.5	12% (45/371)	36% (107/298)	88% (94/107)	8% (9/107)	4% (4/107)
4	20% (74/370)	34% (69/305)	84% (58/69)	13% (9/69)	3% (2/69)
4.5	22% (96/437)	25% (75/303)	93% (70/75)	4% (3/75)	3% (4/75)

Number of nuclei was scored by DAPI under fluorescence microscopy. Among trinucleates the number BrdU positive nuclei was evaluated by immunofluorescence (IF) in the FITC channel.

Table 4.2 Scoring for trinucleate ΔRum1 SIN wee cells between 2 and 3 hours after shift to restrictive temperature.

hours at 36.5°C	% trinucleates in pop.	Of trinucleates, % labeled	Of labeled cells, % with 3 of 3 nuclei labeled	% 2 of 3	% 1 of 3
2	5% (13/266)	43% (38/89)	58% (22/38)	37% (14/38)	8% (3/38)
2.5	17% (75/446)	26% (62/242)	60% (37/62)	39% (24/62)	2% (1/62)
3	22% (49/219)	31% (64/208)	61% (39/64)	31% (20/64)	8% (5/64)

Number of nuclei was scored by DAPI under fluorescence microscopy. Among trinucleates the number BrdU positive nuclei was evaluated by IF in the FITC channel.

4.5. MBF-dependent gene products localize to G1 and G2 nuclei in a common cytoplasm

How might G2 nuclei be licensed to re-replicate? We speculated that the presence of replication factors expressed by the G1 nuclei might have an effect on the G2 nucleus. We used a marker for G1/S MBF-dependent gene expression, Tos4-GFP (Kiang et al., 2009), to determine if all the nuclei in a cell contain Tos4-GFP and possibly other G1/S specific factors. In SIN and SIN wee mutants containing Tos4-GFP, we observed Tos4-GFP localization to all-or-none of the nuclei in a cell (Figure 4.11). While we cannot distinguish which nucleus or nuclei may be responsible for expression of Tos4-GFP, the presence of fluorescent signal in all nuclei in a given cell indicates that they each have access to MBF-dependent gene products regardless of whether the nuclei are in G1 or G2.

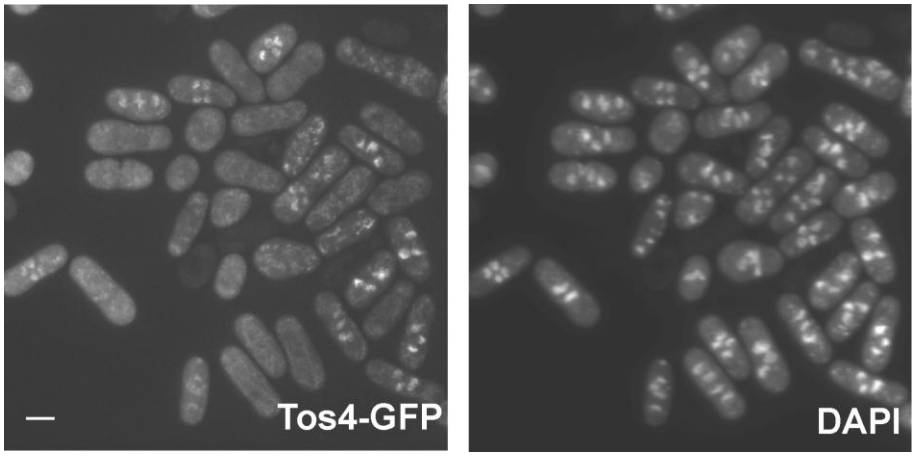

Figure 4.11 Tos4-GFP localizes to all-or-none of the nuclei in multinucleate cells.
SIN wee *tos4-GFP* cells were shifted to restrictive temperature for 4 hours, then fixed in ice cold ethanol. Fixed cells were DAPI stained. Tos4-GFP is visualized on the FITC channel. Scale bar is 5μm.

4.6. The frequency of re-replication in a common cytoplasm is decreased in the absence of *rum1*

In endoreduplication induced by depletion of the B-type cyclin (*cdc13* s/o) we have attributed the ability to re-initiate to periodic dips in CDK activity so that cells return to a G1-like state. We considered whether the same might apply in the multinucleate cells. Successful division of one of the two nuclei in a binucleate cell would require APC/C activity which might lead to degradation of all Cdc13 in the cell. Despite not having divided, the G2 nucleus could return to a G1 state should its CDK activity fall. In *cdc13* s/o, deletion of the CDK inhibitor *rum1* attenuated re-replication (Figure 2.11), possibly by raising CDK activity to a level at which re-initiation is inhibited, but which is insufficient to trigger mitosis. We reasoned that the same attenuation might be seen in the SIN wee mutants, that is, G2 nuclei may not re-replicate. *Rum1* was deleted in the strain by replacement with a Kanamycin resistance cassette (Bähler et al., 1998), cells were shifted to restrictive temperature, and trinucleates were scored for numbers of labeled nuclei (Figure 4.12).

In the absence of *rum1*, the percentage of labeled trinucleate cells with all nuclei BrdU positive decreased from 90% in SIN wee (Table 4.1) to about 60% (Table 4.2). Those with 2 of 3 nuclei labeled increased from about 8% in SIN wee to 36% in *Δrum1* SIN wee, suggesting that in those cells, the undivided nucleus ceased to re-replicate. To verify this, we estimated the relative DNA content of nuclei by DAPI staining. We calculated the relative DNA contents of nuclei within trinucleate cells where 2 of 3 nuclei were BrdU labeled. The nucleus lacking BrdU had about two-fold the DNA content of each of the other two BrdU-positive nuclei (Figure 4.12). Therefore, the BrdU negative

nuclei appear to represent the undivided nucleus which is not re-replicating. In the absence of *rum1*, the percentage of labeled trinucleates with 2 of 3 BrdU-positive nuclei increases and in these cells the G2 undivided nucleus is BrdU negative. This suggests that Rum1 is important for the ability of G2 undivided SIN wee nuclei to re-replicate, since in its absence, re-replication is diminished.

Figure 4.12 Relative DNA content of nuclei in trinucleate cells undergoing DNA synthesis

Δ*rum1* SIN wee *tk hENT* cells shifted to 36.5°C for 3 hours were BrdU labeled for 10 minutes then fixed (Materials and methods). Cells were imaged using 63x (top panel) and 100x (bottom panel) objectives and nuclei were numbered from 1-3. DNA content was estimated from single medial plane (black text) or from the sum of a stack (red) and relative DNA content of nuclei within a cell was then determined as described in text. Cells depicted are random and representative of the 15 measured. Scale bars are 5μm.

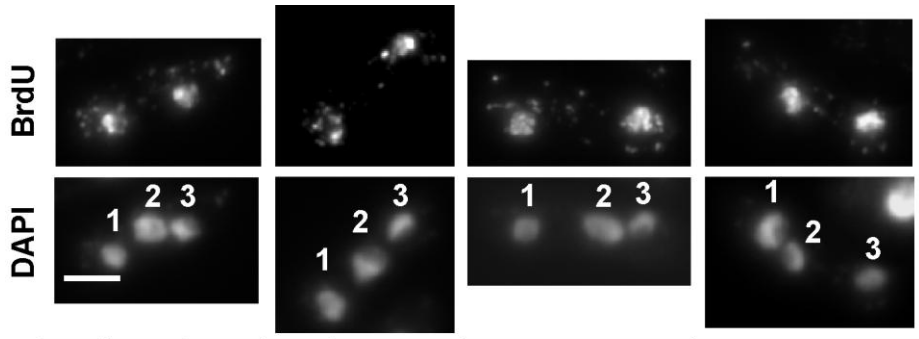

nucleus no.	1	2	3	1	2	3	1	2	3	1	2	3
relative DNA content	1	1.9	1.1	1.1	1.7	1	1	2.0	1.2	2.2	1.1	1
	1	2.0	1.0	1.2	1.5	1	1	2.1	1.1	2.3	1.2	1

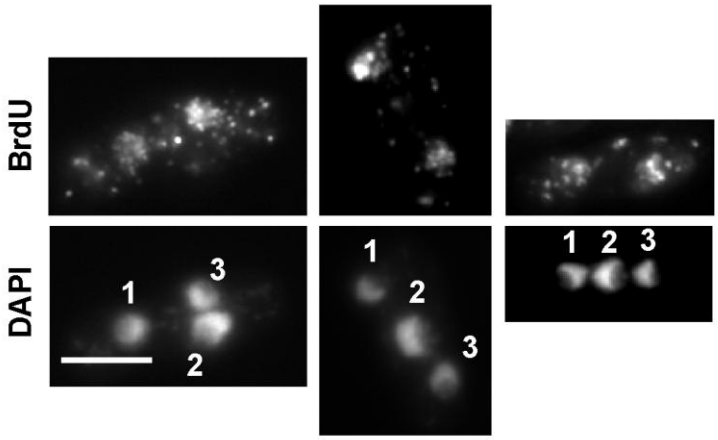

nucleus no.	1	2	3	1	2	3	1	2	3
relative DNA content	1	1.9	1.1	1	2.6	1.2	1.1	1.6	1

We interpret these findings to suggest that in the SIN wee mutants, Rum1 inhibits CDK activity in the undivided nucleus to allow re-initiation of replication. When *rum1* is deleted, increased CDK activity may inhibit re-initiation of S-phase in a fraction of the trinucleate cells. This finding is consistent with our observation that lack of *rum1* attenuates re-replication in *cdc13* s/o.

4.7. Discussion

We set out to determine whether S-phase and M-phase in *S. pombe* are nuclear autonomous or cytoplasmically driven activities. When Wee1 activity was removed from cells, we observed (1) a reduction in synchrony in nuclear division among nuclei of the same cytoplasm. Wee1 activity therefore has a role in coordinating nuclear division in multinucleate cells. (2) In trinucleate cells, nuclei that had undergone asynchronous nuclear division went on to perform DNA synthesis in sync. Timing of DNA synthesis was coordinated, and in the undivided nuclei re-initiation of synthesis was therefore not contingent upon the previous mitosis. (3) Further removal of *rum1* led to partial loss of synchronous DNA synthesis as undivided nuclei in some cells failed to re-replicate. In this study we have assumed that mitosis occurs with nuclear division. We feel that equal segregation of the genome is the most likely consequence of these nuclear divisions, though this has not been formally demonstrated. We have also assumed that the rereplicating nuclei have not initiated mitosis prior to re-initiation of DNA synthesis, but microscopy studies of microtubules could help to provide clarification. We conclude that functions which can inhibit G1/S and G2/M CDK activities play roles in coordinating S-phase and M-phase respectively among multiple nuclei in a common cytoplasm, since in their absence synchrony of DNA synthesis or nuclear division is lost. Since asynchrony

is possible for both S-phase and M-phase, we propose that these activities are nuclear autonomous in multinucleate fission yeast cells, and that the CDK inhibitors Rum1 and Wee1 may act as coordinators to synchronize these cell cycle events in the common cytoplasm. In support of this model, Wee1 is localized to medial cortical nodes, the spindle pole body, and the nucleus in the normal cell cycle, so it is well positioned to coordinate nuclear and cytoplasmic activities (Moseley et al., 2009). Any differences in G2/M CDK activity among nuclei in a multinucleate cell could be buffered or dampened by Wee1 which shuttles in and out of the nucleus. Sister nuclei could then reach the CDK activity threshold for the G2/M transition concomitantly. Some variation in nuclear activity has also been observed in *Xenopus* extracts when wee1 inhibition of Cdc2 is perturbed (Pomerening et al., 2005). More generally, this implies that CDK activity and cell cycle transitions can vary among nuclei residing in the same cytoplasm and within the same cell.

How can the undivided, presumably G2, nucleus in a multinucleate cell be induced to re-initiate DNA replication? One nucleus successfully divides, so APC/C activity must decrease the level of Cdc13 in the cell. We speculate that the overall level of CDK activity decreases, effectively resetting the higher ploidy nucleus to G1 from where it can enter S-phase again. The undivided nucleus in these multinucleate cells 1) likely experiences a drop in CDK activity as its sister nucleus undergoes division and 2) is exposed to MBF-dependent Tos4-GFP, and likely Cdc18 and Cdt1, so it can assemble PreRCs. CDK activity is artificially decreased in *cdc13* s/o where the mitotic cyclin is depleted and in SIN wee cells where Cdc13 must be degraded triggering the sister nucleus to undergo mitosis. In both *cdc13* s/o and SIN wee mutants, an undivided

nucleus re-initiates DNA synthesis and this re-initiation is partially dependent on the presence of the CDK inhibitor *rum1*, so control of CDK activity is important for the ability of a cell to re-initiate DNA synthesis. Past studies show that low level overexpression of *cdc18* and overexpression of *cdt1* alone is insufficient to induce re-replication (Nishitani et al., 2000; Nishitani and Nurse, 1995), so exposure of the undivided nucleus to helicase loaders is unlikely to solely account for its ability to re-replicate. Induction of re-replication in multinucleate cells seems to depend predominantly on the effect of CDK decrease rather than the presence of replication factors present in a G2 nucleus.

In trinucleate cells, we observe that re-replication is attenuated in the absence of *rum1*. The fraction of trinucleate cells with 3 of 3 BrdU positive nuclei decreases but is not completely eliminated, and the fraction with only the two G1 nuclei BrdU positive increases. This raises several questions. First, what can account for the remaining fraction with 3 of 3 nuclei labeled? Is another CDK inhibitor at work in the absence of *rum1* and *wee1*? Second, why would absence of *rum1* inhibit DNA synthesis in this nucleus preferentially over the 2 divided G1 nuclei? One explanation could be that the absolute level of CDK activity is already higher in a nucleus which has not progressed fully through mitosis resetting CDK activity to a low level. Removal of a CDK inhibitor could increase the CDK activity level to above the threshold permissive for PreRC assembly and induction of DNA synthesis. Another explanation is that the divided and undivided nuclei might have different proportions of cyclins contributing to CDK activity. If we consider the divided nuclei to be in G1 and the undivided nucleus to be in G2, the former might have more Cig2-Cdc2 activity and the latter more Cdc13-Cdc2

activity. Since Rum1 is a stronger inhibitor of Cdc13-Cdc2, it would have a more pronounced effect in disinhibiting CDK activity of the undivided nucleus.

How can we reconcile our observation of asynchronous mitosis with cell fusion experiments which rarely detected asynchronous mitosis (Johnson and Rao, 1970; Rao and Johnson, 1970)? A key difference is that the nuclear envelope breaks down in mammalian mitosis, while fission yeast undergo a closed mitosis. Maintaining the nuclear compartment might preserve any degree of heterogeneity in cyclin content or CDK levels. Also, since the 26S proteasome responsible for degrading mitotic cyclin is almost entirely localized within the inner nuclear envelope in fission yeast (Wilkinson et al., 1999), differences in cyclin degradation among nuclei in the same cell could contribute differences in CDK activity among nuclei. *Ashbya gosypii*, in which asynchronous mitosis is normal, also undergoes a closed mitosis and additionally has semipermeable septa dividing segments of the syncytium. The increased density of mitoses at hyphal branchpoints is thought to be mediated by local inhibition of AgSwe1, the Wee1 homologue (Helfer and Gladfelter, 2006), and the spatial range of inhibition may be limited by septa. The extent of compartmentalization of CDK activators and inhibitors allowing differences in CDK activity among nuclei in the same cytoplasm seems to be key in determining synchrony of cell cycle transitions.

Chapter 5

GENERAL DISCUSSION

We set out to investigate the block over re-initiation of S-phase in G2 and the restriction of origin re-firing within S-phase. We also aimed to distinguish whether S-phase and M-phase are nuclear or cytoplasmically driven activities within the cell.

Towards the first aim, we have found that depletion of mitotic CDK activity induces endoreduplication—repeated rounds of a largely normal S-phase program without mitosis. Periodic rounds of DNA synthesis are accompanied by MBF-dependent G1/S gene expression and are re-initiated at doublings close to the normal minimal size for S-phase. Mostly mitotic S-phase origins and some additional origins are activated coordinately to result in even replication of the genome. Further, endoreduplication is attenuated upon deletion of cyclins or *rum1*. This would be expected to lower and raise CDK activity respectively and possibly to abolish feedback loops driving periodic oscillation of CDK activity. We therefore conclude that 1) G2/M CDK activity inhibits re-initiation of S-phase in G2, since in its absence a mostly normal S-phase program is induced and 2) CDK levels and/or oscillation are likely to be important for the ability to endoreduplicate.

Replication in the presence of excess helicase loaders did not resemble endoreduplication. Therefore, regulation of helicase loaders can at best only partially account for the block to re-initiation mediated by the G2/M CDK. DNA synthesis was continuous, not re-initiated at discrete cell sizes and was not accompanied by G1/S gene expression. While most of the genome was restricted to approximately even replication

using mitotic S-phase origins together with some newly activated origins, specific S-phase origins escaped this regulation and re-fired leading to local amplification.

We identified AT-richness as the strongest predictor of a re-firing origin, a feature that is associated with early and efficient firing in S-phase, which in turn is correlated with nucleosome depletion (Field et al., 2008). Since these origins were also embedded within extended intergenic regions, we speculate that location in long, open stretches of nucleosome-depleted chromatin makes origins more accessible to replication factors and machinery, potentiating re-firing. Through origin deletion and integration studies we have demonstrated that specific origins are necessary for local amplification but sufficient to induce amplification only within a permissive chromosome context. We propose that the ability of an origin to re-fire, leading to local amplification, is not determined by a single parameter. Rather, a combination of sequence features, most importantly AT-richness, and position within the chromosome determines amplification behavior.

In multinucleate fission yeast the ability of nuclei to undergo asynchronous mitosis was revealed by depleting Wee1 which inhibits CDK activity. We assessed the simplest product of an asynchronous mitosis, trinucleate cells, finding that DNA synthesis remained highly synchronous despite lack of prior division in one of the three replicating nuclei. Synchrony of DNA synthesis among the three nuclei was partially lost in the absence of CDK inhibition by *rum1*, and the undivided nucleus failed to re-initiate S-phase. We conclude that S-phase and M-phase can be driven in a nuclear autonomous fashion in the absence of Rum1 and Wee1 and that regulation of CDK activity may normally serve to coordinate synchronous cell cycle transitions in multinucleate cells.

The DNA synthesis induced by perturbing normal CDK activity and PreRC formation resembles forms of overreplication found in nature (Figure 5.1). By depletion of G2/M CDK, endoreduplication is induced where cells progress through alternating synthesis and gap phases. Since MBF-dependent G1/S gene expression accompanies each S-phase at least part of the Gap must consists of a G1-like phase. In overexpression of helicase loaders there is no Gap as cells continuously synthesize DNA. Since around 90% of the genome is approximately evenly replicated on average, this suggests that coordination of origin firing is maintained for much of the genome, and is lost chiefly at specific origins which re-fire leading to local amplification. Since we have evaluated a bulk culture at a single point in time, it is not possible to ascertain how DNA content at different regions in the genome increases over time. One possibility shown in Figure 5.1 is that the genome is replicated in rounds with the 9 amplifying origins re-firing in a fraction of rounds, and possibly with other origins re-firing less frequently thereby leading to lower levels of amplification.

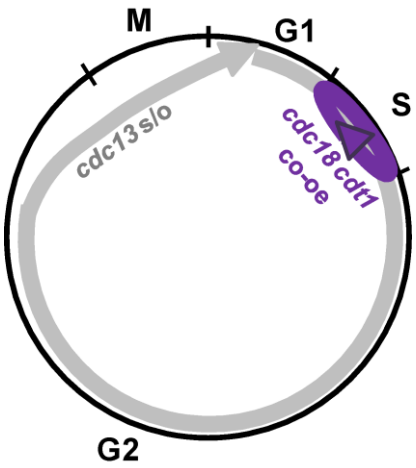

Figure 5.1 Abbreviated cell cycles in re-replicating mutants

In *cdc13* s/o (grey), endoreduplication occurs and post S-phase cells return to G1, bypassing mitosis. In *cdc18 cdt1* co-oe (purple), one model to explain our microarray results would be that cells progress continuously through rounds of S-phase and re-firing occurs mainly at the 9 privileged origins identified in our study to result in local amplification.

Our results in the *cdc13* s/o cells and the multinucleate cells can be considered jointly according to CDK activity. In a trinucleate cell, the nucleus which fails to undergo division but re-initiates S-phase resembles an endoreduplicating nucleus. Viewed through the scope of the quantitative model (Fisher and Nurse, 1996; Stern and Nurse, 1996), in both situations G2/M CDK activity is depleted, and without passage through mitosis, DNA synthesis is re-initiated. The overreplicating nucleus of the trinucleate cell is unlikely to have an intrinsic oscillator as in *cdc13* s/o, rather Cdc13 degradation in the cell due to the mitosis of the sister nucleus may reset the undivided nucleus to G1. In both cases, absence of G2/M CDK activity may trigger the bypass of mitosis and the return to G1, from which point S-phase can be re-initiated. In both *cdc13*

s/o and the trinucleate cells, re-replication was attenuated in the absence of *rum1*, suggesting Rum1 has a role in maintaining CDK activity at a level permissive for PreRC re-loading. Our experimental results are interpreted via the quantitative model in Figure 5.2, in some cases showing alternate explanations for replication behavior. For re-initiation of S-phase, activity must begin at a low level which permits PreRC assembly at origins and must rise to the threshold triggering S-phase. For periodic re-initiation, activity must not remain above the inhibitory threshold for S-phase but must oscillate between a low level permitting PreRC formation and an intermediate level initiating S-phase.

Figure 5.2 Schematic of CDK activity levels in cdc13 s/o and multinucleate cells

Shown are models of changing CDK activity in time to provide potential explanations for our experimental observations. We draw these to illustrate how we are thinking about possible patterns of CDK activity, but variations of these models could also be possible and the precise patterns are not known.

A) Wild type cells begin the cell cycle with a low level of CDK activity necessary for PreRCs to load. Activity rises reaching a threshold which triggers S-phase; after S-phase, re-initiation is inhibited. A sharp peak of CDK activity triggers mitosis. APC/C degradation of Cdc13 brings down CDK activity to begin the cycle anew in G1.

B) In *cdc13* s/o (grey) CDK activity oscillates between a level permissive for PreRC loading and a level that triggers S-phase initiation. Feedback loops between Cig2-Cdc2 and Rum1 and/or Cig2-Cdc2 and MBF could drive this oscillation. When *rum1* or *cig2* is deleted cells progress through one DNA doubling but do not re-initiate subsequent S-phases. In *Δrum1 cdc13* s/o (green) this can be attributed to an oscillation of CDK activity at levels which do not permit PreRC loading and therefore block S-phase (green solid) and /or lack of oscillation (green dashed). In *Δcig2 cdc13* s/o (blue), CDK activity may not reach the level required for S-phase (blue solid) and/or may not oscillate (blue dashed). Failure to re-replicate at all in *Δcig1 Δcig2 cdc13* s/o suggests that CDK activity may be very low and likely not oscillating (red).

C) and **D)** represent two nuclei of a binucleate SIN wee cell which undergoes asynchronous mitosis. Wee1 inhibition of CDK activity during G2 maintains a plateau of CDK activity at an intermediate level. Lack of inhibition by Wee1 would be expected to result in a steadily increasing CDK activity level throughout G2, leading to M. When **C)** undergoes division and **D)** fails to divide, the cell becomes trinucleate. APC/C activity of **C)** likely decreases CDK activity of **D),** allowing PreRC loading despite lack of previous mitosis. Both daughter nuclei of **C)** and the undivided nucleus **D)** then go on to initiate DNA synthesis in synchrony with **D)** re-replicating.

E) and **F)** represent two nuclei of a binucleate *Δrum1* SIN wee mutant cell which undergoes asynchronous mitosis. Rum1 inhibition of CDK activity during M/G1 is thought to maintain a plateau of CDK activity at low level. Absence of Rum1 would be expected to result a steady increase in CDK activity during G1. Lack of inhibition by Rum1 and Wee1 would result in higher CDK activity throughout G1 and G2. When **E)** divides and **F)** does not, the cell becomes a trinucleate. CDK activity in both nuclei decreases owing to APC/C activity associated with the dividing nucleus **E)**. In the absence of *rum1*, CDK activity in a subset of undivided nuclei such as **F)** may be too high to allow PreRC loading so re-replication does not occur. Both daughter nuclei of **E)** then go on to initiate DNA synthesis while **F)** does not, so within the cell S-phase is not synchronous. In some undivided *Δrum1* SIN wee nuclei, CDK activity is low enough to permit PreRC assembly in G1 and the G2 nucleus re-initiates S-phase as in **D)**.

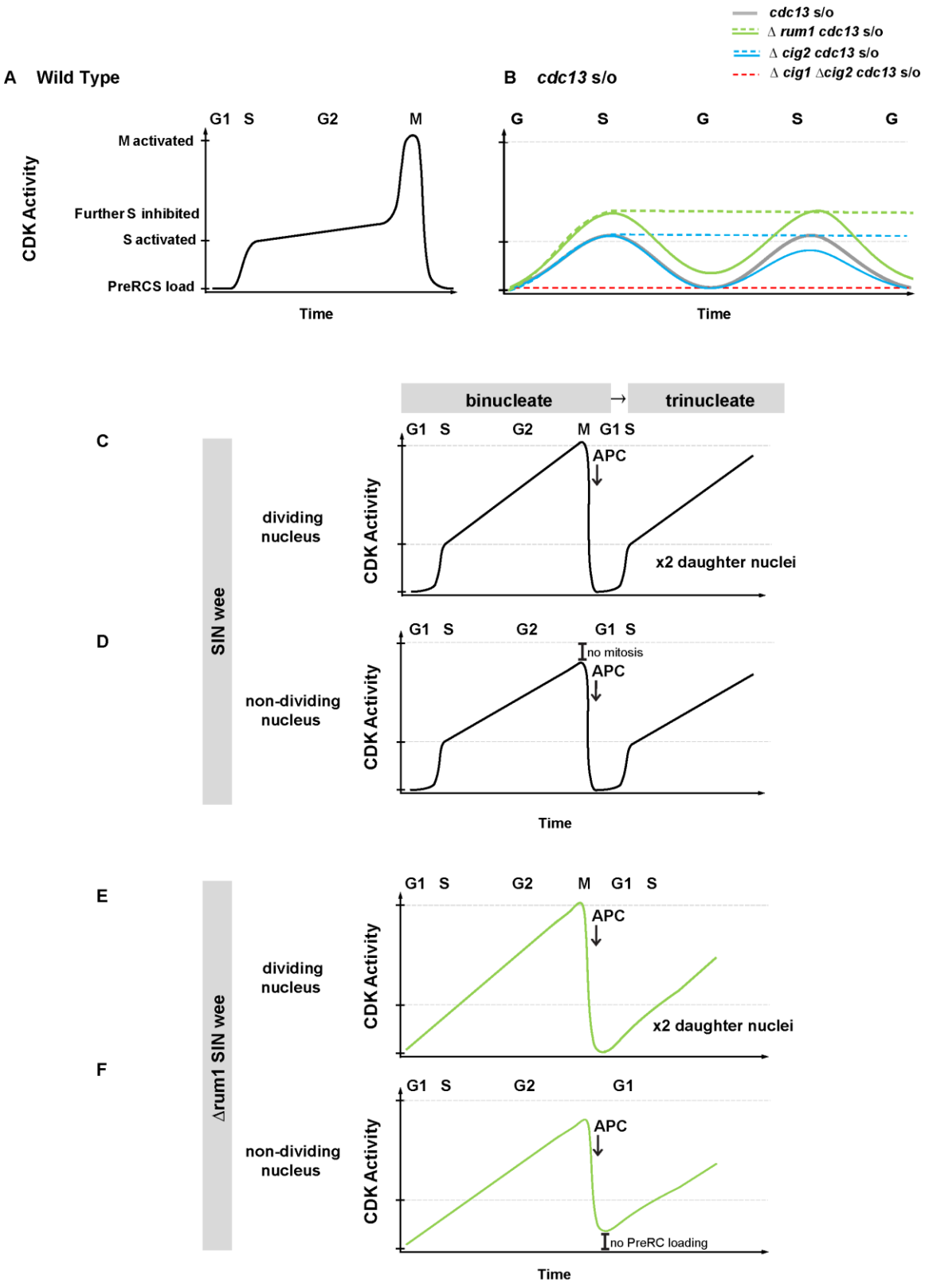
A Wild Type
B cdc13 s/o
cdc13 s/o
Δ rum1 cdc13 s/o
Δ cig2 cdc13 s/o
Δ cig1 Δcig2 cdc13 s/o
G1 S G2 M
M activated
Further S inhibited
S activated
PreRCS load
CDK Activity
Time
G S G S G
Time
binucleate → trinucleate
C
D
SIN wee
dividing nucleus
non-dividing nucleus
G1 S G2 M G1 S
APC
x2 daughter nuclei
G1 S G2 G1 S
no mitosis
APC
CDK Activity
Time
E
F
Δrum1 SIN wee
dividing nucleus
non-dividing nucleus
G1 S G2 M G1 S
APC
x2 daughter nuclei
G1 S G2 G1
APC
no PreRC loading
CDK Activity
Time

The principles established by the cell fusion experiments of Rao and Johnson can be attributed to modulation of CDK levels in time and among nuclei in a common cytoplasm. In fission yeast 1) re-initiation of S-phase in G2 may be inhibited by maintenance of CDK activity above a critical threshold and 2) S-phase and mitosis may be nuclear driven activities and inhibition of CDK activity may coordinate uniform CDK activity levels among nuclei so that S-phase and M-phase occur in synchrony.

Chapter 6

MATERIALS AND METHODS

6.1. Fission yeast growth conditions

Standard growth conditions and methods were used (Moreno et al., 1991); all experiments were performed in EMM4S (Edinburgh Minimal Medium with supplements) unless otherwise stated.

6.2. Strains and strain construction

Strains used in this thesis are listed in Table 6.1.

Tetrad analysis was performed for each cross unless otherwise noted.

6.2.1. BrdU pulse labeling strains

The *S. pombe* strain for pulse labeling, *leu1-32 ade6-210 his7-366 adh1-tk-his7+ adh1-hENT1-leu1+ h-* contains the human nucleoside transporter, *hENT*, and thymidine kinase from herpes simplex virus, *tk* (Sivakumar et al., 2004). With the plasma membrane transporter hENT, cells can take up exogenous thymidine or a thymidine analog and phosphorylate it to dTMP using thymidine kinase; the exogenous nucleotides are incorporated into DNA during replication. Though pJL218 is linked to the *his7* gene, it has been integrated randomly, not at the *his7* locus. The pFS181 integrant contains multiple copies at an unknown number of loci. This strain is healthy and has the same mass doubling time as wild type cells (Sivakumar et al., 2004).

Table 6.1. Strains used in this thesis

*strains originating in this study

Genotype	Additional names/ shorthand	Lab collection No.
leu1-32 ura4-D18 ade6-210 his7-366 adh1-tk-his7+ adh1-hENT-leu1+ h-		PN10597
wee1-50 adh1-hENT-leu1+ adh1-tk-his7+ leu1-32 his7-366		PN10632*
ade6-M210 tos4-GFP-kanMX6 h-		PN10633*
wee1-50 ade6-M210 tos4-GFP-kanMX6 h-		PN10634*
cdc25-22 ade6-M210 tos4-GFP-kanMX6		PN10635*
Δcdc13::ura4+ pREP45 cdc13+ ade6-704	cdc13 s/o	PN1414
Δcdc13::ura4+ pREP45 cdc13+ adh1-hENT-leu1+ adh1-tk-his7+	AK10-3	PN10636
Δcdc13::ura4+ pREP45 cdc13+ ade6-704 tos4-GFP-kanMX6		PN10637*
cdc10-v50 Δcdc13::ura4+pREP45 cdc13+ ade6-704 tos4-GFP-kanMX6		PN10638*
Δcig2::ura4+ Δcdc13::ura4+ pREP45 cdc13+ h-		PN10639*
Δcig1::ura4+ Δcig2::ura4+ Δcdc13::ura4+ pREP45 cdc13+		PN10640*
Δrum1::ura4+ Δcdc13::ura4+ pREP45 cdc13+ adh1-hENT-leu1+ adh1-tk-his7+		PN10641*
cdc25-22 rep3x-cdc18+ leu1-32 ura4-D18 h-	*cdc18* oe	PN1803
cdc25-22 rep3x-cdc18+ pREP4-cdt1+ leu1-32 ura4- h-	*cdc18 cdt1* co-oe	PN3613
cdc25-22 rep3x-cdc18+ pREP4-cdt1+ adh1-tk-his7+ adh1-hENT1-ade6+ leu1-32 ura4-D18 his7-366 ade6-210 h+	KK61E	PN10642*
cdc25-22 rep3x-cdc18 pREP4-cdt1 leu1-32 ura4-D18 tos4-GFP-kanMX6		PN10643*
Δori2040.0.0:: kanMX6 cdc25-22 rep3X-cdc18+ pREP4-cdt1::ura4 ade6-D1 ura4-D18 leu1-32 h-		PN10644*
Δori2040.0.0:: kanMX6 ars2004::2040.0.0-ade6+ cdc25-22 rep3X-cdc18+ pREP4-cdt1::ura4 ade6-D1 ura4-D18 leu1-32		PN10645*
ars2004::2040.0.0-ade6+ cdc25-22 rep3X-cdc18+ pREP4-cdt1::ura4 ade6-D1 ura4-D18 leu1-32		PN10646*
Δori2040.0.0:: kanMX6 C19F5.02::2040.0.0-ade6+ cdc25-22 rep3X-cdc18+ pREP4-cdt1::ura4 ade6-D1 ura4-D18 leu1-32		PN10647*
Δori3049.0.0:: kanMX6 cdc25-22 rep3X-cdc18::leu1 pREP4-cdt1::ura4 ade6-D1 ura4-D18 leu1-32		PN10648*
cdc15-287 h-	SIN	PN1439
cdc15-287 wee1-50	SIN wee	PN10649*
cdc15-287 wee1-50 tos4-GFP-kanMX6	SIN wee *tos4-GFP*	PN10650*
cdc15-287 wee1-50 adh1-hENT-leu+ adh1-tk-his7+ leu1-32 his7-366	SIN wee *tk hENT*	PN10651*
Δrum1::kanMX6 cdc15-287 wee1-50 adh1-hENT-leu+ adh1-tk-his7+ leu1-32 his7-366	Δ *rum1* SIN wee	PN10652*

6.2.2. Tos4-GFP

SPAP14E8.02 was tagged with a single copy of GFP (S65T) with a *kanMX6* cassette at the C-terminus using a PCR-based method (Bähler et al., 1998) and referred to as *tos4-GFP*. The integration was checked by PCR.

6.2.3. *cdc13* s/o *cig1* and *cig2* deletion strains

*cdc13*Δ*::ura4+ pREP45 cdc13+ adh1-hENT-leu1+ adh1-tk-his7+ h-* was crossed to PN1401 *Δcig1::ura4+ Δcig2::ura4+ ura4-D18 h+*. After tetrad dissection, ura+ re-replicating isolates were screened by PCR to distinguish whether *cig1, cig2* or both were deleted.

6.2.4. *Δrum1 cdc13s/o* strain

Rum1 was deleted in *h- cdc13*Δ*::ura4+ pREP45 cdc13+ adh1-hENT-leu1+ adh1-tk-his7+* by gene replacement with a kanamycin resistance cassette according to the methods in (Bähler et al., 1998). Deletion was confirmed by PCR.

6.2.5. Creation of *cdc18 cdt1* co-oe strain for BrdU pulse labeling

6.2.5.1. Crosses

Strains and cloning were constructed in collaboration with Atanas Kaykov, so the strains and plasmid are called **K**aykov **K**iang (KK). The strain yFS240 (obtained from Nick Rhind) *leu1-32 ura4-D18 ade6-210 his7-366 adh1-tk-his7+ adh1-hENT1-leu1+ h*$^{-}$ was crossed to strain AK32 *leu1-32 ura4-d18 his7-366 h+* to yield strain KK1 *leu1-32 his7-366 adh1-tk-his7+ ade6-210 ura4-d18 h+*. KK1 was transformed with linearized plasmid pKK1 (described below) containing *adh1-hENT1-ade6+* for plasmid integration. The progeny KK2 (LK53) *leu1-32 his7-366 adh1-tk-his7+ ade6-210 adh1-hENT1-ade6+*

ura4-d18 h+ were crossed to strain KK5 *rep3x-cdc18 pREP4-cdt1+ leu1-32 ura4-d18 his7-366 ade6-210 h-*. KK5 was generated first by crossing PN559 *ade6-210 leu1-32 ura4-d18 h-* to AK32 to yield KK3 *leu1-32 ura4-D18 his7-366 ade6-210 h+*, which was then crossed to PN3613 *cdc25-22 rep3x-cdc18+ pREP4-cdt1+ leu1-32 ura4-D18 h-* to yield KK5 (LK67). The progeny of the KK2 and KK5 cross were KK7 (LK83) *rep3x-cdc18 pREP4-cdt1+ adh1-tk-his7+ade6+*; KK7 was crossed to *cdc25-22 ade6-210 his7-366 leu1-32 ura4-D18 h-* to yield KK61E, *cdc25-22 rep3x-cdc18+ pREP4-cdt1-ura+ adh1-tk-his7+ adh1-hENT1-ade6+ leu1-32 ura4-D18 his7-366 ade6-210 h+*, the final pulse labeling strain. Crosses were done by random spore analysis.

6.2.5.2. pKK1 cloning

To create the *adh1-hENT-ade6+* shuttle vector pKK1, *pFS181 (adh1-hENT1-leu1+)* was cut with AatII and PflM1. The fragment containing *adh1-hENT ampR* was gel purified, blunt ended using T4 DNA polymerase and 3' phosphate was removed by Calf Intestinal Phosphatase reaction to prevent self-ligation. A fragment of pFS119 containing *ade6* was generated by digestion with BstB1 and SpeI and gel purified. The fragment and vector were ligated using T4 DNA ligase and transformed into *E. coli* by the TOPO/genequick kit. DNA preps were cut with AatII and BlpI to ensure that the linearized plasmid was of the right length, about 7.1 kb. Both AatII and BlpI are unique cutters for the newly constructed plasmid pKK1 and both cut within the insert, ade6. The plasmid was linearized by digestion with BlpI and was used to transform Strain KK1 according to a Cold Spring Harbor course protocol. From colonies, tested KK2 (LK53) isolates by pulse labeling for the presence of *hENT* and *tk*.

6.2.6. Origin 2040.0.0 and 3049.0.0 deletion and integration strains

Deletion of origins was accomplished by gene replacement with a Kanamycin resistance cassette (Bähler et al., 1998). Origins 2040.0.0 and neighboring origins under the amplification peak (origin 2039.0.0 and origin 2042.0.0) as well as origin 3049.0.0, and its neighbor under the peak origin 3048.0.0 were each deleted in separate strains. Ars2004 (origin 2050.0.0) was also deleted with *kanMX6* before integration of the ectopic origin 2040.0.0. Origin 2040.0.0 was integrated ectopically at ars2004 (origin 2050.0.0) and at SPAC19F5.02 on chromosome II as follows: A 3650 bp fragment of origin 2040.0.0 was first cloned into the SmaI site of pFS119, and a 921bp fragment of ars2004 was cloned into the SmaI site of pFS119 as a control. Using these templates, primers specific to the sites of integration (the endogenous ori2040.0.0 site, ars2004 on the left arm of Chromosome II and C19F5.02 on the right arm of Chromosome II) were used to PCR amplify fragments containing ade6 and the origin of interest. Fragments were digested with AvrII and SpeI then transformed into *Δori2040.0.0:: kanMX6 ade6-D1 ura4-D18 leu1-32* or *h+ Δars2004:: kanMX6 ade6-D1 ura4-D18 leu1-32 h+* cells. Correct integration was checked by PCR, then strains were crossed to PN3613 *cdc25-22 rep3x-cdc18+ pREP4-cdt1+ leu1-32 ura4-D18 h-*. Crosses were performed and after random spore analysis, proper integrations were confirmed by PCR.

6.2.7. *Δrum1* SIN wee mutant

Rum1 was deleted in *cdc15-287 wee1-50 adh1-hENT-leu1+ adh1-tk-his7+ leu1-32 his7-366* by gene replacement with a *KanMX6* according to the methods in (Bähler et al., 1998). Deletion was confirmed by PCR.

6.3. BrdU pulse labeling

BrdU pulse labeling and immunofluorescence processing was performed as described (Sivakumar et al., 2004) using 10 minute pulses of 300μM BrdU.

6.4. Use of Tos4-GFP as a marker of MBF-dependent gene expression

6.4.1. Growth conditions and microscopy

Tos4-GFP strains were grown in EMM4S with 750 mg/l adenine to reduce autofluorescence (P. Perez, personal communications). Cells were visually scored for the presence of strong GFP signal.

6.4.2. Cell cycle analysis of Tos4-GFP: G2 block and release

Cdc25-22^{ts} ade6-M210 tos4-GFP-kanMX6 cells grown to 1.2 x10^6/ml were synchronized by shifting to 36.5°C to block cells in G2, then releasing cells synchronously into the cell cycle at 25°C.

6.4.3. *cdc10*-dependence of Tos4-GFP: G1 block

For a *cdc10* block without re-replication, a *cdc10-v50* Δ*cdc13::ura4+pREP45 cdc13+ ade6-704 tos4-GFP-kanMX6* culture in the absence of thiamine was grown to 1.2 x10^6/ml and shifted to 36.5°C.

6.5. Induction of re-replication

6.5.1. Induction of overreplication in *cdc13* s/o

To induce re-replication in *cdc13* s/o for pulse labeling, Δ*cdc13::ura4+ pREP45 cdc13+ ade6-704 adh1-hENT-leu1+ adh1-tk-his7+* (from Atanas Kaykov) cells grown at 25°C to 3.6 x10^6/ml were filtered, washed 4 times with EMM-N, and resuspended at 2.4 x10^6/ml in EMM-N. After 12 hours, 5 μg/ml thiamine was added to the culture; 8 hours later NH_4Cl was added back to the culture with all supplements and the culture was

shifted to 32°C to begin the time course. The same protocol was used for Δ*cdc13::ura4+ pREP45 cdc13+ ade6-704 tos4-GFP-kanMX6*. To impose a *cdc10* block and release in endoreduplicating cells, re-replication was induced as above in *cdc10-v50* Δ*cdc13::ura4+ pREP45 cdc13+ ade6-704 tos4-GFP-kanMX6* cells at 25°C. Once cells had begun endoreduplication, cells were shifted to 36.5°C at 6h; they were then released synchronously into endoreduplication to 25°C at 9h. For origin mapping studies, re-replication was induced in Δ*cdc13::ura4+ pREP45-cdc13+ ade6-704* cells by 5 hours of nitrogen starvation at 25°C in the presence of thiamine 5 μg/ml. Cultures were then shifted to 32°C while NH_4Cl and all supplements were added back, with or without 11 mM HU.

6.5.2. Induction of overreplication in *cdc18 cdt1* co-overexpression

An exponentially growing *cdc25-22 rep3x-cdc18 pREP4-cdt1+ leu1-32 ura4-D18* culture or variants containing *tk* and *hENT or tos4-GFP* in media containing 5μg/ml thiamine was filtered and resuspended in media lacking thiamine to derepress the nmt1 promoter. After 11 hours, the culture was shifted to 35.5°C or 36.5°C. The onset of overreplication occurs sooner at 35.5°C but the extent of overreplication is the same at both temperatures.

To determine the efficiency of ori2040.0.0 firing in ectopic loci, exponentially growing cultures of the *cdc18 cdt1* co-overexpression strain *cdc25-22 rep3x-cdc18+ pREP4- cdt1+ leu1-32 ura4-D18 h-,* the ars2004::2040 strain *Δori2040.0.0::kanMX6 ars2004::2040.0.0-ade6+ cdc25-22 rep3X-cdc18-leu1+, pREP4-cdt1-ura4+ ade6-D1 ura4-D18 leu1-32,* and the C19F5.02:: 2040 strain *Δori2040.0.0::kanMX6 C19F5.02::2040.0.0-ade6+ cdc25-22 rep3X-cdc18-leu1+, pREP4-cdt1+ ade6-D1 ura4-*

D18 leu1-32 were synchronized by shifting up to 36.5°C for 3.5 hours. Upon release to 25°C, cultures were split and 11mM HU was added to half each culture. At 120 minutes after release cells were harvested by filtration and washed in ice-cold MOPS buffer with and then without 0.1% sodium azide. Genomic DNA was extracted as previously described (Heichinger et al., 2006). The fold-increase over one was determined for ori2040.0.0 at its native locus and at the ars2004 and quiet loci by quantitative PCR. Values were normalized to the same non-origin region as in the amplification studies above; non-firing regions are also shown for comparison.

6.6. Microarray experiments

Microarray design, DNA preparation, microarray hybridizations as well as data acquisition and analysis were as described for HU experiments in (Heichinger et al., 2006). Data analysis was based on the genome sequence of June 2006. This and current sequence data can be obtained from the Sanger Institute ftp server at ftp://ftp.sanger.ac.uk/pub/yeast/pombe/Chromosome_contigs/. Microarray data are available at ArrayExpress, accession numbers E-MTAB-105 and E-MTAB-139. At least two biological repeats were carried out for each microarray experiment. In some cases signal ratios for wild type mitotic S-phase have been reassigned in mapping the 904 origins, so efficiencies for 3.8% (34/904) of origins deviate from (Heichinger et al., 2006) and from (Lygeros et al., 2008) (31/904). For all analysis, cv values >30% have been removed.

The cdc13 experiment without HU was performed twice using ORF arrays and once in conjunction with intergenic arrays; the reference DNA from G1-arrested cells was also used for the self:self. The reference DNA for all other microarray experiments

was from cells blocked in G2 with 2C DNA content. Data from two biological repeats were averaged for origin mapping in *cdc13* s/o.

Each *cdc18 cdt1* co-oe origin mapping profile depicts the average of two experiments analyzed using ORF and intergenic tiling microarrays. Amplification profiles comparing *cdc18* oe and *cdc18 cdt1* co-oe are each the average of duplicate ORF array experiments, and a moving average is shown. Control amplification profiles in all other figures depict the clearest representative profile: for chromosomes I and II this is the origin 3048.0.0 deletion strain since deletion has no effect on amplification and the profile is unaltered; on chromosome III it is the origin 2040.0.0 deletion for which the amplification profile is also the same.

%AT-content was defined as the highest %AT in a 500 bp window (50 bp step) in the intergenic region with at least 65% AT-richness that maps to or close to the origin. Intergenic length refers to the number of base pairs in the intergenic region to which the AT-rich island of the origin maps. Efficiency of origins was determined as in (Heichinger et al., 2006).

6.7. Analysis of PreRC colocalization with origins

A custom made Perl script was used to map signal $\log_2$ ratios from genome-wide ChIP on chip analysis by Hayashi et al. to each origin in our study. Briefly, among probes with p-values which conform to the criteria described in Hayashi et al. (>0.025), it detects the peak signal ratio in the vicinity of origins by performing iterative searches for a defined threshold within increasing range of the origin. The data from this analysis using a cutoff signal $\log_2$ ratio of 0.5 and range of 4 kb about the origin were pooled (from

highest to lowest threshold). Our second more stringent analysis followed a cutoff of signal $\log_2$ ratio greater than 0.8 as in Hayashi et al.

6.8. Quantitative PCR

For quantitative PCR, genomic DNA was isolated as described (Heichinger et al., 2006). DNA was diluted to 0.0625 ng/µl and mixed with relevant primers and SYBR Green PCR mix (Applied Biosystems) and analyzed with an Applied Biosystems 7900HT system. The starting quantity of DNA was estimated from the number of cycles (Ct value) required to reach the threshold.

6.8.1. qPCR primers

Primers specific to the centers of origins 2040.0.0, ars2004 (also contained within the integrated fragments) and 3049.0.0, as well as regions to the left and right of the ori2040, ars2004 and C19F5.02 loci and control non-origin regions were designed (Table 6.2). The Ct value for each region in all experiments was normalized to the same non-origin region. The relative quantity of DNA for each region was determined, dividing by the value for the corresponding region in the G2-blocked reference to exclude any effect of primer pair variability. At least two primer pairs were used to probe each region, and each primer pair was used at least in duplicate in each experiment; results were averaged for the region. Representative data are shown.

Table 6.2 Quantitative PCR primers used

region	primer number	sequence
non-origin control region	21_FW	CTTCGTCCCATCGACGCTTAA
	21_RV	ACAGAGCACTGGAGCAAGAAAAAAG
ori2040.0.0 region	14_FW	AGCCAGATGTGTTGAAATAGGCGAC
	14_RV	CCCTAGAGCATTGCGCTACCT
	15_FW	GCTTCCATAGACAGCGCCATTCTA
	15_RV	CCTCAGCTTCAGCAGGTAGCAAAG
	16_FW	GCAAAGCAACAAGAACTTCAACCAC
	16_RV	TGTAACAGGTTCGGCTCAATCTCTC
ars2004 region	40_FW	CGATACAGTTAATCCTGCCGACCC
	40_RV	GGATCCATTCTCGGCATTTTGTC
	41_FW	AAAGGTTCATCTCGCCGGAATTC
	41_RV	AGAGCAGCTTGTCGATTGCGTTC
C19F5.02 quiet region	61_FW	TCGAGCGAAAGGATACGAGACGT
	61_RV	TATTTGACATTAGTGGTGGCCCAG
	62_FW	CGCCAACTTCAATGAAACTGAGCA
	62_RV	CCGCGGGTCTGAACATGTGAATA
	63_FW	AGAATGGCGTTGTACGCTCCAAC
	63_RV	AGCACCCAGCGACCTATACAGCT
3049.0.0 region	25_FW	ATGTCTGCTGCTGAAAAGAAACCC
	25_RV	CGCTTCTTATCAGCAGACTTCATG
	26_FW	CCCGTGAAATCCAGACTGCTGTT
	26_RV	CGGATTTGGTACCTTCGGTAACG
	27_FW	AACAACACAGGTGCAGCACATCAC
	27_RV	CAACTCCACGAACCGGTCATAGA
non-firing region	33_FW	AAGCTTTAAGCGAAAGCACGCAG
	33_RV	CCCATTGACGTTGTCTAGCTCTCG
non-firing region	64_FW	AGGTTGGGTAGGAGAGTGCGTTT
	64_RV	ATTCCCTGGTAGAGCCTATTGCCC
2040.0.0 efficiency test	86_FW	GCTTCTTTATGGGTCACAAAGGTGT
	86_RV	CATTGCACAACTTTAAGAGTGTTGGA

6.9. Microscopy and cell measurements

Microscopy was performed on a Zeiss Axioplan 2 using a 63x objective, Photometrics Coolsnap HQ camera and Metamorph software, and cell length and width measurements were done in ImageJ. Cell volume (fL) was calculated by estimating the shape of the cell as a cylinder with a half-sphere at each end. Cells from the 0-3 hour time points in the *cdc13* s/o pulse labeling experiment were excluded from analysis as BrdU signal was not reliably detectable in those cells, potentially due to prior nitrogen starvation.

6.9.1. Cell measurements

To find the cell volume per nucleus, we considered binucleate and septated cells as two nuclei within a single cell. All cell volumes were binned in discrete intervals, and the percentage of nuclei that incorporated BrdU in each volume cohort was determined. Experiments were performed at least in triplicate unless otherwise noted; representative data are shown.

6.9.2. Quantitation of DNA content by DAPI staining

DNA content of nuclei in multinucleate cells was estimated as:

(average pixel intensity of nucleus in medial plane – background intensity of cytoplasm) x area of nuclear cross section

Relative DNA content of nuclei within a cell was then determined by dividing each nucleus' value by the lowest value for that cell. Similar results were obtained using the sum of a Z-stack rather than a single medial plane.

Chapter 7: APPENDIX

List of DNA replication origins

Origin no.: In sequential order of the chromosomes (first digit); includes the positions for all 904 mitotic S-phase origins (Kiang et al., 2009) and the additional origins that are active in the *cdc13 s/o* and *cdc18 cdt1* co-oe backgrounds. Origin numbers have the format xxxx.x.x. The first four digit number represents the 401 ‘strong‘ origins mapped in (Heichinger et al., 2006). The second number describes the order of the 503 ‘weaker‘ origins which fall between strong origins. The third number denotes additional origins not activated in mitotic S-phase by their position between S-phase origins and ends with “r” for **r**e-replication. All 401 strong origins mapped in (Heichinger et al., 2006) have the suffix 0.0.

Class:

1) Origins that are active in the mitotic cell cycle only, and not in the *cdc13* s/o or *cdc18 cdt1* co-oe backgrounds

2) Origins that are active in the mitotic cell cycle and in the *cdc13* s/o background, but not in *cdc18 cdt1* co-oe

3) Origins that are active in the mitotic cell cycle and in the *cdc18 cdt1* co-oe background, but not in *cdc13* s/o

4) Origins that are active in the mitotic cell cycle and in the *cdc18 cdt1* co-oe and *cdc13* s/o backgrounds, but do not amplify

5) Origins that are active in the mitotic cell cycle and in the *cdc18 cdt1* co-oe and *cdc13* s/o backgrounds and amplify

6) Origins that are active in the *cdc13* s/o background only, and not in the mitotic cell cycle or *cdc18 cdt1* co-oe

7) Origins that are active in the *cdc18 cdt1* co-oe background only, and not in the mitotic cell cycle or *cdc13* s/o

8) Origins that are active in the *cdc13* s/o and *cdc18 cdt1* co-oe backgrounds, but not in the mitotic cell cycle

Central Map Position: Position of the microarray probe that gave the highest signal ratio within the peak where the origin was mapped on the microarray profiles.

Central Probe: Name of the gene that is closest to the central map position where the origin was mapped on the microarray profiles.

Gene AT island L and R: Name of the left and right gene, respectively, flanking the intergenic region containing the AT-rich island to which the origin maps.

%AT content: defined as the highest %AT in a 500 bp window (50 bp step) in the intergenic region with at least 65% AT-richness that maps to or close to the origin.

IG length: Intergenic length refers to the number of base pairs in the intergenic region to which the AT-rich island of the origin maps.

IG context: direction of transcription about the intergenic region to which the origin maps. Convergent (conv), divergent (div), tandem (tan), centromeric (cen)

Mitosis, *cdc13* s/o efficiency, *cdc18 cdt1* co-oe efficiency: determined as in (Heichinger et al., 2006). Entries in bold type indicates entries that were changed with respect to the list published in (Lygeros et al., 2008). These changes were made on the basis of fine-mapping origins and efficiencies with respect to the position of AT-rich islands of the complete set of mitotic origins, which were identified for the present analysis (see Materials and methods).

Orc4 ≥ 0.5, ≥ 0.8 (Y/N): Comparison to Orc4 ChIP on chip analysis of Hayashi et al. Indicates whether Orc4 localizes to the intergene containing the origin at or above a threshold of signal $\log_2$ ratio 0.5 or 0.8, respectively (Materials and methods).

Origin No.	Class	Central Map Position	Central Probe	Gene AT island L	Gene AT island R	% AT	IG Length (bp)	IG Context	Replication Time Mitosis (min)	Mitosis Efficiency	*cdc13* s/o Efficiency	*cdc18cdt1* co-oe Efficiency	Orc4 signal ≥ 0.5 (Y/N)	Orc4 signal ≥ 0.8 (Y/N)
1000. 1. 0	4	14270	c212.06c	c212.07c	c212.06c	74.6	3486	tan	85	4	0	0	Y	Y
1000. 2. 0	4	31133	c212.01c	c977.01	c977.02	75.8	1513	tan	85	5	0	4	Y	Y
1000. 2. 1r	8	72882	prl37	c977.17	pj695.01c	75.4	8638	conv			10	10	Y	Y
1001. 0. 0	4	90532	C1F8.04c	c1f8.04c	isp3	73.8	2128	div	80	**0**	7	14	Y	Y
1001. 0. 1r	8	100911	fta5	fta5	c1f8.07c	72.4	591	conv			33	5	Y	Y
1002. 0. 0	4	113878	c11d3.04c	c11d3.03c	c11d3.04c	75.6	1003	tan	79	15	13	10	Y	Y
1003. 0. 0	4	127765	c11d3.11c	c11d3.09	c11d3.10	75.8	1552	tan	78	**21**	7	10	Y	Y
1003. 1. 0	4	150496	c5h10.02c	c5h10.02c	c5h10.03	70.8	2977	div	81	13	5	4	Y	Y
1003. 2. 0	2	166578	gmh1	gmh1	c5h10.12c	71.8	589	tan	82	7	1		N	N
1003. 3. 0	2	176626	rps3-a1	rad8	rps3-a1	73.8	639	tan	81	6	17		Y	Y
1003. 4. 0	3	190844	c13g6.08	rps601	c13g6.08	72.2	813	div	82	17		19	Y	Y
1004. 0. 0	4	199596	c24b11.02	c24b11.02	aps1	79.6	1003	tan	78	23	7	23	Y	Y
1005. 0. 0	3	230517	c806.10: c24b11.14	hem3	c806.02c	73.0	565	conv	83	21		7	Y	Y
1005. 1. 0	4	240549	c806.04c	c806.11	c806.04c	72.4	3995	tan	83	2	0	4	Y	Y
1005. 2. 0	2	245963	c806.06c	c806.04c	c806.05	76.8	1789	div	83	15	2		Y	Y
1005. 3. 0	4	275789	yam8	shk2	yam8	70.0	167	tan	85	7	5	11	N	N
1005. 4. 0	4	293465	c1f5.02	c1f5.02	c1f5.01	79.0	1163	tan	83	19	5	3	Y	Y
1005. 5. 0	4	299645	tup11	tup11	c18b11.09c	74.6	1449	div	83	11	1	2	Y	Y
1005. 5. 1r	8	309281	c18b11.05: gpi18	ncs1	c18b11.03c	75.8	829	div			13	0	Y	Y
1005. 7. 0	1	322363	c12g12.14c: pfs2	sif3	pfs2	74.0	1032	div	80	9			Y	N
1006. 0. 0	3	326142	c12g12.12	c12g12.12	c12g12.11c	77.6	1413	div	78	33		17	Y	Y

Origin No.	Class	Central Map Position	Central Probe	Gene AT island L	Gene AT island R	% AT	IG Length (bp)	IG Context	Replication Time Mitosis (min)	Mitosis Efficiency	*cdc13* s/o Efficiency	*cdc18cdt1* co-oe Efficiency	Orc4 signal ≥ 0.5 (Y/N)	Orc4 signal ≥ 0.8 (Y/N)
1006. 1. 0	1	334715	c12g12.08: mrp16	c12g12.09	mrp16	72.0	951	tan	82	9			N	N
1006. 2. 0	2	338390	c12g12.06c	c12g12.07c	c12g12.06c	73.4	482	tan	81	6	1		N	N
1006. 3. 0	3	342733	hsp60: mcp60	hsp60: mcp60	cip2	70.8	1543	tan	83	24		2	Y	Y
1006. 4. 0	3	351698	act2: arp3	c630.02	arp3	69.2	564	tan	83	10		27	N	N
1007. 0. 0	3	357003	c630.05: gyp7	c630.04c	gyp7	74.8	972	div	78	**11**		27	N	N
1007. 1. 0	4	361057	c630.08c	c630.07c	erg25	71.2	1174	tan	80	15	0	32	Y	Y
1008. 0. 0	4	367214	c630.10	c630.09c	c630.10	79.4	1947	div	80	23	11	44	Y	Y
1008. 1. 0	3	374824	gti1	tup12	gti1	71.0	1027	tan	80	13		18	N	N
1008. 2. 0	1	386037	c1751.04	gti1	c1751.04	69.0	4272	div	82	0			Y	Y
1009. 0. 0	4	396462	mis4	c31a2.04c	mis4	74.4	664	tan	81	15	4	0	Y	Y
1009. 1. 0	4	404006	c31a2.08: mrp20	dbp10	mrp20	71.0	865	div	85	6	0	0	N	N
1009. 2. 0	4	419538	c31a2.15c: dcc1	dcc1	gef2	69.4	733	div	82	7	0	0	N	N
1009. 3. 0	4	432169	c13c5.05c	c13c5.04	c13c5.05c	73.4	685	conv	80	6	0	26	Y	N
1010. 0. 0	4	441014	gaf2: fep1	rad32	fep1	77.2	5199	tan	80	**8**	0	6	Y	Y
1010. 1. 0	4	464149	uba3	uba3	c24h6.11c	73.8	2025	tan	81	3	6	18	Y	Y
1011. 0. 0	4	473764	c24h6.09: gef1	gef1	c24h6.08	76.6	1135	tan	80	12	12	25	Y	Y
1012. 0. 0	4	490207	c24h6.02c	c24h6.02c	pb21f2.01	78.4	665	tan	77	33	0	12	Y	Y
1012. 1. 0	2	507212	c227.08c: yth1	pab1	yth1	71.6	977	tan	82	13	0		N	N
1012. 2. 0	3	515516	c227.11c	c227.09	c227.10	72.8	770	tan	83	2		0	N	N
1012. 2. 1r	6	521833	c227.14	c227.14	c227.15	69.4	1524	tan			11		Y	N
1013. 0. 0	3	528151	c227.15	c227.15	c227.16c	73.8	2135	conv	83	12		7	Y	Y
1013. 0. 1r	8	539295	C2F7.04: pmc2	c2f7.02c	pom1	70.8	1052	tan			8	13	Y	Y

Origin No.	Class	Central Map Position	Central Probe	Gene AT island L	Gene AT island R	% AT	IG Length (bp)	IG Context	Replication Time Mitosis (min)	Mitosis Efficiency	*cdc13* s/o Efficiency	*cdc18cdt1* co-oe Efficiency	Orc4 signal ≥ 0.5 (Y/N)	Orc4 signal ≥ 0.8 (Y/N)
1013. 2. 0	2	549421	c2f7.09c	c2f7.10	nrd1	72.2	3691	tan	81	9	5		Y	Y
1014. 0. 0	4	565470	c2f7.15: rsm24	c2f7.14c	rsm24	76.6	2202	div	77	19	7	27	Y	Y
1014. 1. 0	2	581247	c13a11.03: mcp7	mcp7	ubp8	72.8	472	conv	80	10	4		Y	N
1014. 2. 0	1	594636	c3h8.05c	c3h8.03	c3h8.04	72.6	1187	tan	82	9			Y	Y
1015. 0. 0	2	607709	c3h8.09c: nab3	nab3	spo20	75.8	2142	div	78	1	4		Y	Y
1015. 1. 0	3	612286	C3H8.11: rrp6	spo20	rrp6	71.8	726	tan	83	7		12	Y	Y
1015. 2. 0	4	622229	c1f3.04c	c1f3.04c	c1f3.05	69.6	1080	div	82	2	0	5	Y	N
1015. 3. 0	4	625949	c1f3.06c: spo15	c1f3.05	spo15	70.6	343	conv	84	7	0	10	Y	N
1015. 4. 0	3	635123	c1f3.09: mug161	c1f3.08c	mug161	69.2	1462	div	85	12		0	N	N
1016. 0. 0	4	645865	cct2	csk1	pis1	77.6	1420	div	81	12	0	0	Y	Y
1016. 1. 0	4	656074	c1d4.10	c1d4.10	lkh1	71.4	519	div	83	1	0	10	Y	Y
1016. 2. 0	2	664220	rad15: rhp3	lkh1	rad15: rhp3	71.2	5949	div	83	8	1		Y	Y
1016. 3. 0	4	684297	rgs1	tsc1	rgs1	72.2	1937	div	83	16	6	8	Y	N
1016. 4. 0	1	690868	c22f3.08c: rok1	rok1	atp20	72.2	601	tan	81	6			N	N
1017. 0. 0	4	707806	atf31	c22f3.01	cox4	71.8	1277	div	77	23	5	14	Y	Y
1018. 0. 0	4	713029	sxa2	sxa2	mug65	79.2	1465	div	79	33	8	35	Y	Y
1019. 0. 0	4	717473	c1296.05c	c1296.05c	c1296.06	74.0	1642	div	79	51	0	38	Y	Y
1019. 1. 0	2	734516	c22g7.04: ubp13	c22g7.05	ura1	71.2	579	conv	79	14	0		Y	Y
1019. 2. 0	1	751047	c22g7.08: ppk8	c22g7.07c	ppk8	73.4	1545	div	81	13			Y	Y
1019. 2. 1r	7	754604	c22g7.10	sss1	c4g8.03c	72.8	1122	tan				11	Y	N
1019. 3. 0	2	768789	c4g8.04	c4g8.03c	c4g8.04	79.4	7158	div	81	8	10		Y	Y
1019. 4. 0	4	782034	c4g8.09	atp10	c4g8.12c	72.6	1530	tan	81	8	0	5	Y	Y
1020. 0. 0	4	793036	c16c9.02c	c16c9.02c	c16c9.03	78.0	1323	div	80	14	4	0	Y	Y

Origin No.	Class	Central Map Position	Central Probe	Gene AT island L	Gene AT island R	% AT	IG Length (bp)	IG Context	Replication Time Mitosis (min)	Mitosis Efficiency	*cdc13* s/o Efficiency	*cdc18cdt1* co-oe Efficiency	Orc4 signal ≥ 0.5 (Y/N)	Orc4 signal ≥ 0.8 (Y/N)
1020. 1. 0	3	823439	smn1: yab8	ptc3	yab8	72.0	627	tan	82	5		11	N	N
1020. 1. 1r	6	832927	hus2: rqh1: rad12	prh1	hus2: rqh1: rad12	67.2	527	div			4		N	N
1021. 0. 0	3	844330	c521.02	tgs1	c521.02	76.8	742	div	76	40		14	Y	Y
1021. 0. 1r	6	847231	C521.04c	c521.02	c521.03	75.0	1060	tan			17		Y	Y
1022. 0. 0	3	876434	c23g3.06	c23g3.05c	c23g3.06	75.8	1383	div	77	27		5	Y	Y
1023. 0. 0	2	881992	c23g3.07c: snf30	snf30	ubp7	75.8	833	tan	77	19	4		Y	Y
1023. 1. 0	2	889888	c23g3.12c	c23g3.12c	mug35	73.0	1598	tan	77	2	1		Y	Y
1024. 0. 0	4	904005	rpc19: rpa17	c22h12.05c	rpc19: rpa17	77.2	1347	div	74	51	8	8	Y	Y
1024. 1. 0	2	913275	rpl44: rpl28	rpl44: rpl28	c1687.07	71.2	1978	div	77	4	4		Y	Y
1024. 2. 0	4	920092	c1687.10: mcp1	c1687.09	mcp1	72.4	741	tan	78	5	4	14	Y	N
1024. 3. 0	4	949456	c222.04c: ies6	mss1: c222.05c	mak16	71.6	509	div	81	13	6	5	N	N
1024. 3. 1r	7	954013	c222.06: mak16	hri2	c222.08c	73.8	1171	tan				8	Y	Y
1025. 0. 0	4	967448	c222.11: hem13	byr4	hem13	78.0	1995	div	78	41	10	10	Y	Y
1026. 0. 0	3	978693	meu13	c222.14c	meu13	71.4	975	div	77	5		1	Y	N
1026. 1. 0	4	995263	slp1	moc3	slp1	71.8	2230	tan	81	7	10	10	Y	Y
1026. 2. 0	4	1011039	orb6	c955.01c	c955.02c	72.0	1037	tan	81	6	5	10	N	N
1027. 0. 0	4	1020574	c139.02c: oac1	c955.02c	oac1	72.0	736	tan	78	20	13	30	Y	N
1027. 1. 0	4	1030288	c139.05	fap2	c139.05	78.8	2838	div	81	5	5	25	Y	Y
1027. 2. 0	4	1039035	c23c4.05c	c23c4.03	c23c4.05c	71.2	1070	conv	80	14	4	22	N	N
1027. 3. 0	1	1043427	c23c4.09c	c23c4.09c	sec2	70.0	920	div	81	6			Y	N
1027. 4. 0	4	1047446	c23c4.11: atp18	atp18	hhp2	72.2	1443	tan	82	14	5	4	Y	Y
1027. 5. 0	3	1055325	rpb5	rpb5	atg15	71.8	498	conv	82	3		4	N	N

Origin No.	Class	Central Map Position	Central Probe	Gene AT island L	Gene AT island R	% AT	IG Length (bp)	IG Context	Replication Time Mitosis (min)	Mitosis Efficiency	*cdc13* s/o Efficiency	*cdc18cdt1* co-oe Efficiency	Orc4 signal ≥ 0.5 (Y/N)	Orc4 signal ≥ 0.8 (Y/N)
1027. 6. 0	4	1059781	c23c4.17	atg15	c23c4.17	69.4	979	div	80	5	10	6	N	N
1027. 6. 1r	7	1069631	c1a6.02: c23c4.21	c1a6.03c	plb1	73.2	2763	tan				34	N	N
1028. 0. 0	4	1082417	meu31	plb1	c1a6.05c	78.4	3402	tan	74	57	19	34	Y	Y
1029. 0. 0	4	1088084	c1a6.08c: mug125	lag1	c30d11.15c	74.6	1686	div	74	31	22	33	Y	Y
1030. 0. 0	4	1094898	hus5: ubc9	hus5	rpl3802	74.8	1496	tan	73	44	20	26	Y	Y
1030. 0. 1r	7	1105764	c30D11.08c: phf2	cwf19	phf2	70.8	1116	div				10	Y	N
1030. 1. 1r	6	1120278	c30D11.02c	c30d11.02c	c56f8.01	72.6	784	tan			1		Y	Y
1030. 2. 0	4	1131055	ppt1: coq2	c56f8.02	c56f8.03	72.2	827	tan	78	13	16	0	N	N
1031. 0. 0	3	1141098	ddi1: mud1	mud1	rrp8	72.0	378	tan	78	20		0	N	N
1032. 0. 0	4	1156828	c22a12.01c: pso2	esc1	pso2	74.6	1135	conv	77	20	13	6	Y	Y
1032. 1. 0	2	1164048	rpc11	csn4	rps2201	73.2	891	tan	79	14	1		Y	N
1032. 1. 1r	8	1173370	sap114	c22a12.10	dak1	70.4	1283	tan			16	0	N	N
1033. 0. 0	4	1188713	c22a12.16	bip1	c22a12.16	73.8	1010	div	74	38	19	14	Y	Y
1034. 0. 0	4	1198285	c4c5.01	ryh1	c4c5.03	78.2	1958	div	74	49	16	14	Y	Y
1034. 1. 0	4	1218247	vip1	ubc6	vip1	71.4	1242	div	78	8	7	2	N	N
1034. 2. 0	3	1229737	mam4	mam4	c10f6.13c	72.8	717	tan	80	13		1	N	N
1034. 3. 0	3	1235693	b8647-4: c10f6.16: mug134	mug134	c56e4.01c	68.6	896	conv	82	5		8	Y	Y
1035. 0. 0	4	1257102	c56e4.05: mug69	cut6	mug69	76.6	2031	div	76	60	7	41	Y	Y
1036. 0. 0	4	1275377	csn2	csn2	rpl3703	74.8	1022	div	76	26	16	12	Y	Y

Origin No.	Class	Central Map Position	Central Probe	Gene AT island L	Gene AT island R	% AT	IG Length (bp)	IG Context	Replication Time Mitosis (min)	Mitosis Efficiency	*cdc13* s/o Efficiency	*cdc18cdt1* co-oe Efficiency	Orc4 signal ≥ 0.5 (Y/N)	Orc4 signal ≥ 0.8 (Y/N)
1037. 0. 0	3	1282801	pb17e12.10c	pb17e12.10c	pb17e12.11	74.0	594	div	76	28		10	N	N
1037. 0. 1r	6	1295383	C1565.03	c1565.03	ste4	75.2	574	conv			5		Y	Y
1037. 1. 0	2	1315334	c6f12.04	fsv1	c6f12.04	72.4	1634	div	81	13	0		Y	Y
1037. 1. 1r	8	1365746	cdr2	pas1	cdr2	72.4	1039	tan			0	0	N	N
1038. 0. 0	3	1375738	pof1	mug10: c57a10.04	sgf11	73.4	441	conv	79	17		23	Y	Y
1038. 1. 0	4	1382406	c57a10.09c	c57a10.09c	sla1	70.2	1005	tan	78	14	2	1	N	N
1039. 0. 0	4	1388312	cdc17	ura3	cdc17	74.0	1102	div	77	33	0	4	Y	Y
1039. 1. 0	1	1398795	cdc15	c20g8.04c	cdc15	71.6	1874	tan	79	1			Y	N
1039. 2. 0	4	1411409	c20g8.07c: erg2	c20g8.06	erg2	72.0	851	conv	78	3	4	18	N	N
1040. 0. 0	4	1423140	c3a12.02	c3a12.01	c3a12.02	75.0	1448	div	77	46	2	9	Y	Y
1040. 1. 0	4	1435283	rpb11	rpb11	c3a12.08	72.4	723	tan	81	15	7	18	N	N
1040. 2. 0	4	1439786	rpl20-1: rpl2001	cwf2	atp11	73.8	565	div	78	20	6	40	Y	Y
1041. 0. 0	4	1442837	c3a12.13c	c3a12.13c	cam1	77.8	1801	div	74	42	16	38	Y	Y
1042. 0. 0	4	1454947	zwf1	zwf1	c9.02c	72.2	613	conv	74	27	12	51	Y	N
1043. 0. 0	4	1475393	c9.06c	c9.07c	c9.08c	76.0	1106	tan	76	**55**	16	10	Y	Y
1044. 0. 0	2	1487141	c9.11	atp12	cwf16	74.6	714	tan	77	11	6		Y	Y
1044. 0. 1r	8	1498047	C5D6.09c: mug86	mug86	mes1	71.4	1123	tan			11	19	Y	Y
1045. 0. 0	4	1504439	c5d6.05: sep11	c5d6.05	c5d6.04	72.6	852	tan	78	**23**	8	33	N	N
1046. 0. 0	4	1509675	C5D6.02c	c5d6.04	mug165	76.2	3204	div	73	**33**	5	14	Y	Y
1047. 0. 0	4	1574967	pip1: rbx1	c23h4.19	rbx1	73.8	4149	div	76	37	12	0	Y	Y
1047. 1. 0	4	1588598	alp13	cnl2	thi4	72.8	507	tan	81	12	11	4	Y	N
1047. 2. 0	2	1598438	gln1	c23h4.08	srp102	74.6	740	div	83	8	20		Y	Y

Origin No.	Class	Central Map Position	Central Probe	Gene AT island L	Gene AT island R	% AT	IG Length (bp)	IG Context	Replication Time Mitosis (min)	Mitosis Efficiency	*cdc13* s/o Efficiency	*cdc18cdt1* co-oe Efficiency	Orc4 signal ≥ 0.5 (Y/N)	Orc4 signal ≥ 0.8 (Y/N)
1048. 0. 0	2	1620493	p27g11.06c	vps41	p27g11.06c	72.0	788	tan	81	17	6		N	N
1048. 1. 0	2	1624785	p27g11.09c	p27g11.09c	nup184	74.4	657	tan	81	4	0		N	N
1048. 3. 0	2	1640654	c343.01c: erg8	erg8	img1	72.0	869	div	82	10	4		Y	Y
1048. 4. 0	4	1645110	c343.04c: gnr1	gnr1	vma1	71.0	1624	div	83	9	1	2	Y	Y
1048. 5. 0	4	1651637	c343.07: mug28	vma1	c343.06c	71.0	396	conv	82	2	0	11	Y	N
1048. 5. 1r	7	1659375	C343.11c: msc1	ubx3	met11	71.0	722	tan				71	N	N
1049. 0. 0	3	1669401	rds1	msc1	rds1	75.0	4829	div	77	14		27	Y	Y
1049. 0. 1r	7	1674847	C343.15	c343.15	lys2	70.0	478	tan				21	N	N
1049. 1. 0	1	1683817	c824.01	c824.01	c824.02	73.4	1362	tan	80	2			Y	N
1049. 2. 0	4	1695580	c824.06: tim14	tim14	c824.07	72.4	946	tan	78	13	6	5	Y	Y
1050. 0. 0	4	1710321	c664.03	c664.02c	c664.03	74.2	1741	div	76	35	52	14	Y	Y
1051. 0. 0	3	1718596	c664.08c	c664.08c	ggt1	74.8	1775	div	75	25		12	Y	Y
1052. 0. 0	4	1735334	c664.14: amt2	amt2	c664.15	78.2	1827	tan	74	37	6	17	Y	Y
1052. 1. 0	4	1748489	c105.03c	c105.03c	pex6	73.2	1048	div	77	14	2	7	N	N
1052. 2. 0	1	1770871	c17a5.09c	ulp2	c17a5.08	75.8	1091	div	80	5			Y	N
1052. 3. 0	4	1777203	c17a5.13	c17a5.13	exo2	72.8	1177	tan	79	4	0	0	Y	Y
1052. 4. 0	3	1791786	c1610.01: c17a5.17	c17a5.16	c17a5.17	73.0	932	tan	80	11		0	Y	N
1052. 5. 0	1	1795829	c1610.04: mug99	crp79	mug99	73.6	1327	div	80	9			Y	Y
1052. 6. 0	4	1824895	C1002.12c	c1002.12c	psu1	72.2	1744	tan	76	13	12	14	Y	Y
1053. 0. 0	4	1827930	c1002.15c: pmc5	pmc5	c1002.16c	79.2	809	tan	74	30	20	23	Y	Y
1054. 0. 0	3	1836175	c1002.19: urg1	urg3	c1002.21	78.2	1218	conv	76	**40**		30	Y	Y
1054. 1. 0	4	1843145	c1399.04c	fur4	c1399.02	73.0	2439	tan	80	17	17	25	Y	Y

Origin No.	Class	Central Map Position	Central Probe	Gene AT island L	Gene AT island R	% AT	IG Length (bp)	IG Context	Replication Time Mitosis (min)	Mitosis Efficiency	*cdc13* s/o Efficiency	*cdc18cdt1* co-oe Efficiency	Orc4 signal ≥ 0.5 (Y/N)	Orc4 signal ≥ 0.8 (Y/N)
1055. 0. 0	1	1857815	p11e10.02c: mam3	mam3	pb1a10.02	71.6	1792	div	77	32			N	N
1055. 1. 0	1	1865913	cwp1	cwp1	pb1a10.05	73.2	1553	div	77	13			Y	Y
1055. 2. 0	4	1887064	pb1a10.12c: alo1	pb1a10.11c	alo1	73.0	565	tan	80	4	6	0	Y	N
1055. 3. 0	4	1901859	c140.04	c140.04	ppk1	72.0	5061	tan	81	1	0	6	Y	Y
1055. 4. 0	2	1921023	pss1	pss1	p14e8.02	73.8	2795	div	81	5	7		Y	Y
1055. 5. 0	4	1928605	p14e8.04: oma1	bos1	oma1	72.2	806	tan	80	1	10	6	Y	Y
1055. 6. 0	2	1940651	c3h1.05	mdm31	c3h1.05	71.6	917	div	81	4	2		N	N
1055. 7. 0	4	1949795	c3h1.09c	c3h1.10	hsr1	76.6	8310	div	82	6	8	14	Y	Y
1055. 8. 0	1	1963087	c3h1.12c	hsr1	snt2	71.0	650	conv	79	0			Y	Y
1056. 0. 0	4	1974174	rpl30: rpl30-1: rpl3001	rpl3001	oxa101	75.8	1230	div	77	34	12	13	Y	Y
1056. 1. 0	4	1980373	c9g1.06c: cyk3	cyk3	c9g1.07	73.4	1074	div	77	11	6	16	Y	Y
1056. 2. 0	3	2009050	c17h9.03c: rdl1	rdl1	c17h9.04c	71.4	1063	tan	81	6		8	N	N
1056. 3. 0	4	2014231	c17h9.05: ebp2	c17h9.04c	ebp2	70.6	1212	div	82	2	8	2	Y	Y
1056. 4. 0	4	2017794	c17h9.07	c17h9.07	c17h9.08	73.4	1427	tan	82	1	0	30	Y	N
1056. 5. 0	1	2022451	c17h9.10c: ddb1	ddb1	c17h9.11	75.4	892	div	79	11			Y	Y
1056. 6. 0	4	2027252	c17h9.12c	c17h9.12c	c17h9.13c	71.0	380	tan	79	7	4	0	N	N
1056. 7. 0	3	2030386	c17h9.14c	c17h9.13c	c17h9.14c	72.8	476	tan	79	19		0	N	N
1057. 0. 0	4	2042881	snu13	snu13	c607.04	76.0	1026	div	79	27	5	4	Y	Y
1057. 0. 1r	7	2044742	rpn9	c607.04	rpn9	76.6	545	tan				18	Y	Y
1057. 1. 0	2	2051708	c607.09c/btn1	btn1	spo3	71.8	2292	div	80	8	5		Y	N
1057. 2. 0	2	2067716	rhp55	c732.03c	c3c7.02c	73.2	1211	tan	79	1	8		Y	Y
1057. 3. 0	2	2078793	c3c7.07c	mug191	pit1	73.6	1061	conv	79	17	4		Y	Y

Origin No.	Class	Central Map Position	Central Probe	Gene AT island L	Gene AT island R	% AT	IG Length (bp)	IG Context	Replication Time Mitosis (min)	Mitosis Efficiency	*cdc13* s/o Efficiency	*cdc18cdt1* co-oe Efficiency	Orc4 signal ≥ 0.5 (Y/N)	Orc4 signal ≥ 0.8 (Y/N)
1058. 0. 0	1	2084908	c3c7.09: set8	elf1	set8	70.6	1071	div	79	14			Y	Y
1058. 1. 0	1	2088021	cal1: cnx1	cnx1	tip1	72.8	1489	div	81	12			Y	Y
1059. 0. 0	4	2101912	c25a8.02	obr1	c3c7.15c	77.4	1490	tan	80	12	1	14	Y	Y
1059. 1. 0	2	2113677	c20h4.01: c631.02	c631.02	c631.03	72.6	1309	tan	83	9	4		Y	Y
1059. 2. 0	1	2119459	c20h4.04: mfh2	c20h4.05c	c20h4.06c	73.0	319	tan	84	4			Y	Y
1059. 3. 0	1	2123654	rhp57	c20h4.06c	rhp57	69.8	1081	div	83	4			N	N
1060. 0. 0	4	2135567	c23c11.01	rho5	c23c11.01	69.8	823	div	79	20	0	10	Y	N
1061. 0. 0	2	2141705	c23c11.05	pnk1	c23c11.05	77.8	1090	div	81	7	7		Y	Y
1061. 1. 0	2	2166330	plo1	plo1	c23c11.17	71.8	878	tan	82	12	0		Y	Y
1061. 2. 0	2	2176426	c13f5.03c	ptr6	c13f5.03c	73.0	1255	tan	79	4	4		Y	Y
1061. 3. 0	4	2190160	c1783.01	c13f5.07c	c1783.01	71.4	2371	div	76	9	0	12	Y	Y
1061. 4. 0	4	2193211	hst4	hst4	hrp1	76.4	1535	div	78	19	2	13	Y	Y
1062. 0. 0	4	2208653	c1327.01c	c1783.09c	c18g6.01c	72.6	1800	tan	79	14	5	17	Y	Y
1062. 1. 0	1	2216746	ypt3	chp1	ypt3	70.0	1955	div	77	5			Y	Y
1063. 0. 0	4	2230620	c18g6.06	c18g6.05c	c18g6.06	76.6	1674	div	77	22	10	16	Y	Y
1063. 0. 1r	7	2235498	c18g6.10	mra1	C18G6.09	72.0	1737	tan				22	N	N
1064. 0. 0	4	2242233	rps7	rps7	mal3	76.2	1112	div	76	16	5	8	Y	Y
1065. 0. 0	4	2251481	c13d6.03c	byr3	c13d6.03c	76.4	1889	tan	76	**34**	0	16	Y	Y
1066. 0. 0	4	2255736	c4g9.02	alp11	c4g9.02	69.8	415	tan	75	**6**	0	24	N	N
1067. 0. 0	4	2264812	b8647-3: mug133	c4g9.06c	mug133	72.6	1251	div	76	16	4	2	Y	Y
1067. 1. 0	4	2274255	arg3	arg11	arg3	73.4	1335	div	78	7	5	10	Y	Y
1068. 0. 0	4	2280746	c4g9.14	vps26	c4g9.14	78.0	1188	div	74	30	2	12	Y	Y

Origin No.	Class	Central Map Position	Central Probe	Gene AT island L	Gene AT island R	% AT	IG Length (bp)	IG Context	Replication Time Mitosis (min)	Mitosis Efficiency	*cdc13* s/o Efficiency	*cdc18cdt1* co-oe Efficiency	Orc4 signal ≥ 0.5 (Y/N)	Orc4 signal ≥ 0.8 (Y/N)
1068. 1. 0	2	2285764	c4g9.17c: mrps5	mrps5	c4g9.19	70.2	1583	div	78	6	10		Y	N
1068. 2. 0	2	2304975	c13g7.05	mac1	c13g7.05	72.2	2552	div	82	17	16		Y	Y
1069. 0. 0	2	2312095	crb3	crb3	c13g7.09c	73.2	726	tan	79	22	0		N	N
1070. 0. 0	4	2317847	c13g7.12c	c13g7.12c	msa1	76.0	800	tan	80	35	2	13	Y	Y
1070. 0. 1r	8	2328158	prl57	c6c3.02c	c6c3.03c	74.0	1168	tan			7	13	Y	Y
1071. 0. 0	1	2337467	c6c3.07: mug68	c6c3.06c	mug68	76.6	671	div	77	**25**			Y	Y
1072. 0. 0	4	2343102	c6c3.09	c6c3.08	c6c3.09	78.0	866	tan	77	**21**	0	20	Y	Y
1072. 1. 0	2	2349452	c17g8.04c: arc15	arc15	med20	73.8	1137	div	78	7	4		Y	Y
1072. 2. 0	4	2355393	c17g8.07	c17g8.06c	c17g8.07	73.2	1233	div	80	1	4	12	Y	Y
1072. 3. 0	2	2358804	c17g8.09: shg1	c17g8.11c	c17g8.12	73.0	2054	div	82	5	6		Y	Y
1072. 3. 1r	6	2368305	pck1	pck1	c22h10.02	70.0	1135	div			7		Y	N
1072. 4. 0	3	2376539	kap114	kap114	c22h10.04	72.2	969	div	83	1		11	N	N
1072. 5. 0	2	2391974	alp21:sto1	c22h10.11c	gdi1	71.8	1155	tan	83	5	19		Y	N
1073. 0. 0	1	2397682	c15f9.01c	c15f9.01c	seh1	76.0	1232	div	80	7			Y	Y
1073. 0. 1r	7	2407564	c1b9.03c: c6b12.01	sck1	c6b12.01	76.0	2057	div				16	Y	Y
1074. 0. 0	4	2425576	c6b12.08: mug185	c6b12.07c	mug185	72.8	3029	div	77	6	25	33	Y	Y
1074. 0. 1r	7	2434292	C6B12.12: tom70	drc1	tom70	72.2	1284	tan				14	Y	Y
1075. 0. 0	4	2441473	c6b12.15: cpc2	c6b12.14c	cpc2	75.4	2068	tan	78	33	49	31	Y	Y
1076. 0. 0	4	2451372	c32a11.03c: phx1	c32a11.02c	phx1	76.6	2215	tan	77	20	1	30	Y	Y
1076. 1. 0	4	2471981	upf2	upf2	c19a8.07c	72.0	2773	div	79	5	0	5	Y	Y
1077. 0. 0	4	2499146	c23h3.03c	c23h3.03c	c23h3.04	73.4	1608	div	78	18	6	0	Y	N

Origin No.	Class	Central Map Position	Central Probe	Gene AT island L	Gene AT island R	% AT	IG Length (bp)	IG Context	Replication Time Mitosis (min)	Mitosis Efficiency	*cdc13* s/o Efficiency	*cdc18cdt1* co-oe Efficiency	Orc4 signal ≥ 0.5 (Y/N)	Orc4 signal ≥ 0.8 (Y/N)
1077. 1. 0	2	2506121	apl6	mrp2	bub3	72.6	454	tan	80	9	4		Y	Y
1077. 2. 0	4	2516139	c23h3.12c	gpa2	c23h3.14	74.2	3382	div	82	0	1	12	Y	Y
1077. 3. 0	1	2528176	c25h1.02: jmj1	c23h3.15c	jmj1	75.4	1310	div	82	17			Y	Y
1077. 4. 0	2	2533213	c25h1.06	c25h1.06	c25h1.07	70.0	1141	tan	82	0	0		N	N
1077. 5. 0	3	2540433	mde5: meu30	c25h1.08c	mde5	74.6	560	div	83	9		19	Y	Y
1077. 6. 0	1	2561514	c4a8.08c: vas1	vas1	cwf21	76.0	1296	tan	84	12			Y	Y
1078. 0. 0	4	2580003	cdc3	prs1	cdc3	75.6	1217	conv	75	31	13	11	Y	Y
1078. 0. 1r	8	2589763	tlg2	c823.04	tlg2	70.6	242	conv			11	7	Y	Y
1078. 1. 0	2	2594596	c823.09c	c823.08c	c823.09c	73.4	877	tan	77	17	10		Y	N
1078. 2. 0	1	2600532	c823.11	c823.11	c823.12	73.8	1573	tan	76	11			Y	Y
1078. 2. 1r	7	2605159	C823.13c	c823.13c	c823.14	71.0	972	div				8	Y	Y
1078. 3. 0	1	2608045	c823.14	ppa1	c823.16c	71.0	436	conv	76	5			N	N
1079. 0. 0	2	2617190	c7d4.12c	c7d4.12c	sec39	75.8	653	tan	78	8	8		Y	Y
1079. 1. 0	2	2627609	c7d4.06c	c7d4.06c	c7d4.05	72.6	1569	conv	77	3	0		Y	Y
1080. 0. 0	4	2640153	c7d4.02c	c7d4.03c	c7d4.02c	74.4	854	tan	78	5	6	8	Y	Y
1080. 0. 1r	7	2644524	hcs	itr1	hcs1	74.8	2195	div				15	Y	Y
1080. 0. 2r	6	2658944	C4F8.11	stg1: c4f8.10c	mug114	75.6	2198	conv			8		Y	Y
1081. 0. 0	4	2674970	c644.02: mrp140	did4	pct1	74.4	1169	div	79	30	10	10	N	N
1081. 1. 0	2	2682408	cdr1:nim1	cdr1	c644.07	71.8	4859	div	81	9	4		Y	Y
1081. 2. 0	1	2698190	rhp51:rad51	c644.13c	rhp51	74.4	911	tan	83	6			N	N
1081. 3. 0	4	2704153	bet3	mrp19	bet3	70.8	1128	tan	81	0	8	12	N	N
1082. 0. 0	4	2720544	pb2b4.05: vma5	b2b4.04c	vma5	75.4	4022	div	76	22	11	26	Y	Y

Origin No.	Class	Central Map Position	Central Probe	Gene AT island L	Gene AT island R	% AT	IG Length (bp)	IG Context	Replication Time Mitosis (min)	Mitosis Efficiency	*cdc13* s/o Efficiency	*cdc18cdt1* co-oe Efficiency	Orc4 signal ≥ 0.5 (Y/N)	Orc4 signal ≥ 0.8 (Y/N)
1082. 0. 1r	7	2733424	C6F6.02c	pof5	c6f6.03c	71.2	538	tan				21	N	N
1083. 0. 0	4	2748489	cdc16	cdc16	c6f6.09	72.2	1058	div	78	15	12	10	Y	Y
1084. 0. 0	4	2761477	ypt5	c6f6.13c	ypt5	78.6	3467	div	75	34	10	32	Y	Y
1084. 1. 0	3	2776464	c1805.02c	c1805.02c	trm13	74.0	411	tan	79	12		13	Y	N
1085. 0. 0	4	2785797	hem2	cki3	hem2	73.4	1006	conv	78	24	8	13	Y	Y
1086. 0. 0	4	2802175	c1805.16c	c1805.16c	crm1	72.4	2607	div	75	35	20	16	Y	Y
1087. 0. 0	4	2815286	c1b2.04: cox6	c1b2.03c	cox6	71.6	1882	div	76	3	4	4	Y	Y
1087. 1. 0	1	2830048	c3f10.07c: mug91	mug91	c3f10.08c	73.0	2625	tan	81	16			Y	Y
1087. 2. 0	2	2835094	map3	map3	abc2	72.6	2279	tan	81	5	1		Y	N
1087. 3. 0	2	2849837	c3f10.15c: spo12	ucp6	spo12	72.0	555	conv	81	7	4		N	N
1087. 3. 1r	6	2854690	rpl41-2: rpl4102	rpl1402	c8f11.02c	72.4	1402	tan			14		Y	Y
1088. 0. 0	3	2861565	c8f11.05c: mug130	mug130	c8f11.06	77.2	933	div	76	25		10	Y	Y
1088. 1. 0	4	2875990	cunk4.17	cunk4.17	mug153	72.8	1638	div	82	8	19	0	Y	Y
1089. 0. 0	4	2882186	cunk4.14: mdb1	cunk4.15	mdb1	76.2	1452	tan	77	0	24	12	Y	Y
1090. 0. 0	2	2913872	mfm2	c513.02	mfm2	72.8	638	conv	75	34	11		Y	Y
1090. 1. 0	4	2938599	c2e1p3.05c	c2e1p3.05c	pb2c8.01	74.4	6285	div	79	18	13	11	Y	Y
1091. 0. 0	4	2959802	pb24d3.08c	pb24d3.07c	pb24d3.08c	79.4	2272	tan	75	48	26	29	Y	Y
1092. 0. 0	3	2984146	pb1a11.03	pb1a11.02	pb1a11.03	72.8	3196	tan	77	19		15	Y	Y
1092. 1. 0	3	2998536	c31g5.07	c31g5.07	ups1	72.2	930	tan	79	21		3	N	N
1093. 0. 0	4	3011299	rpn11	maf1	c31g5.21	78.2	1158	div	74	41	14	10	Y	Y
1094. 0. 0	4	3023991	c31g5.18c	c31g5.18c	c31g5.19	77.4	2684	div	76	16	20	18	Y	Y
1095. 0. 0	4	3060156	bgs2: meu21	bgs2	c24c9.08	77.6	2328	div	76	36	14	20	Y	Y

Origin No.	Class	Central Map Position	Central Probe	Gene AT island L	Gene AT island R	% AT	IG Length (bp)	IG Context	Replication Time Mitosis (min)	Mitosis Efficiency	*cdc13* s/o Efficiency	*cdc18cdt1* co-oe Efficiency	Orc4 signal ≥ 0.5 (Y/N)	Orc4 signal ≥ 0.8 (Y/N)
1095. 1. 0	4	3079630	c16a10.01	c16a10.01	c16a10.02	71.8	843	tan	80	6	5	1	Y	N
1095. 2. 0	4	3088914	c16a10.06c: nse2	rho4	dad1	74.6	1008	conv	80	12	5	11	Y	Y
1095. 3. 0	2	3103397	c589.06c	c589.06c	c589.07c	73.2	623	tan	82	4	10		Y	N
1095. 4. 0	4	3117651	c688.03c	c688.03c	gst3	71.0	624	tan	79	11	2	10	Y	N
1096. 0. 0	3	3129233	c688.08: srb8	srb8	c688.09	76.0	657	tan	77	42		4	Y	Y
1096. 0. 1r	7	3136055	c688.11	rev3	end4	72.0	834	tan				20	Y	Y
1097. 0. 0	4	3147434	c3g9.15c: fcf2	c688.14	bet5	78.4	2179	tan	76	33	10	2	Y	Y
1097. 0. 1r	7	3161130	C3G9.11c	c3g9.11c	ski6	71.6	1278	tan				5	N	N
1097. 1. 0	2	3167139	tif211	ski6	tif211	75.2	2347	tan	80	10	6		Y	Y
1097. 1. 1r	7	3172484	C3G9.06: frs2	frs2	c3g9.05	71.0	600	tan				6	N	N
1097. 1. 2r	7	3177388	C3G9.04: ssu72	ssu72	rpl2301	71.8	2331	tan				15	Y	Y
1098. 0. 0	4	3186732	c1486.01	c3g9.01	c1486.01	75.6	2442	div	77	23	19	19	Y	Y
1098. 1. 0	1	3207386	c1486.08	c1486.08	c1486.09	73.0	1920	tan	79	19			Y	Y
1098. 1. 1r	8	3215590	C6G10.02c: tea3	tea3	c6g10.03c	72.4	884	tan			12	0	Y	Y
1098. 2. 0	4	3226420	c6g10.05c	c6g10.05c	c6g10.06	71.8	685	div	77	9	12	2	N	N
1098. 3. 0	4	3236474	c6g10.09	idp1	c6g10.09	72.8	814	tan	76	11	0	11	N	N
1099. 0. 0	4	3246083	c6g9.03c	nop9	mug183	76.2	1262	tan	74	44	20	12	Y	Y
1099. 0. 1r	8	3254413	C6G9.05: mug79	c6g9.04	c6g9.05	71.2	958	tan			0	12	Y	N
1099. 0. 2r	8	3260604	C6G9.08: ubp6	rpl24	sen1	72.8	541	tan			5	10	Y	N
1100. 0. 0	2	3269618	chs5: c6g9.12: cfr1	snc1: syb1	cfr1	76.0	1494	tan	75	38	7		Y	Y
1100. 0. 1r	6	3277551	C6G9.15c	c6g9.15c	c6g9.16c	68.8	803	tan			11		N	N

Origin No.	Class	Central Map Position	Central Probe	Gene AT island L	Gene AT island R	% AT	IG Length (bp)	IG Context	Replication Time Mitosis (min)	Mitosis Efficiency	*cdc13* s/o Efficiency	*cdc18cdt1* co-oe Efficiency	Orc4 signal ≥ 0.5 (Y/N)	Orc4 signal ≥ 0.8 (Y/N)
1100. 2. 0	4	3286625	pb1e7.03: rpc82	mcl1	rpc82	72.2	856	div	77	40	32	60	N	N
1101. 0. 0	4	3300727	pb1e7.08	eme1	glt1	77.6	3762	div	77	14	20	40	Y	Y
1102. 0. 0	4	3319504	pb1e7.13: mns1	rps602	mns1	77.8	2933	conv	76	42	38	38	Y	Y
1102. 1. 0	3	3334485	sxa1	c2e1p5.05	sxa1	73.4	1732	tan	81	3		36	Y	N
1102. 2. 0	3	3339136	rpl20-2: rpl2002	rpl2002	chc1	65.6	857	tan	82	10		15	N	N
1102. 2. 1r	8	3347235	rpl11-1: rpl1101	smb1	rga2	72.2	1007	conv			45	0	N	N
1102. 3. 0	4	3370739	c26a3.16: dph1	dph1	c8e11.11	71.6	601	conv	85	3	23	0	N	N
1102. 4. 0	3	3378715	c8e11.06	c8e11.05c	c8e11.04c	71.0	1467	tan	81	17		1	Y	Y
1102. 5. 0	4	3385784	rad24	rad24	c959.01	69.0	559	tan	80	16	6	1	N	N
1102. 5. 1r	8	3398924	c959.06c	c959.06c	rps403	74.4	554	div			29	17	N	N
1103. 0. 0	4	3406007	p32a8.02	apc5	p32a8.02	77.6	2244	div	75	**53**	28	35	Y	Y
1104. 0. 0	4	3410586	p32a8.03c	p32a8.03c	rpl501	76.4	1425	div	76	50	27	31	Y	Y
1105. 0. 0	4	3445462	rpt5: tbp1	c3h5.02	rpt5	76.0	1656	div	74	42	11	0	Y	Y
1106. 0. 0	4	3463386	mvp1	mvp1	kms1	70.6	1205	div	76	28	2	7	Y	Y
1106. 1. 0	3	3476866	c328.02	c328.02	tps1	73.8	2238	tan	84	4		14	Y	N
1107. 0. 0	4	3495064	c328.09	rps502	c16e8.01	75.8	1662	div	75	29	22	28	Y	Y
1107. 1. 0	4	3505545	c16e8.02	c16e8.01	c16e8.02	69.6	803	tan	76	8	33	34	N	N
1107. 2. 0	3	3511395	c16e8.06c	nop12	vph1	73.6	411	tan	75	13		27	Y	Y
1108. 0. 0	4	3525569	c16e8.13	c16e8.12c	c16e8.13	74.2	1273	div	75	42	19	30	Y	Y
1109. 0. 0	4	3550027	bsu1	c1b1.04c	bsu1	77.2	3410	div	75	59	26	48	Y	Y
1109. 1. 0	3	3560706	c17a2.04c	c17a2.04c	c17a2.05	72.6	2607	div	74	18		24	Y	Y
1109. 1. 1r	6	3563911	C17A2.06c: vps8	c17a2.05	vps8	70.2	423	conv			25		N	N
1109. 1. 2r	6	3571347	csx1	c17a2.15	csx1	74.4	935	conv			35		Y	Y

Origin No.	Class	Central Map Position	Central Probe	Gene AT island L	Gene AT island R	% AT	IG Length (bp)	IG Context	Replication Time Mitosis (min)	Mitosis Efficiency	*cdc13* s/o Efficiency	*cdc18cdt1* co-oe Efficiency	Orc4 signal ≥ 0.5 (Y/N)	Orc4 signal ≥ 0.8 (Y/N)
1110. 0. 0	5	3578643	c17a2.11	c17a2.10c	c17a2.11	80.2	1421	div	74	56	42	56	Y	Y
1110. 1. 0	3	3595831	c17g6.03	tco1	c17g6.03	71.2	3105	div	79	20		12	Y	Y
1110. 2. 0	4	3601720	c17g6.07c	c17g6.07c	pep7	70.6	1023	div	78	6	8	4	N	N
1111. 0. 0	3	3610600	c17g6.11c	c17g6.11c	cul1	73.6	2384	div	78	**19**		13	Y	Y
1112. 0. 0	4	3637139	c1142.06	c1142.04	ctr5	78.2	2105	tan	74	**41**	39	40	Y	Y
1112. 1. 0	3	3661398	c8c9.11	c8c9.11	c8c9.19	73.2	976	tan	81	3		8	Y	N
1112. 2. 0	2	3673963	c8c9.16c: mug63	mug63	spc34	74.8	1200	tan	80	20	6		N	N
1113. 0. 0	4	3688876	c15a10.06	mug182	c15a10.06	73.4	2508	div	74	**27**	14	0	Y	Y
1114. 0. 0	4	3702490	meu16	mde6	ubr11	78.0	2957	tan	73	**37**	42	25	Y	Y
1114. 1. 0	4	3721830	fat1: bud6	sgo2	bud6	70.6	492	tan	79	0	22	2	N	N
1115. 0. 0	4	3730356	c15e1.08	moa1	c15e1.08	73.4	772	div	74	21	28	6	Y	Y
1116. 0. 0	4	3737463	p7g5.02c: gua2	gua2	p7g5.03	78.2	1355	div	74	**50**	18	12	Y	Y
1117. 0. 0	4	3745050	p7g5.06	rpl1002	p7g5.06	73.8	4865	tan	68	39	51	7	Y	Y
1118. 0. 0	1	3760557	dh.cen.repeat-matk.rc: dhI repeat / dgI repeat	dhI repeat / dgI repeat	dhI repeat / dgI repeat	76.4		cen	68	**46**			Y	Y
1119. 0. 0	2	3774933	chr1.1605.1	imrIR	imrIR	75.0		cen	74	10	23		Y	Y
1120. 0. 0	4	3789432	dh.cen.repeat-matk	dhI repeat	dhI repeat	74.6		cen	70	**54**	40	6	Y	Y
1120. 1. 0	4	3805640	chr1.1616.1: pmm1	meu2	pmm1	71.0	889	tan	79	10	15	10	N	N
1121. 0. 0	4	3810912	c1f12.03c	p23fy	c1f12.04c	72.8	1031	tan	78	**30**	1	20	Y	N

Origin No.	Class	Central Map Position	Central Probe	Gene AT island L	Gene AT island R	% AT	IG Length (bp)	IG Context	Replication Time Mitosis (min)	Mitosis Efficiency	*cdc13* s/o Efficiency	*cdc18cdt1* co-oe Efficiency	Orc4 signal ≥ 0.5 (Y/N)	Orc4 signal ≥ 0.8 (Y/N)
1121. 1. 0	3	3823078	c4h3.01	c1f12.10c	c4h3.01	71.4	1549	div	76	15		17	Y	N
1122. 0. 0	4	3838394	c4h3.07c	c4h3.07c	c4h3.08	74.2	2200	div	72	**43**	31	29	Y	Y
1123. 0. 0	4	3855254	c4h3.13	c4h3.12c	c4h3.13	75.4	861	div	74	50	16	10	Y	Y
1124. 0. 0	4	3863634	c1071.03c	c1071.04c	c1071.05	70.4	1018	div	74	**22**	24	23	Y	N
1124. 0. 1r	7	3867488	C1071.06: arp9	c1071.05	arp9	72.2	1045	tan				40	Y	N
1125. 0. 0	5	3875559	pma1	pma1	c1071.11	81.4	7847	div	77	45	44	79	Y	Y
1126. 0. 0	4	3884142	c1071.11	pma1	c1071.11	77.4	7847	div	75	56	45	53	Y	Y
1127. 0. 0	4	3898021	c926.08c	dlc2	c926.08c	78.4	1455	tan	77	35	24	20	Y	Y
1127. 1. 0	2	3912979	c323.03c	c323.01c	c323.02c	72.4	593	tan	81	12	5		Y	Y
1127. 2. 0	2	3934961	kap104	kap104	c2f3.07c	71.2	1459	tan	81	9	5		Y	N
1128. 0. 0	4	3952385	c2f3.14c	c2f3.14c	lsk1	76.6	2955	div	74	73	30	26	Y	Y
1128. 0. 1r	8	3960798	C11G7.01	c11g7.01	pub1	70.8	1814	tan			33	14	N	N
1129. 0. 0	5	3992829	pb15e9.02c	pb15e9.02c	tf2-5	82.6	3978	tan	76	59	54	63	Y	Y
1129. 0. 1r	8	4006750	C27E2.03c	c27e2.01	c27e2.02	72.6	992	tan			29	41	Y	N
1129. 1. 0	4	4010394	c27e2.11c	c27e2.03c	c27e2.11c	73.0	2544	tan	78	6	42	17	Y	Y
1130. 0. 0	4	4016502	c27e2.06c	c27e2.06c	pvg2	76.2	1884	div	73	31	27	37	Y	Y
1130. 0. 1r	7	4028014	mak2	tf2-6	mak2	70.6	620	tan				18	Y	Y
1130. 1. 0	1	4038170	rpsa-2: rps002	rfc3	rps002	71.2	940	tan	81	3			N	N
1130. 1. 1r	7	4039044	prp12: sap130	rps002	prp12	70.8	557	tan				18	N	N
1130. 2. 0	3	4050599	c19g12.04	c19g12.04	c19g12.05	71.4	933	tan	79	2		4	N	N
1130. 2. 1r	7	4057858	C19G12.08	c19g12.08	c19g12.09	72.0	1962	tan				8	Y	Y
1131. 0. 0	4	4069681	c19g12.12: dlp1	c19g12.13c	its3	76.0	1619	div	73	40	37	11	Y	Y
1131. 0. 1r	8	4076167	tpp1	tpp1	adg2	73.6	1217	tan			37	26	Y	Y
1132. 0. 0	1	4088333	c23a1.05	mnl1	c23a1.05	77.8	1430	div	73	61			Y	Y

Origin No.	Class	Central Map Position	Central Probe	Gene AT island L	Gene AT island R	% AT	IG Length (bp)	IG Context	Replication Time Mitosis (min)	Mitosis Efficiency	*cdc13* s/o Efficiency	*cdc18cdt1* co-oe Efficiency	Orc4 signal ≥ 0.5 (Y/N)	Orc4 signal ≥ 0.8 (Y/N)
1132. 0. 1r	8	4093229	C23A1.07	cmk2	c23a1.07	68.8	249	div			40	32	N	N
1132. 0. 2r	8	4098234	rpl13a-2: rpl16-2: rpl1602	ef1a-b	rpl1602	70.4	749	tan			13	12	N	N
1132. 1. 0	3	4118055	c26h5.02c	c26h5.02c	c26h5.03	72.2	925	div	78	11		13	Y	N
1133. 0. 0	4	4136477	bgl2	bgl2	c26h5.09c	75.6	1985	tan	76	42	18	7	Y	Y
1133. 1. 0	4	4143111	tif51	c26h5.09c	tif51	72.0	3057	tan	80	19	12	4	Y	Y
1133. 2. 0	4	4152695	c26h5.13c	c26h5.13c	dap1	72.0	2978	div	77	11	6	7	Y	Y
1133. 2. 1r	6	4157439	C25B8.02	c25b8.02	c25b8.03	68.4	1485	tan			15		N	N
1133. 3. 0	1	4161251	c25b8.03	c25b8.03	c25b8.04c	74.6	473	conv	79	12			Y	Y
1133. 3. 1r	6	4173846	C25B8.10	c25b8.10	c25b8.11	70.6	1112	tan			19		N	N
1133. 3. 2r	8	4181441	isp7	isp7	mal2	74.8	3788	div			22	8	Y	Y
1134. 0. 0	2	4187324	mal2	isp7	mal2	78.8	3788	div	76	30	18		Y	Y
1134. 0. 1r	6	4192140	C25B8.17	c25b8.16	c25b8.17	70.0	709	tan			17		N	N
1135. 0. 0	3	4195850	c683.03	c683.03	c694.01c	71.4	1699	conv	79	**23**		10	Y	Y
1135. 1. 0	4	4206893	c694.03	c694.02	c694.03	72.4	426	tan	79	6	10	2	Y	Y
1135. 2. 0	2	4223016	c1f7.03: pkd2	pkd2	rho1	72.6	2046	tan	81	7	8		Y	Y
1135. 3. 0	4	4232075	c1f7.06	cdc22	c1f7.06	71.4	1116	tan	80	11	12	21	Y	Y
1135. 4. 0	4	4243426	c1f7.09c	fio1	c1f7.09c	73.0	4508	conv	77	13	15	22	Y	Y
1136. 0. 0	4	4253423	pcr1: mts2	pcr1	ppr1	76.6	1941	div	77	42	11	56	Y	Y
1136. 1. 0	4	4264942	c2c4.04c	c2c4.04c	c2c4.05	73.8	1013	div	75	19	22	16	Y	Y
1137. 0. 0	3	4276774	c2c4.09	c2c4.07c	c2c4.08	77.6	1090	div	74	46		22	Y	Y
1137. 1. 0	4	4285351	c2c4.14c: ppk11	vma16	c2c4.14c	71.4	1422	conv	79	5	16	6	Y	N
1137. 2. 0	4	4291797	c25g10.01: c2c4.18	c2c4.17c	c2c4.18	73.2	4452	div	77	16	10	0	Y	Y

Origin No.	Class	Central Map Position	Central Probe	Gene AT island L	Gene AT island R	% AT	IG Length (bp)	IG Context	Replication Time Mitosis (min)	Mitosis Efficiency	*cdc13* s/o Efficiency	*cdc18cdt1* co-oe Efficiency	Orc4 signal ≥ 0.5 (Y/N)	Orc4 signal ≥ 0.8 (Y/N)
1137. 3. 0	4	4301928	rec10	rec10	his1	72.4	911	tan	77	19	4	6	Y	N
1137. 3. 1r	7	4320559	cdc8	c25g10.09c	cdc8	70.6	1054	tan				36	Y	Y
1138. 0. 0	3	4325978	c27f1.05c	c27f1.05c	c27f1.10	79.4	1381	tan	75	60		33	Y	Y
1138. 1. 0	3	4331353	c27f1.08: pdt1	c27f1.07	pdt1	68.8	882	tan	79	10		25	N	N
1138. 2. 0	3	4339346	c23d3.01	rfc2	c23d3.03c	69.6	329	conv	80	6		16	N	N
1138. 3. 0	4	4352827	c23d3.07: pup1	pup1	usp108	69.4	579	tan	83	10	5	0	N	N
1138. 4. 0	2	4367069	c23d3.13c	c23d3.12	c23d3.13c	78.6	3126	conv	83	11	6		Y	Y
1138. 5. 0	4	4390086	sec7b: sec72	c1527.03	sec72	73.2	869	conv	82	17	12	8	Y	Y
1138. 6. 0	4	4404539	c29e6.02	abc4	pof11	69.6	1675	div	80	3	11	4	N	N
1139. 0. 0	4	4414057	c29e6.06c: c30.10c	c30.10c	c30.11	77.6	904	div	78	30	12	10	Y	Y
1139. 1. 0	3	4416558	tbp1 : tdf1	c30.13	c30.14c	72.8	464	conv	76	21		8	N	N
1139. 2. 0	4	4428634	c16.03c: ura2	ura2	dus3	72.2	878	div	77	15	10	10	N	N
1140. 0. 0	4	4438136	c9e9.17c	c9e9.17c	leu2	74.8	2233	div	78	33	11	8	Y	Y
1140. 0. 1r	8	4449814	ypt2	ypt2	rad26	77.6	1597	div			11	31	Y	Y
1140. 1. 0	4	4470788	vps24	ybt1	wos2	72.6	873	tan	79	2	2	2	Y	Y
1140. 1. 1r	7	4476769	c17c9.14	c9e9.16	c17c9.15c	72.8	1030	tan				17	Y	N
1141. 0. 0	4	4483143	stm1	stm1	tim13	75.8	1302	div	76	28	10	13	Y	Y
1142. 0. 0	4	4491913	c17c9.05c	alg8: c17c9.07	sam50	72.4	716	tan	76	25	4	1	Y	Y
1142. 1. 0	3	4498681	nuc2	tif471	lys7	70.0	665	div	80	11		10	N	N
1142. 2. 0	2	4510723	c27d7.02c	c27d7.02c	mei2	73.2	1189	tan	79	7	19		Y	N
1143. 0. 0	1	4518600	c27d7.04	mei2	omt2	72.8	4249	div	78	20			Y	Y
1144. 0. 0	4	4534926	ssm4	c27d7.11c	but1	77.6	2663	tan	76	33	15	7	Y	Y

Origin No.	Class	Central Map Position	Central Probe	Gene AT island L	Gene AT island R	% AT	IG Length (bp)	IG Context	Replication Time Mitosis (min)	Mitosis Efficiency	*cdc13* s/o Efficiency	*cdc18cdt1* co-oe Efficiency	Orc4 signal ≥ 0.5 (Y/N)	Orc4 signal ≥ 0.8 (Y/N)
1144. 1. 0	2	4542343	c637.03	tpr1	c637.03	68.6	2299	div	78	20	16		Y	N
1144. 2. 0	2	4551856	moe1	vma2	c637.06	74.0	1097	div	79	15	1		Y	Y
1144. 3. 0	4	4558164	c637.09	rpn10	c637.11	69.6	656	div	80	6	0	118	N	N
1145. 0. 0	4	4577418	c12b10.02c	c12b10.02c	c12b10.03	73.0	1691	div	79	25	4	0	Y	Y
1146. 0. 0	3	4585551	c12b10.06c	c12b10.05	c12b10.06c	69.2	216	conv	79	24		4	N	N
1146. 1. 0	4	4590471	c12b10.10	c12b10.09	c12b10.10	72.0	690	tan	80	10	7	33	N	N
1146. 2. 0	3	4596683	rhp4a	rhp41	c12b10.13	71.0	649	div	83	13		13	N	N
1147. 0. 0	4	4601582	c12b10.16c: mug157	mug157	c12b10.18	74.8	4410	div	80	23	0	9	Y	Y
1147. 1. 0	3	4607112	c1093.01: c12b10.18	c12b10.18	c1093.02	70.6	713	tan	85	6		2	N	N
1148. 0. 0	4	4619130	c1093.04c	c1093.04c	c1093.05	72.8	1552	div	81	10	0	0	Y	Y
1148. 1. 0	4	4637595	c30c2.02: mmd1	dhc1	mmd1	71.8	990	div	83	8	10	0	Y	Y
1149. 0. 0	4	4650391	c1635.01	c144.01	c144.02	75.8	2030	div	81	**2**	7	5	Y	Y
1149. 1. 0	4	4658468	ade2 : min10	spe1	c144.05	72.0	1237	div	82	7	4	0	N	N
1149. 2. 0	4	4666550	C144.07c	c144.07c	c144.08	72.6	532	div	83	7	6	30	N	N
1150. 0. 0	2	4682800	klp8	cog1	c144.16	69.8	1180	div	83	8	0		Y	N
1150. 1. 0	2	4700003	h4.1: hhf1	hht1	alg9	74.8	2348	tan	87	10	0		Y	Y
1150. 2. 0	4	4705216	c1834.06c	pmo25	klp3	76.0	995	div	87	1	0	0	Y	Y
1151. 0. 0	4	4723000	sec18	sec18	pex7	70.8	1901	div	78	29	0	3	Y	Y
1152. 0. 0	4	4739355	vps34	c458.04c	pik3	78.4	1522	div	75	34	10	1	Y	Y
1152. 1. 0	2	4754248	pyug7.05	rpb9	pyug7.05	70.4	461	div	83	0	1		N	N
1152. 2. 0	3	4760930	c1782.02c	c1782.02c	c1782.03	71.8	920	div	83	0		18	Y	Y
1152. 2. 1r	7	4766865	C1782.06c	c1782.05	c1782.06c	71.4	458	conv				8	Y	N

Origin No.	Class	Central Map Position	Central Probe	Gene AT island L	Gene AT island R	% AT	IG Length (bp)	IG Context	Replication Time Mitosis (min)	Mitosis Efficiency	*cdc13* s/o Efficiency	*cdc18cdt1* co-oe Efficiency	Orc4 signal ≥ 0.5 (Y/N)	Orc4 signal ≥ 0.8 (Y/N)
1153. 0. 0	4	4778225	c11h11.03c	mug162	c11h11.03c	79.4	751	tan	77	25	0	24	Y	Y
1153. 0. 1r	7	4786061	C22F8.02c: pvg5	pvg5	c22f8.03c	70.6	2213	tan				16	Y	Y
1153. 1. 0	4	4791819	c22f8.05	c22f8.04	c22f8.05	68.8	1367	tan	81	0	6	4	Y	Y
1154. 0. 0	4	4804713	c22f8.09: rrp16	c22f8.08	rrp16	75.2	643	tan	78	14	8	4	Y	Y
1154. 1. 0	3	4822772	hus1	hri1	hus1	72.4	1117	tan	81	7		0	N	N
1155. 0. 0	4	4845092	c4f10.08: mug126	atg13	mug126	70.4	1410	div	77	30	2	11	Y	Y
1156. 0. 0	4	4855456	spn1	c4f10.10c	spn1	76.0	1764	div	75	22	1	10	Y	Y
1156. 0. 1r	8	4864860	C4F10.16c	wsp1	c4f10.16c	71.2	512	tan			6	2	Y	N
1157. 0. 0	2	4874446	grx1	c19b12.02c	bgs3	77.8	3544	div	72	39	0		Y	Y
1157. 1. 0	1	4897390	c19b12.07c	c19b12.07c	c19b12.08	72.0	1297	div	78	10			Y	Y
1157. 2. 0	2	4903246	c19b12.11c	c19b12.11c	yip11	70.8	1331	tan	76	6	13		N	N
1158. 0. 0	4	4924760	pb8e5.08	pb8e5.08	pb8e5.09	75.2	372	tan	77	26	13	7	Y	Y
1159. 0. 0	2	4934397	c1b3.04c	c1b3.04c	c1b3.05	72.4	1290	div	77	15	2		Y	Y
1159. 1. 0	4	4939040	c1b3.06c	c1b3.05	c1b3.06c	72.0	1247	conv	77	1	4	2	N	N
1159. 2. 0	2	4941622	vps28	c1b3.06c	vps28	70.2	1856	tan	79	2	2		Y	Y
1159. 3. 0	3	4948390	c1b3.10c	c1b3.20	ypt4	70.8	373	conv	80	3		14	N	N
1160. 0. 0	4	4964717	c1b3.17: clr2	vht1	clr2	78.2	4475	div	76	42	7	23	Y	Y
1160. 0. 1r	8	4970791	C1952.02	c1952.02	c1952.03	73.0	471	tan			5	31	Y	Y
1161. 0. 0	2	4980632	rad1	c1952.06c	rad1	75.8	1178	div	77	12	0		Y	Y
1161. 0. 1r	7	4982233	C1952.09c	c1952.09c	c1952.10c	73.6	2194	tan				54	Y	Y
1161. 1. 0	1	4990124	csn7a: csn71	ure2	csn71	70.0	801	tan	78	6			N	N
1161. 2. 0	2	4996116	c1952.14c: mrp125	ned1	mrp125	75.6	663	conv	80	0	1		Y	Y

Origin No.	Class	Central Map Position	Central Probe	Gene AT island L	Gene AT island R	% AT	IG Length (bp)	IG Context	Replication Time Mitosis (min)	Mitosis Efficiency	*cdc13* s/o Efficiency	*cdc18cdt1* co-oe Efficiency	Orc4 signal ≥ 0.5 (Y/N)	Orc4 signal ≥ 0.8 (Y/N)
1161. 3. 0	1	5002866	alp7	c890.01c	alp7	70.2	794	tan	80	15			N	N
1161. 4. 0	1	5014479	c890.06	c890.04c	c890.05	71.6	949	div	78	9			N	N
1161. 4. 1r	8	5019025	rpl31	c890.09	c22e12.02	73.4	1516	tan			53	6	Y	Y
1162. 0. 0	3	5023091	c22e12.03c	c22e12.03c	ccs1	76.8	1183	div	76	41		11	Y	Y
1162. 1. 0	2	5034396	c22e12.08	rrn10	krp1	70.0	616	conv	78	4	5		N	N
1163. 0. 0	4	5044477	rpl24-3: rpl2403	rpl2403	sck2	78.2	1904	tan	75	20	29	12	Y	Y
1163. 1. 0	2	5066571	c1006.01: psp3	wtf1	psp3	71.4	1608	tan	79	9	5		Y	N
1163. 1. 1r	6	5082004	C1006.06: rgf2	rgf2	c1006.07	71.6	882	tan			7		N	N
1164. 0. 0	4	5098334	ubc14	rpl3002	atl1	75.8	1302	div	79	20	20	5	Y	Y
1164. 0. 1r	7	5111331	C29A4.18: prw1	prw1	c29a4.17c	69.4	1267	div				15	N	N
1164. 1. 0	4	5121402	c29a4.13	c29a4.13	mug108	72.0	3199	div	80	6	2	0	Y	Y
1164. 1. 1r	8	5137066	C29A4.06c	cam2	c29a4.04c	74.0	2420	div			2	19	Y	Y
1165. 0. 0	4	5140115	c29a4.04c	cam2	c29a4.04c	74.0	2420	div	77	16	19	20	Y	Y
1166. 0. 0	4	5155963	c26f1.12c	c26f1.12c	c26f1.11	77.6	2929	conv	76	38	24	46	Y	Y
1166. 1. 0	4	5175504	gpm1	c26f1.07	gpm1	72.2	2123	tan	78	17	10	70	Y	Y
1167. 0. 0	4	5180320	c26f1.04c: etr1	mug106	etr1	72.2	2998	div	78	18	14	19	Y	Y
1167. 1. 0	2	5189450	pj691.03	pj691.02	pj691.03	73.8	1160	tan	82	12	46		Y	Y
1167. 2. 0	4	5218635	c19d5.04: ptr1	cid1	ptr1	72.6	640	tan	79	5	5	0	N	N
1168. 0. 0	4	5234575	b22918-2	mek1	b22918-2	76.0	1726	tan	78	**28**	5	4	Y	Y
1168. 0. 1r	7	5241691	C14C4.07	c14c4.06c	c14c4.07	69.0	974	div				8	N	N
1169. 0. 0	4	5252907	rad17	c14c4.12c	rad17	76.0	1323	div	81	13	6	14	Y	Y
1169. 1. 0	4	5262630	app1	adg1	c2h10.01	79.4	7817	div	83	0	20	32	Y	Y
1169. 2. 0	3	5277780	c2h10.02c	c2h10.02c	swr1	72.4	590	tan	86	1		7	N	N
1169. 3. 0	4	5291946	c11e3.05	c11e3.05	map1	73.0	431	tan	86	5	4	0	Y	Y

Origin No.	Class	Central Map Position	Central Probe	Gene AT island L	Gene AT island R	% AT	IG Length (bp)	IG Context	Replication Time Mitosis (min)	Mitosis Efficiency	*cdc13* s/o Efficiency	*cdc18cdt1* co-oe Efficiency	Orc4 signal ≥ 0.5 (Y/N)	Orc4 signal ≥ 0.8 (Y/N)
1169. 4. 0	4	5298628	cor1: nse6	nse6	pyp3	73.2	1104	div	85	0	0	1	Y	N
1169. 5. 0	1	5308924	c11e3.13c	c11e3.13c	c11e3.14	72.6	3822	div	86	1			Y	Y
1170. 0. 0	4	5317376	p8a3.02c	hsp9	p8a3.05	78.2	1921	div	81	1	5	0	Y	Y
1170. 1. 0	4	5328421	p8a3.07c	p8a3.07c	cdc4	71.0	1108	div	85	8	8	0	Y	Y
1170. 1. 1r	6	5341926	P8A3.13c	p8a3.13c	p8a3.14c	71.6	1203	tan			2		N	N
1170. 2. 0	2	5353592	c4d7.02c	c4d7.02c	pop2	71.4	1458	div	83	5	5		N	N
1170. 3. 0	4	5361223	tif34:sum1	c4d7.04c	sum1	70.2	556	div	82	0	0	0	N	N
1170. 4. 0	4	5366841	ade4 : min13	ade4	tif223	71.4	1586	div	85	4	0	0	Y	Y
1170. 4. 1r	8	5384854	C3G6.03c	c3g6.03c	rnp24	71.6	744	div			10	12	Y	Y
1171. 0. 0	3	5393545	c3g6.08	c3g6.07	erv1	76.6	1037	tan	77	17		17	Y	Y
1171. 0. 1r	6	5395545	C3G6.09c: tps2	erv1	tps2	70.4	409	conv			15		Y	Y
1171. 1. 0	2	5402750	c29b12.01: ino80	rpl4101	ino80	70.2	1007	tan	80	6	7		N	N
1171. 2. 0	4	5413756	spd1	spd1	snz1	73.6	2322	tan	81	4	10	8	Y	Y
1171. 2. 1r	8	5420896	sec16	rcd1	sec16	70.6	1185	div			10	5	N	N
1172. 0. 0	3	5437726	c29b12.11c	c29b12.10c	c29b12.11c	75.4	2264	tan	76	36		8	Y	Y
1172. 0. 1r	8	5442647	prl28	prl28	c1039.01	74.4	3755	div			6	13	Y	Y
1173. 0. 0	3	5449302	c1039.02	c1039.01	c1039.02	76.6	2663	tan	77	31		16	Y	Y
1173. 0. 1r	8	5455800	C1039.04	c1039.03	c1039.04	71.0	1146	tan			10	10	N	N
1173. 1. 0	2	5462253	c1039.06	c1039.06	c1039.07c	69.4	628	conv	83	6	8		N	N
1174. 0. 0	4	5471857	c922.01: mmf2	c922.02c	c922.03	76.8	2328	div	79	28	1	4	Y	Y
1174. 1. 0	4	5480929	c922.03	c922.04	c922.05c	75.8	2717	conv	82	16	8	10	Y	Y
1175. 0. 0	3	5486445	c922.06	c922.06	c922.07c	73.4	968	conv	80	33		8	Y	Y
1176. 0. 0	4	5499355	c869.08: pcm2	c869.09	pcm2	77.8	881	tan	80	4	11	17	Y	Y

Origin No.	Class	Central Map Position	Central Probe	Gene AT island L	Gene AT island R	% AT	IG Length (bp)	IG Context	Replication Time Mitosis (min)	Mitosis Efficiency	*cdc13* s/o Efficiency	*cdc18cdt1* co-oe Efficiency	Orc4 signal ≥ 0.5 (Y/N)	Orc4 signal ≥ 0.8 (Y/N)
1176. 0. 1r	7	5503474	C869.06c	mel1	c869.06c	74.8	1482	tan				10	Y	Y
1176. 1. 0	4	5513265	c869.03c	c869.03c	c869.02c	74.0	3216	tan	85	0	5	6	Y	Y
1176. 2. 0	4	5523977	c869.01	c869.02c	c869.01	75.8	2114	conv	84	3	0	7	Y	Y
1176. 3. 0	2	5536755	c186.03	c186.02c	c186.03	74.8	4237	div	87	0	0		Y	Y
1176. 3. 1r	7	5539473	C186.04c	c186.04c	c186.05c	76.0	1332	tan				5	Y	Y
1176. 4. 0	4	5548668	c186.08c	c186.06	c186.07c	76.2	2641	conv	87	0	0	12	Y	Y
1177. 0. 0	4	5558266	c186.09	c186.09	c750.01	75.2	1186	tan	85	0	10	16	Y	Y
1178. 0. 0	4	5576092	C750.07	c750.06c	c750.07c	83.4	5389	tan	85	0	5	11	Y	Y
2000. 0. 1r	7	36901	C1348.13	c1348.13	ght7	78.4	1323	conv				18	Y	Y
2000. 0. 2r	8	47428	PB8B6.03	pb8b6.02c	pb8b6.03	72.6	596	div			29	8	Y	Y
2000. 1. 0	4	67024	pb21e7.06	pb21e7.05	pb21e7.06	75.6	1129	tan	79	3	7	0	Y	Y
2001. 0. 0	2	95383	pb10d8.04c	pb10d8.03	pb10d8.04c	78.0	2694	conv	76	15	11		Y	Y
2001. 1. 0	4	113905	c359.03c	alr2	c359.03c	77.8	2437	conv	77	2	10	18	Y	Y
2002. 0. 0	4	129902	c359.06: mug14	mug14	c1683.01	75.8	4704	tan	77	6	7	6	Y	Y
2003. 0. 0	4	140082	c1683.03c	c1683.03c	c1683.04	78.4	2327	div	77	14	11	4	Y	Y
2004. 0. 0	4	149656	c1683.06c	c1683.05	c1683.06c	77.4	1384	conv	77	14	22	7	Y	Y
2004. 0. 1r	8	165330	c1683.10: pcl1	pcl1	c1683.11c	70.0	1633	tan			21	0	Y	N
2004. 1. 0	3	171214	c1683.12	c1683.13c	c1198.01	72.4	833	div	84	1		0	Y	N
2004. 2. 0	4	183177	c1198.05	zas1	c1198.05	75.8	1086	div	87	8	16	0	Y	N
2004. 3. 0	4	195776	c660.02: mfr1	reb1	mfr1	73.0	1135	div	84	1	6	0	N	N
2004. 4. 0	4	208542	ntp1	c660.05	c660.06	76.4	1681	tan	84	2	13	0	Y	Y
2004. 5. 0	2	218399	c660.12c	c660.12c	ssb1	74.8	1182	tan	82	2	11		Y	Y
2004. 6. 0	2	235120	c31e1.01c: atg2	atg2	pmr1	71.6	856	tan	85	0	4		N	N
2004. 7. 0	4	246667	ubl4: hub1	pmr1	hub1	73.4	1541	tan	79	1	4	13	Y	Y

Origin No.	Class	Central Map Position	Central Probe	Gene AT island L	Gene AT island R	% AT	IG Length (bp)	IG Context	Replication Time Mitosis (min)	Mitosis Efficiency	*cdc13* s/o Efficiency	*cdc18cdt1* co-oe Efficiency	Orc4 signal ≥ 0.5 (Y/N)	Orc4 signal ≥ 0.8 (Y/N)
2005. 0. 0	4	259783	clr3	clr3	rpl4301	76.2	2691	conv	80	18	16	16	Y	Y
2005. 1. 0	3	265692	c800.07c: tsf1	gcd10	sum2	72.0	591	tan	77	7		8	N	N
2006. 0. 0	4	279184	c800.12c	c800.11	c800.12c	75.0	1170	conv	75	38	21	16	Y	Y
2007. 0. 0	4	289429	c1773.04	c1773.03c	c1773.04	70.4	2206	div	76	29	17	11	Y	Y
2008. 0. 0	3	318308	c1773.15	arg7	c1773.15	77.8	1279	tan	76	39		33	Y	Y
2009. 0. 0	4	326041	car1	car1	p26c9.03c	76.0	2829	tan	76	48	30	39	Y	Y
2009. 0. 1r	8	328892	P26C9.03c	p26c9.03c	c1271.15c	74.6	4641	div			26	30	Y	Y
2009. 1. 0	4	342517	c1271.13: mrp18	c1271.14	mrp18	74.2	2831	tan	78	7	22	10	Y	Y
2010. 0. 0	2	359839	c1271.07c	mug96	c1271.05c	72.2	3098	tan	76	19	12		Y	N
2010. 1. 0	4	372533	c1271.01c: pof13	stt3	pof13	71.0	1483	div	81	5	17	0	N	N
2010. 2. 0	2	390762	cut4	mug2	cut4	71.8	2257	div	79	10	16		Y	N
2011. 0. 0	4	408532	c106.16	idi1	c106.16	77.8	1818	tan	76	41	35	13	Y	Y
2011. 1. 0	2	432057	rpn7	rpn7	c582.08	75.0	769	div	81	7	37		Y	N
2012. 0. 0	2	448794	c428.04	pho4	c428.04	74.8	2125	div	76	28	10		Y	Y
2013. 0. 0	4	462896	c428.10	c428.06	meu6	73.2	1190	div	79	**1**	6	4	Y	Y
2013. 0. 1r	6	471552	C428.14	c428.11	c428.12c	71.8	1211	conv			6		Y	Y
2013. 1. 0	4	487818	c902.03	c902.03	c902.04	70.6	1109	tan	80	9	8	2	Y	N
2013. 2. 0	4	502445	c1685.04	sec11	vma9	72.6	1533	tan	79	6	12	17	Y	N
2014. 0. 0	4	512980	cid11	c1685.07c	c1685.08	73.6	1749	div	76	44	30	34	Y	Y
2015. 0. 0	5	518689	c1685.11: rlp1	rlp1	c1685.13	80.0	6627	div	74	40	58	56	Y	Y
2015. 1. 0	4	537904	rhp14	rps1902	rhp14	73.8	997	tan	79	12	14	6	Y	Y
2015. 2. 0	4	551228	c354.04	c354.04	sre2	72.4	955	conv	82	3	8	6	Y	Y

Origin No.	Class	Central Map Position	Central Probe	Gene AT island L	Gene AT island R	% AT	IG Length (bp)	IG Context	Replication Time Mitosis (min)	Mitosis Efficiency	*cdc13* s/o Efficiency	*cdc18cdt1* co-oe Efficiency	Orc4 signal ≥ 0.5 (Y/N)	Orc4 signal ≥ 0.8 (Y/N)
2016. 0. 0	4	570157	c354.09c	c354.09c	c354.10	77.2	3366	div	76	43	24	16	Y	Y
2016. 0. 1r	8	576673	C354.11c	c354.10	c354.11c	69.6	1820	conv			30	24	Y	Y
2017. 0. 0	3	594429	c1706.01: tea4	tea4	fzo1	73.6	1993	tan	74	22		19	Y	Y
2017. 0. 1r	6	600328	C839.03c	c839.03c	rpl803	73.6	1097	div			22		Y	N
2018. 0. 0	4	604687	rps17-1: rps1701	rpl803	rps1701	75.8	1661	conv	74	28	32	16	Y	Y
2018. 1. 0	4	621879	c839.11c: hut1	hut1	rpc31	69.2	728	div	79	0	5	2	N	N
2019. 0. 0	4	637463	c115.03	c839.18c	c115.02c	75.4	2203	div	76	38	20	12	Y	Y
2019. 1. 0	4	645536	c947.14c	c947.13	kms2	73.0	928	tan	77	6	5	7	Y	Y
2020. 0. 0	3	648407	kms2	kms2	elg1	73.6	990	div	75	16		7	Y	Y
2020. 1. 0	4	657434	c947.09	c947.09	c947.08c	70.8	1976	div	80	2	2	0	Y	N
2021. 0. 0	4	673538	c947.04	c947.04	c947.03c	81.0	3967	div	75	30	37	41	Y	Y
2022. 0. 0	4	685043	dps: dps1	dps1	pj4664.02	74.2	2355	tan	74	41	26	21	Y	Y
2022. 0. 1r	6	713412	rpn3	rpn3	ubc4	69.6	1237	tan			10		Y	N
2023. 0. 0	4	719088	c119.03	ubc4	c119.03	69.2	1739	tan	78	22	9	9	Y	Y
2023. 0. 1r	6	734575	C119.09c	c119.09c	asn1	68.4	1180	div			12		N	N
2023. 1. 0	4	742342	c119.12	c119.12	prp31	71.8	482	conv	76	25	16	22	Y	Y
2024. 0. 0	4	745220	c119.18	c119.18	rti1	75.2	1694	tan	76	62	26	8	Y	Y
2025. 0. 0	4	756559	c577.03c	c577.01	rpl3801	72.2	836	tan	76	32	29	14	Y	Y
2025. 1. 0	1	776260	c577.12: mug71	c577.11	mug71	69.4	1132	tan	82	3			Y	N
2025. 1. 1r	8	781972	C577.15c	spa1	c577.15c	73.2	1202	tan			8	0	Y	Y
2025. 2. 0	1	787519	c530.02	c530.02	bag102	73.0	1955	conv	79	9			Y	Y
2025. 3. 0	2	794461	c530.04	mod5	c530.05	72.4	1582	tan	79	9	13		Y	N
2025. 4. 0	1	805432	c530.06c	c530.06c	c530.07c	70.6	1513	tan	80	23			Y	Y

Origin No.	Class	Central Map Position	Central Probe	Gene AT island L	Gene AT island R	% AT	IG Length (bp)	IG Context	Replication Time Mitosis (min)	Mitosis Efficiency	*cdc13* s/o Efficiency	*cdc18cdt1* co-oe Efficiency	Orc4 signal ≥ 0.5 (Y/N)	Orc4 signal ≥ 0.8 (Y/N)
2025. 4. 1r	8	810425	C530.09c	c530.08	c530.09c	70.2	243	conv			18	1	N	N
2026. 0. 0	3	818330	c530.12c: pdf1	pdf1	c530.13	75.4	1281	div	73	65		15	Y	Y
2026. 0. 1r	8	829991	dsk1	c661.01	c36.01c	73.2	2520	tan			15	12	Y	Y
2027. 0. 0	4	840165	c36.02c	c36.02c	c36.03c	76.2	4222	tan	76	37	20	18	Y	Y
2027. 1. 0	4	871728	ubpd	ubp21	c713.03	70.2	1463	div	85	0	11	0	N	N
2027. 2. 0	2	883547	c713.08: tom13	tom13	c713.09	71.8	2283	tan	87	9	15		Y	Y
2027. 2. 1r	6	893579	C713.12: erg1	pmp3	erg1	76.8	4527	div			11		Y	Y
2027. 3. 0	4	902850	c216.03	mcp5	c216.03	71.4	960	tan	83	4	2	0	N	N
2028. 0. 0	1	919729	tor2	swi1	tor2	77.0	677	tan	81	15			Y	Y
2029. 0. 0	4	938970	c646.08c	c646.08c	int6	74.0	608	tan	79	11	2	0	Y	Y
2029. 0. 1r	6	951781	sds23: moc1	gap1	sds23	77.6	3478	div			7		Y	Y
2030. 0. 0	4	957997	c646.16	c646.15c	c646.16	77.4	1169	div	78	16	5	9	Y	Y
2030. 1. 0	4	973319	p35g2.06c: nup131	p35g2.04c	cki2	73.6	922	tan	82	5	9	0	Y	Y
2030. 2. 0	4	991031	p35g2.13c: swc2	p35g2.11c	p35g2.12	72.2	1720	div	83	4	0	0	Y	N
2030. 3. 0	4	1009012	c146.04	cut3	c146.04	79.2	1554	div	80	6	1	0	Y	Y
2031. 0. 0	4	1021416	c146.10: mug57	lsd1	mug57	74.0	750	div	80	14	0	0	Y	Y
2031. 1. 0	3	1034630	c337.02c	c337.02c	c337.03	71.6	1761	div	77	6		7	Y	Y
2032. 0. 0	4	1048973	c337.09: erg28	ubi4	erg28	71.0	1968	div	80	16	1	0	Y	N
2033. 0. 0	3	1057797	gtr1	gtr1	rpb4	73.2	957	div	80	26		12	Y	Y
2033. 1. 0	4	1089225	suc1	atp3	suc1	71.6	1350	conv		10	11	5	N	N
2034. 0. 0	4	1107356	sks2: hsc1	cyp3	sks2	76.2	1848	div	76	27	26	17	Y	Y
2034. 1. 0	4	1120149	c1709.09	c1709.10c	png2	72.6	763	tan	79	10	14	14	Y	Y

Origin No.	Class	Central Map Position	Central Probe	Gene AT island L	Gene AT island R	% AT	IG Length (bp)	IG Context	Replication Time Mitosis (min)	Mitosis Efficiency	*cdc13* s/o Efficiency	*cdc18cdt1* co-oe Efficiency	Orc4 signal ≥ 0.5 (Y/N)	Orc4 signal ≥ 0.8 (Y/N)
2034. 2. 0	4	1123753	c1709.12: rid1	png2	rid1	72.6	878	div	78	2	5	9	Y	Y
2035. 0. 0	4	1141686	psh1: skp1	skp1	uch2	77.2	1414	tan	73	41	30	27	Y	Y
2036. 0. 0	4	1157276	c409.10: ade7	mis13	ade7	75.4	1516	div	73	29	20	16	Y	Y
2036. 1. 0	3	1167105	c409.14c: mrps17	c409.12c	c409.13	71.0	2398	div	78	16		4	N	N
2037. 0. 0	2	1169916	c409.16c	c409.17c	c409.18	73.2	1379	div	78	21	6		Y	N
2037. 0. 1r	7	1177761	sec66	psh3	sec66	72.8	995	div				5	Y	Y
2037. 1. 0	2	1201815	c725.01	c725.01	mpr1	71.8	1782	tan	84	2	11		Y	N
2037. 2. 0	4	1211576	c725.04	c725.03	c725.04	71.8	1151	tan	83	8	11	14	N	N
2037. 3. 0	2	1218935	pex5	c725.06c	pex5	71.0	1097	div	82	5	15		Y	N
2037. 3. 1r	8	1225874	C725.10	hob3	c725.10	70.6	1777	div			18	5	Y	Y
2037. 4. 0	2	1228956	c725.12: mug118	php2	mug118	71.0	847	div	79	16	8		Y	N
2037. 5. 0	4	1232601	res1: sct1	ura5	res1	73.2	1608	tan	79	10	11	19	Y	N
2038. 0. 0	4	1240584	c651.03c: gyp10	nog1	c651.02	72.2	1008	div	76	32	16	18	Y	Y
2038. 1. 0	4	1246420	c651.04	gyp10	c651.04	74.2	1901	div	77	24	29	30	Y	Y
2039. 0. 0	4	1255201	C651.09c	rpc1	c651.09c	75.8	1256	tan	75	17	24	36	Y	Y
2040. 0. 0	5	1263905	cwl1	cwl1	but2	83.8	6144	div	75	53	82	70	Y	Y
2041. 0. 0	4	1272086	c3d6.02: but2	but2	c3d6.03c	71.2	1057	conv	75	32	73	54	Y	N
2042. 0. 0	4	1279970	c3d6.05: ptp4	mad1	ptp4	78.6	1259	div	74	58	54	38	Y	Y
2042. 0. 1r	8	1288306	C3D6.10	c3d6.08c	dpb4	72.6	1058	div			18	28	N	N
2042. 0. 2r	8	1301412	C30B4.01c: wsc1	c3d6.13c	wsc1	72.2	3608	tan			5	15	Y	Y
2043. 0. 0	2	1312584	c30b4.04c: sol1	c30b4.03c	sol1	75.0	3130	tan	77	37	27		Y	Y

Origin No.	Class	Central Map Position	Central Probe	Gene AT island L	Gene AT island R	% AT	IG Length (bp)	IG Context	Replication Time Mitosis (min)	Mitosis Efficiency	*cdc13* s/o Efficiency	*cdc18cdt1* co-oe Efficiency	Orc4 signal ≥ 0.5 (Y/N)	Orc4 signal ≥ 0.8 (Y/N)
2044. 0. 0	4	1316300	c30b4.05:kap109	sol1	kap109	75.0	1506	div	76	29	29	19	Y	Y
2044. 1. 0	2	1322695	c27b12.01c: mmm1	mmm1	c30b4.10	73.4	639	div	79	8	23		Y	Y
2044. 2. 0	2	1354079	c27b12.12c	c27b12.14	c27b12.12c	75.0	2467	conv	80	5	8		Y	Y
2045. 0. 0	4	1390370	c8d2.17	c8d2.16c	c8d2.17	75.2	1445	div	77	41	25	5	Y	Y
2045. 0. 1r	6	1394354	C8D2.19: mde3	c8d2.18c	mde3	70.0	485	div			24		Y	N
2045. 1. 0	4	1404843	c17a3.02	tim50	c17a3.02	70.0	1470	div	80	7	11	0	Y	Y
2045. 2. 0	4	1414134	pi040: c17a3.06	pgr1	c17a3.08	71.6	319	tan	81	5	13	7	N	N
2045. 3. 0	4	1420712	pi035: c691.01c	pas4	c691.01	70.6	691	tan	79	10	10	4	N	N
2046. 0. 0	3	1428946	pi031: c691.04	apl3	c691.04	74.4	1482	div	77	16		11	Y	Y
2046. 0. 1r	8	1437178	pi028: p22h7.03	p22h7.01c: c691.05c	p22h7.02c	71.2	521	tan			23	22	Y	N
2047. 0. 0	4	1444492	pi025: p22h7.06	p22h7.05c	p22h7.06	77.6	1992	div	75	**27**	50	32	Y	Y
2047. 1. 0	4	1449751	rps10-2: pi023: rps1002	p22h7.10c	nep2	73.4	1082	tan	78	21	78	43	Y	Y
2048. 0. 0	5	1457664	bem46	nep2	bem46	80.8	4229	div	76	41	65	45	Y	Y
2048. 0. 1r	8	1465226	git5	git5	c32h8.08c	74.0	567	conv			48	21	Y	Y
2048. 0. 2r	8	1474094	pi013: mei4	mei4	act1	72.0	1401	conv			17	1	Y	Y
2048. 1. 0	4	1490539	pi008: cog8	his3	cog8	71.6	711	div	83	4	5	0	Y	N
2048. 1. 1r	6	1503542	pht1: pi001	cdc2	pht1	72.0	1113	conv			16		Y	Y
2048. 1. 2r	7	1506318	C1215.01	pht1	shy1	69.2	2260	div				3	Y	Y
2048. 2. 0	2	1514321	rpl37a-2: rpl43-2: rpl4302	rpl4302	tas3	75.0	739	tan	83	21	6		Y	Y
2048. 3. 0	4	1519956	c83.05	tas3	apc15	70.4	598	div	81	3	1	0	N	N
2049. 0. 0	4	1529334	c83.10	c83.09c	c83.10	71.8	940	div	76	20	25	8	Y	Y

Origin No.	Class	Central Map Position	Central Probe	Gene AT island L	Gene AT island R	% AT	IG Length (bp)	IG Context	Replication Time Mitosis (min)	Mitosis Efficiency	*cdc13* s/o Efficiency	*cdc18cdt1* co-oe Efficiency	Orc4 signal ≥ 0.5 (Y/N)	Orc4 signal ≥ 0.8 (Y/N)
2049. 1. 0	4	1536905	rfc5	rfc5	c83.15	71.8	843	div	76	11	29	13	N	N
2049. 1. 1r	8	1542352	C83.19c	c83.16c	c83.19c	74.4	959	tan			43	22	Y	Y
2050. 0. 0	4	1545364	ars2004: c83.18c	c83.18c	atf1	75.6	2894	div	72	51	45	19	Y	Y
2050. 1. 0	4	1565674	c27.01c	c27.01c	ask1	73.4	472	tan	79	2	8	10	Y	Y
2050. 1. 1r	8	1580027	mdm12	mdm12	sfr1	71.0	739	div			18	16	Y	N
2051. 0. 0	4	1587587	C28F2.10c: kap1	kap1	c28f2.11	76.8	1016	div	80	13	29	21	Y	Y
2051. 1. 0	4	1592054	rpb1	rpb1	centromere repeats	73.6		cen	80	19	66	33	Y	Y
2052. 0. 0	4	1649764	c21b10.13c	dgII pericentric repetitive sequence	c21b10.13c	79.2	3484	cen	76	20	49	19	Y	Y
2053. 0. 0	4	1658122	c21b10.08c	c21b10.09	c21b10.08c	73.0	1670	div	78	32	49	27	Y	Y
2054. 0. 0	4	1664975	pop3: wat1	nrf1	c21b10.03c	72.6	2108	tan	78	17	24	12	Y	Y
2054. 0. 1r	7	1671424	C21B10.02	c21b10.02	cdc28	69.0	437	div				10	N	N
2054. 1. 0	2	1680440	c19c2.04c	ubp11	ran1	72.0	5284	div	80	15	13		Y	Y
2054. 2. 0	4	1688574	c19c2.06c: mug124	ran1	mug124	79.2	2494	conv	81	8	20	7	Y	Y
2055. 0. 0	4	1704867	smd3	c19c2.10	c19c2.11c	75.0	893	conv	74	41	31	7	Y	Y
2056. 0. 0	4	1717752	c2f12.12c	c2f12.12c	rep2	72.6	3337	tan	74	17	27	6	Y	Y
2056. 1. 0	4	1730309	rpl8-2: rpk37: rpk5b: rpl802	rpl802	c2f12.05c	69.8	1395	tan	78	12	10	12	N	N
2056. 1. 1r	8	1749201	c1d7.03: mug80	mug80	scr1	73.8	6162	div			31	17	Y	Y
2056. 2. 0	4	1753434	scr1	scr1	c1d7.01	74.2	1223	conv	76	16	25	29	Y	Y

Origin No.	Class	Central Map Position	Central Probe	Gene AT island L	Gene AT island R	% AT	IG Length (bp)	IG Context	Replication Time Mitosis (min)	Mitosis Efficiency	*cdc13* s/o Efficiency	*cdc18cdt1* co-oe Efficiency	Orc4 signal ≥ 0.5 (Y/N)	Orc4 signal ≥ 0.8 (Y/N)
2056. 2. 1r	8	1759607	C11G11.01: fis1	fis1	end3	70.2	555	conv			24	11	Y	N
2057. 0. 0	3	1765886	sme1	sme1	c18h10.01	73.4	1017	div	76	27		11	Y	Y
2058. 0. 0	4	1781829	meu11	meu11	c18h10.05	74.4	3116	div	76	26	28	34	Y	Y
2058. 0. 1r	8	1788396	c18h10.08c: ubp4	ubp4	c18h10.09	68.6	1060	div			22	9	Y	N
2058. 1. 0	4	1791904	rpl7-2: rpl701	rps1402	rps1601	70.6	1143	tan	78	6	11	12	N	N
2058. 2. 0	4	1797195	rps16-1: rps1601	ppk23	c18h10.16	70.6	519	tan	80	3	11	9	N	N
2058. 2. 1r	8	1802531	C18H10.17c	c18h10.17c	c18h10.18c	73.0	1097	tan			24	4	Y	N
2059. 0. 0	4	1808026	c18h10.19	c18h10.18c	c18h10.19	74.8	3927	div	77	20	18	15	Y	Y
2059. 1. 0	4	1833724	c9b6.09c	c9b6.07	clc1	70.8	1665	tan	87	4	2	0	Y	Y
2059. 2. 0	3	1837685	c9b6.12c: apc13	apc13	c9b6.13	70.6	1031	div	86	5		0	N	N
2059. 3. 0	4	1845199	c28e12.04	c28e12.04	esf2	71.0	630	tan	86	2	0	0	N	N
2059. 3. 1r	6	1866577	C3H7.10	c3h7.10	mug142	70.2	788	tan			11		Y	Y
2060. 0. 0	1	1870330	c3h7.08c	mug142	c3h7.08c	76.4	1802	div	82	9			Y	Y
2060. 1. 0	4	1880179	c3h7.04	c3h7.04	c3h7.03c	70.8	4179	div	82	12	10	12	N	N
2060. 2. 0	2	1895505	mcs2	spo14	mcs2	71.6	1499	div	82	12	12		Y	Y
2060. 3. 0	4	1918104	c16e9.01c: php4	p16f5.08c	php4	70.6	2370	tan	80	9	0	4	Y	Y
2060. 3. 1r	8	1925786	C16E9.05: erg6	uvi31	mug100	72.4	1145	div			8	6	Y	Y
2060. 4. 0	3	1929243	c16e9.07: mug100	c16e9.09c	c16e9.10c	72.2	574	tan	77	17		6	Y	N
2061. 0. 0	4	1941985	pab2	pab2	ksp1	75.8	2470	div	75	42	35	17	Y	Y
2062. 0. 0	4	1955244	rem1	c16e9.16c	rem1	75.2	3163	tan	79	28	33	29	Y	Y
2063. 0. 0	2	1964686	c1e8.03c	c1e8.03c	tf2-10-pseudo	73.4	3572	div	76	18	33		Y	Y
2063. 1. 0	4	1987173	c1a4.05	c1a4.06c	c1a4.07c	74.4	632	tan	81	8	15	0	Y	Y

Origin No.	Class	Central Map Position	Central Probe	Gene AT island L	Gene AT island R	% AT	IG Length (bp)	IG Context	Replication Time Mitosis (min)	Mitosis Efficiency	*cdc13* s/o Efficiency	*cdc18cdt1* co-oe Efficiency	Orc4 signal ≥ 0.5 (Y/N)	Orc4 signal ≥ 0.8 (Y/N)
2064. 0. 0	4	2027780	p23a10.12	p23a10.11c	p23a10.12	80.8	3259	div	75	30	17	60	Y	Y
2065. 0. 0	4	2035403	p23a10.15c	qcr1	sdh4	75.2	1175	div	75	34	10	34	Y	Y
2065. 0. 1r	8	2045563	his7	c29a3.03c	rpl8	71.6	1731	div			26	31	Y	N
2066. 0. 0	4	2056510	c29a3.08: pof4	c29a3.07c	pof4	76.2	2337	div	77	30	24	29	Y	Y
2066. 0. 1r	8	2062903	c29a3.13	rps902	c29a3.13	71.0	732	conv			14	8	N	N
2067. 0. 0	1	2072281	c29a3.17	c29a3.16	gef3	77.4	1492	tan	79	10			Y	Y
2067. 1. 0	4	2077564	c18e5.01	cyt1	c29a3.19	72.2	1334	tan	80	11	10	4	N	N
2067. 1. 1r	8	2084287	C18E5.05c	rps21	c18e5.07	70.8	1437	tan			26	8	Y	N
2067. 2. 0	4	2091888	c18e5.14c	c18e5.15	c18e5.10	73.8	616	tan	83	6	10	0	Y	Y
2067. 3. 0	1	2100904	chr2.854.1: ctr6	ctr6	nif1	73.6	384	conv	81	1			Y	Y
2067. 4. 0	4	2109310	c23g7.06c	nif1	sui1	79.4	2134	div	84	0	23	8	Y	Y
2068. 0. 0	4	2115820	matmc: c23g7.09	matmc_2	c23g7.10c	79.4	3239	conv	75	**15**	22	22	Y	Y
2069. 0. 0	4	2133124	matmi: c1711.01	rpp202	matmi_1	77.4	4175	tan	81	**25**	24	19	Y	Y
2070. 0. 0	4	2139624	c1711.03	matmc_1	c1711.03	75.2	4968	tan	76	18	19	20	Y	Y
2070. 1. 0	3	2145514	rpl4: rpl401	rpl401	c1711.07	71.6	2027	tan	80	7		21	N	N
2071. 0. 0	4	2163634	his2	c1711.15c	c1711.16	71.4	2066	div	77	25	12	4	Y	Y
2071. 0. 1r	8	2173657	C17G9.03c	c17g9.03c	nup85	70.6	468	tan			15	13	N	N
2072. 0. 0	3	2180590	c17g9.05: rct1	nup85	rct1	71.8	1905	div	76	27		25	Y	Y
2073. 0. 0	4	2190182	csx2	csx2	tif213	74.2	3035	div	79	30	16	52	Y	Y
2074. 0. 0	4	2207092	c14c8.02: tim44	cut2	tim44	72.2	1332	div	79	25	8	8	Y	Y
2074. 1. 0	3	2216239	sop2	meu17	arc1	71.0	1065	div	79	20		12	N	N
2074. 2. 0	4	2231868	c14c8.15	pol5	c14c8.15	71.6	1239	div	79	22	12	6	Y	N
2074. 3. 0	1	2238603	c14c8.17c	oca3	c15c4.02	74.2	1032	div	77	12			Y	N

Origin No.	Class	Central Map Position	Central Probe	Gene AT island L	Gene AT island R	% AT	IG Length (bp)	IG Context	Replication Time Mitosis (min)	Mitosis Efficiency	*cdc13* s/o Efficiency	*cdc18cdt1* co-oe Efficiency	Orc4 signal ≥ 0.5 (Y/N)	Orc4 signal ≥ 0.8 (Y/N)
2075. 0. 0	2	2252074	c21h7.01c: c15c4.06c	c15c4.06c	taf10	72.8	1795	div	79	18	15		Y	Y
2075. 0. 1r	8	2268466	his5	c21h7.06c	his5	73.8	1635	tan			8	7	Y	Y
2075. 1. 0	1	2282820	prp43.a: prp43	c16h5.09c	c16h5.08c	73.2	549	tan	82	12			Y	Y
2076. 0. 0	4	2318853	c12d12.06: trx2	trx2	ned8	79.0	1419	tan	76	32	9	16	Y	Y
2077. 0. 0	3	2322243	ubl1	c24c6.02	c24c6.03	73.4	691	tan	75	32		18	Y	Y
2077. 0. 1r	7	2326089	c24c6.04	sec28	gpa1	70.4	1921	tan				15	N	N
2077. 1. 0	4	2347730	msh2	msh2	c19g7.02	74.0	741	div	81	21	5	7	Y	Y
2077. 2. 0	1	2357183	cps1: drc1: bgs1	bgs1	mbx1	69.0	3185	div	81	1			Y	Y
2078. 0. 0	4	2373967	c19g7.11c	c19g7.11c	trf1	70.8	1249	div	81	14	12	0	N	N
2078. 1. 0	4	2379949	c19g7.16: iws1	nup44	iws1	70.6	1372	tan	82	9	7	25	Y	Y
2078. 2. 0	4	2389680	c36b7.04	sec63	c36b7.04	70.4	628	tan	83	8	4	0	N	N
2078. 3. 0	2	2403598	p18g5.02	rpl3701	rad60	71.2	870	div	84	8	5		Y	N
2078. 4. 0	1	2412894	mex67	mex67	c1921.04c	76.4	956	tan	84	12			Y	Y
2079. 0. 0	4	2434427	c21d10.09c	c21d10.07	map4	73.4	2153	div	76	22	17	25	Y	Y
2080. 0. 0	4	2448612	c12c2.12c	ucp3	fnx1	77.8	3194	tan	78	21	5	48	Y	Y
2080. 1. 0	4	2465317	c12c2.07c	dnm1	c12c2.07c	69.4	1704	div	82	5	14	5	N	N
2080. 2. 0	1	2485034	nak1	nak1	rga5	70.8	2486	div	80	10			Y	N
2080. 3. 0	4	2491092	pim1: dcd1	pim1	ppk29	70.0	1219	div	80	14	2	0	N	N
2080. 4. 0	3	2499479	c365.20c	c557.06c	c365.01	74.6	2328	div	80	8		13	Y	Y
2080. 5. 0	4	2503770	rpl21	cox10	rpl2101	70.6	702	tan	81	12	18	3	Y	Y
2081. 0. 0	4	2527412	alp4	c365.14c	alp4	74.6	1135	div	78	37	12	10	Y	Y
2081. 0. 1r	8	2532788	C365.16	alp4	c365.16	73.0	4572	tan			14	14	Y	Y
2081. 1. 0	3	2547320	exo1	psm1	exo1	71.8	1104	tan	79	2		53	Y	Y

Origin No.	Class	Central Map Position	Central Probe	Gene AT island L	Gene AT island R	% AT	IG Length (bp)	IG Context	Replication Time Mitosis (min)	Mitosis Efficiency	*cdc13* s/o Efficiency	*cdc18cdt1* co-oe Efficiency	Orc4 signal ≥ 0.5 (Y/N)	Orc4 signal ≥ 0.8 (Y/N)
2082. 0. 0	3	2557464	C29A10.09c	c29a10.07	c29a10.08	81.0	1599	tan	78	27		45	Y	Y
2082. 1. 0	3	2559093	C29A10.10c	c29a10.10c	vps902	74.6	798	tan	79	0		34	Y	N
2082. 1. 1r	8	2569630	atp7	atp7	rec8	73.0	709	tan			11	22	Y	N
2083. 0. 0	4	2596041	rpc25	rpc25	c2g5.08	78.4	1293	div	76	29	22	27	Y	Y
2084. 0. 0	4	2601808	mam1	mam1	c25b2.03	69.0	1848	div	76	25	7	12	N	N
2084. 1. 0	2	2609155	c25b2.06c	c25b2.07c	c25b2.08	69.8	1665	div	81	2	7		Y	Y
2084. 2. 0	4	2614037	c25b2.08	c25b2.08	c25b2.09c	76.0	463	conv	81	6	16	0	Y	Y
2085. 0. 0	4	2622205	c25b2.12c: mot1	c6b1.03c	mde4	75.6	1057	div	80	6	12	2	Y	Y
2085. 1. 0	2	2641131	c6b1.06c: ubp14	upb14	prp1	75.4	1980	div	83	0	8		Y	Y
2085. 2. 0	2	2662387	hsp16	hsp16	c3e7.05c	71.8	4744	tan	79	6	12		Y	Y
2086. 0. 0	4	2673881	c3e7.07c	c3e7.06c	c3e7.07c	73.2	2018	tan	78	10	11	22	Y	Y
2086. 0. 1r	8	2693818	C4F6.05c	c4f6.05c	kin1	73.0	1995	div			25	12	Y	N
2087. 0. 0	4	2703235	c4f6.08c: mrp139	mrp139	str1	75.0	4273	div	76	29	5	2	Y	Y
2087. 0. 1r	8	2711648	C4F6.11c	c4f6.11c	c4f6.12	71.4	1017	div			18	12	Y	N
2087. 0. 2r	7	2716224	C4F6.13c	c4f6.12	c4f6.13c	75.0	539	conv				11	N	N
2087. 1. 0	4	2723006	c4f6.16c: ero11	ero11	c4f6.17c	71.4	837	tan	80	6	8	12	N	N
2088. 0. 0	4	2742002	c336.02	c336.02	efc25	77.6	2257	tan	75	34	18	33	Y	Y
2088. 1. 0	3	2749420	cdc6: pol3: pold: mis10	rnh1	sfc3	71.4	1145	div	79	10		16	N	N
2088. 2. 0	1	2766183	c336.13c	ppk26	pic1	73.6	1580	div	79	18			Y	Y
2088. 2. 1r	7	2776497	C685.03	c685.03	aps2	72.8	429	conv				6	Y	Y
2089. 0. 0	4	2778285	aps2	aps2	gpi15	72.8	925	div	78	5	17	32	Y	Y
2090. 0. 0	4	2789729	rec14	rec14	gpx1	72.8	1131	conv	75	30	4	32	Y	N

Origin No.	Class	Central Map Position	Central Probe	Gene AT island L	Gene AT island R	% AT	IG Length (bp)	IG Context	Replication Time Mitosis (min)	Mitosis Efficiency	*cdc13* s/o Efficiency	*cdc18cdt1* co-oe Efficiency	Orc4 signal ≥ 0.5 (Y/N)	Orc4 signal ≥ 0.8 (Y/N)
2091. 0. 0	4	2792440	tug1: gtb1	gpx1	tug1	80.2	1922	div	75	44	28	46	Y	Y
2092. 0. 0	4	2799830	c32f12.08c: duo1	duo1	rum1	74.4	2081	div	77	47	17	71	Y	Y
2092. 1. 0	4	2812552	c32f12.12c	c32f12.12c	c32f12.13c	71.8	788	tan	80	1	6	17	N	N
2092. 2. 0	4	2822096	cyr1: git2	ubr1	cyr1	70.4	782	tan	83	9	2	11	Y	N
2092. 3. 0	2	2851918	p19a11.02c	p19a11.02c	mts4	70.4	1015	tan	84	6	7		N	N
2092. 4. 0	4	2871220	c1346.03: p4h10.02c	oxa102	ppb1	74.0	869	tan	85	8	11	9	Y	Y
2092. 5. 0	3	2880262	cut14	cut14	p4h10.07	70.6	436	div	85	7		2	N	N
2093. 0. 0	4	2900409	p4h10.14c	p4h10.14c	p4h10.15	83.6	3896	div	80	14	13	27	Y	Y
2093. 1. 0	4	2916236	p4h10.20: nhm1	p4h10.19c	nhm1	73.6	762	div	80	3	9	12	Y	Y
2093. 2. 0	3	2926087	c1703.05	mlh1	c1703.05	73.8	501	tan	81	3		6	Y	Y
2093. 3. 0	3	2930902	c1703.08c	c1703.08c	c1703.09	76.4	573	div	79	6		9	Y	N
2093. 4. 0	2	2935558	ypt1	c1703.09	ypt1	72.6	569	tan	79	12	7		Y	N
2094. 0. 0	4	2942660	c1703.13c	ubp9	c1703.13c	77.2	1912	conv	77	28	14	8	Y	Y
2094. 0. 1r	8	2958269	c2a9.05	c2a9.04c	c2a9.05c	71.6	1427	tan			17	7	Y	Y
2094. 1. 0	1	2962766	c2a9.13	c2a9.09	c2a9.10	72.4	551	tan	80	2			Y	Y
2094. 2. 0	2	2967941	c2d10.02: orc6	c2d10.01c	orc6	72.4	832	div	80	3	10		N	N
2094. 3. 0	2	2976815	c2d10.04	c2d10.03c	c2d10.04	70.6	3400	div	82	4	11		N	N
2094. 4. 0	3	2983316	c2d10.09	c2d10.08c	c2d10.09	70.6	615	div	80	17		22	Y	N
2095. 0. 0	3	2986841	c2d10.11c	c2d10.11c	rhp23	74.8	1115	div	78	21		5	Y	Y
2095. 1. 0	3	3006087	c2d10.19c	c2d10.19c	ubc1	76.0	597	div	84	0		0	Y	N
2095. 2. 0	4	3017563	slm9	c15d4.02	slm9	72.6	960	tan	85	0	11	4	Y	N
2095. 3. 0	4	3025845	c15d4.06	gpt2	c15d4.05	73.4	1268	tan	84	13	12	0	Y	Y

Origin No.	Class	Central Map Position	Central Probe	Gene AT island L	Gene AT island R	% AT	IG Length (bp)	IG Context	Replication Time Mitosis (min)	Mitosis Efficiency	*cdc13* s/o Efficiency	*cdc18cdt1* co-oe Efficiency	Orc4 signal ≥ 0.5 (Y/N)	Orc4 signal ≥ 0.8 (Y/N)
2095. 4. 0	2	3032267	c15d4.11c	c15d4.09c	amo1	70.6	431	tan	81	7	7		Y	Y
2095. 5. 0	3	3036105	c15d4.13c	pho2	cwf22	71.0	877	tan	80	5		6	N	N
2095. 6. 0	1	3039997	c13e7.01: cwf22	cwf22	cwf24	73.4	1309	tan	81	6			Y	Y
2096. 0. 0	3	3051269	c13e7.06	msd1	c13e7.07	77.0	935	tan	78	30		6	Y	Y
2096. 1. 0	4	3059406	c30d10.20: brf1	c30d10.20: brf1	c30d10.19c	75.0	542	div	82	7	12	13	Y	Y
2097. 0. 0	4	3071638	c30d10.14	c30d10.14	pdb1	72.8	1797	div	78	10	6	9	Y	Y
2097. 1. 0	1	3086513	c30d10.09c	mgm101	c30d10.07c	70.6	790	div	81	11			Y	Y
2097. 2. 0	3	3091974	c30d10.05c	lsm4	c30d10.05c	70.6	1103	div	82	5		12	N	N
2098. 0. 0	4	3097222	c1778.01c: zuo1	zuo1	rap1	79.0	2043	div	79	17	10	26	Y	Y
2098. 1. 0	4	3111629	c1778.07	fim1	c1778.07	68.4	1219	div	81	10	7	6	N	N
2098. 2. 0	4	3116780	ppk21	c1778.09	ppk21	72.8	492	conv	85	6	4	39	Y	N
2098. 3. 0	1	3123468	c4c3.09	c4c3.09	mug136	73.6	928	tan	81	14			N	N
2099. 0. 0	4	3138358	c4c3.04c	c4c3.12	c4c3.04c	74.6	2119	div	78	13	0	0	Y	Y
2099. 1. 0	1	3164076	c609.01	c609.01	ptn1	75.2	610	tan	81	2			Y	Y
2100. 0. 0	3	3175543	c776.03	dis2	c776.03	79.2	1595	div	77	37		17	Y	Y
2100. 1. 0	3	3190233	c776.07	c776.06c	c776.07	72.0	834	div	81	3		12	Y	N
2100. 2. 0	4	3199818	hsk1	hsk1	cnd1	76.4	1162	div	83	2	4	0	Y	Y
2100. 2. 1r	7	3205563	plh1	cnd1	plh1	71.2	672	tan				16	Y	N
2100. 3. 0	4	3214362	pmh1	pmh1	mis17	73.0	720	div	80	5	2	0	Y	N
2100. 4. 0	4	3218556	c21.02	c21.03c	med8	71.8	656	div	81	5	4	7	N	N
2100. 4. 1r	7	3223908	ral2	ral2	cdc7	73.8	599	tan				16	Y	N
2101. 0. 0	3	3237173	c19f8.04c	c19f8.04c	c19f8.05	78.4	2849	div	78	17		5	Y	Y

Origin No.	Class	Central Map Position	Central Probe	Gene AT island L	Gene AT island R	% AT	IG Length (bp)	IG Context	Replication Time Mitosis (min)	Mitosis Efficiency	*cdc13* s/o Efficiency	*cdc18cdt1* co-oe Efficiency	Orc4 signal ≥ 0.5 (Y/N)	Orc4 signal ≥ 0.8 (Y/N)
2101. 1. 0	1	3252870	c25h2.14: mug16	mug16	cdc20	74.2	2641	div	79	9			Y	Y
2101. 2. 0	4	3275570	c25h2.06c: hrf1	hrf1	egd2	72.8	1145	conv	81	9	17	5	N	N
2102. 0. 0	4	3289550	C20F10.03	c20f10.02c	c20f10.03	77.2	1329	div	75	23	15	18	Y	Y
2102. 0. 1r	8	3297795	C20F10.07	mad2	c20f10.07	71.2	1021	tan			1	26	N	N
2102. 1. 0	3	3305235	c20f10.10	lsm5	c20f10.10	72.2	1564	tan	79	6		11	N	N
2103. 0. 0	4	3335630	c17d1.03c	c17d1.03c	c17d1.04	76.4	833	div	77	22	11	16	Y	Y
2104. 0. 0	4	3365308	rpl5-2: rpl1502	c11c11.06c	rpl1801	76.0	1920	div	78	34	29	10	Y	Y
2104. 1. 0	4	3398583	php5	php5	arh1	75.0	1927	div	82	11	11	0	Y	Y
2105. 0. 0	2	3405453	c13a2.03	c13a2.04c	c4b4.01c	77.2	3683	tan	82	**6**	7		Y	Y
2105. 1. 0	3	3419511	c4b4.04	nca2	rsc1	69.6	961	div	77	14		14	Y	N
2106. 0. 0	3	3424585	c4b4.06: vps25	smg1	vps25	80.0	866	tan	75	41		20	Y	Y
2106. 1. 0	1	3440203	sbh1	mmf1: c2g2.04c	rpl1603	70.2	587	div	82	2			N	N
2106. 2. 0	4	3455022	c2g2.10c	c2g2.11	c2g2.12	75.4	439	tan	78	7	6	15	Y	Y
2107. 0. 0	4	3467468	c2g2.17c	c2g2.16	c2g2.17c	73.0	417	conv	79	21	8	4	Y	Y
2108. 0. 0	4	3493499	pb7e8.01	zfs1	pb7e8.01	75.2	9848	div	79	21	33	27	Y	Y
2109. 0. 0	4	3516675	exg1	cbp1	exg1	75.0	2798	div	76	19	12	18	Y	Y
2109. 1. 0	2	3531565	h3.3: hht3	hhf3	c1105.13c	68.0	1681	conv	82	1	12		N	N
2109. 2. 0	4	3539857	c1105.16c: rpr2	rpr2	cnp1	74.8	717	div	82	9	4	0	Y	Y
2110. 0. 0	4	3557798	c887.09c	c887.09c	mcs4	76.2	1791	div	79	3	1	0	Y	Y
2110. 1. 0	2	3561732	c887.11: pus2	pus2	c887.12	71.8	1098	tan	79	7	6		N	N
2110. 2. 0	4	3569530	pfh1	pfh1	c887.15c	71.6	1191	tan	82	6	10	0	Y	Y
2111. 0. 0	3	3610155	c16d10.06	mok13	c16d10.06	75.4	3202	tan	80	10		6	Y	Y

Origin No.	Class	Central Map Position	Central Probe	Gene AT island L	Gene AT island R	% AT	IG Length (bp)	IG Context	Replication Time Mitosis (min)	Mitosis Efficiency	*cdc13* s/o Efficiency	*cdc18cdt1* co-oe Efficiency	Orc4 signal ≥ 0.5 (Y/N)	Orc4 signal ≥ 0.8 (Y/N)
2111. 1. 0	2	3618485	pcn1: pcn	c16d10.08c	pcn1	72.8	1608	div	77	10	20		Y	Y
2112. 0. 0	4	3635929	p8b7.01c	p8b7.01c	p8b7.02	79.6	919	div	74	40	5	28	Y	Y
2112. 0. 1r	8	3644989	rpp2-1: rpp201	p8b7.05c	rpp201	70.2	1238	div			12	12	Y	N
2112. 1. 0	2	3646453	p8b7.08c	p8b7.08c	p8b7.09c	70.2	395	tan	77	12	11		N	N
2113. 0. 0	4	3659529	p8b7.15c	dpb2	p8b7.15c	75.6	1420	tan	78	23	5	1	Y	Y
2114. 0. 0	2	3682163	erd2	erd2	p8b7.23	76.2	1304	tan	78	19	0		Y	Y
2114. 1. 0	1	3693112	p8b7.28c	p8b7.28c	p8b7.29	71.8	714	div	80	6			Y	Y
2114. 2. 0	4	3703535	puc1	puc1	c19f5.02c	72.4	3089	tan	83	0	0	0	Y	Y
2114. 3. 0	3	3720420	mcm7	mcm7	suc22	75.4	1834	div	80	14		1	Y	Y
2115. 0. 0	2	3725567	trm1	suc22	trm1	76.0	452	tan	77	16	2		Y	Y
2115. 1. 0	4	3738188	c13g1.05	c13g1.04c	c13g1.05	72.8	1029	div	82	14	22	5	Y	Y
2116. 0. 0	3	3756712	c13g1.12: did2	did2	tfb2	72.4	675	tan	77	17		11	Y	N
2117. 0. 0	3	3764707	c31f10.07	sar1	c31f10.07	77.4	1340	div	75	34		15	Y	Y
2117. 1. 0	4	3780241	c31f10.14c: hip3	hip3	atp15	71.4	1516	tan	80	2	4	7	N	N
2118. 0. 0	4	3803892	c21c3.02c: sds3	sds3	c21c3.03	74.6	1244	div	75	16	6	6	Y	Y
2119. 0. 0	3	3818098	c21c3.12c	c21c3.12c	rps1901	73.2	882	div	76	31		26	Y	Y
2120. 0. 0	4	3827825	spo4	c21c3.17c	spo4	73.4	963	div	77	16	19	16	Y	Y
2121. 0. 0	3	3841437	C23E6.02	pj758.01	c23e6.02	74.8	2372	div	76	24		10	Y	Y
2121. 1. 0	1	3855342	rfc1	sat1	ssn6	74.0	5208	tan	83	9			Y	Y
2121. 2. 0	4	3869682	c23e6.10c	c23e6.10c	rsm10	72.8	1703	div	83	4	12	5	Y	Y
2121. 3. 0	2	3886485	c211.06	ubc8	c211.08c	70.8	900	tan	83	0	6		Y	N
2122. 0. 0	3	3900253	c1604.19c	c1604.19c	c1604.18c	76.6	709	tan	80	5		0	Y	Y
2122. 1. 0	2	3904410	c1604.16c	c1604.18c	c1604.17c	76.8	497	tan	84	0	8		Y	Y
2123. 0. 0	4	3916478	c1604.09c	c1604.09c	imp1	77.2	1073	tan	78	32	26	7	Y	Y

Origin No.	Class	Central Map Position	Central Probe	Gene AT island L	Gene AT island R	% AT	IG Length (bp)	IG Context	Replication Time Mitosis (min)	Mitosis Efficiency	*cdc13* s/o Efficiency	*cdc18cdt1* co-oe Efficiency	Orc4 signal ≥ 0.5 (Y/N)	Orc4 signal ≥ 0.8 (Y/N)
2123. 1. 0	3	3928190	c1604.03c	c1604.04	c1604.03c	71.8	1703	div	80	18		14	Y	Y
2124. 0. 0	4	3938481	c1677.03c	c1677.03c	thi2	77.4	2907	div	77	35	25	33	Y	Y
2124. 1. 0	2	3953780	c26h8.04c	sec9	cho2	75.2	2316	div	80	16	5		Y	Y
2124. 2. 0	4	3962583	c26h8.14c: cox17	cox17	nda3	71.8	1996	tan	77	5	1	4	Y	Y
2124. 3. 0	1	3970452	c26h8.09c: snf59	snf59	dis3	74.2	865	div	83	4			Y	Y
2124. 4. 0	2	3990318	c32c12.03c: ppk25	ppk25	c3b9.01	75.2	1380	div	81	4	8		Y	N
2124. 5. 0	2	4002516	c3b9.06c: apg3	apg3	rpa43	74.4	837	tan	78	9	7		Y	Y
2124. 6. 0	4	4007606	vti1	dad4	ctf1	72.6	522	tan	78	2	21	8	Y	Y
2125. 0. 0	3	4022194	c3b9.18c	nup120	isa2	77.8	1541	div	75	23		13	Y	Y
2126. 0. 0	4	4033745	git11	csn1	git11	74.6	995	div	78	27	1	21	Y	Y
2126. 1. 0	2	4051434	c215.10	erg10	c215.10	74.4	1952	div	81	7	4		Y	Y
2126. 2. 0	2	4071488	c1347.04	c1347.05c	cki1	72.6	1170	tan	83	5	0		Y	Y
2126. 3. 0	1	4076171	c1347.07: rex2	c1347.08c	c1347.09	70.4	1728	div	84	7			N	N
2126. 4. 0	4	4081184	cdc23	c1347.09	cdc23	71.8	1134	tan	83	11	5	3	Y	N
2126. 5. 0	2	4089537	c56f2.12	met6	alg5	71.4	1501	div	84	11	11		Y	Y
2126. 6. 0	3	4098783	c56f2.08c	c56f2.08c	c56f2.07c	73.2	1650	tan	84	6		5	Y	Y
2126. 7. 0	3	4110594	c56f2.06	mug147	c56f2.05c	76.6	6051	div	82	1		7	Y	Y
2126. 8. 0	4	4125259	rpl19-1	c56f2.03	rpl1901	72.6	510	tan	81	9	8	15	Y	Y
2127. 0. 0	4	4144648	b8647-1: c1861.04c	c1861.04c	c1861.05	75.2	1343	div	77	25	11	33	Y	Y
2127. 1. 0	4	4169757	c14f5.07	c14f5.07	med7	74.4	1156	tan	84	7	13	0	Y	N
2128. 0. 0	4	4176724	c14f5.10c	c14f5.10c	mug186	73.8	897	tan	83	10	17	6	Y	Y

Origin No.	Class	Central Map Position	Central Probe	Gene AT island L	Gene AT island R	% AT	IG Length (bp)	IG Context	Replication Time Mitosis (min)	Mitosis Efficiency	*cdc13* s/o Efficiency	*cdc18cdt1* co-oe Efficiency	Orc4 signal ≥ 0.5 (Y/N)	Orc4 signal ≥ 0.8 (Y/N)
2129. 0. 0	4	4201876	C342.01c	alg6	c342.02	75.6	1714	div	78	16	9	12	Y	Y
2129. 1. 0	4	4218106	c16g5.02c	c16g5.02c	c16g5.03	69.8	1570	div	80	3	15	2	Y	Y
2130. 0. 0	4	4228211	c16g5.09	c16g5.07c	trp4	74.2	1943	div	81	8	0	6	Y	Y
2131. 0. 0	4	4239024	c16g5.13	top3	c16g5.13	75.6	1084	div	81	26	19	19	Y	Y
2131. 1. 0	3	4252369	erg24	erg24	c16g5.19	75.6	565	tan	83	4		3	Y	Y
2131. 2. 0	3	4268616	c16a3.16	c16a3.16	nda2	71.6	900	div	85	5		0	Y	N
2131. 3. 0	4	4277149	c16a3.12c	meu7	c16a3.12c	73.2	591	div	84	4	10	4	N	N
2131. 4. 0	4	4291694	rae1	rsm25: c16a3.04	lyn1	77.8	1908	div	85	2	8	5	Y	Y
2132. 0. 0	4	4296568	lyn1	lyn1	c16a3.02c	70.6	2010	tan	80	0	6	8	Y	Y
2132. 1. 0	4	4303482	c543.02c	c543.02c	pku80	73.4	525	tan	83	15	5	0	Y	Y
2132. 2. 0	1	4310678	c543.04	dbp8	pek1	72.6	1006	div	85	9			Y	Y
2132. 3. 0	2	4316724	c543.08	c543.08	c543.09	73.4	1047	tan	88	9	6		Y	Y
2132. 4. 0	4	4322099	c16c6.01c: c543.11c	c543.11c	vps1302	72.0	679	tan	85	0	14	11	N	N
2132. 5. 0	1	4339109	pep1: vps10	c16c6.05	pep1	72.6	767	tan	82	7			N	N
2133. 0. 0	4	4362350	sid4	c244.02c	sid4	76.0	1180	tan	79	18	15	0	Y	Y
2133. 0. 1r	7	4365816	C1539.02	c1539.03c	c1539.04	70.8	1621	div				11	Y	Y
2134. 0. 0	4	4377939	c1539.08	c1539.07c	c1539.08	73.8	781	div	78	12	1	2	Y	Y
2134. 1. 0	3	4398329	c1289.08	c1289.06c	rpc40	74.0	616	tan	82	0		0	N	N
2135. 0. 0	1	4412059	c1289.13c	c1289.13c	c8e4.10c	72.2	3187	div	79	1			Y	Y
2135. 1. 0	2	4426827	c8e4.07c: c1289.15	tf2-11	c8e4.07c	75.0	2754	tan	79	10	15		Y	Y
2136. 0. 0	4	4438357	c8e4.03	c8e4.03	c8e4.02c	77.8	7546	div	80	0	13	2	Y	Y
2137. 0. 0	4	4448854	pho1	pho1	p4g3.03	76.8	4159	tan	79	0	9	7	Y	Y

Origin No.	Class	Central Map Position	Central Probe	Gene AT island L	Gene AT island R	% AT	IG Length (bp)	IG Context	Replication Time Mitosis (min)	Mitosis Efficiency	*cdc13* s/o Efficiency	*cdc18cdt1* co-oe Efficiency	Orc4 signal ≥ 0.5 (Y/N)	Orc4 signal ≥ 0.8 (Y/N)
2138. 0. 0	4	4468755	pb2b2.05	pb2b2.05	pb2b2.06c	76.0	1684	conv	79	2	8	6	Y	Y
2138. 1. 0	2	4479544	PB2B2.07c	pb2b2.06c	pb2b2.07c	74.4	3428	tan	82	3	8		Y	Y
2138. 1. 1r	8	4480910	PB2B2.09c	pb2b2.08	pb2b2.09c	73.2	2435	tan			15	0	Y	Y
2138. 2. 0	4	4490285	pb2b2.13	pb2b2.13	pb2b2.14c	74.6	2529	conv	85	0	4	6	Y	Y
3001. 0. 0	3	33072	c1884.01	p20c8.03	c1884.01	74.8	3578	tan	71	37		29	Y	Y
3002. 0. 0	4	53520	c757.05c	c757.05c	ctt1	70.0	2814	div	72	26	16	30	Y	N
3002. 1. 0	1	63551	c757.08	ctt1	c757.08	72.8	4533	div	77	12			Y	Y
3003. 0. 0	4	67657	c757.10	vph2	c757.11c	72.2	405	conv	76	26	18	12	Y	Y
3004. 0. 0	4	74211	c757.12	c757.12	c757.13	76.6	2683	tan	75	45	38	12	Y	Y
3004. 1. 0	2	83162	c757.14	c757.14	c613.02	71.6	819	tan	75	13	29		Y	N
3004. 2. 0	4	88239	rng3	c613.02	c613.03	74.4	1009	tan	76	2	25	9	Y	N
3004. 3. 0	2	89852	rpl9-2: rpl902	rpl902	c613.07	70.0	1336	tan	76	13	28		N	N
3004. 4. 0	1	97972	c613.10	qcr2	meu23	73.2	719	conv	75	14			Y	Y
3005. 0. 0	4	107375	c330.02	rhp7	c330.19c	73.4	585	conv	72	25	22	7	Y	Y
3006. 0. 0	4	118893	pmp20: c330.06c	c330.06c	c330.07c	78.2	2019	tan	72	64	45	46	Y	Y
3007. 0. 0	4	123235	c330.07c	c330.07c	alg11	78.6	2147	div	73	50	67	29	Y	Y
3007. 1. 0	4	142698	c320.12: c330.17c	c330.15c	ark1	70.6	1468	div	78	7	7	4	Y	Y
3007. 2. 0	4	172314	c320.02c	c320.03	c320.02c	71.8	5657	div	82	4	7	1	Y	N
3008. 0. 0	4	189261	c1235.06: sif1	c1235.05c	sif1	70.6	2381	div	74	29	6	24	Y	Y
3009. 0. 0	5	203746	ght6: meu12	ght6	ght5	82.6	5972	tan	71	52	65	92	Y	N
3009. 1. 0	2	221807	wtf3	wtf3	wtf4	71.8	915	tan	74	27	37		Y	N
3010. 0. 0	5	233612	ght1	ght8	ght1	78.6	4433	tan	74	**30**	43	54	Y	Y

Origin No.	Class	Central Map Position	Central Probe	Gene AT island L	Gene AT island R	% AT	IG Length (bp)	IG Context	Replication Time Mitosis (min)	Mitosis Efficiency	*cdc13* s/o Efficiency	*cdc18cdt1* co-oe Efficiency	Orc4 signal ≥ 0.5 (Y/N)	Orc4 signal ≥ 0.8 (Y/N)
3011. 0. 0	4	247585	c794.03	c794.03	c794.04c	75.8	922	conv	72	14	12	18	Y	Y
3012. 0. 0	4	256477	c794.14	c794.04c	c794.06	75.2	10242	div	76	13	42	36	Y	Y
3012. 0. 1r	6	269479	tef1-e: ef1a-e: ef1a-a	ef1a-a	c794.10	72.0	1486	div			22		Y	N
3013. 0. 0	4	280953	c553.11c	mae2	c794.15	70.6	1694	div	74	18	24	24	Y	Y
3014. 0. 0	3	288104	c553.09c	c553.10	spb70	76.6	3168	div	73	46		25	Y	Y
3014. 1. 0	4	299321	c553.04: cyp9	wtf6	cyp9	73.2	2081	tan	75	17	8	8	Y	Y
3014. 2. 0	2	308448	c553.02	c553.02	c736.01c	75.2	2057	div	78	18	14		Y	Y
3015. 0. 0	4	314888	c736.02	c736.01c	c736.02	75.2	496	tan	75	14	7	0	Y	Y
3016. 0. 0	4	332126	c736.09c	mrps8	ago1	74.0	1653	div	76	33	4	0	Y	Y
3017. 0. 0	4	368974	c594.07c	c594.07c	qcr9	77.4	2234	div	73	43	46	35	Y	Y
3017. 1. 0	4	382413	c1682.06	c1682.05c	c1682.06	72.0	1342	div	72	9	21	20	Y	Y
3018. 0. 0	4	397693	c1682.13	ubp16	c1682.13	76.0	2823	div	74	49	33	14	Y	Y
3018. 1. 0	4	411015	cnd2	c306.02c	cnd2	74.2	1015	tan	76	9	20	6	N	N
3018. 2. 0	4	429780	wtf8	wtf8	c306.11	70.2	2024	tan	79	11	5	3	Y	Y
3018. 3. 0	4	442665	c4g3.16	c4g3.18	c4g3.17	72.0	640	tan	81	0	0	0	Y	N
3018. 4. 0	4	454392	c4g3.09c	rhp42	gyp3	75.4	873	tan	78	18	10	0	Y	Y
3018. 5. 0	2	463582	mus81	phf1: c4g3.07c	mrp14	70.2	448	tan	77	13	17		Y	N
3019. 0. 0	4	471015	c364.07: c4g3.01	c4g3.01	c364.06	77.6	2321	tan	77	34	22	2	Y	Y
3019. 1. 0	4	482235	rpl17-2: rpl1702	rpl1702	bis1	71.2	786	div	77	7	2	2	Y	Y
3020. 0. 0	4	507467	mob2	c970.06	rpl3601	75.2	1889	tan	76	25	29	22	Y	Y
3021. 0. 0	4	518748	rad16: rad10: rad20: swi9	rad16	prp11	74.6	1636	div	73	62	31	23	Y	Y

Origin No.	Class	Central Map Position	Central Probe	Gene AT island L	Gene AT island R	% AT	IG Length (bp)	IG Context	Replication Time Mitosis (min)	Mitosis Efficiency	*cdc13* s/o Efficiency	*cdc18cdt1* co-oe Efficiency	Orc4 signal ≥ 0.5 (Y/N)	Orc4 signal ≥ 0.8 (Y/N)
3021. 1. 0	4	525748	p31b10.02	med31	p31b10.04	73.4	911	div	73	18	9	17	Y	Y
3022. 0. 0	2	530741	p31b10.05	p31b10.05	mug190	71.8	2538	tan	73	18	6		Y	N
3022. 1. 0	3	551122	cut15	cut15	rps1201	72.2	1083	div	77	8		6	Y	Y
3023. 0. 0	4	557218	bpb1: sf1	bpb1	c1672.01	70.8	1861	div	75	7	26	11	Y	Y
3024. 0. 0	4	565937	c1672.03c	sap1	c1672.03c	77.6	2773	tan	74	48	40	39	Y	Y
3025. 0. 0	4	575026	c1672.07	asp1	c1672.07	74.8	1064	div	74	52	34	40	Y	Y
3025. 1. 0	4	582170	c1672.09	c1672.09	mis16	72.2	1939	tan	76	9	16	17	Y	Y
3026. 0. 0	4	604102	ung1	ung1	c1183.07	74.4	2207	tan	74	35	12	13	Y	Y
3026. 1. 0	4	610398	c1183.07	rpl101	pmp31	69.4	794	tan	75	16	20	2	N	N
3027. 0. 0	2	614675	c1183.09c	pmp31	wtf10	70.2	1879	div	74	5	26		Y	Y
3027. 1. 0	4	623745	c31h12.02c	c31h12.01	mug73	73.4	547	conv	79	6	14	0	N	N
3027. 2. 0	2	633017	sec23a: sec231	sds21	mug111	74.2	1804	div	76	12	23		Y	Y
3028. 0. 0	4	642400	taf72	taf72	cut1	78.6	1367	div	76	38	28	9	Y	Y
3028. 1. 0	4	650744	c5e4.05c	c5e4.05c	c5e4.10c	74.2	829	tan	76	10	23	4	N	N
3028. 2. 0	2	664707	c16c4.03: pin1	pin1	c16c4.04	76.2	1830	tan	76	22	1		Y	Y
3029. 0. 0	4	669270	c16c4.05	c16c4.04	c16c4.05	74.0	516	tan	76	22	23	0	Y	Y
3029. 1. 0	2	687965	pef1	c16c4.10	pef1	74.0	961	tan	78	3	5		N	N
3029. 2. 0	2	706984	pj732.02c	vps5	pj732.02c	72.6	635	conv	77	17	7		N	N
3030. 0. 0	4	718849	c18b5.02c	c18b5.02c	wee1	75.6	3364	div	76	47	45	22	Y	Y
3030. 0. 1r	6	727030	C18B5.05c	c18b5.05c	erf1	71.6	1119	div			23		Y	Y
3030. 1. 0	1	738425	c18b5.10c	c18b5.08c	c18b5.09c	71.8	1177	tan	78	24			N	N
3030. 2. 0	4	755699	c1020.13c	c1020.11c	oca2	74.0	1098	conv	76	25	15	0	Y	Y
3031. 0. 0	4	766179	c1020.09	oca2	c1020.09	78.4	5316	tan	76	30	35	18	Y	Y
3031. 1. 0	4	790566	pma2	spc7	pma2	71.4	2564	tan	82	16	13	0	Y	Y

Origin No.	Class	Central Map Position	Central Probe	Gene AT island L	Gene AT island R	% AT	IG Length (bp)	IG Context	Replication Time Mitosis (min)	Mitosis Efficiency	*cdc13* s/o Efficiency	*cdc18cdt1* co-oe Efficiency	Orc4 signal ≥ 0.5 (Y/N)	Orc4 signal ≥ 0.8 (Y/N)
3031. 2. 0	1	801635	c1393.05	fta4	c1393.05	72.6	578	tan	80	22			N	N
3031. 3. 0	4	806310	c1393.07c: mug4	mug4	c1393.08	71.8	3799	div	78	4	12	23	Y	Y
3032. 0. 0	4	821150	ctr4	ctr4	c1393.11	75.0	2315	tan	73	53	35	9	Y	Y
3032. 0. 1r	6	827546	prl64	c1393.13	c2h8.02	74.6	2005	tan			35		Y	Y
3032. 1. 0	4	835052	c2h8.03	c63.01c	aah3	72.8	965	tan	74	15	19	5	N	N
3032. 2. 0	4	844051	c63.05	mok14	c63.05	71.2	374	tan	77	18	0	5	Y	Y
3033. 0. 0	4	852566	c63.10c	ppk36	c63.10c	76.8	2046	tan	72	64	35	11	Y	Y
3033. 1. 0	4	877939	dim1: c16a11.05c	dim1	gpi10	72.2	1012	tan	82	12	0	0	N	N
3033. 2. 0	4	888872	c16a11.10c	atg20: c16a11.08	tim23	73.2	927	conv	82	3	0	0	N	N
3034. 0. 0	4	903088	cdc21: mcm4	c16a11.16c	cdc21	74.0	1246	div	77	23	5	14	N	N
3034. 0. 1r	8	921946	C24B10.12	c24b10.10c	c24b10.11c	71.8	615	tan			16	7	N	N
3035. 0. 0	4	936142	c24b10.20	c24b10.19c	c24b10.20	75.4	3356	div	74	52	43	28	Y	Y
3036. 0. 0	4	972909	c1795.12c	c1795.13	c1795.12c	78.8	8851	div	75	45	68	62	Y	Y
3037. 0. 0	4	986420	map2	c1795.07	map2	74.6	1087	tan	76	49	62	23	Y	Y
3037. 1. 0	2	1007495	c895.06	c895.06	alp14	72.0	885	tan	80	27	8		Y	N
3037. 2. 0	3	1015638	c895.08c	alp14	c895.08c	73.2	456	conv	84	15		0	Y	N
3037. 3. 0	4	1024312	c825.01	ucp12	c825.01	70.8	1389	div	82	21	1	0	Y	N
3037. 4. 0	2	1029103	sso1: psy1	psy1	c825.04c	71.8	1109	tan	81	7	2		Y	Y
3037. 5. 0	4	1035111	c1259.02c	c1259.02c	rpa12	74.2	3252	div	82	9	0	0	Y	Y
3038. 0. 0	4	1042644	rpa12	c1259.02c	rpa12	74.2	3252	div	79	2	8	0	Y	Y
3038. 1. 0	4	1046529	c1259.07	c1259.07	c1259.08	70.2	2034	tan	78	7	7	5	Y	Y
3039. 0. 0	4	1053603	c1259.11c	gyp2	c1259.12c	70.2	466	tan	76	4	47	27	N	N

Origin No.	Class	Central Map Position	Central Probe	Gene AT island L	Gene AT island R	% AT	IG Length (bp)	IG Context	Replication Time Mitosis (min)	Mitosis Efficiency	*cdc13* s/o Efficiency	*cdc18cdt1* co-oe Efficiency	Orc4 signal ≥ 0.5 (Y/N)	Orc4 signal ≥ 0.8 (Y/N)
3040. 0. 0	4	1061738	chk1: rad27	c1259.12c	ubc11	71.8	700	tan	79	26	46	41	N	N
3041. 0. 0	4	1065271	meu27: b8647-6	meu27	centromere	78.8	1849	cen	79	26	39	24	Y	Y
3042. 0. 0	4	1144065	c4b3.18	centromere	c4b3.18	73.0		cen	77	23	67	0	Y	Y
3042. 1. 0	4	1166153	c4b3.06c	c4b3.08	c4b3.07	72.4	876	tan	80	17	5	0	Y	N
3042. 2. 0	4	1178803	p25a2.01c	c4b3.03c	c4b3.02c	72.4	1229	tan	80	14	9	6	Y	N
3043. 0. 0	4	1193147	c550.05: nse1	gpi2: c550.04c	nse1	73.6	1125	div	75	40	26	12	Y	Y
3043. 1. 0	4	1202595	c550.09	c550.08	c550.09	72.4	802	tan	77	15	38	0	N	N
3043. 2. 0	4	1213271	c550.12: arp6	c550.11	arp6	73.2	918	tan	83	6	2	0	Y	Y
3043. 3. 0	4	1229658	c645.02	c645.02	isa1	70.2	751	conv	79	4	4	0	N	N
3044. 0. 0	4	1255450	snd1: c645.08c	snd1	mrp137	76.0	2351	div	74	56	33	30	Y	Y
3044. 1. 0	1	1281777	c23b6.04c	ssb3	c23b6.06	71.8	797	div	78	9			N	N
3044. 2. 0	3	1298289	c1322.06	c1322.05c	kap113	73.2	1043	div	80	16		0	N	N
3044. 3. 0	1	1308642	c1322.09	srk1	c1322.09	70.6	1328	tan	81	6			Y	N
3045. 0. 0	3	1322786	c1322.16: phb2	rpl3402	phb2	76.0	1948	tan	70	52		21	Y	Y
3046. 0. 0	4	1340542	c338.18	c338.18	rad21	74.6	1469	div	73	55	47	19	Y	Y
3046. 0. 1r	8	1345936	rad21	pof3	c338.15	70.8	694	tan			41	26	N	N
3046. 0. 2r	8	1350270	c338.14	c338.15	c338.14	72.4	663	tan			29	24	N	N
3047. 0. 0	4	1369233	c338.02	c338.03c	ags1	76.4	4827	tan	71	48	30	65	Y	Y
3048. 0. 0	4	1396804	c1281.06c	c1281.06c	c1281.07c	72.2	3495	conv	73	43	43	86	Y	Y
3049. 0. 0	5	1409066	c622.05	c622.01c	hta1	78.6	6768	tan	69	57	67	163	Y	Y
3050. 0. 0	4	1416334	c622.10c	c622.10c	c622.11	77.8	949	div	72	53	37	148	Y	Y
3050. 0. 1r	8	1438640	rpl6	rpl6	jmj4	69.4	634	tan			42	33	N	N

Origin No.	Class	Central Map Position	Central Probe	Gene AT island L	Gene AT island R	% AT	IG Length (bp)	IG Context	Replication Time Mitosis (min)	Mitosis Efficiency	*cdc13* s/o Efficiency	*cdc18cdt1* co-oe Efficiency	Orc4 signal ≥ 0.5 (Y/N)	Orc4 signal ≥ 0.8 (Y/N)
3051. 0. 0	4	1451189	c61.04c	c61.04c	c61.05	76.4	2228	div	72	46	40	25	Y	Y
3051. 1. 0	3	1471600	c11e10.07c	c11e10.07c	rik1	72.6	2167	div	78	12		2	Y	Y
3051. 2. 0	4	1485038	srp54	srp54	ccq1	70.8	1166	div	80	2	0	0	Y	Y
3051. 2. 1r	6	1498880	C584.07c	c188.09c	c584.07c	74.8	3212	tan			18		Y	N
3052. 0. 0	4	1511153	c584.11c	dcr1	c584.11c	76.2	1292	tan	74	28	12	8	Y	Y
3052. 0. 1r	8	1521706	C584.15c	c584.15c	c584.16c	72.6	1325	tan			22	6	Y	Y
3053. 0. 0	4	1531714	c584.02: cuf2	c584.01c	cuf2	76.8	2633	div	71	45	18	2	Y	Y
3053. 1. 0	4	1542795	ssb2	ssb2	git3	70.4	1266	tan	76	11	13	0	N	N
3054. 0. 0	2	1558661	c162.11c	c1753.06c	c162.11c	73.0	2249	div	75	43	10		Y	Y
3055. 0. 0	4	1578378	C162.06C	ent1	c162.06c	74.4	3089	div	74	42	29	23	Y	Y
3056. 0. 0	4	1594674	c13b11.03c	c13b11.02c	c13b11.03c	80.8	1223	tan	72	53	68	62	Y	Y
3057. 0. 0	4	1608596	c777.06c	c777.06c	c777.07	78.8	2077	div	70	52	41	49	Y	Y
3057. 1. 0	4	1615755	c777.09c	c777.08c	c777.09c	77.0	759	tan	75	13	18	31	Y	Y
3057. 2. 0	1	1625914	c777.15	c777.15	ekc1	70.4	864	conv	81	1			N	N
3057. 3. 0	4	1640448	pmd1	pmd1	rpl39	71.0	958	tan	81	15	1	0	Y	N
3058. 0. 0	4	1655583	c663.11	c663.11	cid12	72.8	956	tan	79	24	6	1	Y	Y
3058. 1. 0	4	1658391	c663.14c	c663.14c	c663.15c	70.0	498	tan	80	8	0	0	N	N
3059. 0. 0	4	1683073	c417.07c: mto1	mto1	tef3	76.2	2394	div	74	49	17	18	Y	Y
3060. 0. 0	4	1691448	tef3	tef3	c417.09c	78.4	2972	conv	73	49	18	7	Y	Y
3060. 0. 1r	8	1709134	C191.02c	c417.12	c417.13	72.4	5159	div			29	29	Y	Y
3060. 0. 2r	8	1715428	cyc1	c191.05c	c191.06	71.2	1184	div			26	60	Y	N
3061. 0. 0	4	1717654	c191.08	c191.08	gst1	77.6	2169	conv	73	76	40	39	Y	Y
3062. 0. 0	4	1722830	c191.10	c191.12c	c191.13	76.6	1744	div	73	49	25	43	Y	Y
3062. 0. 1r	8	1733051	C1450.03	c1450.03	tef5	72.8	622	tan			30	35	Y	Y

Origin No.	Class	Central Map Position	Central Probe	Gene AT island L	Gene AT island R	% AT	IG Length (bp)	IG Context	Replication Time Mitosis (min)	Mitosis Efficiency	*cdc13* s/o Efficiency	*cdc18cdt1* co-oe Efficiency	Orc4 signal ≥ 0.5 (Y/N)	Orc4 signal ≥ 0.8 (Y/N)
3062. 0. 2r	7	1736327	C1450.06c	tef5	rox3	72.2	1101	conv				25	Y	Y
3062. 1. 0	4	1741516	c1450.09c	c1450.09c	c1450.10c	74.0	2834	tan	75	10	7	12	Y	Y
3063. 0. 0	4	1753518	cek1	cek1	c1450.12	74.0	1637	div	75	48	12	21	Y	Y
3063. 1. 0	4	1758406	c1450.13c	c1450.13c	ero12	70.0	1181	tan	77	32	16	21	N	N
3063. 2. 0	2	1782355	c1442.08c: cox12	c1442.07c	cox12	72.4	1044	tan	80	10	15		N	N
3063. 3. 0	4	1794867	c1142.15c: cox18	cox18	zta1	72.8	604	tan	79	10	6	10	Y	N
3063. 4. 0	4	1812940	cgs2: pde1	cgs2	c285.10c	72.0	1703	tan	75	17	20	9	Y	Y
3064. 0. 0	4	1821777	c285.13c	c285.13c	c285.14	76.8	2046	div	72	42	33	31	Y	Y
3065. 0. 0	4	1843516	c1223.04c	c285.18	nmt1	77.6	1570	tan	76	52	37	21	Y	Y
3065. 1. 0	4	1858637	c1223.10c: eaf1	c1223.09	eaf1	71.6	2533	tan	78	14	21	10	Y	Y
3066. 0. 0	4	1869591	meu10	ptc2	meu10	74.8	3610	conv	74	27	8	7	Y	Y
3067. 0. 0	3	1886985	c737.01c	c737.01c	qcr7	71.6	887	tan	77	9		0	Y	N
3067. 1. 0	4	1896728	c737.06c	c737.04	c737.05	73.4	1702	tan	81	6	4	0	Y	N
3068. 0. 0	4	1930800	c74.03c: ssp2	c74.02c	ssp2	74.8	1609	tan	75	**25**	14	16	Y	Y
3069. 0. 0	4	1966937	c18.06c: caf1	caf1	rpc53	73.8	2499	div	72	38	33	23	Y	Y
3070. 0. 0	4	1976530	c18.10	c18.09c	c18.10	73.8	1080	div	72	21	20	23	Y	Y
3070. 1. 0	1	1985155	c18.15	c18.15	fmn1	72.4	568	conv	78	13			Y	Y
3070. 2. 0	2	1994696	rpc34	rpc34	nup186	75.2	476	conv	79	20	6		Y	Y
3070. 3. 0	1	2001220	nup186	nup186	ams2	71.8	1975	div	80	20			Y	Y
3070. 4. 0	2	2011666	c4f11.05	c4f11.05	mpg1	72.4	2052	tan	75	13	7		Y	N
3071. 0. 0	4	2022227	wtf20	wtf20	c1906.05	70.4	4221	tan	72	23	12	1	Y	Y
3072. 0. 0	4	2035807	c1739.05: set5	c1739.04c	set5	75.8	1754	div	69	48	29	10	Y	Y

Origin No.	Class	Central Map Position	Central Probe	Gene AT island L	Gene AT island R	% AT	IG Length (bp)	IG Context	Replication Time Mitosis (min)	Mitosis Efficiency	*cdc13* s/o Efficiency	*cdc18cdt1* co-oe Efficiency	Orc4 signal ≥ 0.5 (Y/N)	Orc4 signal ≥ 0.8 (Y/N)
3072. 1. 0	4	2046290	c1739.09c	c1739.08c	cox13	71.0	2593	tan	74	17	8	12	Y	Y
3073. 0. 0	4	2069384	pb1c11.01: amt1	wtf21	amt1	76.0	4024	tan	76	25	38	24	Y	Y
3073. 1. 0	4	2076986	pb1c11.03	pb1c11.03	pb1c11.04c	73.4	625	conv	78	14	37	20	Y	Y
3073. 1. 1r	8	2083547	C576.02	c576.02	tpx1	70.2	1678	conv			39	12	Y	Y
3073. 2. 0	4	2094845	ret3	ret3	rps2	71.2	813	conv	80	0	8	8	N	N
3074. 0. 0	4	2104673	c576.14	ksg1	wtf22	77.0	2922	conv	78	28	32	14	Y	Y
3075. 0. 0	4	2116823	c126.01c: c576.18c	c576.18c	pku70	74.6	861	tan	73	32	13	10	Y	N
3075. 1. 0	4	2127134	c126.06	c126.06	c126.07c	71.0	451	conv	77	5	0	1	N	N
3075. 2. 0	2	2134335	iah1	c126.09	iah1	71.6	1243	tan	77	18	15		Y	N
3076. 0. 0	2	2141517	c126.12	c126.12	c126.13c	72.6	1442	conv	77	24	12		Y	Y
3076. 0. 1r	8	2149628	C1620.03: mug163	wtf23	mug163	72.6	1469	tan			7	11	Y	Y
3076. 1. 0	1	2152468	c1620.05	mug55	c1620.05	72.4	1280	div	82	13			Y	Y
3076. 2. 0	4	2159427	c1620.08	c1620.07c	c1620.08	71.8	2148	div	81	3	4	0	Y	Y
3076. 3. 0	4	2169269	c1620.12c	c1620.12c	c1620.13	72.8	1881	div	80	14	0	0	N	N
3076. 4. 0	3	2187653	c830.04c: mug128	mug128	ep11	73.4	1380	tan	75	16		6	Y	N
3077. 0. 0	4	2204942	c830.10	c830.09c	c830.10	77.0	1824	div	69	54	26	18	Y	Y
3077. 1. 0	4	2207771	c1919.02	ppk34	c1919.02	73.0	637	tan	73	13	15	21	Y	N
3078. 0. 0	4	2220027	wtf9: wtf25	wtf25	c1919.07	71.2	1391	div	73	11	0	2	Y	Y
3078. 1. 0	2	2223435	tif6	tif6	myo52	70.8	790	conv	78	8	0		N	N
3078. 2. 0	4	2236847	c1919.13c	c1919.13c	bdp1	73.6	423	tan	77	4	6	0	Y	Y
3078. 3. 0	2	2248700	c790.04c: mog1	mog1	bgs4	72.4	1114	tan	79	10	1		Y	Y
3078. 4. 0	4	2262826	pse1: sal3	bgs4	sal3	73.6	5135	div	79	7	15	11	Y	Y

Origin No.	Class	Central Map Position	Central Probe	Gene AT island L	Gene AT island R	% AT	IG Length (bp)	IG Context	Replication Time Mitosis (min)	Mitosis Efficiency	*cdc13* s/o Efficiency	*cdc18cdt1* co-oe Efficiency	Orc4 signal ≥ 0.5 (Y/N)	Orc4 signal ≥ 0.8 (Y/N)
3078. 5. 0	4	2270016	c1840.06	c1840.07c	c1840.08c	73.6	523	tan	77	10	11	19	Y	N
3079. 0. 0	3	2277456	lsm8	c1840.09	lsm8	78.2	2703	div	72	32		24	Y	Y
3079. 1. 0	2	2292222	thp1	c965.04c	thp1	71.6	1776	tan	76	14	5		Y	Y
3080. 0. 0	3	2300593	c965.09	prl45	c965.09	74.2	2005	div	73	23		0	Y	Y
3081. 0. 0	1	2336653	c1494.08c	c1494.06c	c1494.07	73.4	2073	div	74	24			Y	Y
3082. 0. 0	4	2362302	c70.05c	c70.05c	c70.06	74.8	3473	div	74	27	10	1	Y	Y
3082. 1. 0	4	2368801	c70.08c	c70.08c	mug9	73.2	471	tan	74	17	4	27	Y	N
3083. 0. 0	4	2384723	c1827.05c	c1827.03c	c1827.04	79.6	2708	div	71	49	21	29	Y	Y
3083. 1. 0	3	2391951	p1e11.02: ppk38	p1e11.01c	ppk38	73.2	1200	div	74	19		11	Y	Y
3083. 2. 0	4	2405446	p1e11.07c: cwf18	apl4	cwf18	72.4	537	conv	77	19	7	0	Y	N
3083. 3. 0	3	2409900	p1e11.10	p1e11.11	ade5	73.2	514	tan	76	19		5	Y	Y
3084. 0. 0	4	2420654	c569.06	c569.05c	c569.04	75.8	1152	conv	74	24	7	12	Y	Y
3085. 0. 0	3	2431896	c569.03	c569.04	c569.03	75.2	2749	tan	74	39		24	Y	Y

Chapter 8

BIBLIOGRAPHY

Adachi, Y., Usukura, J., and Yanagida, M. (1997). A globular complex formation by Nda1 and the other five members of the MCM protein family in fission yeast. Genes Cells *2*, 467-479.

Arentson, E., Faloon, P., Seo, J., Moon, E., Studt, J. M., Fremont, D. H., and Choi, K. (2001). Oncogenic potential of the DNA replication licensing protein CDT1. Oncogene *21*, 1150-1158.

Arias, E. E., and Walter, J. C. (2005). Replication-dependent destruction of Cdt1 limits DNA replication to a single round per cell cycle in Xenopus egg extracts. Genes Dev *19*, 114-126.

Arias, E. E., and Walter, J. C. (2006). PCNA functions as a molecular platform to trigger Cdt1 destruction and prevent re-replication. Nat Cell Biol *8*, 84-90.

Arias, E. E., and Walter, J. C. (2007). Strength in numbers: preventing rereplication via multiple mechanisms in eukaryotic cells. Genes Dev *21*, 497-518.

Austin, R. J., Orr-Weaver, T. L., and Bell, S. P. (1999). Drosophila ORC specifically binds to ACE3, an origin of DNA replication control element. Genes Dev *13*, 2639-2649.

Ayté, J., Schweitzer, C., Zarzov, P., Nurse, P., and DeCaprio, J. A. (2001). Feedback regulation of the MBF transcription factor by cyclin Cig2. Nat Cell Biol *3*, 1043-1050.

Baccini, V., Roy, L., Vitrat, N., Chagraoui, H., Sabri, S., Couedic, J.-P. L., Debili, N., Wendling, F., and Vainchenker, W. (2001). Role of p21Cip1/Waf1 in cell-cycle exit of endomitotic megakaryocytes. Blood *98*, 3274-3282.

Bähler, J. (2005). Cell-cycle control of gene expression in budding and fission yeast. Annu Rev Genet *39*, 69-94.

Bähler, J., Wu, J.-Q., Longtine, M. S., Shah, N. G., III, A. M., Steever, A. B., Wach, A., Philippsen, P., and Pringle, J. R. (1998). Heterologous modules for efficient and versatile PCR-based gene targeting in Schizosaccharomyces pombe. Yeast *14*, 943-951.

Bates, S., Ryan, K. M., Phillips, A. C., and Vousden, K. H. (1998). Cell cycle arrest and DNA endoreduplication following p21Waf1/Cip1 expression. Oncogene *17*, 1691-1703.

Bell, S. P., and Dutta, A. (2002). DNA Replication in Eukaryotic Cells. Annu Rev Biochem *71*, 333.

Bell, S. P., and Stillman, B. (1992). ATP-dependent recognition of eukaryotic origins of DNA replication by a multiprotein complex. Nature *357*, 128-134.

Benito, J., Martín-Castellanos, C., and Moreno, S. (1998). Regulation of the G1 phase of the cell cycle by periodic stabilization and degradation of the p25rum1 CDK inhibitor. EMBO *17(2)*, 482–497.

Broek, D., Bartlett, R., Crawford, K., and Nurse, P. (1991). Involvement of the p34cdc2 in establishing the dependency of S phase on mitosis. Nature *349*, 388-393.

Calvi, B. R., Lilly, M. A., and Spradling, A. C. (1998). Cell cycle control of chorion gene amplification. Genes Dev *12*, 734-744.

Chesnokov, I., Remus, D., and Botchan, M. (2001). Functional analysis of mutant and wild-type Drosophila origin recognition complex. Proc Natl Acad Sci U S A *98*, 11997-12002.

Chuang, R.-Y., and Kelly, T. J. (1999). The fission yeast homologue of Orc4p binds to replication origin DNA via multiple AT-hooks. Proc Natl Acad Sci U S A *96*, 2656-2661.

Claycomb, J. M., MacAlpine, D. M., Evans, J. G., Bell, S. P., and Orr-Weaver, T. L. (2002). Visualization of replication initiation and elongation in Drosophila. J Cell Biol *159*, 225-236.

Clutterbuck, A. J. (1970). Synchronous Nuclear Division and Septation in Aspergillus nidulans. J Gen Microbiol *60*, 133-135.

Correa-Bordes, J., Gulli, M.-P., and Nurse, P. (1997). p25rum1 promotes proteolysis of the mitotic B-cyclin p56cdc13 during G1 of the fission yeast cell cycle. EMBO *16*, 4657-4664.

Correa-Bordes, J., and Nurse, P. (1995). p25rum1 orders S phase and mitosis by acting as an inhibitor of the p34cdc2 mitotic kinase. Cell *83*, 1001-1009.

Coverley, D., Pelizon, C., Trewick, S., and Laskey, R. A. (2000). Chromatin-bound Cdc6 persists in S and G2 phases in human cells, while soluble Cdc6 is destroyed in a cyclin A-cdk2 dependent process. J Cell Sci *113*, 1929-1938.

Dahmann, C., Diffley, J. F. X., and Nasmyth, K. A. (1995). S-phase-promoting cyclin-dependent kinases prevent re-replication by inhibiting the transition of replication origins to a pre-replicative state. Curr Biol *5*, 1257-1269.

Dai, J., Chuang, R.-Y., and Kelly, T. J. (2005). DNA replication origins in the Schizosaccharomyces pombe genome. Proc Natl Acad Sci U S A *102*, 337-342.

de Cicco, D. V., and Spradling, A. C. (1984). Localization of a cis-acting element responsible for the developmentally regulated amplification of drosophila chorion genes. Cell *38*, 45-54.

Decottignies, A., Zarzov, P., and Nurse, P. (2001). In vivo localisation of fission yeast cyclin-dependent kinase cdc2p and cyclin B cdc13p during mitosis and meiosis. J Cell Sci *114*, 2627-2640.

Demeter, J., Lee, S. E., Haber, J. E., and Stearns, T. (2000). The DNA Damage Checkpoint Signal in Budding Yeast Is Nuclear Limited. Mol Cell *6*, 487-492.

DePamphilis, M. L. (2005). Cell cycle dependent regulation of the origin recognition complex. Cell Cycle *4*, 70-79.

DePamphilis, M. L., Blow, J. J., Ghosh, S., Saha, T., Noguchi, K., and Vassilev, A. (2006). Regulating the licensing of DNA replication origins in metazoa. Curr Opin Cell Biol *18*, 231-239.

Donti, T. R., Datta, S., Sandoval, P. Y., and Kapler, G. M. (2009). Differential targeting of Tetrahymena ORC to ribosomal DNA and non-rDNA replication origins. EMBO J *28*, 223-233.

Dorn, E. S., Chastain, P. D., II, Hall, J. R., and Cook, J. G. (2009). Analysis of re-replication from deregulated origin licensing by DNA fiber spreading. Nucl Acids Res *37*, 60-69.

Ducommun, B., Tollon, Y., Gares, M., Beach, D., and Wright, M. (1990). Cell cycle regulation of p34cdc2 kinase activity in Physarum polycephalum. J Cell Sci *96*, 683-689.

Dunham, M. J., Badrane, H., Ferea, T., Adams, J., Brown, P. O., Rosenzweig, F., and Botstein, D. (2002). Characteristic genome rearrangements in experimental evolution of Saccharomyces cerevisiae. Proc Natl Acad Sci U S A *99*, 16144-16149.

Edgar, B., and Orr-Weaver, T. (2001). Endoreduplication Cell Cycles: More for Less. Cell *105*, 297-306.

Fantes, P. (1979). Epistatic gene interactions in the control of division in fission yeast. Nature *279*, 428-430.

Feng, W., Collingwood, D., Boeck, M. E., Fox, L. A., Alvino, G. M., Fangman, W. L., Raghuraman, M. K., and Brewer, B. J. (2006). Genomic mapping of single-stranded DNA in hydroxyurea-challenged yeasts identifies origins of replication. Nat Cell Biol *8*, 148-155.

Field, Y., Kaplan, N., Fondufe-Mittendorf, Y., Moore, I. K., Sharon, E., Lubling, Y., Widom, J., and Segal, E. (2008). Distinct Modes of Regulation by Chromatin Encoded through Nucleosome Positioning Signals. PLoS Comput Biol *4*, e1000216.

Fisher, D., and Nurse, P. (1996). A single fission yeast mitotic cyclin B p34cdc2 kinase promotes both S-phase and mitosis in the absence of G1 cyclins. EMBO *15*, 850-860.

Follette, P. J., Duronio, R. J., and O'Farrell, P. H. (1998). Fluctuations in Cyclin E levels are required for multiple rounds of endocycle S phase in Drosophila Curr Biol *8*, 235-238.

Friedman, K. L., Brewer, B. J., and Fangman, W. L. (1997). Replication profile of Saccharomyces cerevisiae chromosome VI. Genes Cells *2*, 667-678.

Gall, J., HC, M., and ME, K. (1969). Gene amplification in the oocytes of Dytiscid water beetles. Chromosoma *26*, 169-187.

Gall, J. G. (1968). Differential synthesis of the genes for ribosomal RNA during amphibian oögenesis. Proc Natl Acad Sci USA *60*, 553-560.

Gladfelter, A. S. (2006). Nuclear anarchy: asynchronous mitosis in multinucleated fungal hyphae. Curr Opin Microbiol *9*, 547-552.

Gladfelter, A. S., Hungerbuehler, A. K., and Philippsen, P. (2006). Asynchronous nuclear division cycles in multinucleated cells. J Cell Biol *172*, 347-362.

Goff, L., and Coleman, A. (1990). Red algal plasmids. Curr Genet *18*, 557-565.

Gonzalez, M. A., Tachibana, K.-e. K., Adams, D. J., van der Weyden, L., Hemberger, M., Coleman, N., Bradley, A., and Laskey, R. A. (2006). Geminin is essential to prevent endoreduplication and to form pluripotent cells during mammalian development. Genes Dev *20*, 1880-1884.

Gopalakrishnan, V., Simancek, P., Houchens, C., Snaith, H. A., Frattini, M. G., Sazer, S., and Kelly, T. J. (2001). Redundant control of rereplication in fission yeast. PNAS *98*, 13114-13119.

Gould, K. L., and Nurse, P. (1989). Tyrosine phosphorylation of the fission yeast cdc2+ protein kinase regulates entry into mitosis. Nature *342*, 39-45.

Green, B. M., Morreale, R. J., Ozaydin, B., DeRisi, J. L., and Li, J. J. (2006). Genome-wide Mapping of DNA Synthesis in Saccharomyces cerevisiae Reveals That Mechanisms Preventing Reinitiation of DNA Replication Are Not Redundant. Mol Biol Cell *17*, 2401-2414.

Hahn, M. W. (2009). Distinguishing Among Evolutionary Models for the Maintenance of Gene Duplicates. J Hered, esp047.

Hartwell, L. H. (1973). Three Additional Genes Required for Deoxyribonucleic Acid Synthesis in Saccharomyces cerevisiae. J Bacteriol *115*, 966-974.

Hartwell, L. H., Culotti, J., Pringle, J. R., and Reid, B. J. (1974). Genetic Control of the Cell Division Cycle in Yeast. Science *183*, 46-51.

Hayashi, M., Katou, Y., Itoh, T., Tazumi, A., Yamada, Y., Takahashi, T., Nakagawa, T., Shirahige, K., and Masukata, H. (2007). Genome-wide localization of pre-RC sites and identification of replication origins in fission yeast. EMBO *26*, 1327-1339.

Hayles, J., Fisher, D., Woollard, A., and Nurse, P. (1994). Temporal order of S phase and mitosis in fission yeast is determined by the state of the p34cdc2-mitotic B cyclin complex. Cell *78*, 813-822.

Heichinger, C., Penkett, C. J., Bähler, J., and Nurse, P. (2006). Genome-wide characterization of fission yeast DNA replication origins. EMBO *25*, 5171-5179.

Heim, R., Cubitt, A. B., and Tsien, R. Y. (1995). Improved green fluorescence. Nature *373*, 663-664.

Helfer, H., and Gladfelter, A. S. (2006). AgSwe1p Regulates Mitosis in Response to Morphogenesis and Nutrients in Multinucleated Ashbya gossypii Cells. Mol Biol Cell *17*, 4494-4512.

Hofmann, J. F. X., and Beach, D. (1994). cdt1 is an essential target of the Cdc10/Sct1 transcription factor: requirement for DNA replication and inhibition of mitosis. EMBO *13*, 425-434.

Houchens, C. R., Lu, W., Chuang, R.-Y., Frattini, M. G., Fuller, A., Simancek, P., and Kelly, T. J. (2008). Multiple Mechanisms Contribute to Schizosaccharomyces pombe Origin Recognition Complex-DNA Interactions. J Biol Chem *283*, 30216-30224.

Hourcade, D., and Dressler (1973). The amplification of ribosomal RNA genes involves a rolling circle intermediate. Proc Natl Acad Sci USA *70*, 2926-2930.

Hua, X. H., and Newport, J. (1998). Identification of a Preinitiation Step in DNA Replication That Is Independent of Origin Recognition Complex and cdc6, but Dependent on cdk2. J Cell Biol *140*, 271-281.

Itzhaki, J. E., Gilbert, C. S., and Porter, A. C. G. (1997). Construction by gene targeting in human cells of a 'conditional' CDC2 mutant that rereplicates its DNA. Nat Genet *15*, 258-265.

Jallepalli, P. V., Brown, G. W., Muzi-Falconi, M., Tien, D., and Kelly, T. J. (1997). Regulation of the replication initiator protein p65cdc18 by CDK phosphorylation. Genes Dev *11*, 2767-2779.

Jallepalli, P. V., Tien, D., and Kelly, T. J. (1998). sud1+ targets cyclin-dependent kinase-phosphorylated Cdc18 and Rum1 proteins for degradation and stops unwanted diploidization in fission yeast. Proc Natl Acad Sci U S A *95*, 8159-8164.

Johnson, R., and Rao, P. (1970). Mammalian cell fusion: induction of premature chromosome condensation in interphase nuclei. Nature *226*, 717-722.

Jorgensen, P., and Tyers, M. (2004). How Cells Coordinate Growth and Division. Curr Biol *14*, R1014-R1027.

Karakaidos, P., Taraviras, S., Vassiliou, L. V., Zacharatos, P., Kastrinakis, N. G., Kougiou, D., Kouloukoussa, M., Nishitani, H., Papavassiliou, A. G., Lygerou, Z., and Gorgoulis, V. G. (2004). Overexpression of the Replication Licensing Regulators hCdt1 and hCdc6 Characterizes a Subset of Non-Small-Cell Lung Carcinomas: Synergistic Effect with Mutant p53 on Tumor Growth and Chromosomal Instability--Evidence of E2F-1 Transcriptional Control over hCdt1. Am J Pathol *165*, 1351-1365.

Kelly, T. J., GS, M., Forsburg, S. L., Stephen, R., Russo, A., and Nurse, P. (1993). The fission yeast cdc18+ gene product couples S phase to START and mitosis Cell *74*, 371-382.

Kiang, L., Heichinger, C., Watt, S., Bahler, J., and Nurse, P. (2009). Cyclin-Dependent Kinase Inhibits Reinitiation of a Normal S-Phase Program during G2 in Fission Yeast. Mol Cell Biol *29*, 4025-4032.

Kikuchi, J., Furukawa, Y., Iwase, S., Terui, Y., Nakamura, M., Kitagawa, S., Kitagawa, M., Komatsu, N., and Miura, Y. (1997). Polyploidization and functional maturation are two distinct processes during megakaryocytic differentiation: involvement of cyclin-dependent kinase inhibitor p21 in polyploidization. Blood *89*, 3980 - 3990.

Klemm, R. D., Austin, R. J., and Bell, S. P. (1997). Coordinate Binding of ATP and Origin DNA Regulates the ATPase Activity of the Origin Recognition Complex. Cell *88*, 493-502.

Kominami, K.-i., Ochotorena, I., and Toda, T. (1998). Two F-box/WD-repeat proteins Pop1 and Pop2 form hetero- and homo-complexes together with cullin-1 in the fission yeast SCF (Skp1-Cullin-1-F-box) ubiquitin ligase. Genes Cells *3*, 721-735.

Kong, D., and DePamphilis, M. L. (2001). Site-Specific DNA Binding of the Schizosaccharomyces pombe Origin Recognition Complex Is Determined by the Orc4 Subunit. Mol Cell Biol *21*, 8095-8103.

Koszul, R., Caburet, S., Dujon, B., and Fischer, G. (2004). Eucaryotic genome evolution through the spontaneous duplication of large chromosomal segments. EMBO J *23*, 234-243.

Krasinska, L., Besnard, E., Cot, E., Dohet, C., Mechali, M., Lemaitre, J.-M., and Fisher, D. (2008). Cdk1 and Cdk2 activity levels determine the efficiency of replication origin firing in Xenopus. EMBO J *27*, 758-769.

Krishan, A., and Ray-Chaudhuri, R. (1969). Asynchrony of Nuclear Development in Cytochalasin-Induced Multinucleate Cells. The Journal of Cell Biology *43*, 618-621.

Kubrakiewicz, J. (2002). Extrachromosomal rDNA amplification in the oocytes of Polystoechotes punctatus (Fabricius) (Insecta-Neuroptera-Polystoechotidae). Arthropod Structure & Development *31*, 23-31.

Kubrakiewicz, J., and Bilinski, S. M. (1995). Extrachromosomal amplification of rDNA in oocytes of Hemerobius spp. (Insecta, Neuroptera). Chromosoma *103*, 606-612.

Labbe, J. C., Lee, M. G., Nurse, P., Picard, A., and Doree, M. (1988). Activation at M-phase of a protein kinase encoded by a starfish homologue of the cell cycle control gene cdc2+. Nature *335*, 251-254.

Labib, K., Tercero, J. A., and Diffley, J. F. X. (2000). Uninterrupted MCM2-7 Function Required for DNA Replication Fork Progression. Science *288*, 1643-1647.

Larkins, B. A., Dilkes, B. P., Dante, R. A., Coelho, C. M., Woo, Y.-m., and Liu, Y. (2001). Investigating the hows and whys of DNA endoreduplication. J Exp Bot *52*, 183-192.

Lee, M. G., and Nurse, P. (1987). Complementation used to clone a human homologue of the fission yeast cell cycle control gene cdc2. Nature *327*, 31-35.

Liang, C., and Gerbi, S. A. (1994). Analysis of an origin of DNA amplification in Sciara coprophila by a novel three-dimensional gel method. Mol Cell Biol *14*, 1520-1529.

Liang, C., Spitzer, J. D., Smith, H. S., and Gerbi, S. A. (1993). Replication initiates at a confined region during DNA amplification in Sciara DNA puff II/9A. Genes Dev *7*, 1072-1084.

Liang, C., Weinreich, M., and Stillman, B. (1995). ORC and Cdc6p interact and determine the frequency of initiation of DNA replication in the genome. Cell *81*, 667-676.

Lilly, M. A., and Spradling, A. C. (1996). The Drosophila endocycle is controlled by Cyclin E and lacks a checkpoint ensuring S-phase completion. Genes Dev *10*, 2514 - 2526.

Liontos, M., Koutsami, M., Sideridou, M., Evangelou, K., Kletsas, D., Levy, B., Kotsinas, A., Nahum, O., Zoumpourlis, V., Kouloukoussa, M., *et al.* (2007). Deregulated Overexpression of hCdt1 and hCdc6 Promotes Malignant Behavior. Cancer Res *67*, 10899-10909.

Loog, M., and Morgan, D. O. (2005). Cyclin specificity in the phosphorylation of cyclin-dependent kinase substrates. Nature *434*, 104-108.

Lopez-Girona, A., Mondesert, O., Leatherwood, J., and Russell, P. (1998). Negative Regulation of Cdc18 DNA Replication Protein by Cdc2. Mol Biol Cell *9*, 63-73.

Lunyak, V. V., Ezrokhi, M., Smith, H. S., and Gerbi, S. A. (2002). Developmental Changes in the Sciara II/9A Initiation Zone for DNA Replication. Mol Cell Biol *22*, 8426-8437.

Lygeros, J., Koutroumpas, K., Dimopoulos, S., Legouras, I., Kouretas, P., Heichinger, C., Nurse, P., and Lygerou, Z. (2008). Stochastic hybrid modeling of DNA replication across a complete genome. Proc Natl Acad Sci U S A *105*, 12295-12300.

Lygerou, Z., and Nurse, P. (1999). The fission yeast origin recognition complex is constitutively associated with chromatin and is differentially modified through the cell cycle. J Cell Sci *112*, 3703-3712.

Mailand, N., and Diffley, J. F. (2005). CDKs promote DNA replication origin licensing in human cells by protecting Cdc6 from APC/C-dependent proteolysis. Cell *122*, 915 - 926.

Maines, J. Z., Stevens, L. M., Tong, X., and Stein, D. (2004). Drosophila dMyc is required for ovary cell growth and endoreplication. Development *131*, 775-786.

Malumbres, M., Sotillo, R., SantamarIa, D., Galán, J., Cerezo, A., Ortega, S., Dubus, P., and Barbacid, M. (2004). Mammalian Cells Cycle without the D-Type Cyclin-Dependent Kinases Cdk4 and Cdk6. Cell *118*, 493-504.

Marks, J., Fankhauser, C., Reymond, A., and Simanis, V. (1992). Cytoskeletal and DNA structure abnormalities result from bypass of requirement for the cdc10 start gene in the fission yeast Schizosaccharomyces pombe. J Cell Sci *101*, 517-528.

Martín-Castellanos, C. (2000). The puc1 Cyclin Regulates the G1 Phase of the Fission Yeast Cell Cycle in Response to Cell Size. Mol Biol Cell *11*, 543-554.

Masui, Y., and Markert, C. (1971). Cytoplasmic control of nuclear behavior during meiotic maturation of frog oocytes. J Exp Zool *177*, 129-145.

Melixetian, M., Ballabeni, A., Masiero, L., Gasparini, P., Zamponi, R., Bartek, J., Lukas, J., and Helin, K. (2004). Loss of Geminin induces rereplication in the presence of functional p53. J Cell Biol *165*, 473-482.

Mendez, J., and Stillman, B. (2000). Chromatin Association of Human Origin Recognition Complex, Cdc6, and Minichromosome Maintenance Proteins during the Cell Cycle: Assembly of Prereplication Complexes in Late Mitosis. Mol Cell Biol *20*, 8602-8612.

Mickle, K., Oliva, A., Huberman, J., and Leatherwood, J. (2007). Checkpoint effects and telomere amplification during DNA re-replication in fission yeast. BMC Molecular Biology *8*, 119.

Mihaylov, I. S., Kondo, T., Jones, L., Ryzhikov, S., Tanaka, J., Zheng, J., Higa, L. A., Minamino, N., Cooley, L., and Zhang, H. (2002). Control of DNA Replication and Chromosome Ploidy by Geminin and Cyclin A. Mol Cell Biol *22*, 1868-1880.

Mitchison, J. M., and Creanor, J. (1971). Further measurements of DNA synthesis and enzyme potential during cell cycle of fission yeast Schizosaccharomyces pombe. Exp Cell Res *69*, 244-247.

Mondesert, O., McGowan, C., and Russell, P. (1996). Cig2, a B-type cyclin, promotes the onset of S in Schizosaccharomyces pombe. Mol Cell Biol *16*, 1527-1533.

Monesi, N., Fernandez, M. A., Fontes, A. M., Jr, L. R. B., Nakanishi, Y., Baron, B., Buttin, G., and Paçó-Larson, M. L. (1995). Molecular characterization of an 18 kb segment of DNA puff C4 of Bradysia hygida(Diptera, Sciaridae). Chromosoma *103*, 715-724.

Moreno, S., Klar, A., and Nurse, P. (1991). Molecular genetic analysis of fission yeast Schizosaccharomyces pombe. Methods Enzymol *194*, 795-823.

Moreno, S., Labib, K., Correa, J., and Nurse, P. (1994). Regulation of the cell cycle timing of Start in fission yeast by the rum1+ gene. J Cell Sci *18*, 63-68.

Moreno, S., and Nurse, P. (1994). Regulation of progression through the Gl phase of the cell cycle by the rum1+ gene. Nature *367*, 236-242.

Moseley, J. B., Mayeux, A., Paoletti, A., and Nurse, P. (2009). A spatial gradient coordinates cell size and mitotic entry in fission yeast. Nature *459*, 857-860.

Muzi-Falconi, M., Brown, G. W., and Kelly, T. J. (1996). cdc18+ regulates initiation of DNA replication in Schizosaccharomyces pombe. PNAS *93*, 1566-1570.

Nasmyth, K., Nurse, P., and Fraser, R. (1979). The effect of cell mass on the cell cycle timing and duration of S-phase in fission yeast. J Cell Sci *39*, 215-233.

Nguyen, V. Q., Co, C., and Li, J. J. (2001). Cyclin-dependent kinases prevent DNA re-replication through multiple mechanisms. Nature *411*, 1068-1073.

Nishitani, H., Lygerou, Z., Nishimoto, T., and Nurse, P. (2000). The Cdt1 protein is required to license DNA for replication in fission yeast. Nature *404*, 625-628.

Nishitani, H., and Nurse, P. (1995). p65cdc18 plays a major role controlling the initiation of DNA replication in fission yeast. Cell *83*, 397-405.

Nishitani, H., Sugimoto, N., Roukos, V., Nakanishi, Y., Saijo, M., Obuse, C., Tsurimoto, T., Nakayama, K. I., Nakayama, K., Fujita, M., *et al.* (2006). Two E3 ubiquitin ligases, SCF-Skp2 and DDB1-Cul4, target human Cdt1 for proteolysis. EMBO J *25*, 1126-1136.

Nurse, P. (1975). Genetic control of cell size at cell division in yeast. Nature *256*, 547-551.

Nurse, P., and Bissett, Y. (1981). Gene required in G1 for commitment to cell cycle and in G2 for control of mitosis in fission yeast. Nature *292*, 558-560.

Nurse, P., and Thuriaux, P. (1977). Controls over the timing of DNA replication during the cell cycle of fission yeast. Exp Cell Res *107*, 365-375.

Nurse, P., Thuriaux, P., and Nasmyth, K. (1976). Genetic Control of the Cell Division Cycle in the Fission Yeast Schizosaccharomyces pombe. Molec gen Genet *146*, 167-178.

Ohno, S. (1970). Evolution by gene duplication (Berlin: Springer-Verlag).

Ohno, S. (1999). Gene duplication and the uniqueness of vertebrate genomes circa 1970-1999. Semin Cell Dev Biol *10*, 517-522.

Okuno, Y., Satoh, H., Sekiguchi, M., and Masukata, H. (1999). Clustered Adenine/Thymine Stretches Are Essential for Function of a Fission Yeast Replication Origin. Mol Cell Biol *19*, 6699-6709.

Osheim, Y. N., Miller, O. L., Jr., and Beyer, A. L. (1988). Visualization of Drosophila melanogaster chorion genes undergoing amplification. Mol Cell Biol *8*, 2811-2821.

Parisi, T., Beck, A. R., Rougier, N., McNeil, T., Lucian, L., Werb, Z., and Amati, B. (2003). Cyclins E1 and E2 are required for endoreplication in placental trophoblast giant cells. EMBO J *22*, 4794 - 4803.

Patel, P. K., Kommajosyula, N., Rosebrock, A., Bensimon, A., Leatherwood, J., Bechhoefer, J., and Rhind, N. (2008). The Hsk1/Cdc7 Replication Kinase Regulates Origin Efficiency. Mol Biol Cell *19*, 5550-5558.

Petersen, B. O., Wagener, C., Marinoni, F., Kramer, E. R., Melixetian, M., Denchi, E. L., Gieffers, C., Matteucci, C., Peters, J.-M., and Helin, K. (2000). Cell cycle- and cell growth- regulated proteolysis of mammalian CDC6 is dependent on APC-CDH1. Genes Dev *14*, 2330-2343.

Poloumienko, A., Dershowitz, A., De, J., and Newlon, C. S. (2001). Completion of Replication Map of Saccharomyces cerevisiae Chromosome III. Mol Biol Cell *12*, 3317-3327.

Pomerening, J. R., Kim, S. Y., and Ferrell, J. E. (2005). Systems-Level Dissection of the Cell-Cycle Oscillator: Bypassing Positive Feedback Produces Damped Oscillations. Cell *122*, 565-578.

Ralph, E., Boye, E., and Kearsey, S. E. (2006). DNA damage induces Cdt1 proteolysis in fission yeast through a pathway dependent on Cdt2 and Ddb1. EMBO rep *7*, 1134-1139.

Rane, S. G., Dubus, P., Mettus, R. V., Galbreath, E. J., Boden, G., Reddy, E. P., and Barbacid, M. (1999). Loss of Cdk4 expression causes insulin-deficient diabetes and Cdk4 activation results in [beta]-islet cell hyperplasia. Nat Genet *22*, 44-52.

Rao, P., and Johnson, R. (1970). Mammalian cell fusion: studies on the regulation of DNA synthesis and mitosis. Nature *10*, 159-164.

Rossi, S. G., Vazquez, A. E., and Rotundo, R. L. (2000). Local Control of Acetylcholinesterase Gene Expression in Multinucleated Skeletal Muscle Fibers: Individual Nuclei Respond to Signals from the Overlying Plasma Membrane. J Neurosci *20*, 919-928.

Russell, P., and Nurse, P. (1986). cdc25+ functions as an inducer in the mitotic control of fission yeast. Cell *45*, 145-153.

Russell, P., and Nurse, P. (1987). Negative regulation of mitosis by wee1+, a gene encoding a protein kinase homolog. Cell *49*, 559-567.

Rustici, G., Mata, J., Kivinen, K., Lio, P., Penkett, C. J., Burns, G., Hayles, J., Brazma, A., Nurse, P., and Bähler, J. (2004). Periodic gene expression program of the fission yeast cell cycle. Nat Genet *36*, 809-817.

Saha, P., Chen, J., Thome, K. C., Lawlis, S. J., Hou, Z.-h., Hendricks, M., Parvin, J. D., and Dutta, A. (1998). Human CDC6/Cdc18 Associates with Orc1 and Cyclin-cdk and Is Selectively Eliminated from the Nucleus at the Onset of S Phase. Mol Cell Biol *18*, 2758-2767.

Santamaria, D., Barriere, C., Cerqueira, A., Hunt, S., Tardy, C., Newton, K., Caceres, J. F., Dubus, P., Malumbres, M., and Barbacid, M. (2007). Cdk1 is sufficient to drive the mammalian cell cycle. Nature *448*, 811 - 815.

Sauer, K., Knoblich, J. A., Richardson, H., and Lehner, C. F. (1995). Distinct modes of cyclin E/cdc2c kinase regulation and S-phase control in mitotic and endoreduplication cycles of Drosophila embryogenesis. Genes Dev *9*, 1327-1339.

Schimke, R. T., Sherwood, S. W., Hill, A. B., and Johnston, R. N. (1986). Overreplication and recombination of DNA in higher eukaryotes: potential consequences and biological implications. Proc Natl Acad Sci U S A *83*, 2157-2161.

Segurado, M., Luis, A. d., and Antequera, F. (2003). Genome-wide distribution of DNA replication origins at A+T islands in Schizosaccharomyces pombe. EMBO rep *4*, 1048-1053.

Seo, J., Chung, Y. S., Sharma, G. G., Moon, E., Burack, W. R., Pandita, T. K., and Choi, K. (2005). Cdt1 transgenic mice develop lymphoblastic lymphoma in the absence of p53. Oncogene *24*, 8176-8186.

Shcherbata, H. R., Althauser, C., Findley, S. D., and Ruohola-Baker, H. (2004). The mitotic-to-endocycle switch in Drosophila follicle cells is executed by Notch-dependent regulation of G1/S, G2/M and M/G1 cell-cycle transitions. Development *131*, 3169-3181.

Sigrist, S. J., and Lehner, C. F. (1997). Drosophila fizzy-related down-regulates mitotic cyclins and is required for cell proliferation arrest and entry into endocycles. Cell *90*, 671 - 681.

Simanis, V., and Nurse, P. (1986). The cell cycle control gene cdc2+ of fission yeast encodes a protein kinase potentially regulated by phosphorylation. Cell *45*, 261-268.

Sivakumar, S., Porter-Goff, M., Patel, P. K., Benoit, K., and Rhind, N. (2004). In vivo labeling of fission yeast DNA with thymidine and thymidine analogs. Methods *33*, 213-219.

Smith, L. D., and Ecker, R. E. (1971). The interaction of steroids with Rana pipiens oocytes in the induction of maturation. Dev Biol *25*, 232-247.

Stanojcic, S., Lemaitre, J.-M., Brodolin, K., Danis, E., and Mechali, M. (2008). In Xenopus Egg Extracts, DNA Replication Initiates Preferentially at or near Asymmetric AT Sequences. Mol Cell Biol *28*, 5265-5274.

Stern, B., and Nurse, P. (1996). A quantitative model for the cdc2 control of S phase and mitosis in fission yeast. Trends Genet *12*, 345-350.

Tanaka, H., Tanaka, K., Murakami, H., and Okayama, H. (1999). Fission Yeast Cdc24 Is a Replication Factor C- and Proliferating Cell Nuclear Antigen-Interacting Factor Essential for S-Phase Completion. Mol Cell Biol *19*, 1038-1048.

Tanny, R. E., MacAlpine, D. M., Blitzblau, H. G., and Bell, S. P. (2006). Genome-wide Analysis of Re-replication Reveals Inhibitory Controls That Target Multiple Stages of Replication Initiation. Mol Biol Cell *17*, 2415-2423.

Tetsu, O., and McCormick, F. (2003). Proliferation of cancer cells despite CDK2 inhibition. Cancer Cell *3*, 233-245.

Tröster, H., Edström, J.-E., Trendelenburg, M. F., and Hofmann, A. (1990). Structural organization of Acheta rDNA : Evidence for differential amplification of soma and germ-line-specific rDNA sequences. J Mol Biol *216*, 533-543.

Tsuyama, T., Tada, S., Watanabe, S., Seki, M., and Enomoto, T. (2005). Licensing for DNA replication requires a strict sequential assembly of Cdc6 and Cdt1 onto chromatin in Xenopus egg extracts. Nucl Acids Res *33*, 765-775.

Ullah, Z., Kohn, M. J., Yagi, R., Vassilev, L. T., and DePamphilis, M. L. (2008). Differentiation of trophoblast stem cells into giant cells is triggered by p57/Kip2 inhibition of CDK1 activity. Genes Dev *22*, 3024-3036.

Varshavsky, A. (1981). On the possibility of metabolic control of replicon "misfiring": relationship to emergence of malignant phenotypes in mammalian cell lineages. Proc Natl Acad Sci U S A *78*, 3673-3677.

Vas, A., Mok, W., and Leatherwood, J. (2001). Control of DNA Rereplication via Cdc2 Phosphorylation Sites in the Origin Recognition Complex. Mol Cell Biol *21*, 5767-5777.

Vashee, S., Cvetic, C., Lu, W., Simancek, P., Kelly, T. J., and Walter, J. C. (2003). Sequence-independent DNA binding and replication initiation by the human origin recognition complex. Genes Dev *17*, 1894-1908.

Vaziri, C., Saxena, S., Jeon, Y., Lee, C., Murata, K., Machida, Y., Wagle, N., Hwang, D. S., and Dutta, A. (2003). A p53-Dependent Checkpoint Pathway Prevents Rereplication. Mol Cell *11*, 997-1008.

Wilkinson, C. R. M., Penny, M., McGurk, G., Wallace, M., and Gordon, C. (1999). The 26S proteasome of the fission yeast Schizosaccharomyces pombe. Philos Trans R Soc Lond B Biol Sci *354*, 1523-1532.

Wilmes, G. M., Archambault, V., Austin, R. J., Jacobson, M. D., Bell, S. P., and Cross, F. R. (2004). Interaction of the S-phase cyclin Clb5 with an 'RXL' docking sequence in the initiator protein Orc6 provides an origin-localized replication control switch. Genes Dev *18*, 981-991.

Wood, V., Gwilliam, R., Rajandream, M. A., Lyne, M., Lyne, R., Stewart, A., Sgouros, J., Peat, N., Hayles, J., Baker, S., *et al.* (2002). The genome sequence of Schizosaccharomyces pombe. Nature *415*, 871-880.

Wu, P.-Y. J., and Nurse, P. (2009). Establishing the Program of Origin Firing during S Phase in Fission Yeast. Cell *136*, 852-864.

Wuarin, J., Buck, V., Nurse, P., and Millar, J. B. A. (2002). Stable Association of Mitotic Cyclin B/Cdc2 to Replication Origins Prevents Endoreduplication. Cell *111*, 419-431.

Yabuuchi, H., Yamada, Y., Uchida, T., Sunathvanichkul, T., Nakagawa, T., and Masukata, H. (2006). Ordered assembly of Sld3, GINS and Cdc45 is distinctly regulated by DDK and CDK for activation of replication origins. EMBO J *25*, 4663-4674.

Yamano, H., Kitamura, K., Kominami, K.-i., Lehmann, A., Katayama, S., Hunt, T., and Toda, T. (2000). The Spike of S Phase Cyclin Cig2 Expression at the G1–S Border in Fission Yeast Requires Both APC and SCF Ubiquitin Ligases. Mol Cell *6*, 1377-1387.

Yamano, H., Kominami, K.-i., Harrison, C., Kitamura, K., Katayama, S., Dhut, S., Hunt, T., and Toda, T. (2004). Requirement of the SCFPop1/Pop2 Ubiquitin Ligase for Degradation of the Fission Yeast S Phase Cyclin Cig2. J Biol Chem *279*, 18974-18980.

Yanow, S. K., Lygerou, Z., and Nurse, P. (2001). Expression of Cdc18/Cdc6 and Cdt1 during G2 phase induces initiation of DNA replication. EMBO *20*, 4648-4656.

Yao, M.-C., Kimmel, A. R., and Gorovsky, M. A. (1974). A Small Number of Cistrons for Ribosomal RNA in the Germinal Nucleus of a Eukaryote, Tetrahymena pyriformis. Proc Natl Acad Sci USA *71*, 3082-3086.

Yu, Q., Sicinska, E., Geng, Y., Ahnström, M., Zagozdzon, A., Kong, Y., Gardner, H., Kiyokawa, H., Harris, L. N., Stål, O., and Sicinski, P. (2006). Requirement for CDK4 kinase function in breast cancer. Cancer Cell *9*, 23-32.

Zhang, H., and Tower, J. (2004). Sequence requirements for function of the Drosophila chorion gene locus ACE3 replicator and ori-{beta} origin elements. Development *131*, 2089-2099.

Zhang, Y., Wang, Z., Liu, D. X., Pagano, M., and Ravid, K. (1998). Ubiquitin-dependent Degradation of Cyclin B Is Accelerated in Polyploid Megakaryocytes. J Biol Chem *273*, 1387-1392.

Zhong, W., Feng, H., Santiago, F. E., and Kipreos, E. T. (2003). CUL-4 ubiquitin ligase maintains genome stability by restraining DNA-replication licensing. Nature *423*, 885-889.

Zou, L., and Stillman, B. (2000). Assembly of a Complex Containing Cdc45p, Replication Protein A, and Mcm2p at Replication Origins Controlled by S-Phase Cyclin-Dependent Kinases and Cdc7p-Dbf4p Kinase. Mol Cell Biol *20*, 3086-3096.